



COPYRIGHT AND USE OF THIS THESIS

This thesis must be used in accordance with the provisions of the Copyright Act 1968.

Reproduction of material protected by copyright may be an infringement of copyright and copyright owners may be entitled to take legal action against persons who infringe their copyright.

Section 51 (2) of the Copyright Act permits an authorized officer of a university library or archives to provide a copy (by communication or otherwise) of an unpublished thesis kept in the library or archives, to a person who satisfies the authorized officer that he or she requires the reproduction for the purposes of research or study.

The Copyright Act grants the creator of a work a number of moral rights, specifically the right of attribution, the right against false attribution and the right of integrity.

You may infringe the author's moral rights if you:

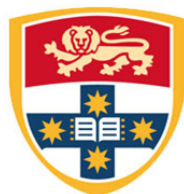
- fail to acknowledge the author of this thesis if you quote sections from the work
- attribute this thesis to another author
- subject this thesis to derogatory treatment which may prejudice the author's reputation

For further information contact the University's Director of Copyright Services

sydney.edu.au/copyright

**Role of mineralocorticoid receptor
regulation during experimental
myocardial infarction**

Thi Yen Loan Le



THE UNIVERSITY OF
SYDNEY

A thesis submitted for fulfilment of the requirements for
the degree of Doctor of Philosophy, 2014.

Faculty of Medicine, The University of Sydney

Declaration

The work described in this thesis was performed by the author at the Kolling Institute of Medical Research, Sydney, Australia between the years 2009 and 2013, to fulfill the requirements of the degree of Doctor of Philosophy in the Faculty of Medicine, University of Sydney. The work presented was conducted under the supervision of my primary supervisor Dr Anastasia Susie Mihailidou. None of the contents of this thesis has been submitted previously for the purpose of obtaining another degree.

Thi Yen Loan Le

18th September 2013

Abstract

Ischaemic heart disease (IHD) remains the leading cause of morbidity and mortality worldwide. During ischaemia, coronary perfusion is interrupted which triggers oxidative stress due to the imbalance between free radical generation and/or inadequate antioxidant defense and increased cardiomyocyte apoptosis which contributes to ventricular remodelling and deterioration in cardiac function. The primary clinical strategy is to quickly restore blood flow to the heart muscle (myocardial reperfusion), although this may induce further injury known as myocardial reperfusion injury. During ischaemia and reperfusion several processes are activated which include sodium and calcium overload, generation of reactive oxygen species (ROS) while myocardial antioxidant defence systems are impaired, activation of immediate stress-related gene transcription, autophagy and cell death processes, apoptosis and necrosis leading to further aggravated cardiac damage.

Advances in treatment strategies have decreased mortality rates although myocardial infarction still remains one of the leading global burdens of disease and hence further studies are required to identify additional mechanisms involved. Therefore the first aim of this thesis was to develop an experimental model of myocardial infarction (MI). This was achieved by using the *ex-vivo* rat heart and inducing MI to determine direct effects of treatment without interference by circulatory reflexes. Hearts were isolated from anaesthetised male Sprague Dawley (SD) rats and perfused on a Langendorff apparatus. Following a stabilisation period, hearts were subjected to regional ischaemia by occluding a branch of the left coronary artery (30 minutes) and then releasing the occlusion and allowing reperfusion (150 minutes). Increased levels of superoxide and

oxidised glutathione (GSSG) with activated cellular pathways autophagy and apoptosis, comparable to previous studies validated this model of MI. Although there were increased expression levels of autophagy proteins (Beclin-1, Atg5-Agt12 conjugate, LC3-II), there was also activation of pro-apoptotic proteins (caspase-3, caspase-9), with suppression of anti-apoptotic proteins (B-cell lymphoma-2 (Bcl-2), X-linked inhibitor of apoptosis protein (XIAP) and anti-apoptotic repressor protein with a caspase domain (ARC)), leading to increased cardiomyocyte apoptosis and aggravated infarct size.

The incidence of IHD in men is twice that of age-matched women, although most studies focus on protection by oestrogen, with less attention on androgen receptor (AR) mediated actions. Expression levels of mineralocorticoid receptors (MR) have been shown to increase in MI and heart failure, which may also contribute to cardiac damage, although there have been no previous studies whether there is sexual dimorphism of MR expression following myocardial ischaemia-reperfusion (I-R) injury. The second aim for this thesis was to determine the role of androgens in the sex differences in cardiac damage during MI and whether there are gender differences in expression levels of MR.

Studies were in age-matched male and female SD rats either intact or surgically gonadectomised (Gx) \pm hormone replacement with testosterone, as androgen replacement, or 17 β -oestradiol as oestrogen replacement via subdermal silastic implants; a subset of male rats received dihydrotestosterone. After 21 days, hearts were subjected to *ex-vivo* myocardial I-R. Hearts from intact males had larger infarcts than hearts from intact females following I-R; Gx produced the opposite effect, suggesting a key role for sex steroid action during MI. Levels of MR did not significantly change

during the various treatments suggesting gonadal steroids do not modify MR expression. Novel mechanisms were identified for I-R induced aggravated cardiac damage in male animals through increased AR and receptor for advanced glycation end products (RAGE) expression shifting the balance between autophagy and apoptosis towards increased apoptosis. In contrast, myocardial I-R in females produced less cardiac damage reflecting enhanced autophagy and decreased apoptosis. RAGE expression is the key regulator of this switch since testosterone administration to females, aggravated cardiac damage during myocardial I-R which was mediated by upregulation of AR and RAGE expression. This may be relevant for postmenopausal women receiving testosterone and also provide a platform for tailored therapeutic strategies.

Primary treatment strategies for MI are directed to timely restoration of blood flow to the ischaemic myocardium using drug therapy (thrombolytics) or catheter procedures (percutaneous coronary intervention, PCI), however a high incidence of mortality persists and hence additional treatment strategies are needed. Elevated plasma levels of aldosterone during PCI for MI are an independent risk factor for mortality therefore targeting aldosterone or mineralocorticoid receptors (MR) is an important therapy strategy. Our laboratory has previously shown aldosterone aggravated cardiac damage during experimental MI, which was mediated via its cognate receptor MR. The next aim was to determine whether this aggravated cardiac damage involved genomic signalling pathways through the intracellular MR alone or whether there non-genomic pathways involved the G protein-coupled receptor 30 (GPR30), which has not been previously reported.

Aldosterone (Ald) and the membrane impermeable aldosterone-3-carboxymethoxylamine-TFP ester reacted with an 8-branched PEG amine (Aldo-PEG) were used in rat ventricular myoblast cells H9c2 and *ex-vivo* I-R in rat hearts. Both Ald and Aldo-PEG ligand activated extracellular signal-regulated kinase 1/2 (ERK1/2) phosphorylation in H9c2 cells, confirming biological activity of the Aldo-PEG ligand and comparable to that of the GPR30 selective agonist, G1. The specific GPR30 antagonist, G36, but not MR antagonist, spironolactone, prevented Ald and Aldo-PEG - induced ERK1/2 phosphorylation suggesting these rapid non-genomic actions of Ald were mediated via GPR30. In contrast, only Ald increased transcript levels of MR-responsive genes serum/glucocorticoid regulated kinase-1 (Sgk-1) and plasminogen activator inhibitor type-1 (PAI-1). In separate *ex-vivo* I-R studies in rat hearts, Ald (10 nM) increased infarct size and aggravated apoptosis, whereas Aldo-PEG (10 or 100 nM) had no effect. These studies suggest that aldosterone aggravated cardiac damage during reperfusion injury requires activation of genomic pathways.

Blockade of MR prevents aldosterone-aggravated cardiac damage and has been shown to be an effective treatment strategy in both experimental and clinical studies. Large randomised trials have shown MR antagonists (spironolactone or eplerenone) added to standard therapy reduced morbidity and mortality in patients with heart failure and heart failure post MI, although the mechanisms were not fully defined. In these trials, the levels of plasma aldosterone were within the normal range and low doses of MR antagonists were used. Therefore the next aim was to identify how MR blockade alone, in the absence of other corticosteroids, may prevent cardiac damage during myocardial I-R. Dose response studies for MR antagonists, spironolactone and eplerenone showed

that low doses of MR antagonists (10 nM spironolactone and 100 nM eplerenone) reduced infarct size. Low dose MR antagonists prevented degradation of anti-apoptotic protein ARC, which prevented initiation of apoptosis and provides a novel mechanism for low-dose MR blockade during I-R.

Since redox signaling during myocardial I-R regulates both apoptosis and stress response pathways, the final aim was to determine whether low-dose MR blockade may also regulate redox balance and immediate early gene transcription to protect the myocardium during I-R. Low-dose spironolactone during I-R decreased superoxide levels, maintained redox balance and prevented I-R induced activation of immediate early gene transcription. In separate studies, H9c2 cells were exposed to low dose spironolactone during oxidant stress simulated using the pro-oxidant agent buthionine sulfoximine (BSO). The antioxidant effects of low-dose spironolactone were maintained whereas oxidative stress enhanced expression of MR-responsive genes (*Sgk-1* and *PAI-1*) were prevented, indicating ligand-independent MR regulation. These studies suggest that the cardioprotective effects of SPIRO involve both a reduction in ROS formation as well as blockade of MR activation.

In summary the results from these studies provide the mechanisms for low dose MR antagonists to protect the myocardium during MI. The novel findings in this thesis provide direct evidence that these agents have actions beyond preventing ligands access to the mineralocorticoid receptor and for including MR antagonists as standard treatment regimens in conditions where there is increased oxidative stress and apoptosis.

Acknowledgements

Working on the PhD has been a wonderful and real learning experience. I am indebted to many people for their support, help and encouragement throughout this journey.

First of all, I am deeply grateful to my primary supervisor, Dr Anastasia Susie Mihailidou. She gave me the opportunity to undertake PhD in the Cardiovascular & Hormonal Research Laboratory. I am very appreciative of her constant support, encouragement, help and guidance, especially with my writing. This thesis would not have been possible without her help and support.

I would like to thank my co-supervisors, in particular Dr Anthony Ashton for his support, help, guidance and teaching with molecular studies; Dr Mahidi Mardini for his support and providing training with infarct analysis and Prof John Funder for his support.

I would like to acknowledge Prof Celso Gomez-Sanchez (University of Mississippi Medical Center, USA) for the supply of Aldo-PEG compound and MR antibodies, Prof David Handelsman (Anzac Research Institute, AUS) and Prof Peter Stanton (Prince Henry's Institute, AUS) for the supply of steroid implants.

I would like to express gratitude to the staff at the Kolling Institute of Medical research for not only allowed me to use the facilities but also provided valuable discussions about the technique. In particular, I would like to thank Dr Viive Howell for her generosity in giving me her time training and guidance with RNA/PCR studies. I would

like to thank Dr Rosanna Cazzolli, Dr Jenny Park and Dr Sharon McCracken for teaching me protein extraction and western blot and answering questions whenever I asked. Thanks also to Dr Jane Radford (University of Sydney) and Mrs Sue Smith (Kolling Institute of Medical Research) for their friendly advice and help with sectioning and immunohistochemistry. In addition, I would like to acknowledge Mrs Giselle Bellamy and the staff of the Kearns Facility for looking after the animals. Thanks also go to all my friends at the Kolling Institute of Medical Research for giving me encouragement and support throughout this journey.

I would like to extend my deepest gratitude to my mom, brother and sisters. They always have provided infinite support, love and encouragement. Without their support it would not have been possible to complete this thesis. Thank you for believing in me!

Finally, I would like to acknowledge the Royal North Shore Hospital & University of Sydney (co-funded postgraduate scholarship) and the National Health and Medical Research Council of Australia (NHMRC, Dora Lush postgraduate scholarship) for providing financial support during my candidature and the National Heart Foundation of Australia for providing project support.

Publications arising from this work

Publication (Refereed Journals)

- **Le TYL**, Ashton AW, Mardini M, Stanton PG, Funder JW, Handelsman DJ, Mihailidou AS. Role of androgens in sex differences in cardiac damage during myocardial infarction. *Endocrinology*. 2014;155:568-575.
- **Le TYL**, Mardini M, Howell VM, Funder JW, Ashton AW, Mihailidou AS. Low-dose spironolactone prevents apoptosis repressor with caspase recruitment domain degradation during myocardial infarction. *Hypertension*. 2012;59:1164-1169.

Manuscripts in preparation/submitted

- **Le TYL**, Ashton AW, Mardini M, Gomez-Sanchez CE, Mihailidou AS. Aldosterone-induced Cardiac Damage during Myocardial Infarction: Is there a Role for Non-genomic Pathways.

Published abstracts

- **Le TYL**, Ashton AW, Gomez Sanchez, Mihailidou AS. Novel regulator for aldosterone action in myocardial infarction: apoptotic repressor protein with a caspase domain (ARC). *J Hypertension*. 2012; 30:e325.
- **Le TYL**, Howell VM, Ashton AW, Mihailidou AS. Low Doses of Mineralocorticoid Receptor Antagonists regulate Early Gene Transcription during Myocardial Ischemia-Reperfusion Injury. *Hypertension*. 2012;60:487-502.

- **Le TYL**, Ashton AW, Mardini M, Mihailidou AS. Spironolactone restores redox balance during myocardial ischemia-reperfusion. *Endocrine reviews*. 2011;32: P1-25.
- **Le TYL**, Ashton AW, Mardini M, Funder JW, Mihailidou AS. Cardioprotective action of Mineralocorticoid receptor antagonists during experimental myocardial infarction: role of apoptosis repressor with caspase recruitment domain (ARC). *Hypertension*. 2011;58:114-132.
- Mihailidou AS, **Le TYL**, Ashton AW, Funder JW, Mardini M, Stanton P. Myocardial damage during Ischemia-Reperfusion: Role of ARC in gender differences. *Journal of Hypertension*. 2010.
- **Le TYL**, Mardini M, Ashton A, Funder JW, Mihailidou AS. Mechanism of anti-apoptotic action of Mineralocorticoid receptor blockade in experimental myocardial infarction. *Hypertension*. 2010;55:1492-1513.
- Mihailidou AS, **Le TYL**, Mardini M, Ashton AW, Funder JW. Gonadal steroids and experimental myocardial infarction. *Endocrine reviews*. 2010;31(3):S894.

Table of Contents

<i>Declaration</i>	<i>i</i>
<i>Abstract</i>	<i>ii</i>
<i>Acknowledgements</i>	<i>vii</i>
<i>Publications arising from this work</i>	<i>ix</i>
<i>Table of Contents</i>	<i>xi</i>
<i>List of Figures</i>	<i>xviii</i>
<i>List of Tables</i>	<i>xxi</i>
<i>Abbreviations</i>	<i>xxii</i>
CHAPTER 1: LITERATURE REVIEW	1
1.1 OVERVIEW OF ISCHAEMIC HEART DISEASE	2
1.2 DEFINITION OF MYOCARDIAL ISCHAEMIA-REPERFUSION (I-R) INJURY	3
1.3 MECHANISMS OF MYOCARDIAL I-R INJURY	3
1.3.1 Cellular redox regulatory mechanisms during myocardial I-R.....	7
1.3.1.1 Generation of reactive oxygen species.....	7
1.3.1.2 Antioxidant defences systems	11
1.3.2 Redox-mediated mechanisms in regulation of cellular processes: role of gene transcription.....	14
1.3.3 Autophagy.....	17
1.3.3.1 Molecular mechanisms involved in autophagy	17
1.3.3.2 Regulation of autophagy during myocardial I-R	19
1.3.4 Apoptosis	23
1.3.4.1 Molecular mechanisms involved in apoptosis.....	23

1.3.4.2	<i>Regulation of apoptosis during myocardial I-R</i>	27
1.3.5	<i>Necrosis</i>	31
1.3.6	<i>Necroptosis</i>	33
1.4	EXPERIMENTAL MODELS OF MYOCARDIAL INFARCTION.....	36
1.4.1	<i>Ex-vivo Langendorff isolated rat preparations</i>	36
1.4.2	<i>Advantages and limitations of the ex-vivo experimental technique</i>	37
1.4.3	<i>Regional versus global ischaemia</i>	38
1.4.4	<i>Duration of ischaemia and reperfusion during myocardial I-R</i>	39
1.5	GENDER DIFFERENCE IN ISCHAEMIC HEART DISEASE.....	40
1.5.1	<i>Overview</i>	40
1.5.2	<i>Sex hormones and ischaemic heart disease: controversy</i>	41
1.5.3	<i>Gonadal steroid receptors</i>	43
1.5.3.1	<i>Oestrogens and oestrogen receptors</i>	43
1.5.3.2	<i>Androgens and androgen receptors</i>	46
1.5.4	<i>Sex hormones in myocardial I-R injury</i>	47
1.5.4.1	<i>Effects of oestrogens during myocardial I-R</i>	48
1.5.4.2	<i>Effects of androgens during myocardial I-R</i>	50
1.6	CORTICOSTEROIDS AND THE MINERALOCORTICOID RECEPTOR (MR).....	52
1.6.1	<i>Overview</i>	52
1.6.2	<i>Corticosteroids</i>	54
1.6.3	<i>Structural & functional domain of MR</i>	56
1.6.4	<i>MR expression</i>	60
1.6.5	<i>Mechanism of action for MR: genomic and non-genomic</i>	62
1.6.6	<i>Effects of MR regulation in the cardiovascular system</i>	65

1.6.6.1	<i>Oxidative stress</i>	66
1.6.6.2	<i>Inflammation, fibrosis and atherosclerosis</i>	68
1.6.6.3	<i>Apoptosis</i>	68
1.6.7	<i>MR regulation during MI: cardiac damage & mechanisms involved</i>	70
1.7	HYPOTHESES & AIMS	75
CHAPTER 2: GENERAL METHODS		77
2.1	ANIMALS	78
2.2	MYOCARDIAL ISCHAEMIA-REPERFUSION MODEL	78
2.2.1	<i>Induction of regional ischaemia-reperfusion</i>	79
2.2.2	<i>Collection of heart tissue</i>	80
2.3	MEASUREMENT OF INFARCT SIZE	80
2.4	MEASUREMENT OF APOPTOSIS USING <i>TUNEL</i> METHOD	82
2.5	MYOCARDIAL PROTEIN EXPRESSION	83
2.5.1	<i>Immunohistochemistry</i>	83
2.5.2	<i>Protein extraction from heart tissue</i>	84
2.5.3	<i>Western blots</i>	85
2.6	MYOCARDIAL GENE EXPRESSION	87
2.6.1	<i>Total RNA extraction from heart tissue</i>	87
2.6.2	<i>RNA quantitation and determination</i>	89
2.6.3	<i>RNA cleanup</i>	89
2.6.4	<i>First strand cDNA synthesis from RNA</i>	90
2.7	STUDIES USING H9C2 CELLS	91
2.7.1	<i>Cell culture and passage</i>	91

2.7.2	<i>Cell quantification and viability by Trypan Blue</i>	92
2.7.3	<i>Protein extraction from H9c2 cells</i>	93
2.7.4	<i>Total RNA extraction from H9c2 cells</i>	93
2.8	STATISTICAL ANALYSIS.....	94

CHAPTER 3: VALIDATION OF THE MODEL OF MYOCARDIAL ISCHAEMIA-REPERFUSION INJURY AND TIMING OF TREATMENT 95

3.1	INTRODUCTION	96
3.2	METHODS	98
3.3	RESULTS	98
3.3.1	<i>I-R induces increased infarct area</i>	98
3.3.2	<i>I-R induces increased cardiomyocyte apoptosis</i>	100
3.3.3	<i>Regulation of apoptosis during I-R</i>	103
3.3.4	<i>Regulation of autophagy during I-R</i>	106
3.3.5	<i>Mineralocorticoid receptor blockade protects against cardiac damage during myocardial I-R: timing of treatment</i>	108
3.4	DISCUSSION	110

CHAPTER 4: SEX DIFFERENCES IN CARDIAC DAMAGE DURING MYOCARDIAL INFARCTION 113

4.1	INTRODUCTION	114
4.2	METHODS	116
4.2.1	<i>Gonadectomy surgical procedures</i>	116
4.2.2	<i>Treatments</i>	117
4.2.3	<i>Ex-vivo myocardial ischaemia-reperfusion</i>	118

4.2.4	<i>Western blots</i>	118
4.2.5	<i>Statistical analysis</i>	119
4.3	RESULTS	120
4.3.1	<i>Role of sex steroids on infarct size</i>	122
4.3.2	<i>Differential regulation of AR levels during myocardial I-R</i>	124
4.3.3	<i>Regulation of autophagy by sex steroids during myocardial I-R</i>	126
4.3.4	<i>Differential regulation of RAGE by sex steroids during myocardial I-R</i> ...	128
4.3.5	<i>Sex differences in regulation of apoptosis during myocardial I-R</i>	130
4.3.6	<i>Regulation of MR levels by sex steroids during myocardial I-R</i>	133
4.4	DISCUSSION	134

**CHAPTER 5: CARDIAC EFFECTS OF MINERALOCORTICOID RECEPTOR
ACTIVATION DURING MYOCARDIAL INFARCTION..... 139**

5.1	INTRODUCTION	140
5.2	METHODS	142
5.2.1	<i>Reagents</i>	142
5.2.2	<i>Cell culture and treatment</i>	143
5.2.3	<i>Measurement of superoxide generation</i>	144
5.2.4	<i>Subcellular fractionation</i>	145
5.2.5	<i>Immunofluorescence staining</i>	146
5.2.6	<i>Western blots</i>	146
5.2.7	<i>Quantitative real time RT-PCR (qRT-PCR)</i>	147
5.2.8	<i>Ex-vivo myocardial ischaemia-reperfusion studies</i>	148
5.2.9	<i>Statistical analysis</i>	149

5.3 RESULTS	149
5.3.1 <i>MR and GPR30 expression in cardiomyocytes</i>	149
5.3.2 <i>Aldo-PEG regulates nongenomic signaling pathways similar to Ald</i>	154
5.3.3 <i>Aldo-PEG does not activate transcription of Ald-responsive genes</i>	160
5.3.4 <i>Activation of MR genomic signalling pathways mediate Ald-aggravated cardiac damage</i>	162
5.4 DISCUSSION	164
CHAPTER 6: CARDIAC EFFECTS OF BLOCKADE OF MINERALOCORTICOID RECEPTORS DURING MYOCARDIAL INFARCTION.....	169
INTRODUCTION.....	170
STATEMENT OF AUTHORSHIP CONTRIBUTION	171
MANUSCRIPT.....	174
SUPPLEMENTAL METHOD: <i>IN SITU</i> PROXIMITY LIGATION ASSAY.....	187
SUPPLEMENTAL RESULT: MR-ARC INTERACT BASED ON <i>IN SITU</i> PLA.....	188
SUPPLEMENTAL DISCUSSION	191
CHAPTER 7: OTHER ACTIONS OF BLOCKADE OF MINERALOCORTICOID RECEPTORS DURING MYOCARDIAL INFARCTION.....	192
7.1 INTRODUCTION	193
7.2 METHODS	195
7.2.1 <i>Protocol for collection of left ventricular tissue following ex-vivo myocardial I-R</i>	195

7.2.2	<i>Measurement of myocardial glutathione levels</i>	195
7.2.3	<i>Measurement of myocardial I-R triggered superoxide generation</i>	196
7.2.4	<i>Measurement of myocardial nicotinamide adenine dinucleotide (NAD⁺)</i> .	197
7.2.5	<i>Dose-response for BSO ± SPIRO in H9c2 cells</i>	197
7.2.6	<i>Measurement of glutathione and superoxide levels in H9c2 cells</i>	198
7.2.7	<i>qRT-PCR: rat heart tissue and H9c2 cells</i>	199
7.2.8	<i>Western blot: rat heart tissue and H9c2 cells</i>	200
7.2.9	<i>Statistical analysis</i>	200
7.3	RESULTS	200
7.3.1	<i>Low-dose SPIRO restores redox balance during I-R</i>	200
7.3.2	<i>Low-dose SPIRO restores PGC-1α and PGC-1β gene expression</i>	204
7.3.3	<i>Low dose SPIRO prevents the onset of the immediate early gene response in the myocardium after I-R injury</i>	206
7.3.4	<i>Low-dose SPIRO prevents I-R induced MR activation</i>	208
7.3.5	<i>BSO induced oxidant stress in H9c2 cells</i>	210
7.3.6	<i>Effects of BSO on SPIRO action in H9c2 cells</i>	213
7.3.7	<i>Low-dose SPIRO regulates MR genomic signaling</i>	218
7.4	DISCUSSION	221
	CHAPTER 8: SUMMARY AND FUTURE PERSPECTIVES	227
	APPENDICES	235
	BIBLIOGRAPHY	242

List of Figures

Figure 1.1: Mechanisms activated during myocardial ischaemia-reperfusion	6
Figure 1.2: Schematic of oxidative stress induced expression of transcription factors during myocardial ischaemia-reperfusion injury	15
Figure 1.3: Schematic illustration of four phases of autophagy	19
Figure 1.4: Regulation of autophagy during myocardial ischaemia-reperfusion	22
Figure 1.5: Extrinsic (left) and intrinsic (right) mechanisms of apoptosis and the cross talk that occurs between these pathways	24
Figure 1.6: The molecular pathway of necroptosis	35
Figure 1.7: Sex steroid hormones synthesis pathways	45
Figure 1.8: Synthesis pathway for the renin-angitensin aldosterone system.....	53
Figure 1.9: Mineralocorticoid (aldosterone) and glucocorticoid (cortisol in human and corticosterone in rodents) synthesis pathways.....	55
Figure 1.10: Structure of the MR.....	57
Figure 1.11: Genomic (right) and non-genomic (left) action of aldosterone	63
Figure 2.1: Cross-sectional of a heart slice after staining with TTC	81
Figure 3.1: Myocardial infarct size in hearts subjected to ischaemia (30 minutes) followed by reperfusion (150 minutes).....	99
Figure 3.2: Cardiomyocytes apoptosis detected after ischaemia-reperfusion by TUNEL assay.....	102
Figure 3.3: Caspase-3 is activated during ischaemia-reperfusion	104
Figure 3.4: Ischaemia-reperfusion induced decreased anti-apoptotic protein Bcl-2 ...	105
Figure 3.5: Autophagy is activated during myocardial ischaemia-reperfusion.....	107

Figure 3.6: Myocardial infarct size during treatment with 10 nM spironolactone, on reperfusion and 15 minutes before ischaemia.....	109
Figure 4.1: Sex differences in left ventricular infarct size and apoptosis.....	121
Figure 4.2: Effect of gonadectomy and steroid treatment on left ventricular infarct size in males and females.....	123
Figure 4.3: Regulation of left ventricular sex steroid receptor expression.....	125
Figure 4.4: Effects of sex steroids on autophagy markers.....	127
Figure 4.5: Effects of sex steroids on RAGE expression	129
Figure 4.6: Effect of sex steroids on caspase-3 and -9 processing during myocardial ischaemia-reperfusion.....	131
Figure 4.7: Effects of sex steroids on anti-apoptotic regulators of the intrinsic pathway of apoptosis.....	132
Figure 4.8: Effects of sex steroids on MR protein expression during I-R.....	133
Figure 4.9: Schematic summary of pathways activated during myocardial I-R injury in male and female myocardium.....	138
Figure 5.1: Structure of Aldosterone-3-carboxymethoxylamine-PEG-amine (M.W. 40,000) compared to aldosterone (M.W. 360.44).....	149
Figure 5.2: Expression and localisation of MR and GPR30 in H9c2 cells.....	151
Figure 5.3: Expression and localisation of MR and GPR30 in rat heart	153
Figure 5.4: Aldo, Aldo-PEG and G1 mediated ERK1/2 phosphorylation	155
Figure 5.5: Effects of G36 on G1 mediated ERK1/2 phosphorylation.....	156
Figure 5.6: Effects of antagonists on Ald, Aldo-PEG and G1 mediated ERK1/2 phosphorylation	158
Figure 5.7: Aldosterone and Aldo-PEG mediated superoxide generation	159

Figure 5.8: MR activation by Ald but not Aldo-PEG regulates Sgk-1 and PAI-1 gene expression	161
Figure 5.9: Aldo-PEG induces superoxide production but maintains apoptosis and infarct size by preventing MR activation.....	163
Figure 6.1: Interaction of MR-ARC by <i>in situ</i> PLA during myocardial I-R.....	190
Figure 7.1: Low-dose SPIRO restores redox balance.....	202
Figure 7.2: Low-dose SPIRO did not modify G6PD gene expression	203
Figure 7.3: Low-dose SPIRO restores PGC-1 α and PGC-1 β gene expression	205
Figure 7.4: Low-dose SPIRO reduces heat shock proteins and immediate early genes and proteins expression.....	207
Figure 7.5: Low-dose SPIRO suppresses transcription of MR-responsive genes during I-R	209
Figure 7.6: Effects of BSO \pm SPIRO (10 nM) exposure on reduced glutathione (GSH) levels in H9c2 cells	211
Figure 7.7: Low-dose SPIRO prevents BSO-induced superoxide generation in H9c2 cells	212
Figure 7.8: BSO-induced various genes expression in H9c2 cells.....	215
Figure 7.9: Low-dose SPIRO reduces BSO-induced various genes expression in H9c2 cells	216
Figure 7.10: Low-dose SPIRO reduces BSO-induced stress responsive protein expression in H9c2 cells	217
Figure 7.11: Low-dose SPIRO regulates MR genomic signaling	219
Figure 7.12: Low-dose SPIRO reduces infarct size and persists in the presence of actinomycin D.....	220

List of Tables

Table 1.1: Animal studies examining effects of MR antagonists on cardiac damage and mechanisms involved during <i>ex-vivo</i> and <i>in situ</i> experimental myocardial ischaemia-reperfusion	72
Table 1.2: Animal studies examining effects of MR antagonists on cardiac damage and mechanisms involved during <i>in vivo</i> experimental myocardial infarction (MI)	73
Table 1.3: Clinical MR blockade trials in MI and HF	74
Table 4.1: Body weights of male and female rats in the various treatment groups	120
Table 5.1: Preparation of the qRT-PCR reaction cocktail	148
Table A1: Details of primary antibodies and concentrations used in western blots (WB) and immunohistochemistry (IHC)	239
Table A2: Formulation for SDS - separating and stacking gels	241

Abbreviations

11 β -HSD2	11beta-hydroxysteroid dehydrogenase
Ald	Aldosterone
Aldo-PEG	Aldosterone-3-carboxymethoxylamine-PEG amine
AAR	Area-at-risk
Acinus	Apoptotic chromatin condensation inducer in the nucleus
Akt	known as protein kinase B (PKB)
AMI	Acute myocardial infarction
AMPK	AMP-activated protein kinase
ANOVA	Analysis of variance
AR	Androgen receptor
ARC	Apoptosis Repressor with Caspase recruitment domain
Atg	Autophagy-related gene
ATP	Adenosine 5'- triphosphates
Bcl-2	B-cell lymphoma-2
Bcl-xL	B-cell lymphoma-extra large
BSA	Bovine serum albumin
BSO	Buthionine sulfoximine
CAD	Coronary artery disease
CARD	Caspase recruitment domain
Caspase	Cysteine-dependent aspartate-directed proteases
cDNA	Complementary deoxyribonucleic acid
CHD	Coronary heart disease
CVD	Cardiovascular disease

CyD	Cyclophilin D
DBD	DNA binding domain
DD	Death domain
DEPC	Diethylpyrocarbonate
DFF	DNA fragmentation factor
DHT	5-dihydrotestosterone
DISC	Death-inducing signalling complex
DMEM	Dulbecco's modified Eagle's medium
DOPS	Danish Osteoporosis Prevention Study
E2	17 β -estradiol
ECs	Endothelial cells
EGFR	Epidermal growth factor receptor
EMPHASIS-HF	Eplerenone in Mild Patients Hospitalization And Survival Study in Heart Failure
EPHESUS	EPlerenone HEart failure and SURvival Study
EPL	Eplerenone
E2-R	Oestrogen receptor
ERK	Extracellular signal-regulated kinases
ETC	Electron transport chain
FADD	Fas-associated protein with death domain
G6PD	Glucose-6-phosphate dehydrogenase
Gapdh	Glyceraldehyde-3-phosphate dehydrogenase
GPR30	G protein-coupled receptor 30 (also known as GPER1)
GR	Glucocorticoid receptor

GSH	Reduced glutathione
GSSG	Oxidised glutathione
Gusb	Glucuronidase beta
HERS	Heart and Estrogen/progestin Replacement Study
HF	Heart failure
HRT	Hormone replacement therapy
Hsp	Heat shock protein
IA	Infarct area
ICAD	Inhibitor of caspase-3-activated DNase
IHD	Ischaemic heart disease
IKK	I kappa B kinase
I-R	Ischaemia-reperfusion
LAD	Left anterior descending
LAMP	Lysosome-associated membrane protein
LBD	Ligand binding domain
LC3	Microtubule-associated protein light chain 3
LV	Left ventricle
MAPK	Mitogen-activated protein kinase
MI	Myocardial infarction
mPTP	Mitochondrial permeability transition pore
MR	Mineralocorticoid receptor
mRNA	Messenger RNA
mTOR	Mammalian target of rapamycin
NAD	Nicotinamide adenine dinucleotide

NADPH	Nicotamide adenine dinucleotide phosphate
NEMO	NF-κB essential modulator
NO	Nitric oxide
NoI3	Nucleolar protein 3 (apoptosis repressor with CARD domain)
NOS	Nitric oxide synthase
NOX	NADPH oxidase
NTD	N-terminal domain
O ₂ ^{•-}	Superoxide
PBS	Phosphate-buffered saline
PAI-1	Plasminogen activator inhibitor type 1
PCI	Percutaneous coronary intervention
PGC-1	Peroxisome proliferator-activated receptor-γ coactivator 1
PI3K	Phosphoinositide 3-kinase
PR	Progesterone receptor
qRT-PCR	Quantitative real-time RT- PCR
RAGE	Receptor for advanced glycation end products
RALES	Randomized ALdosterone Evaluation Study
RAAS	Renin-angiotensin-aldosterone system
RIP	Receptor interacting protein
RIPA	Radioimmunoprecipitation assay buffer
ROS	Reactive oxygen species
RT-PCR	Reverse transcription polymerase chain reaction
SD	Sprague Dawley
SDS-PAGE	Sodium dodecyl sulfate-polyacrylamide gel electrophoresis

SE	Standard error
Sgk-1	Serum/glucocorticoid regulated kinase 1
SPIRO	Spironolactone
STEMI	ST-segment elevation myocardial infarction
SOD	Superoxide dismutase
VSMCs	Vascular smooth muscle cells
WHI	Women's Health Initiative
T	Testosterone
TBS	Tris-buffered saline
TBS/T	Tris-buffered saline + Tween-20
TNF	Tumor necrosis factor
TRADD	TNF receptor-associated death domain
TRAF	TNF receptor-associated factor
TUNEL	Terminal deoxynucleotide transferase-mediated dUTP nick end labeling
XIAP	X-linked inhibitor of apoptosis protein

Chapter 1

Literature review

1.1 Overview of ischaemic heart disease

Ischaemic heart disease [IHD; also known as coronary heart disease (CHD)] is the leading cause of morbidity and mortality worldwide (Mathers and Loncar, 2006). According to a World Health Organisation report, IHD accounts for approximately 7.25 million (representing 12.8 %) of all deaths (WHO, 2011). In Australia, IHD accounted for 22,729 (17%) of all deaths and is responsible for approximately 49% of cardiovascular deaths in 2007 (AIHW, 2011). The current best practice for treatment of patients with IHD is to re-establish blood flow using primary percutaneous coronary intervention (PCI) (Bhatt, 2013), antiplatelet therapy (Boden et al., 2013; Lippi et al., 2013), coronary artery bypass graft surgery (Doggrell, 2013; O'Gara et al., 2013; Sa et al., 2013) and recently stem cell-based therapy (Assmus et al., 2010; Bozdog-Turan et al., 2012; Dill et al., 2009; Surder et al., 2010; Turan et al., 2011). These treatments allow the restoration of coronary artery blood flow to the myocardium and improve cardiac function in patients with IHD. Despite improvements over the last few decades, IHD still remains one of leading global burdens of disease (Forouzanfar et al., 2012).

There are a large number of risk factors that may contribute to an even greater medical and social burden of IHD in the future. These risk factors include diabetes, hypertension (Juarez-Herrera and Jerjes-Sanchez, 2013), coronary artery calcification (Budoff et al., 2013), smoking, hypercholesterolemia, hyperlipidemia, obesity and physical inactivity (Migliaresi et al., 2007; Ram and Trivedi, 2012). Several public health initiatives and implementation of new reperfusion strategies and therapeutics have been effective in improving the quality of life for patients with IHD and reducing associated mortality

(Borden et al., 2012; Bradley et al., 2012; Darling et al., 2013; Heitzler et al., 2012; Isik et al., 2012; Morel et al., 2012; Niles et al., 2010; Purim-Shem-Tov et al., 2012).

1.2 Definition of myocardial ischaemia-reperfusion injury

Myocardial ischaemic injury occurs when blood supply to the heart muscle is interrupted, generally due to occlusion or blockade of coronary arteries, resulting in reduced levels of oxygen and nutrients. This leads to cardiac muscle damage and cardiomyocyte death, known as myocardial infarction (MI). Acute myocardial infarction (AMI) can be the first indication of IHD (Manfroi et al., 2002; Shirani et al., 1994; Zucker et al., 1997). Rapid restoration of blood flow (reperfusion) is needed for myocardial salvage, and improves survival after myocardial ischaemia (Braunwald, 1989; Miura et al., 2002; Ndrepepa et al., 2010). However, the reperfusion of ischaemic tissue itself is deleterious and can exacerbate damage (Hausenloy and Yellon, 2013; Yellon and Hausenloy, 2007). This damage is referred to as “ischaemia-reperfusion injury” or “reperfusion-induced injury”. Ischaemia-reperfusion (I-R) injury can trigger contractile dysfunction and cardiac stunning (Miura et al., 1991), arrhythmias (Tan et al., 1998), oxidative stress (Inafuku et al., 2012; Robin et al., 2007), endothelial dysfunction and cell death (Gottlieb, 2011; Scarabelli et al., 2002).

1.3 Mechanisms of myocardial I-R injury

The pathogenic mechanisms contributing to myocardial I-R injury are complex and induced by both ischaemia and reperfusion and summarised in Figure 1.1. During ischaemia, the O₂ supply is reduced, which arrests mitochondrial oxidative phosphorylation and thus depletes ATP (Kahles et al., 1979; Reimer et al., 1983). As a

result, anaerobic metabolism takes over providing an avenue for continued ATP production (Jennings and Reimer, 1991), but producing intracellular acidosis through accumulation of lactate, protons, and NAD^+ . To normalise this accumulation of H^+ ions, the Na^+/H^+ exchanger eliminates excess H^+ ions, producing in turn a large influx of Na^+ ions (Murphy and Steenbergen, 2008). The Na^+ ions are, in turn, exchanged for Ca^{2+} by the $\text{Na}^+/\text{Ca}^{2+}$ exchanger (Chen and Li, 2012). Reduction of ATP during ischaemia also inactivates Na^+/K^+ ATPase, reduces active Ca^{2+} efflux, and limits the reuptake of Ca^{2+} by the endoplasmic reticulum (ER), thereby resulting in Ca^{2+} overload in the cell (Shintani-Ishida et al., 2012). Furthermore, in ischaemia, increased Ca^{2+} levels induce opening of the mitochondrial permeability transition pores (mPTP) leading to mitochondrial swelling and ultimately to cardiomyocyte necrosis (Abdallah et al., 2011; Assaly et al., 2012; Gorenkova et al., 2013; Ruiz-Meana et al., 2007). Activation of mPTP alters mitochondrial membrane potential and induces production of reactive oxygen species (ROS); finally the influx of water causes swelling and rupture of the mitochondria (Abdallah et al., 2011). In the heart, these cellular changes activate number of molecules including proteases, phospholipase, ATPases and endonucleases which damage myofibrils and produce hypercontracture and contracture band necrosis (Ruiz-Meana et al., 2007).

Although timely reperfusion restores the supply of oxygen and nutrients required for aerobic ATP generation and pH normalisation, reperfusion itself leads to further cardiac damage (Yellon and Hausenloy, 2007). At the onset of reperfusion, massive increases in mitochondrial Ca^{2+} , oxidative stress and pH normalisation induce opening of the mPTP (Abdallah et al., 2011; Assaly et al., 2012; Saotome et al., 2009). The restoration

of blood flow also triggers an inflammatory process (Kawaguchi et al., 2011; Takahashi, 2011). Different factors, such as generation of ROS, secretion of chemokines and cytokines, as well as expression of adhesion molecules on the endothelial cell surface promote neutrophil recruitment (Albertine et al., 1994; Chandrasekar et al., 2001). In turn, infiltrated neutrophils secrete inflammatory molecules and ROS to contribute to tissue damage (Kaminski et al., 2002). Furthermore, cytoplasmic Ca^{2+} overload in the reperfused myocardium is in part due to the metabolic disturbance during the ischaemic episode, but is also aggravated at the onset of reperfusion by ROS-induced sarcoplasmic reticulum dysfunction and by $\text{Na}^+/\text{Ca}^{2+}$ exchange (Peters and Piper, 2007; Wei et al., 2007). Transient peaks of Ca^{2+} cause uncontrolled contractile activation of the myofibrils, resulting in hypercontracture (Ruiz-Meana et al., 2007).

Overall, I-R injury is associated with endothelial dysfunction (Qi et al., 1998), complement activation (Yasojima et al., 1998), an inflammatory response (Kawaguchi et al., 2011), pH change, Ca^{2+} overload, opening of the mPTP and generation of ROS (Shintani-Ishida et al., 2012) (Figure 1.1). Such damage promotes activation of autophagy (Dong et al., 2010; Ma et al., 2012b) and cell death pathways including apoptosis, necroptosis and necrosis (Gottlieb et al., 1994; McCully et al., 2004; Smith and Yellon, 2011), which all contribute to myocardial damage and decreased cardiac performance. Thus, understanding the mechanisms involved prepares the way for development of novel therapeutic opportunities that not only reduce the extent of injury induced by I-R but may also extend the time a tissue could be subjected to ischaemia before irreversible injury occurs.

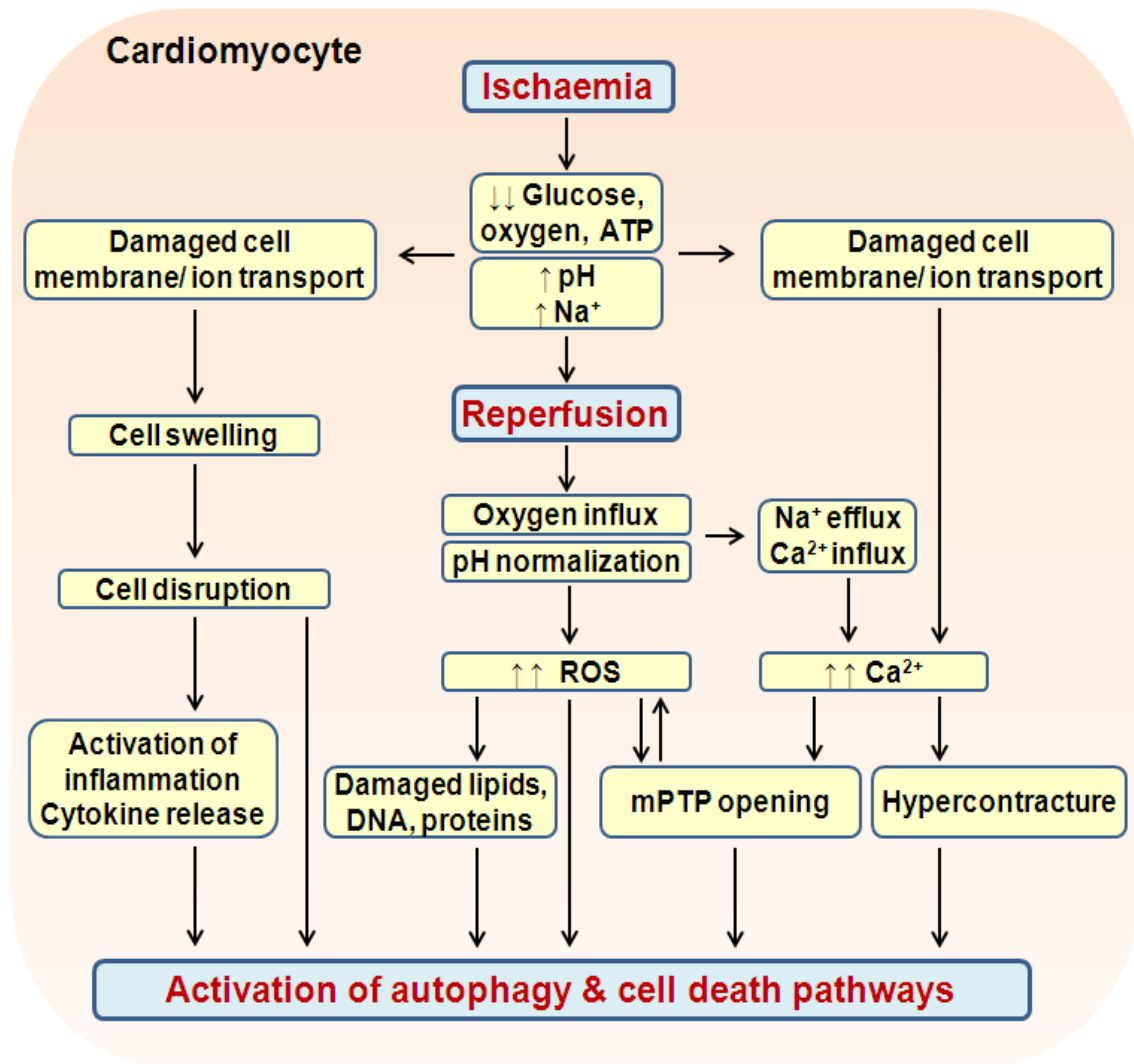


Figure 1.1: Mechanisms activated during myocardial ischaemia-reperfusion.

Reperfused ischaemic myocardium undergoes several biochemical and metabolic changes, which include intracellular Ca^{2+} overload, ROS generation, inflammation, and rapid change of pH. All these changes interact with each other and ultimately lead to mPTP opening and induction of hypercontracture, activation of autophagy and cell death pathways (apoptosis, necrosis and necroptosis). ROS, reactive oxygen species; mPTP, mitochondrial permeability transition pore; ATP, adenosine triphosphate. (Modified from Kalogeris et al., 2012).

1.3.1 Cellular redox regulatory mechanisms during myocardial I-R

The redox system plays an important role in maintaining cellular homeostasis. Under physiologic conditions, cells maintain redox balance through generation and elimination of reactive oxygen/nitrogen species (ROS/RNS), for maintaining cell function and survival. However, the redox homeostasis is disturbed during I-R injury which increases intracellular ROS/RNS levels. Oxidative stress is caused by an imbalance between the oxidant and antioxidant systems of the body in favour of the oxidants. ROS or free radical production during myocardial I-R is harmful to cells (Sies and Cadenas, 1985) and exceeds the capacity of antioxidant defences, triggering cellular dysfunction and eventually cell death (Loor et al., 2011; Robin et al., 2007). Moreover, there is evidence that oxidative stress occurs in patients with coronary artery disease (CAD) during surgical reperfusion, associated with transient LV dysfunction or stunning (Curello et al., 1995; Ferrari et al., 1990). Thus regulation of ROS levels is critical in maintaining cellular homeostasis.

1.3.1.1 Generation of reactive oxygen species

In the heart, ROS can be generated from different cell types including cardiomyocytes, endothelial cells (ECs), vascular smooth muscle cells (VSMCs), fibroblasts and infiltrating inflammatory cells and include superoxide anion radical (dioxide, or $O_2^{\cdot-}$), the hydroxyl radical ($\cdot OH$), the peroxynitrite anion ($ONOO^-$) and hydrogen peroxide (H_2O_2) (Halliwell and Cross, 1994). During an ischaemic event the presence of residual oxygen, Ca^{2+} overload and opening of the mPTP are associated with ROS generation (Feissner et al., 2009; Vanden Hoek et al., 1997a). ROS alter the functional activity of the sarcolemmal Ca^{2+} pump ATPase, decreasing efflux and increasing influx of Ca^{2+} ,

and finally to cytosolic Ca^{2+} overload and cell death (Dixon et al., 1990; Matsubara and Dhalla, 1996). Moreover, increased mitochondria Ca^{2+} induces mPTP opening, ROS production and organelle disruption (Braunersreuther and Jaquet, 2012).

Reperfusion restores the supply of oxygen and nutrients that are required for salvage of myocardium. However, ROS generation occurs very rapidly (within minutes) in post-ischaemic heart tissue, as examined by electron paramagnetic resonance spectroscopy and chemiluminescent techniques (Ambrosio et al., 1991a; Ambrosio et al., 1991b; Henry et al., 1990; Zweier et al., 1989). Similarly, reperfusion augments release of ROS within the myocardium (Angelos et al., 2006; Ferrari et al., 1990; Ytrehus et al., 1986; Zweier et al., 1987; Zweier et al., 1989). Elevated ROS generation induces severe damage to lipids, proteins, deoxyribonucleic acid (DNA) and consequently apoptosis (Becker, 2004; Yellon and Hausenloy, 2007; Zhao et al., 2004). Further changes occur in the mitochondria, such as swelling, membrane instability and cytochrome c release from the intra-membrane space, contributes to mitochondrial membrane depolarisation and signals cell death (Halestrap et al., 2004). Several mechanisms are responsible for the generation of ROS in the reperfused myocardium. These include mitochondrial electron transport chain (ETC), xanthine oxidases, NADPH oxidases (NOX), uncoupled nitric oxide synthases (NOS), cytochrome P450 or from inflammation cells (Braunersreuther and Jaquet, 2012; Raedschelders et al., 2012; Zweier and Talukder, 2006). Of these, the mitochondrial electron transport chain and NADPH oxidases are important sources of ROS generation in cardiomyocytes.

Mitochondrial Electron Transport Chain

Reduction of molecular O₂ by the mitochondrial electron transport chain (ETC) is essential for generating most of the biological energy (Cortassa et al., 2009). However, electron transfer, and therefore mitochondrial ETC, is impaired during I-R when mitochondria are damaged. This results in an electron being gained by molecular O₂, yielding superoxide (O₂^{•-}) (Chen et al., 2008). In myocytes, these reactions occur at complexes I (NADH-ubiquinone oxidoreductase) (Ide et al., 1999; Paradies et al., 2004; Passarelli et al., 2010; Sgobbo et al., 2007) and complex III (ubiquinol-cytochrome c oxidoreductase) (Chen et al., 2003b; Petrosillo et al., 2003) of the mitochondrial ETC. Recent studies have provided evidence that mitochondrial complex II (succinate-ubiquinone oxidoreductase) mediated ROS production also plays an important role in heart failure (HF) and reperfused myocardium (Drose et al., 2011; Moreno-Sanchez et al., 2013; Mourmoura et al., 2011; Redout et al., 2007). During I-R injury both oxidative stress and ROS formation from mitochondrial ETC have been reported by using specific inhibitors of the mitochondrial ETC with cyanide, antimycin, and rotenone, generating sufficient ROS to disturb contractile function and induce cardiomyocyte death (Chen et al., 2006; Lee et al., 2012; Vanden Hoek et al., 1997b). In addition, I-R injury causes decreased endogenous mitochondrial antioxidant capacity which leads to an imbalance between production versus scavenging and thus increases mitochondrial ROS generation (Stowe and Camara, 2009). Furthermore, activation of mPTP causes equilibration of H⁺ across the inner membrane and dissipates the proton electrochemical gradient ($\Delta\Psi_m$), leading to ATP depletion, further ROS generation and ultimately swelling and rupture of the mitochondria (Baines, 2010; Weiss et al., 2003).

NADPH Oxidase

Five NADPH oxidase (NOX) isoforms have been identified (NOX1 – NOX5), each encoded by a separate gene and with distinct tissue distributions (Bedard and Krause, 2007; Lambeth, 2004). The enzymatic activity of NOX depends on additional small protein subunits, which vary according to isoform. NOX1 & NOX4 associate with p22^{phox} subunits. NOX2 (also known as p91^{phox}) associates with p47^{phox}, p67^{phox}, p40^{phox} and Rac1 or Rac2, while NOX1 associates with Rac1, NOXO1 and NOXA1 (homologues of p47^{phox} and p67^{phox} respectively). NOX enzymes work as an electron transfer chain carrying electrons through the cell membrane to reduce extracellular O₂ into O₂^{•-} and using NADPH as an electron donor (Leto et al., 2009). NOX isoforms are expressed in multiple cell types including VSMCs (NOX1, NOX2, NOX4) (Hilenski et al., 2004; Lassegue et al., 2001; Touyz et al., 2002), ECs (NOX2, NOX4, NOX5) (Ago et al., 2004; BelAiba et al., 2007; Gorlach et al., 2000; Jay et al., 2008; Li and Shah, 2002), adventitial cells and fibroblasts (NOX2, NOX4) (Cucoranu et al., 2005; Pagano et al., 1997), and cardiomyocytes (NOX2, NOX4) (Bendall et al., 2002; Byrne et al., 2003; Hingtgen et al., 2006; Li et al., 2006; Xiao et al., 2002). NOX3 is not expressed in cardiovascular cells.

The involvement of NADPH oxidases in post-MI remodelling has been demonstrated in both experimental (Fukui et al., 2001) and clinical (Krijnen et al., 2003) studies, with elevated myocardial levels of NOX2 and p22^{phox} after MI. More recent studies have shown that Nox2^{-/-} or p47^{phox} deficient mice subjected to experimental MI have reduced myocyte apoptosis, preventing left ventricular (LV) remodelling and dysfunction and improving overall survival compared with wild type controls (Doerries et al., 2007;

Looi et al., 2008). Moreover, inhibition of NADPH oxidase with apocynin showed decreased oxidative stress and myocyte apoptosis, and improvement of cardiac function in heart failure (HF) after MI in rabbits (Qin et al., 2007).

Recent evidence shows that NADPH oxidase and the Rac1 pathway mediate ROS production and myocardial contractile dysfunction following acute I-R (Shan et al., 2010; Talukder et al., 2013). Increased expression of Rac1 and/or NADPH oxidases has been reported in animals and humans with MI, HF, diabetes, oxidant stress or inflammation (Dwivedi et al., 2010; Fukui et al., 2001; Krijnen et al., 2003; Maack et al., 2003; Nagase et al., 2012; Talukder et al., 2013). Disruption of Rac1 signalling reduces prolonged myocardial ischaemia-induced Rac1 activity and I-R injury in mice (Shan et al., 2010). Taken together, these studies highlight a crucial role of NADPH oxidases and Rac1 in acute myocardial I-R injury. In summary, ROS may exert multiple actions with all the sources playing some role in ROS mediated damage in I-R injury; although exact contribution of each source remains unclear. The precise role of each of these ROS generators in the pathology of experimental I-R injury is not clear since a particular source may depend upon the experimental protocol used to produce I-R injury.

1.3.1.2 Antioxidant defences systems

During I-R, antioxidant defences (such as glucose-6-phosphate dehydrogenase (G6PD), superoxide dismutase (SOD), reduced glutathione and protein SH groups) are decreased whereas ROS generating enzymes (such as oxidized glutathione, NADPH oxidase) are increased (Ferrari et al., 1985; Krijnen et al., 2003; Usal et al., 1996).

G6PD is a critical cytosolic antioxidant enzyme in adult cardiomyocytes (Jain et al., 2003) and functions as the first and rate-limiting enzyme in the pentose phosphate pathway responsible for generation of NADPH in a reaction coupled to the oxidation of glucose-6-phosphate (Frederiks et al., 2007; Gupte et al., 2006). Decreased G6PD activity lowers NADPH levels and promotes oxidative stress damage (Hecker et al., 2013b; Jain et al., 2003; Leopold et al., 2001; Leopold et al., 2003). G6PD activity is increased in response to a number of stress-induced stimuli, infarcted myocardium and failing hearts (Bing et al., 1969; Gupte et al., 2007; Gupte et al., 2006; Stanton et al., 1991). Studies with G6PD-deficient mice provide evidence for both protective and deleterious effects (Hecker et al., 2013a). G6PD deficiency may provide a protective effect through decreasing cholesterol synthesis and $O_2^{\cdot-}$ production (Matsui et al., 2006), and thus reduce the risk of CHD and cardiovascular associated death observed in humans (Cocco et al., 1998; Meloni et al., 2008). However, recent studies indicate that G6PD-deficient mice are more susceptible to ventricular dilation and greater myocardial oxidative stress in response to MI or pressure overload-induced HF (Hecker et al., 2013b). Moreover, mice with G6PD-deficiency displayed increased cardiac dysfunction during myocardial I-R, associated with depletion of intracellular glutathione and increased oxidative stress (Jain et al., 2004).

The glutathione redox cycle is a major antioxidant defense mechanism against ROS. This redox cycle detoxifies ROS by reaction with reduced glutathione (GSH). GSH is a radical scavenger that directly neutralizes a variety of reactive molecules, such as carbon-centered radicals, superoxide anion and hydroxyl radicals (Dickinson and Forman, 2002; Wu et al., 2004). GSH provides the reducing equivalents necessary for

the conversion of hydrogen peroxide and lipid peroxides to water and lipid alcohols, respectively, thereby preventing degradation to highly toxic free radicals, including hydroxyl and peroxy radicals. GSH is also an essential cofactor for inactivation of hydroperoxides by glutathione peroxidase, for the conjugation of cytotoxic by-products of lipid peroxidation by glutathione-S-transferase, and for the reduction of protein mixed disulfides (Bindoli et al., 2008; Fernandes and Holmgren, 2004; Mieczal et al., 2008; Wu et al., 2004). GSH also has an important role in protecting against oxidation of protein sulfhydryl groups (Thomas et al., 1995). During oxidative stress, reduced GSH is oxidized to glutathione disulfide (GSSG). The majority of GSSG is reduced back to GSH by glutathione reductase and NADPH, an essential cofactor for regeneration of GSH from GSSG (Schafer and Buettner, 2001).

The cellular ratio of GSH-to-GSSG under physiological conditions highly favours reduced GSH and is decreased during oxidative stress. Thus the levels of GSH, GSSG and ratio of GSH-to-GSSG are considered to be sensitive indices of cellular oxidative stress (Ho et al., 2008; Verbunt et al., 1995). In isolated rat hearts, myocardial content of GSSG is increased during post-ischaemic reperfusion (Verbunt et al., 1995), but not during reoxygenation of hypoxic hearts (Darley-Usmar et al., 1989; Park et al., 1991) when compared to control levels. Recent studies have shown GSH depletion and increased content of GSSG in patients with AMI, indicating these patients experience increased oxidative stress (Ho et al., 2008; Usal et al., 1996). Depletion of cardiac GSH exacerbates myocardial I-R injury (Leichtweis and Ji, 2001; Singh et al., 1989; Werns et al., 1992), whereas exogenous supplementation with GSH protects against such injury (Ferrari et al., 1991; Gao et al., 2002; Singh et al., 1989).

Pyridine nucleotides include reduced and oxidized nicotinamide adenine dinucleotide (NADH/NAP⁺) and NADH/NAP⁺ phosphate (NADPH/NADP⁺) and are critical molecules in energy metabolism, ATP production, Ca²⁺ homeostasis, anti-oxidation and reductive biosynthesis (Belenky et al., 2007; Berger et al., 2004; Pollak et al., 2007). NADPH/NADP⁺ also participate in antioxidant defense in the control of cellular oxidative stress and GSH/GSSG redox balance (Ceconi et al., 2000). NAD⁺ and NADH have been used to characterize mitochondrial energy states in isolated hearts and myocardial tissue (Di Lisa et al., 2001; Nuutinen, 1984; Stoner et al., 2004). Adult rat cardiomyocytes subjected to simulated ischaemia produced substantial reduction in NAD⁺-to-NADH and associated energy-dependent processes including contraction and maintenance of ATP (Esumi et al., 1991). NAD⁺ plays an essential role in mediating cell survival by inhibiting apoptosis in response to I-R injury (Hsu et al., 2009; Sukoyan et al., 2005). Furthermore, the cellular content of NAD⁺ has been shown to be regulated by multiple mechanisms including nicotinamide phosphoribosyltransferase (Nampt) (Revollo et al., 2007). Expression of Nampt in the heart is significantly decreased by ischaemia, I-R and pressure overload, leading to significantly decreased NAD⁺ and ATP concentrations (Hsu et al., 2009).

1.3.2 Redox-mediated mechanisms in regulation of cellular processes: role of gene transcription

Redox balance is critical in maintaining cellular homeostasis. Disruption of this balance by increased oxidative stress will alter cellular function. In response to oxidative stress, cells react by activating expression of several stress-related genes. As shown in Figure 1.2, this could lead to the synthesis of proteins involved in cellular protection or repair

of injury. These stress induced gene products can be distinguished by their specific protein structures, functional properties, and their inducing stimuli. Among stress genes, the most common and well known are those coding for heat shock proteins (Hsp) (Subjeck and Shyy, 1986), proto-oncogenes (immediate early genes) and genes for antioxidants (Das et al., 1995).

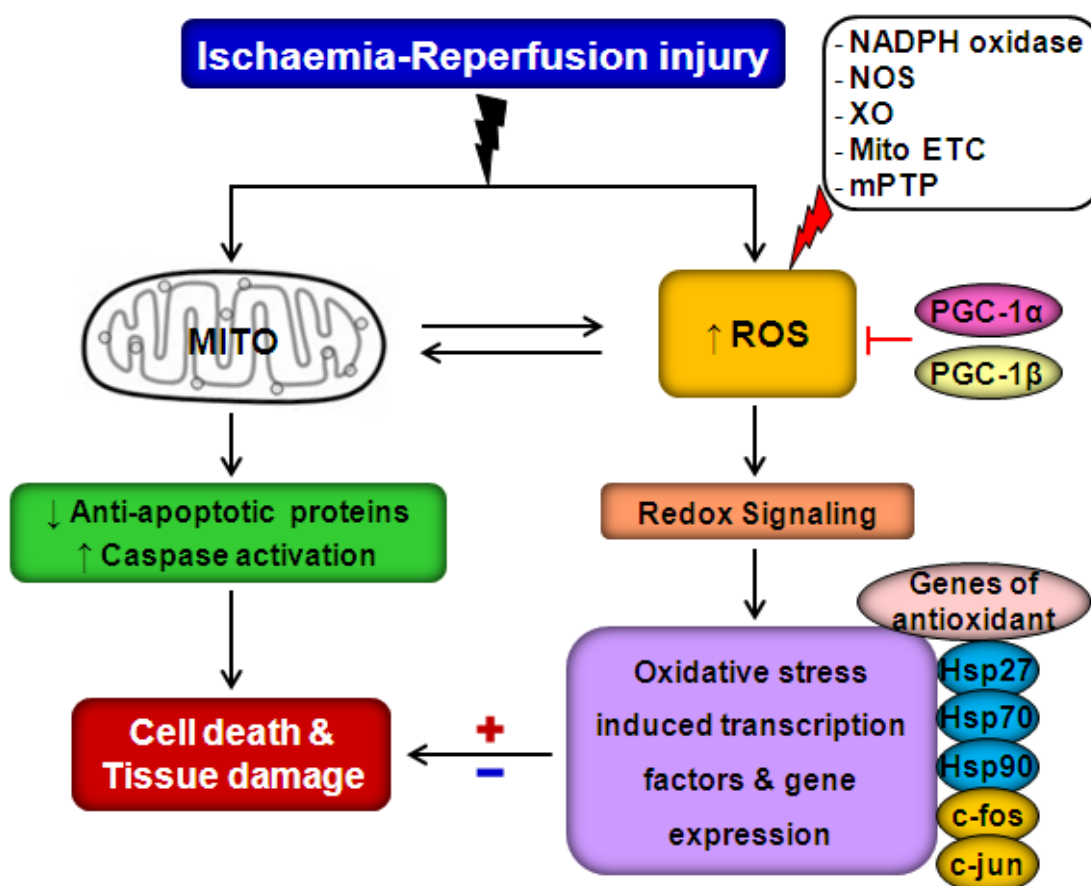


Figure 1.2: Schematic of oxidative stress induced expression of transcription factors during myocardial ischaemia-reperfusion injury.

ROS, reactive oxygen species; Hsp, heat shock protein; PGC, peroxisome proliferator activated receptor-gamma coactivator; MITO, mitochondrial; +, stimulation; -, inhibition. (Modified from Das et al., 1995).

Oxidative stress induced by reperfusion injury leads to the expression of heat shock and immediate early genes. After 20-30 minutes of reperfusion, accumulation of mRNA for *hsp90*, *hsp72* and *hsp70* was detectable in ischaemic myocardium (Nishizawa et al., 1999; Plumier et al., 1996; Schoeniger et al., 1994). Similarly, oxidative stress was shown to induce the expression of Hsp27 (Das et al., 1998; Maulik et al., 1993). I-R injury also induces the expression of a number of immediate early genes - immediately following coronary artery occlusion, mRNAs for *c-fos*, *Egr-1*, *c-jun* and *jun-B* accumulate in the ischaemic region as well as during the reperfusion period (Brand et al., 1992; Xu et al., 2008).

Peroxisome proliferator activated receptor-gamma coactivator (PGC)-1 α and PGC-1 β are two key molecules which play important roles in oxidative metabolism, mitochondrial biogenesis, as well as ROS generation (Garnier et al., 2003; Huss and Kelly, 2005). Both PGC-1 α and -1 β regulate mitochondrial biogenesis and genes encoding enzymes of mitochondrial metabolism and proteins that compose the electron transport chain (Fan et al., 2004; Lin et al., 2003; Meirhaeghe et al., 2003; St-Pierre et al., 2003). The expression of PGC-1 α mRNA was suppressed following acute MI (Sun et al., 2007), congestive heart failure (CHF) (Garnier et al., 2003), and pressure overload (Huss and Kelly, 2004; Lehman and Kelly, 2002). Conversely, pioglitazone, a PGC agonist, attenuated LV remodelling and HF after experimental MI (Shiomi et al., 2002), while PGC-1 β deficient mice exhibited greater degrees of oxidative stress and lower rates of glucose metabolism following pressure overload hypertrophy (Riehle et al., 2011). Dysfunctional mitochondria in I-R injury are either cleared through

autophagy or persist to initiate apoptosis through the intrinsic pathway culminating in myocyte death.

1.3.3 Autophagy

Autophagy is the process for disposal of damaged organelles and non-specific or superfluous cytosolic proteins, thereby participating in homeostatic functions in cells (Dong et al., 2010). It also provides cells with a survival mechanism in response to stressful conditions, such as starvation (nutrient depletion), hypoxia and I-R by generating amino acids and fatty acids for maintenance of cell function (Gurusamy and Das, 2009; Gurusamy et al., 2009; Hamacher-Brady et al., 2006b). However, uncontrolled autophagy may ultimately lead to cell death and aggravate I-R injury (Dong et al., 2010; Ma et al., 2012b).

1.3.3.1 Molecular mechanisms involved in autophagy

Autophagy is tightly regulated and mediated by specific pathways (Figure 1.3). The process of autophagy consists of four main phases. Autophagy is initiated by activation of class III PI3K-associated Beclin-1 and inhibited by class I PI3Ks through mammalian target of rapamycin (mTOR). Beclin-1 bound to anti-apoptotic proteins Bcl-2 or Bcl-xL also inhibits autophagy (Cheng et al., 2013; Hamacher-Brady et al., 2006a; Maiuri et al., 2007; Oberstein et al., 2007). During starvation or stress, mTOR is inactivated and initiates formation of a phagophore, which is further facilitated by another complex consisting of a class III PI3K associated Beclin-1 (Gottlieb and Mentzer, 2010; He and Klionsky, 2009; Levine and Kroemer, 2008). This complex, in turn, recruits autophagy-related genes (Atg): Atg12, Atg5, and Atg8 (also called LC3), which are essential for

the elongation of the membrane and completion of the autophagosome (Figure 1.3). p62, a major selective substrate for autophagic degradation, is recruited to the autophagosomal membrane through interaction with ubiquitinated substrates and LC3, and is degraded during the autophagic process (Bjorkoy et al., 2005; Ichimura et al., 2008; Pankiv et al., 2007). Atg12-Atg5-Atg16 complex is required for recruitment of LC3-II. After autophagosome formation, the remaining membrane-attached LC3-II-phosphatidylethanol-amine (LC3-II-PE) then fuses with lysosomal protease to create an autophagolysosome. The fusion of the autophagosome to the lysosome is mediated by the small GTPase Rab7 and the lysosomal-associated membrane protein 2 (LAMP2) (Gottlieb and Mentzer, 2010; He and Klionsky, 2009; Levine and Kroemer, 2008; Ma et al., 2012b). The contents within this complex are degraded by lysosomal hydrolases and in the process can produce ATP (Gurusamy and Das, 2009; Gurusamy et al., 2009; Hamacher-Brady et al., 2006b).

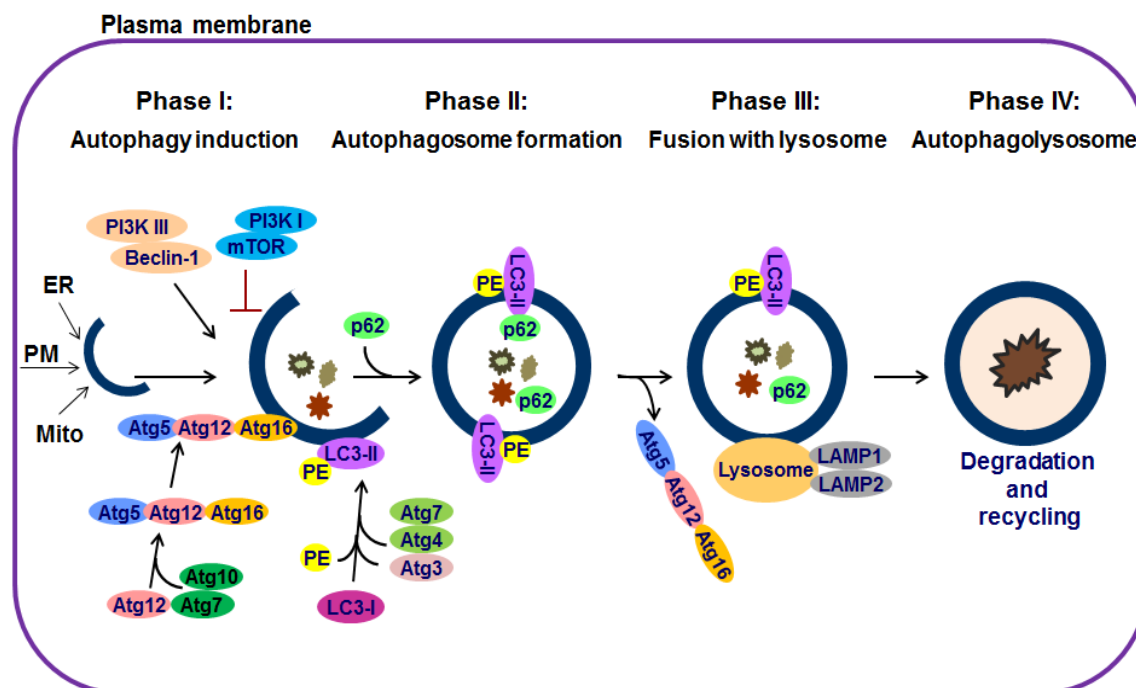


Figure 1.3: Schematic illustration of the four phases of autophagy.

PI3K, phosphatidylinositol-3 kinase; mTOR, mammalian target of rapamycin; Atg, autophagy-related gene; Beclin-1, the mammalian homolog of yeast Atg6; LC3, Microtubule-associated protein 1 light chain 3; PE, phosphatidylethanol-amine; p62, polyubiquitin-binding protein p62 (also called SQSTM1; sequestrome 1); LAMP, lysosomal-associated membrane protein; ER, endoplasmic reticulum; PM, plasma membrane; Mito, mitochondrial.

1.3.3.2 Regulation of autophagy during myocardial I-R

Autophagy is induced by a variety of factors during I-R, such as oxidative stress (Dai and Rabinovitch, 2011; Dutta et al., 2013; Hariharan et al., 2011), endoplasmic reticulum stress, Ca^{2+} overload (Pan et al., 2013), activation of AMPK and inactivation of mTOR (Matsui et al., 2007) and upregulation of Beclin-1 (Ma et al., 2012b). During

the ischaemic phase, autophagy is stimulated through an AMPK/mTOR-dependent mechanism (Takagi et al., 2007), whereas reperfusion stimulates autophagy through an upregulation of Beclin-1-dependent mechanisms rather than by activation of AMPK (De Meyer and Martinet, 2009; Ma et al., 2012b; Matsui et al., 2007); induction of autophagy and cardiac injury during the reperfusion phase is significantly attenuated in Beclin 1^{+/-} mice (Matsui et al., 2007). In Langendorff isolated rabbit hearts, I-R induced autophagy (Decker et al., 1980; Decker and Wildenthal, 1980). These studies showed that 40 min of ischaemia led to an increase in autophagic vacuoles, and that reperfusion after 20 or 40 minutes of ischaemia further enhanced autophagy in the reperfused rabbit heart. When ischaemia was extended to 60 minutes, large and possibly dysfunctional lysosomes were present during reperfusion, suggesting that the prolonged ischaemia impaired autophagic-lysosomal fusion.

Autophagy has been measured in human and pig hearts under chronic myocardial ischaemia (Elsasser et al., 2004; Yan et al., 2006; Yan et al., 2005), as well as in mouse and rat hearts subjected to acute I-R (Hamacher-Brady et al., 2007; Matsui et al., 2007). The extent of autophagy is enhanced during reperfusion compared with ischaemia alone in hearts from rabbit and mice (Decker and Wildenthal, 1980; Matsui et al., 2007). Autophagy has also been examined in isolated neonatal and adult cardiac myocytes subjected to simulated I-R (sI/R) or hypoxia and reoxygenation (H/R), with an increase in the number of autophagic vesicles reported (Valentim et al., 2006). Hamacher-Brady et al. found that when HL-1 myocytes were subjected to sI/R, autophagic activity was inhibited during ischaemia, but re-activated during reperfusion (Hamacher-Brady et al.,

2006a). Taken together, autophagy is induced by ischaemia and further enhanced after reperfusion in the heart (*ex vivo* and *in vivo*) and in cultured cardiac myocytes (*in vitro*). Although it is clear that autophagy is enhanced during I-R, the functional significance of autophagy (beneficial vs. detrimental) in the heart remains controversial. Several studies suggest that up-regulation of autophagy is cardioprotective and attenuates myocardial I-R injury (Dosenko et al., 2006; Hamacher-Brady et al., 2006a; Hamacher-Brady et al., 2006c; McCormick et al., 2012), with inhibition of autophagy worsening tissue damage in I-R (Jiang et al., 2010; Qian et al., 2009; Wei et al., 2013). Pharmacological induction of autophagy also confers protection against I-R (Gurusamy et al., 2010; Sala-Mercado et al., 2010). However, autophagy also leads to detrimental effects in I-R (Ma et al., 2012a; Matsui et al., 2008b) (Figure 1.4). Recent experimental data also show that the clearance of autophagosomes is impaired in myocardial reperfusion injury which is mediated in part by ROS-induced decline in LAMP-2A and upregulation of Beclin-1, contributing to increased cardiomyocyte death (Hariharan et al., 2011; Ma et al., 2012b). Furthermore, Bcl-2 and Bcl-xL directly interact and regulate the autophagy protein inducer Beclin-1 (Cheng et al., 2013; Pattingre et al., 2005). The BH3 domain of Beclin-1 binds and is inhibited by Bcl-2 or Bcl-xL (Maiuri et al., 2007; Oberstein et al., 2007). Dissociation of Beclin-1-Bcl-2/xL complexes promotes autophagy (Zalckvar et al., 2009) and ultimately cell death (Luo and Rubinsztein, 2010). Thus, Bcl-2/xL not only functions as an anti-apoptotic protein, but also as an anti-autophagic protein via its inhibitory interaction with Beclin-1.

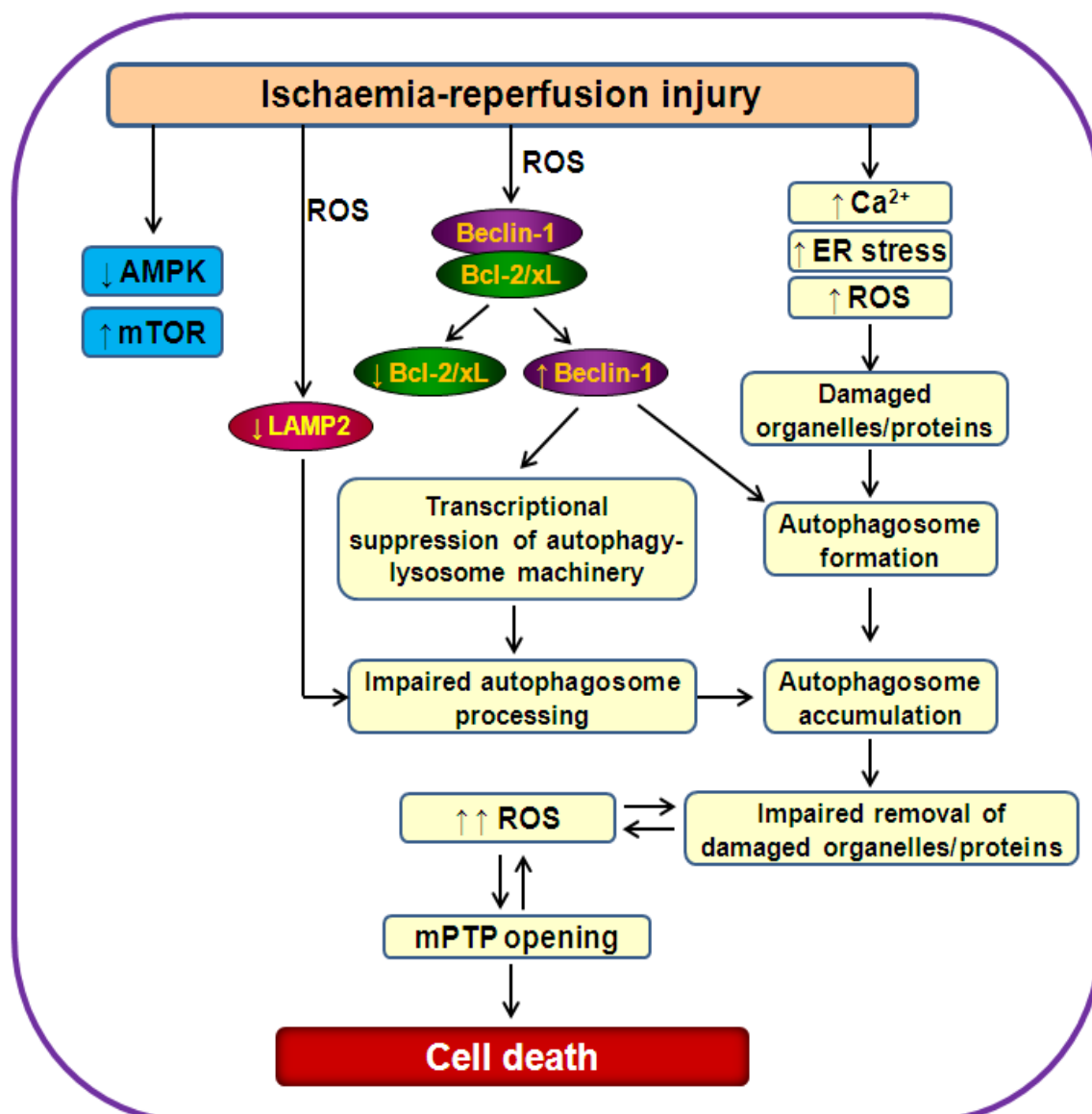


Figure 1.4: Regulation of autophagy during myocardial ischaemia-reperfusion.

ER, endoplasmic reticulum; ROS, reactive oxygen species; mPTP, mitochondrial permeability transition pore; Bcl-2, B-cell lymphoma 2; Bcl-xL; B-cell lymphoma extra large; Beclin-1, the mammalian homolog of yeast autophagy-related gene 6 (Atg6); LAMP2, lysosomal-associated membrane protein 2; AMPK, adenosine monophosphate-activated protein kinase; mTOR, mammalian target of rapamycin; ↑ increased; ↓ decreased.

1.3.4 Apoptosis

Apoptotic cell death was first identified by Kerr, Wyllie and Currie early in the 1970s and can be initiated by two main mechanisms which are referred to as extrinsic and intrinsic pathways of cell death (Kerr et al., 1972; Wyllie et al., 1980). Apoptosis at basal level is required for tissue development and cellular homeostasis (Danial and Korsmeyer, 2004; Kerr et al., 1972). However, enhanced apoptosis is observed in myocardial I-R injury (Fliss and Gattinger, 1996; Gottlieb et al., 1994; Zhao et al., 2000) and during ventricular remodelling after AMI (Hofstra et al., 2000; Krijnen et al., 2002; Olivetti et al., 1996; Palojoki et al., 2001; Saraste et al., 1997).

1.3.4.1 Molecular mechanisms involved in apoptosis

Apoptosis is a mechanism of programmed cell death that results in cell shrinkage and condensation of the cytosol and nucleus to eventually form apoptotic bodies (Arbustini et al., 2008; Kerr et al., 1972; Saraste and Pulkki, 2000). Since apoptotic bodies are surrounded by cell membranes, they can be engulfed and digested by phagocytes without inducing an inflammatory process. Apoptosis can be identified by the presence of DNA condensation, fragmentation and breakdown of the nucleus substrates (Joselin et al., 2006; Sakahira et al., 1999). Figure 1.5 is a schematic of the major apoptotic pathways leading to cell death

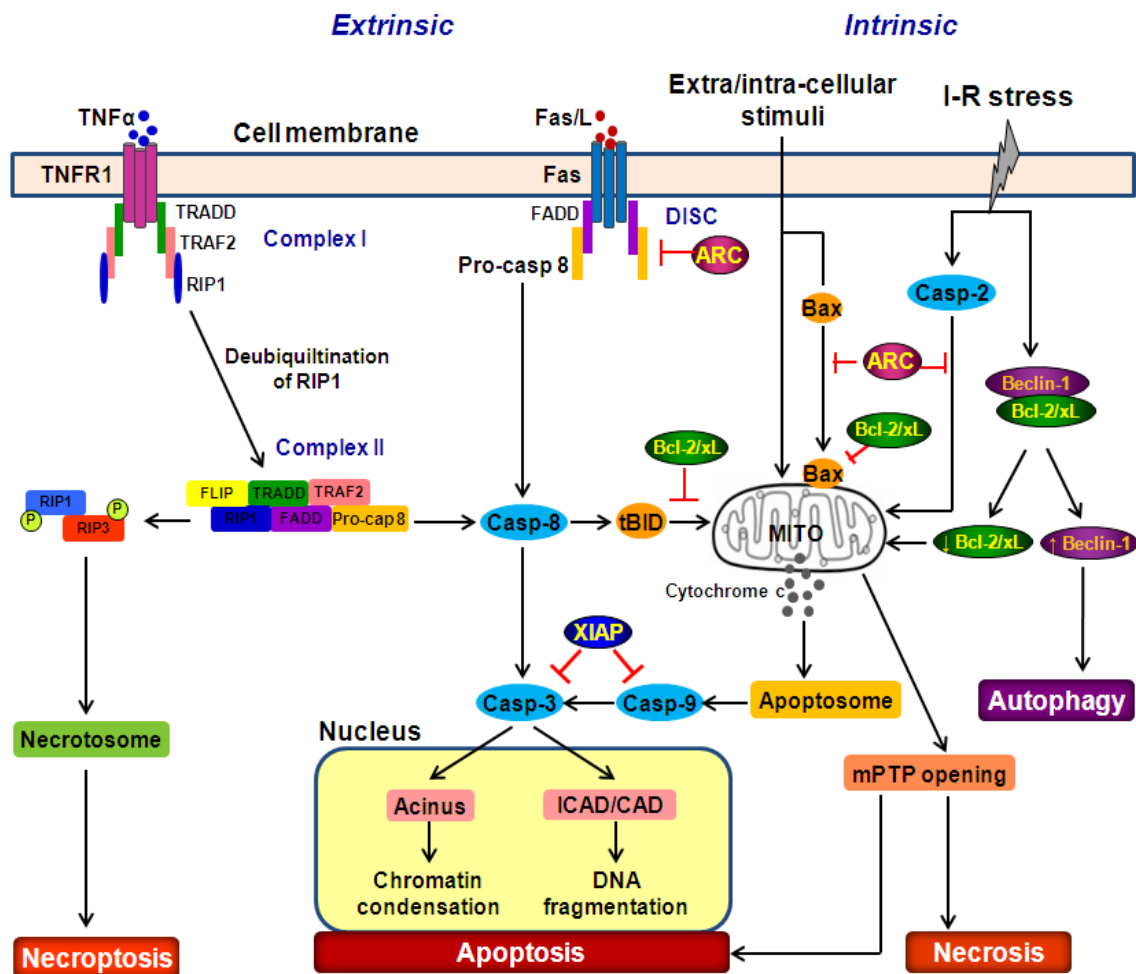


Figure 1.5: Extrinsic (left) and intrinsic (right) mechanisms of apoptosis and the cross talk that occurs between these pathways.

The signalling complexes are induced by death receptor mediated apoptosis or necroptosis (programmed necrosis) and by extra-/intra-cellular stimuli mediated autophagy, apoptosis or necrosis. TNF, tumour necrosis factor; TNFR1, tumour necrosis factor receptor 1; DISC, death-inducing signaling complex; Casp, caspase; tBID, truncated BID; ARC, Apoptosis Repressor with Caspase recruitment domain; Bcl-2, B-cell lymphoma 2; Bcl-xL; B-cell lymphoma extra large; XIAP, X-linked inhibitor of apoptosis; Acinus, ICAD/CAD, inhibitor of caspase-activated DNase/ caspase-activated DNase; I-R, ischaemia-reperfusion; MITO, mitochondrial.

Extrinsic apoptotic pathway: The extrinsic cell death pathway is activated by death receptor ligands such as tumour necrosis factor alpha (TNF α) and Fas ligand (FasL), which bind to specific death receptors (Jeremias et al., 2000; Krown et al., 1996). Activation of these receptors results in their trimerization and recruits a number of death domain-containing proteins such as FADD and TRADD to the receptor complex (Figure 1.5). The death-inducing signalling complex (DISC) and Complex I activate the initiator caspase-8 (Dickens et al., 2012; Kim et al., 2000), which in turn, cleaves and activates the executioner caspase-3 (Stennicke et al., 1998). The release of an active caspase-3 fragment can cleave death substrates such as PARP (poly-ADP ribose polymerase) (O'Brien et al., 2001), fodrin (Janicke et al., 1998), lamin (Rao et al., 1996), acinus (apoptotic chromatin condensation inducer in the nucleus) (Sahara et al., 1999) and ICAD/DFP45 (inhibitor of caspase-activated DNase or DNA fragmentation factor 45) (Enari et al., 1998; Sakahira et al., 1998). Cleavage of these proteins prevent DNA repair and induce DNA fragmentation resulting in increased level of apoptosis.

Intrinsic apoptotic pathway: As shown in Figure 1.5, the intrinsic cell death pathway is mediated by intracellular and extracellular stimuli including I-R, UV irradiation, toxic compounds (etoposide, staurosporine) or oxidative stress, all of which induce the translocation and integration of pro-death members of the Bcl-2 protein family (e.g., Bax, Bak) into the outer mitochondrial membrane (Antignani and Youle, 2006; Kroemer et al., 2007; Nechushtan et al., 1999). These proteins permeabilize the outer membrane, thereby enabling the release of pro-apoptotic proteins from the intermembrane space. Bax and Bak proteins stimulate the release of cytochrome c, Smac/DIABLO, Omi/HtrA2, and endonuclease-G (endoG) from mitochondria (Arnoult

et al., 2003; Kroemer et al., 2007). Cytochrome c, ATP, Apaf-1, and pro-caspase-9 assemble into the “apoptosome” leading to caspase-9 activation, which can cleave and subsequently activate caspase-3 and thus promote nuclear fragmentation (Hu et al., 1999; Kroemer et al., 2007; Zou et al., 1999).

Crosstalk between extrinsic and intrinsic apoptotic cell death pathways: The extrinsic and intrinsic pathways are connected by BID, a direct substrate of caspase-8 (Figure 1.5). After cleavage of cytosolic BID to truncated BID (tBID), the C-terminus of tBID translocates and inserts into the outer mitochondrial membrane and thus transduces apoptotic signals from the cytoplasmic membrane to mitochondria (Li et al., 1998). This has been associated with the loss of mitochondrial membrane potential, activation of Bax and Bak and cytochrome c release and thus cell shrinkage and nuclear fragmentation (Figure 1.5) (Korsmeyer et al., 2000; Li et al., 1998; Madesh et al., 2002). I-R in the rat heart suggested that activation of caspase-9 occurring during reperfusion may depend on caspase-8 cleavage of BID, and tBID relocates to mitochondria where it induces caspase-9 processing (Scarabelli et al., 2002). This shows that although activation of the extrinsic pathway does not directly act in the mitochondria it can activate mechanisms within the intrinsic pathway (Figure 1.5).

Counteracting the induction of apoptotic cascades are the anti-apoptotic proteins which include Bcl-2/xL, XIAP (X-linked inhibitor of apoptosis protein) and ARC (Apoptosis repressor with caspase recruitment domain). Bcl-2 and Bcl-xL, anti-apoptotic proteins at the mitochondrial membrane level, can prevent BID or Bax induced apoptosis by stopping these pro-apoptotic proteins from integrating into the outer mitochondrial

membrane (Billen et al., 2008; Cheng et al., 2001; Yi et al., 2003). XIAP inhibits activation of caspase-9 and -3 (Bratton et al., 2002; Srinivasula et al., 2001), whereas ARC antagonises both the extrinsic and the intrinsic death pathways (Nam et al., 2004) (Figure 1.5). The change in balance between pro-survival and pro-death proteins depends also on the type of apoptotic stimulus (I-R stress, toxic compounds, oxidative stress or DNA damage).

1.3.4.2 Regulation of apoptosis during myocardial I-R

Regulation of apoptosis involves transduction of signalling by apoptotic mediators, both pro- and anti-apoptotic proteins. The current study focuses on the role of apoptotic mediators during myocardial I-R injury.

Caspases

Caspases, the main effectors of apoptosis, are a group of cysteine containing proteases that specifically cleave proteins at aspartate residues (Alnemri et al., 1996). Caspases are constitutively expressed and synthesised as inactive zymogens referred as “pro-caspases”, containing an N-terminal prodomain and a C-terminal catalytic domain; once stimulated mature active fragments, heterotetramers of the smaller cleavage fragments, are generated (Nicholson et al., 1995). Caspases are classed according to their function, as either upstream (initiator) caspases including caspases-2/-8/-9/-10/-12 or downstream (effector, executioner) caspases including caspases-3/-6/-7 (Crow et al., 2004; Nicholson et al., 1995). Caspases play critical roles in I-R induced cell death and numerous studies have demonstrated increased activity of caspase-8, caspase-2, caspase-9, and caspase-3 in myocardial I-R (Fauconnier et al., 2011; Qin et al., 2004; Scarabelli

et al., 2002). Administration of caspase inhibitors such as zVAD-FMK and MX1013 attenuates apoptosis and cell death in response to I-R in kidney (Daemen et al., 1999), liver (Kobayashi et al., 2001), brain (Yang et al., 2003) and heart (Chandrashekhar et al., 2004; Yaoita et al., 1998; Yarbrough et al., 2010). Genetic deletion or knockdown of specific caspases, both in the extrinsic and intrinsic pathways, also ameliorates I-R injury (Contreras et al., 2004; Zhang et al., 2006; Zhang et al., 2010; Zheng et al., 2006). However, targeting caspase inhibition for reducing I-R injury may not be ideal since upstream mitochondria will still be adversely affected (Figure 1.5).

The Bcl-2 family proteins

The Bcl-2 family of proteins include both pro-apoptotic and anti-apoptotic factors that regulate the activation of the intrinsic pathway. Anti-apoptotic factors of the Bcl-2 family proteins, include Bcl-2, Bcl-xL, Bcl-w, inhibit apoptosis by preventing BID or Bax activation/mitochondrial translocation and preventing release of cytochrome c from mitochondria (Billen et al., 2008; Cheng et al., 2001; Yi et al., 2003). During I-R the expression levels of Bcl-2 and Bcl-xL decrease (Lazou et al., 2006; Maulik et al., 1999; Zhao et al., 2000). Conversely, overexpression of anti-apoptosis genes, Bcl-2 and Bcl-xL, block the release of cytochrome c and reduce both myocardial apoptosis and infarct size following I-R (Chen et al., 2001; Huang et al., 2003).

Pro-apoptotic Bcl-2 family members function by binding and inactivating anti-apoptotic factors and ultimately trigger the release of cytochrome c from mitochondria (Mikhailov et al., 2003; Shimizu and Tsujimoto, 2000). BID can also promote the activation of both Bax and Bak by competing for Bcl-2 binding (Kim et al., 2009; Ren et al., 2010).

Activation, upregulation, translocation, and integration of pro-apoptotic Bcl-2 proteins (such as Bax, Bak, Puma, BID and BNIP3) into mitochondrial membranes have been reported in ischaemic tissues (Hamacher-Brady et al., 2007; Toth et al., 2006; Webster, 2006). Bax-, BID-, BNIP3-, or Puma-deficient mice have reduced infarct size, confirming a role for these proteins in the progression of I-R injury (Diwan et al., 2007; Hochhauser et al., 2003; Toth et al., 2006).

Inhibitors of apoptotic proteins (IAPs)

IAPs, such as X-linked inhibitor of apoptosis (XIAP), are major endogenous inhibitors of apoptosis in cardiomyocytes (Potts et al., 2005). XIAP inhibits apoptosis by binding directly to caspases-9 and -3, preventing their processing and activation (Crow et al., 2004; Deveraux et al., 1997; Riedl et al., 2001). XIAP also prevents the proteolytic processing of caspases-3 and -9 by modulating Apaf-1 and cytochrome c-induced activation (Deveraux et al., 1998; Potts et al., 2005). Levels of XIAP are reduced in response to ischaemia or hypoxia (Lyn et al., 2002; Shilkrut et al., 2003), as well as in hearts subjected to I-R (Bhuiyan and Fukunaga, 2008; Liu et al., 2005a; Scarabelli et al., 2004), suggesting that XIAP is involved in I-R induced cardiomyocyte apoptosis. Recent studies have shown that overexpression of XIAP via *in vivo* gene delivery to rabbit hearts decreases expression of cleaved caspase-3, and thus attenuates both myocardial apoptosis and infarction following I-R (Kim et al., 2011).

Apoptosis Repressor with Caspase recruitment domain (ARC)

ARC is an endogenous inhibitor of apoptosis that inhibits both the extrinsic and the intrinsic apoptotic pathways (Gustafsson et al., 2004; Koseki et al., 1998; Nam et al.,

2004). ARC inhibits the extrinsic pathway by direct interaction of the ARC caspase recruitment domain (CARD) with the death domains (DD) of Fas and Fas-associated protein with death domain (FADD), and with the death effector domain (DED) of procaspase-8, thus interfering with DISC formation (Nam et al., 2004). ARC inhibits the intrinsic pathway through several mechanisms. These include the direct interaction between the CARD of ARC and the C-terminus of Bax, inhibiting death stimulus-induced Bax conformational activation and translocation to the mitochondria (Nam et al., 2004). Direct interaction between the ARC C-terminal domain with the p53 tetramerization domain inhibits p53 tetramerization (Foo et al., 2007b). This, in turn, disables p53 transcriptional and exposes a p53 nuclear export signal that relocates p53 to the cytoplasm. Furthermore, phosphorylation of ARC at threonine 149 inhibits oxidative stress-induced caspase-2 activation, cytochrome c release, and translocation of Bax to mitochondria (Zhang and Herman, 2006).

ARC protein levels decrease rapidly in response to hypoxia, I-R and oxidative stress (Ekhterae et al., 1999; Nam et al., 2007b; Neuss et al., 2001). The increased degradation of ARC protein via the ubiquitin-proteasomal pathway (Nam et al., 2007b) is dependent on the p53-induced ubiquitin E3 ligase MDM2 (Foo et al., 2007a). In response to hypoxia, ARC protein abundance falls after p53 repression of ARC transcription (Li et al., 2008). The activity of ARC is also post-translationally regulated. Dephosphorylation of threonine 149 decreases the anti-apoptotic activity of ARC (Li et al., 2002; Murtaza et al., 2008; Tan et al., 2008; Yao et al., 2012; Zhang and Herman, 2006). ARC binds calcium via its C-terminus and can also suppress Ca^{2+} -mediated apoptosis (Jo et al., 2004). Recently, it was demonstrated that oxidative stress results in ARC attenuating

release of Ca^{2+} from the sarcoplasmic reticulum and inhibiting Ca^{2+} elevation in the cytoplasm and mitochondria (Lu et al., 2013). Furthermore, Foxo3a, a member of the forkhead family of transcription factors, inhibits cardiomyocyte apoptosis by maintaining calcium homeostasis through transactivation of ARC (Lu et al., 2013).

ARC plays an important role during MI where rapid proteasomal degradation of endogenous ARC protein (Nam et al., 2007b) has been shown to lead to cell death (Nam et al., 2004). Accordingly, ARC overexpression leads to improved recovery of contractile performance during reperfusion and decrease infarct size (Gustafsson et al., 2002; Pyo et al., 2008). Conversely, increased cardiomyocyte apoptosis (An et al., 2009), larger infarcts and exacerbated pathological cardiac remodelling (Donath et al., 2006) are observed in ARC null mice. Decreased ARC protein levels have been measured in heart muscle from patients with heart failure (Donath et al., 2006).

1.3.5 Necrosis

During MI there is both apoptotic and necrotic myocyte death (Kajstura et al., 1996; McCully et al., 2004). In contrast to apoptosis, I-R induced cell necrosis involves membrane disintegration and dysregulated ion transport, which leads to the absorption of water, cell swelling and eventually membrane rupture (Searle et al., 1982). Release of pro-inflammatory mediators and destruction of cellular organelles subsequently recruits inflammatory cells (such as neutrophils) to the area of necrosis, initiating inflammation and further damage to surrounding tissue (Kajstura et al., 1996; Tavernarakis, 2007; Vanlangenakker et al., 2008). Necrosis does not require energy and it has been suggested that necrosis is the main type of cell death during ischaemia, whereas

apoptosis occurs mainly during reperfusion when the energy supply is restored (Kajstura et al., 1996; McCully et al., 2004).

During reperfusion, restoration of oxygen quickly allows ATP levels to recover and restore mitochondrial membrane potential. These changes generate ROS and increased intracellular Ca^{2+} , which leads to opening of mPTP by cyclophilin D (CyD), and mitochondrial swelling ultimately resulting in cellular necrosis (Devalaraja-Narashimha et al., 2009; Miura et al., 2009). Involvement of mPTP in cardiac I-R responses has been verified in both experimental and clinical studies (Hausenloy et al., 2012; Perrelli et al., 2011). Mice with cardiac-specific overexpression of CyD exhibit mitochondrial swelling and spontaneous cell death, whereas lack of CyD protected cardiac myocytes from Ca^{2+} overload-induced cell death *in vitro* (Baines et al., 2005; Nakagawa et al., 2005). Interestingly, pro-apoptotic protein-induced cytochrome c release did not differ between mitochondria from wild-type and knockout CyD mice, suggesting that CyD does not have a critical role in apoptosis (Baines et al., 2005; Nakagawa et al., 2005). On the other hand, similar mice lacking CyD showed smaller infarct size, improved LV function and less mortality following MI (Lim et al., 2011). Although experimental studies show cardioprotective effects with cyclosporine A (CsA, a mPTP inhibitor) in response to I-R (Boengler et al., 2010), pre-thrombolytic administration of CsA in patients with acute anterior ST-segment elevation MI (STEMI) did not reduce infarct size or improve morbidity and mortality (Ghaffari et al., 2012).

1.3.6 Necroptosis

Recently, another form of cell death has been described, named “necroptosis” or “programmed necrosis”. As shown in Figure 1.6, necroptosis is a caspase independent cell death pathway. The signalling complexes are induced by TNF α stimulation of death receptor TNFR1 leading to the formation of complex I at the cytoplasmic membrane that includes TNF receptor-associated death domain (TRADD), TNF receptor-associated factor-2 (TRAF2), and receptor-interacting protein-1 (RIP1). Ubiquitination of RIP1 at K377 leads to the recruitment of NF- κ B essential modulator (NEMO), a regulatory subunit of I kappa B kinase (IKK) complex that in turn activates NF- κ B pathway. On the other hand, deubiquitination of RIP1 leads to the formation of complex II including FADD and caspase-8 to activate a caspase cascade and mediate apoptosis. Alternatively, RIP1 interacts with RIP3 and phosphorylation of RIP1 and RIP3 leads to the formation of necroptosome and mediates necroptosis (Figure 1.6).

Necroptosis may play an important role in cell death during ischaemia and I-R. Necrostatin-1, a highly specific RIP1 inhibitor, reduces infarct volume in a mouse model of cerebral ischaemia (Degterev et al., 2005) and also lessens structural and functional impairment in a rat model of retinal I-R injury (Rosenbaum et al., 2010). The involvement of necroptosis has also demonstrated in kidney I-R where necrostatin-1 ameliorated functional and morphological changes in kidney damage (Linkermann et al., 2012). In contrast to necrostatin-1 treatment, blockade of apoptosis by zVAD (a pan-caspase inhibitor) did not prevent tissue damage or the increase in urea and creatinine during *in vivo* renal I-R injury. The protective effect of necrostatin-1 was

more pronounced, suggesting the role of necroptosis over apoptosis in the pathophysiology of renal I-R injury (Linkermann et al., 2012).

Although no studies have examined the direct role of necroptosis during myocardial I-R injury, it has been suggested that a group of serine/threonine kinases called receptor-interacting proteins (RIPs) are activated and mediate necroptosis during cellular stress or death receptor activation (Moquin and Chan, 2010; Smith and Yellon, 2011; Vandenabeele et al., 2010). Activation of RIP-1 and -3, in turn, increases ROS production, either through activation of NADPH oxidases (Cho et al., 2009; Kim et al., 2007) or increased mitochondrial oxidant production (Vandenabeele et al., 2010). One potential mitochondrial target for RIP-mediated necroptosis is mPTP. The mPTP opens in response to excessive production of ROS and Ca^{2+} overload of the mitochondrial matrix (Abdallah et al., 2011; Assaly et al., 2012; Saotome et al., 2009), both of which occur during myocardial I-R. This increase in inner membrane permeability dissipates the proton electrochemical gradient, leading to ATP depletion, further ROS production, and ultimately swelling and rupture of the organelle and cell lysis (Figure 1.6).

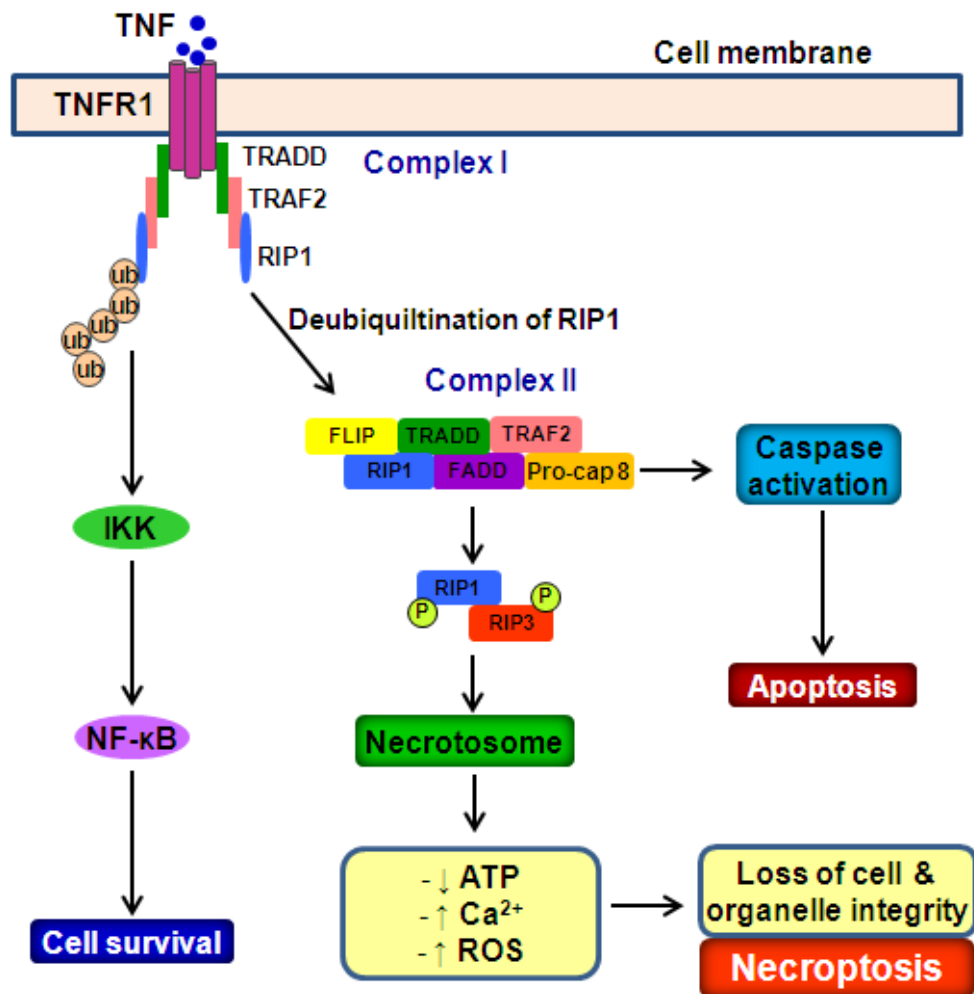


Figure 1.6: The molecular pathway of necroptosis.

The signalling complexes are induced by TNF α to mediate cell survival, apoptosis or necroptosis. Stimulation of TNFR1 by TNF α leads to the formation of “Complex I”. Deubiquitination of RIP1 leads to the formation of “Complex II”. Phosphorylation of RIP1 and RIP3 forms “necrosome” and mediate “necroptosis”. TNF, tumor necrosis factor; TNFR1, TNF receptor 1; IKK, I kappa B kinase; TRADD, TNF receptor-associated death domain; TRAF2, TNF receptor-associated factor-2; RIP, receptor-interacting protein; FLIP, FLICE-like inhibitory protein; FADD, Fas-associated protein with death domain; Pro-casp8; pro-caspase 8; ROS, reactive oxygen species.

1.4 Experimental models of myocardial infarction

Experimental models of MI from small to large animal including sheep, dog, pig, rabbit, rat or mouse (Wang et al., 2001; Wong et al., 2011; Zhang et al., 2011; Zornoff et al., 2009) have been used to identify the mechanisms involved in tissue damage and how new treatments intercept these pathways. Previous studies have shown no significant difference between the extent of tissue damage between rat and rabbit models for MI (Mihailidou et al., 2009; Wong et al., 2011). Further, infarct size, calculated relative to area-at-risk following I-R in rat (Mihailidou et al., 2009), does not differ from other species (Schmidt et al., 2010; Wong et al., 2011; Ytrehus et al., 1994). The rat model for MI has been widely used to study the (patho)physiological alterations caused by occlusion and reperfusion (Fishbein et al., 1978; Selye et al., 1960), including infarct size and post infarction remodelling (Goldman and Raya, 1995; Vidavalur et al., 2008; Zornoff et al., 2009), and it is for this reason that we chose to perform our studies in rats. The progression of changes post- MI include an acute inflammatory response at the edge of the infarct area, chronic inflammation, vascularisation and collagenation, cell death and formation of necrotic tissue (infarction) (Fishbein et al., 1978). Additionally, MI induces myocyte hypertrophy (Anversa et al., 1985; Anversa et al., 1986; Anversa et al., 1984). These features, especially the loss of myocardial cells in the area of injury, are also observed in rat hearts after occlusion of blood flow (Mihailidou et al., 2009).

1.4.1 *Ex vivo* Langendorff isolated heart preparations

The Langendorff isolated organ technique was established in the 1890s by Oscar Langendorff (Langendorff, 1898). This is an *ex vivo* model that consists of the intact heart removed from animal and perfused with blood-like buffer (Krebs-Henseleit buffer,

oxygenated solution) via the aorta. This is referred to as a “retrograde perfusion”, as the perfusate flows directly into the aorta rather than the normal situation where blood enters the aorta from the left ventricles (Bell et al., 2011b; Langendorff, 1898). The perfusate is forced through the ostium at the base of the aorta and into the coronary arteries. Retrograde perfusion of the coronary arteries can be delivered using either at a constant hydrostatic pressure or at a constant flow. Constant flow offers the advantage of greater reproducibility, and it is easy to induce various degrees of flow rate (Vidavalur et al., 2008).

1.4.2 Advantages and limitations of the *ex vivo* experimental technique

Experimental models of MI are usually divided into *in vivo* and *ex vivo* models. There are advantages and limitations of the *ex vivo* experimental technique. The isolated heart method (*ex vivo*) provides highly reproducible results. It allows a wide range of physiological, morphological and biochemical activity of the heart to be measured in a single experiment. Although the hearts are isolated from the body, the method remains reasonably close to normal physiology. Another advantage of this model is it allows the determination of direct actions of drugs or hormones in the whole heart without interference from the peripheral circulation (e.g. circulating hormones, blood cells), sympathetic stimulation or peripheral resistance. The model is also very useful for the study of dose-response relationships of direct actions of agents (Wong et al 2011; Mihailidou et al 2009) as well as assessing new compounds or drugs (Anderson et al., 1990).

Limitations of isolated heart perfusion include lack of the normal humoral background and neuronal regulation of the heart. At very high perfusion flow rate, the retrograde flow of perfusate in the aorta may not pass through the ostium into the coronary arteries/circulation. The different composition of perfusion buffer compared to oxygenated whole blood or red-blood cell enriched solutions produces higher flow rates which alter sheer stress along the endothelium of coronary arteries and may lead to tissue edema (Döring and Dehnert, 1988). Another limitation is the significantly increased possibility of preconditioning during surgical excision of the heart, leading to higher oxidative stress and deterioration of contractile function (Ferdinandy et al., 1999). Despite these limitations, several studies have confirmed that *ex vivo* results correlate well with *in vivo* studies (Penumathsa et al., 2007; Thirunavukkarasu et al., 2006).

1.4.3 Regional versus global ischaemia

Ischaemia can be induced either by stopping perfusate or blood flow (global ischaemia) or by occluding a branch of the left coronary artery (regional ischaemia). Clinically, regional ischaemia is more important than global ischaemia. Global ischaemia for 25-30 minutes can cause irreversible necrotic myocyte injury, resulting in substantial increases in creatine kinase (CK) and severe myocardial dysfunction during reperfusion (Palmer et al., 2004). The presence or absence of collaterals between coronary vascular beds is irrelevant in the study of global ischaemia; however, it is highly relevant to regional ischaemia so that consistency is required in placing the snare in regional ischaemia. Regional ischaemia in the isolated perfused heart is obtained by ligation of one of the branches of the left anterior descending (LAD) coronary artery (Bredde et al.,

1975; Johns and Olson, 1954; Reimer et al., 1981), reducing the oxygen and nutrient supply to the tissue distal to the snare (Liedtke et al., 1975; Neely et al., 1973) and cardiac function progressively declines as reperfusion progresses (Bolli and Marban, 1999; Jennings et al., 1978; Ruiz-Meana et al., 2011).

1.4.4 Duration of ischaemia and reperfusion during myocardial I-R

For regional ischaemia induced by occlusion of either a branch of the left anterior descending or circumflex coronary arteries, the occlusion period varies. Ischaemia for 30 minutes or less is often used while several studies have shown that 15-40 minutes of ischaemia results in potentially reversible cell injury, whereas >40 minutes results in cell death (irreversible necrotic injury) (Jennings et al., 1978; Ruiz-Meana et al., 2011). In the *ex vivo* Langendorff perfused heart, an ischaemic period of 30 minutes followed by 120-150 minutes of reperfusion produces an infarct area between 17% to 80%, with a median infarct size of 42% (Mersmann et al., 2011). This is a significant increase in infarct size and apoptosis compared to 60 minutes reperfusion (Mersmann et al., 2011). No significant difference in infarct size was observed between 120 to 150 minutes reperfusion (Birnbaum et al., 1997; Ferrera et al., 2009; Hausenloy et al., 2003; Mihailidou et al., 2009; Schwarz et al., 2000; Wang et al., 2001; Wong et al., 2011; Ytrehus et al., 1994).

There is now also growing evidence that there are gender differences in outcomes from MI. Whether sex steroid hormones, particularly androgens, regulate the mechanisms activated during MI is not defined and further studies are required to determine the pathways activated during reperfusion injury differ between males and females.

1.5 Gender difference in ischaemic heart disease

1.5.1 Overview

Death rates due to IHD are higher in men than age-matched women (Bener et al., 2013; Papakonstantinou et al., 2013; Tunstall-Pedoe, 1998; Wingard et al., 1983) suggesting sex hormones play an important role. Recent studies highlight distinct gender differences in the epidemiology, pathophysiology and prognosis of IHD (Dunlay and Roger, 2012; Kostapanos et al., 2013), in that the prevalence of IHD in men is higher than in women across all ages (Jacobs, 2009; Kalin and Zumoff, 1990; Roger et al., 2012).

IHD presents in females approximately 10 years later than in males (Anand et al., 2008), which decreases with increasing age, especially after the onset of menopause (Yusuf et al., 2001), with incidence of MI lower in women (Isaksson et al., 2011; Wenger, 2002). Although males have higher STEMI and age-adjusted prevalence of IHD compared to females (Heer et al., 2002; Kosuge et al., 2006), younger females experience more adverse outcomes after MI and coronary artery bypass grafting surgery than do males (Vaccarino et al., 2002), and a higher proportion of females with MI die of sudden cardiac arrest before reaching hospital (Roger et al., 2012; Shaw et al., 2006). The underlying reasons for the gender differences in IHD incidence have not been fully defined and may include genetics, lifestyle differences between genders or levels of endogenous sex hormones (Nordlie et al., 2005; Notarangelo et al., 2012; Silander et al., 2008). Another possible reason for these gender differences may be that most clinical trials do not include adequate numbers of women and older males to allow sex-specific

analyses, suggesting a possible selection bias (Dunlay and Roger, 2012; Kim et al., 2010; Xhyheri and Bugiardini, 2010).

1.5.2 Sex hormones and ischaemic heart disease: controversy

It has been suggested that hormonal differences between men and women may explain the gender differences in the incidence of IHD (Kalin and Zumoff, 1990; Perez-Lopez et al., 2010). Decline in oestrogen levels in post-menopausal women is associated with increased number of coronary deaths (Mosca, 2000; Tunstall-Pedoe, 1998), suggesting oestrogens are cardioprotective. Therefore many studies focused on the potential cardioprotective effects of oestrogens (Baker et al., 2003; Mendelsohn and Karas, 1999), with very few studies investigating the role of androgens in IHD.

Hormone replacement therapy (HRT) with oestrogens to post-menopausal women also produced conflicting results. While observational studies show improved cardiovascular outcomes (Herrington and Klein, 2001; Hodis et al., 2001), prospective randomised controlled studies show HRT either had no significant effects (Angerer et al., 2001; Cushman et al., 1999; Hodis et al., 2003) or adverse effects (Hulley et al., 1998; Kuller, 2003; Vickers et al., 2007). Two trials in particular, the Heart and Estrogen/progestin Replacement Study (HERS) (Hulley et al., 1998) and the Women's Health Initiative (WHI) study (Kuller, 2003) failed to show cardiovascular benefit as expected from the observational studies (Herrington and Klein, 2001), with increased cardiovascular risk in the first few years of HRT. The lack of cardiovascular benefit observed in the WHI and HERS studies was proposed to be due to the timing of treatment (Machens and Schmidt-Gollwitzer, 2003). Cardiovascular benefit was shown when women started

HRT at the onset of menopausal symptoms, prior to the development of any significant vascular disease (Dubey et al., 2005; Hodis et al., 2001). Recently the Danish Osteoporosis Prevention Study (DOPS) shows that 10 years of oestrogen replacement may be beneficial, with significantly decreased risk of MI, HF and mortality when HRT was started early in postmenopause (Schierbeck et al., 2012). Differences between the various trials include the participants recruited. The HERS study was established as a secondary prevention trial that targeted women already carrying significant disease risk (Hulley et al., 1998), whereas the WHI study was a primary prevention trial and included only women with no prior history of CVD (Kuller, 2003). Average age of women in the DOPS trial was younger than in the WHI (50 vs 65 years) at the commencement of treatment (Kuller, 2003; Schierbeck et al., 2012). In summary, endogenous oestrogens may protect younger women against early onset CVD and further prospective studies are required for starting oestrogen therapy earlier in postmenopausal women.

The role of androgens during IHD is also conflicting, with the pro-atherogenic effects of androgens suggested to contribute to their adverse cardiac effects (Hartgens et al., 2003; Hassan et al., 2009; Rockhold, 1993; Sader et al., 2001; Shapiro et al., 1999; Sullivan et al., 1998), whereas low levels of endogenous testosterone (T) in men are associated with increased CVD events (Akishita et al., 2010; Hak et al., 2002; Malkin et al., 2010). Few studies have examined the direct cardiac effects of androgens in males or females (Cattabiani et al., 2012; Mathur and Braunstein, 2010; Miller, 2001; Rosano et al., 2005). Women with polycystic ovary syndrome (PCOS) have elevated levels of endogenous androgens and increased CVD risk (Christakou and Diamanti-Kandarakis,

2013; Christian et al., 2003; Guzick et al., 1996; Wild et al., 2000), while low endogenous testosterone levels in elderly men increased the risk of cardiovascular mortality (Laughlin et al., 2008; Wehr et al., 2011). In separate studies acute administration of testosterone produced arterial dilation, increased blood flow and improved myocardial ischaemia in men with CHD (Rosano et al., 1999; Webb et al., 1999). The mechanism underlying beneficial effects of testosterone is not clearly defined. Since testosterone is converted to 17β -oestradiol by the enzyme aromatase, it may be oestrogen that contributes to the vascular actions of testosterone. The dimorphism for sex steroid action may therefore depend upon the balance between testosterone and oestrogen (Dai et al., 2012; He et al., 2007; Kocoska-Maras et al., 2009; Zheng et al., 2012), rather than absolute levels of androgens or oestrogens alone. Further studies are needed to confirm the role of androgens in the development or prevention of IHD.

1.5.3 Gonadal steroids receptors

Sex hormones mediate their cardiovascular actions through interaction with their specific sex steroid hormone receptors. Both androgen (AR) and oestrogen (E2-R) receptors are expressed in male and female hearts (Lizotte et al., 2009; Nordmeyer et al., 2004). Understanding whether the expression and regulation of these receptors is modified during MI may identify the mechanisms for the gender differences.

1.5.3.1 Oestrogens and oestrogen receptors

Oestrogens are female sex hormones and synthesized by the ovaries in premenopausal women. 17β -oestradiol (E2) is the biologically active oestrogen and oestrone (E1) is a

low-potency oestrogen. The conversion of low potency E1 into E2 is metabolized by the 17 β -hydroxysteroid dehydrogenase (17 β -HSD) enzyme (Figure 1.7). E2 can exert both direct and indirect effects on cells (Miller and Duckles, 2008). E2 bind to the nuclear oestrogen receptors (E2-R α and E2-R β) and the cytosolic E2-R-ligand complex translocates into the nucleus to regulate transcription. Both E2-R α and E2-R β have been shown to be expressed in vascular endothelial cells, VSMCs (Mendelsohn, 2000) and cardiomyocytes (Lizotte et al., 2009; Saunders et al., 1997; Savolainen et al., 2001; Taylor and Al-Azzawi, 2000; Xu et al., 2003). E2 binds with similar binding affinity to both E2-R α and E2-R β (approximately 0.05 to 0.3 nM) (Bologa et al., 2006; Kuiper et al., 1998). E2 also binds to a receptor at the plasma membrane. This receptor is either a membrane-resident E2-R variant (Haynes et al., 2002; Pedram et al., 2006a; Simoncini et al., 2000) or the G protein coupled receptor 30 (GPR30) (Filardo, 2002; Filardo and Thomas, 2005; Revankar et al., 2005), which localises to the endoplasmic reticulum (Revankar et al., 2005) or the plasma membrane (Filardo and Thomas, 2005). E2-mediated effects through the activation of membrane-associated E2-R or GPR30 result in transactivation of the epidermal growth factor receptor (EGFR) (Filardo, 2002) and activating phosphatidylinositol 3-kinase (PI3K), mitogen-activated protein kinase (MAPK), NOS and increased levels of second messengers (e.g. cAMP, calcium) (Filardo, 2002; Haynes et al., 2000; Levin, 2009; Marino et al., 2006; Moriarty et al., 2006), which have been shown to be protective. GPR30, however, has very low affinity for E2 (\sim Kd 10^{-7} M) and proposed as unlikely to have physiologic relevance as an oestrogen receptor (Prossnitz et al., 2008; von Lueder et al., 2013).

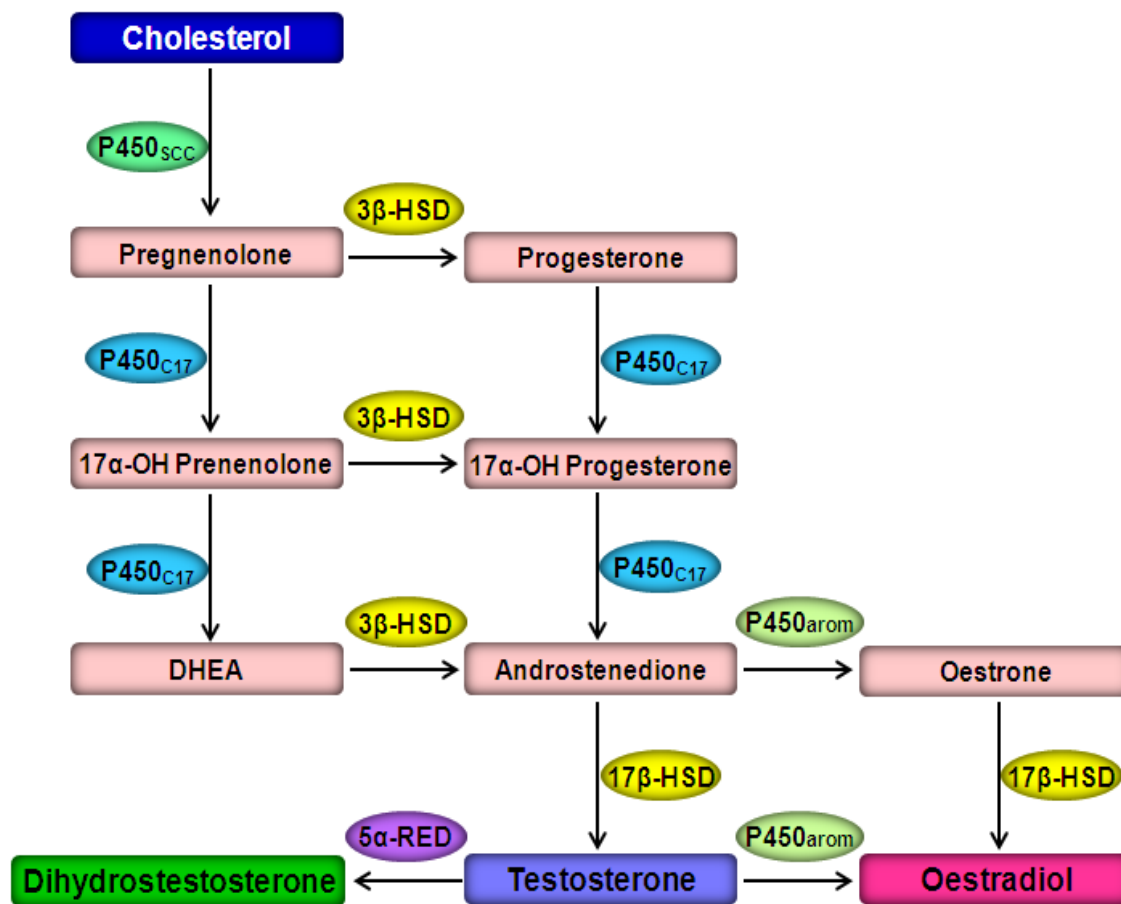


Figure 1.7: Sex steroid hormones synthesis pathways.

All steroid hormones are synthesised from the same precursor, cholesterol. The end product depends on the complement of enzymes present in the cells and tissues. DHEA, dehydroepiandrosterone; P450, cytochrome P450 oxidation enzyme; P450_{SCC}, side chain cleavage; P450_{C17}, 17- α -hydroxylase; 3 β -HSD, 3 β -hydroxysteroid dehydrogenase; 17 β -HSD, 17 β -hydroxysteroid dehydrogenase; P450_{arom}, aromatase; 5 α -RED, 5 α -reductase.

Recently, mitochondrial localised E2-R also been demonstrated in a number of cell types including primary cardiomyocytes (Chen et al., 2009; Pedram et al., 2006b; Yang et al., 2004). The E2-mediated mitochondrial pathway involves the generation of

cellular energy (ATP), mitochondrial respiratory complex and ROS generation that play important roles in regulating cell activities including cell death (Chen et al., 2009). Similarly, Pedram et al. (Pedram et al., 2006b) have shown that E2 inhibits UV-induced release cytochrome c, decrease in mitochondrial membrane potential, ROS production, and apoptosis in breast cancer cells and endothelial cells.

1.5.3.2 Androgens and androgen receptors

Androgens are male sex hormones and primarily synthesized in the testes. The principal androgen is testosterone (T), with active metabolites E2 and dihydrotestosterone (DHT) (Figure 1.7). Cytochrome P450 aromatase converts T to E2 (Diano et al., 1999; Sasano et al., 1999), while 5 α -reductase enzymes reduce T to DHT, a non-aromatisable androgen (Swerdloff and Wang, 1998). DHT is a more potent androgen than T, in that it has higher affinity for the androgen receptor (AR) than T (Saartok et al., 1984; Wilson et al., 1993; Zhou et al., 1995). The effects of T and DHT are mediated by binding to the AR, a member of the steroid receptor superfamily (Mangelsdorf et al., 1995). The classical pathway of androgen action involves steroid binding to the AR; the ligand-receptor complex then translocates into the nucleus to regulate transcription (Mangelsdorf et al., 1995; Quigley et al., 1995). AR have been found in ECs, VSMCs (Liu et al., 2005b) and cardiac myocytes from multiple species including rat and human (Marsh et al., 1998). There appear to be gender differences in AR expression in human vasculature, with higher levels in men than in women (Death et al., 2004; McCrohon et al., 2000; Sader et al., 2005).

1.5.4 Sex hormones in myocardial I-R injury

Gender differences in cardioprotection have been reported in a few animal studies, suggesting that intact females (pre-menopausal) show less cardiac damage following ischaemia-reperfusion than males (Bae and Zhang, 2005; Wang et al., 2006). Female hearts subjected to global ischaemia followed by reperfusion had smaller infarcts (37%) than male hearts (48%) (Bae and Zhang, 2005) and significant improvement in post-ischaemic recovery of the maximum rate of pressure development and relaxation ($+/-dP/dt$) compared to males (Wang et al., 2006). Under conditions of increased contractility or elevated Ca^{2+} , there is reduced I-R injury in female compared to male hearts (Cross et al., 2002; Gabel et al., 2005; Kam et al., 2004). Protection may relate to the ability of the female heart to reduce Ca^{2+} loading during I-R, as it is known that elevated Ca^{2+} levels increase during reperfusion injury (Steenbergen et al., 1987). Lower levels of β 1-adrenergic receptor (β 1-AR) expression in intact females may provide an explanation for the reduced Ca^{2+} overload and protect the heart from injury (Chen et al., 2003a). In contrast to these findings, other *ex vivo* and *in vivo* studies have not demonstrated differences between males and females in I-R injury (Cross et al., 1998; Li and Kloner, 1995; Przyklenk et al., 1995; Schuit et al., 2005).

Gender also appears to be an important determinant of the incidence of cardiomyocyte cell death. In clinical studies less cardiomyocytes necrosis and apoptosis was observed in the normal and failing hearts of females compared to males (Guerra et al., 1999; Mallat et al., 2001; Olivetti et al., 1995). A higher levels of myocyte death in men is associated with an earlier onset heart failure (Guerra et al., 1999). Additionally, sex differences may occur at the cellular level, in that cells from males show a higher

susceptibility to apoptosis than autophagy, while cells from females show a higher resistance to apoptosis and susceptibility to autophagy in response to oxidant stress and metabolic disturbances (Alvarez et al., 1997; Maselli et al., 2009; Straface et al., 2012; Straface et al., 2009). These observations suggest the possibility that female sex hormones, such as oestrogen, may have a cardioprotective role while androgens, such as testosterone, have a detrimental effect on the development of CHD.

1.5.4.1 Effects of oestrogens during myocardial I-R

There have been numerous *in vitro* studies investigating the effects of E2 in multiple cell systems, with the collective findings strongly suggesting protective effects of E2. These effects include preventing TNF- α activated ERK1/2 signaling and reducing apoptosis in human umbilical vein endothelial cells (HUVEC) (Ling et al., 2006), reducing H₂O₂-induced apoptosis (Lu et al., 2007), and increasing levels of the anti-apoptotic Bcl-2 and Bcl-xL in endothelial cells (Florian and Magder, 2008). Similarly, E2 inhibits apoptosis in cardiomyocytes as demonstrated by reduced activity of caspase-3 and NF- κ B transcription factors (Pelzer et al., 2000) and the nuclear accumulation of activated Akt (Camper-Kirby et al., 2001), a protein kinase that regulates a broad range of responses including cell survival (Kandel and Hay, 1999). Furthermore, in cultured neonatal rat cardiomyocytes subjected to *in vitro* system of hypoxia/reoxygenation to simulate I-R injury, E2-activated E2-Rs and suppressed mitochondrial ROS generation through PI3K signalling lead to myocyte survival (Kim et al., 2006a).

In contrast, other studies have demonstrated that E2, at physiological concentrations, increases apoptosis in human coronary artery endothelial cells by upregulation of Fas

and FasL expression (Seli et al., 2006). In human aortic VSMCs, E2-induced apoptosis manifests through a non-genomic mechanism mediated by p38 and E2-R α (Mori-Abe et al., 2003). Moreover, physiological concentrations of E2 have dual effects on rat VSMCs, simultaneously promoting proliferation of VSMCs and inducing apoptosis through up-regulation of Bax via the p38-MAPK pathway (Yang et al., 2007). These findings suggest that E2 has additional effects that may counteract the beneficial actions.

Myocardial salvage achieved by primary PCI for acute MI is greater in women compared with men (Mehilli et al., 2005) with animal studies, showing females had smaller infarct sizes compared with age-matched males (Bae and Zhang, 2005; Johnson et al., 2006; Zheng et al., 2011). Furthermore, replacement or treatment of animals with E2 prior to *in vivo* coronary artery ligation reduced I-R injury in both males and females as indicated by smaller infarct size (Booth et al., 2003; Booth et al., 2007; Booth et al., 2005; Das and Sarkar, 2006; Hale et al., 1997; Lee et al., 2004; Li and Kloner, 1995; Patten et al., 2004; Sbarouni et al., 1998; van Eickels et al., 2003) and less apoptosis (Patten et al., 2004; van Eickels et al., 2003).

Moreover, human myocardial samples from premenopausal females had a greater nuclear accumulation of the activated Akt and reduced cardiomyocyte apoptosis compared with normal males and postmenopausal females (Camper-Kirby et al., 2001). In *ex vivo* experimental myocardial I-R, females constitutively expressed a significantly lower pro-apoptotic Bax-to-Bcl-2 ratio and higher anti-apoptotic protein ARC than male or ovariectomized female rabbits (Bouma et al., 2010). Similarly E2-mediated anti-

apoptotic effects were observed in ovariectomised female mice *in vivo*, in which E2 replacement increased activation of Akt and decreased cardiomyocyte apoptosis after MI (Patten et al., 2004).

Although E2 appears cardioprotective during myocardial I-R damage, some adverse effects of E2 treatment on ventricular remodelling and mortality have been reported in animals with MI (van Eickels et al., 2003; Zhan et al., 2008). The diverse effects of E2 may be due to differences in the levels of E2, with detrimental effects of high E2 concentrations but not at physiological levels (Jovanovic et al., 2000; Meng et al., 2011; Zhan et al., 2008). For example, supplementing E2 to ovariectomised mice for 8 weeks with low-dose E2 (0.42 µg/day), restored plasma levels close to physiological levels and improved cardiac function and remodelling following MI; whereas higher moderate (4.2 µg/day) and very high (18.8 µg/day) doses exacerbated cardiac fibrosis, hypertrophy, dysfunction and dilatation (Zhan et al., 2008).

1.5.4.2 Effects of androgens during myocardial I-R

In comparison with other androgen target organs, the heart can accumulate testosterone at higher concentrations (Krieg et al., 1978), and functional AR are present in isolated cardiomyocytes (Zhang et al., 1998). However, little information exists regarding the role of physiological levels of testosterone in cardiac injury. Testosterone has pro-inflammatory and/or pro-apoptotic effects in vascular cells, with increased VSMC apoptosis in a dose-dependent manner (Bowles et al., 2007). High testosterone levels enhance acute myocardial inflammation and increase cardiac rupture, leading to deterioration of cardiac function after MI (Cavasin et al., 2006). Blocking AR, by

flutamide or removing testosterone by gonadectomy (Gx), decreases myocardial injury and improves myocardial function after I-R in adult male rats (Huang et al., 2010; Wang et al., 2005; Wang et al., 2009). In comparison with untreated males, Gx male and flutamide-treated male hearts had decreased pro-inflammatory cytokines (TNF- α , IL-1, IL-6), decreased pro-apoptotic proteins (caspase-3, FasL), increased anti-apoptotic protein (Bcl-2), decreased activation of p38 MAPK while increased activation of Akt after I-R (Huang et al., 2010; Wang et al., 2005). Acute perfusion of isolated hearts with testosterone increased activation of MAPKs and caspase-3 following I-R; however, there were no significant differences in the myocardial proinflammatory cytokine production (Crisostomo et al., 2006). Consistently, the number of apoptotic cells was increased by testosterone in neonatal and adult cardiomyocytes (Kohno et al., 2007; Welder et al., 1995; Zaugg et al., 2001).

Several animal studies have shown that exogenous T or DHT treatment aggravate cardiac damage during I-R in males and females (Cavasin et al., 2003; Cavasin et al., 2006; Crisostomo et al., 2006; Huang et al., 2010; Wang et al., 2005; Wang et al., 2009). Contrary to the adverse effects, a number of studies show neutral (Nam et al., 2007a; Rubio-Gayosso et al., 2013) or protective effects (Chen et al., 2012a; Kuhar et al., 2007; Liu et al., 2012). The variable results may be related to whether low or high doses were administered (Cavasin et al., 2003; Chen et al., 2012a; Crisostomo et al., 2006; Liu et al., 2012) and the route of administration (Stokes et al., 2000). Additionally, variability may be a result of whether the androgen used was testosterone, which is aromatised to E2, or DHT (Rubio-Gayosso et al., 2013). Metabolism of T to E2 diversifies its action as E2 acts through binding and activation of either of the E2-R

isoforms, E2-R α or E2-R β , resulting in activation of different set of genes to that regulated by T binding its cognate receptor, AR. Indeed, there is increasing evidence that the cardioprotective effects of T in male animals is via its aromatisation to E2 (Bell et al., 2011a; Chen et al., 2012a; Rubio-Gayosso et al., 2013). However, DHT treatment resulted in the opposite effects to T, increasing myocardial damage during I-R in males (Rubio-Gayosso et al., 2013).

1.6 Corticosteroids and the mineralocorticoid receptor

1.6.1 Overview

To determine the actions of corticosteroids and the mineralocorticoid receptor (MR) during MI requires a brief summary of the renin-angiotension-aldosterone system (RAAS) which is important in regulating blood pressure and cardiac function. The system consists of several important components including renin, angiotensin and aldosterone (Figure 1.8). Renin is released from the kidneys into circulation and acts as substrate for angiotensinogen that undergoes proteolytic cleavage to form angiotensin I. Angiotensin I then cleaves off two amino acids by angiotensin converting enzyme (ACE) to form angiotensin II. The formation of angiotensin in blood and tissues, in turn, stimulates the release of aldosterone from the adrenal cortex (Mulrow, 1999; Zaman et al., 2002). Aldosterone secretion is also stimulated by adrenocorticotrophic hormone (ACTH), sodium and potassium levels (Merrill et al., 1989; Quinn and Williams, 1988; Zaman et al., 2002). Activation of RAAS has been implicated in the pathogenesis of CVD including AMI and HF. The hormones in the RAAS, in particular angiotensin II and aldosterone, have direct detrimental effects on the myocardium contributing to cardiac remodelling and cardiac failure (Edelmann et al., 2012; Huggins et al., 2003;

von Lueder et al., 2013; Weir et al., 2011). Blockade of this system with ACE inhibitors or angiotensin receptor blockers (ARB) have shown benefit in MI and HF (Gajarsa and Kloner, 2011; Mentz et al., 2012), although they do not suppress plasma levels of aldosterone. During prolonged treatment with ACE inhibitors or ARB (Borghi et al., 1993; Struthers, 1996), plasma levels of aldosterone are increased indicating targeting blockade of aldosterone is also required.

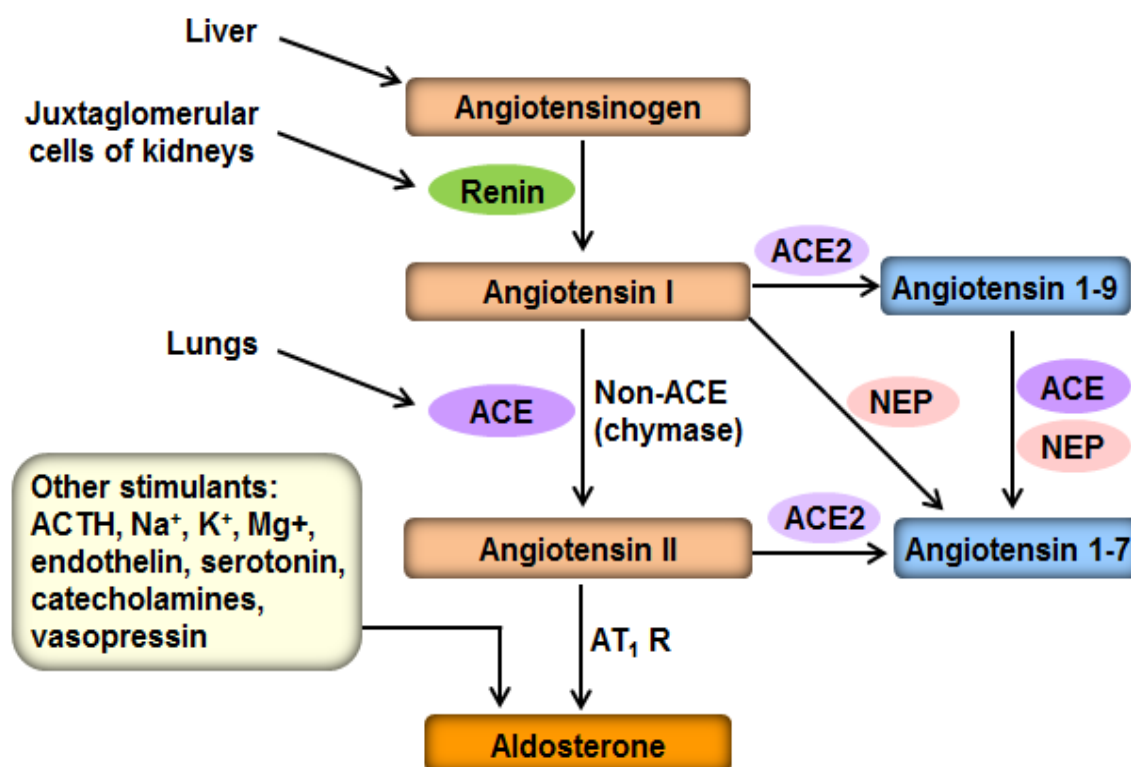


Figure 1.8: Synthesis pathway for the renin-angiotensin-aldosterone system.

ACE, angiotensin-converting enzyme; ACE2, angiotensin-converting enzyme 2; ARB, angiotensin receptor blockers; NEP, neutral endopeptidase; AT₁R, angiotensin II type 1 receptor; ACTH, adrenocorticotropic hormone. (Modified from von Lueder et al., 2013 and Zaman et al., 2002).

1.6.2 Corticosteroids

Both mineralocorticoids (include aldosterone) and glucocorticoids (include cortisol) hormones are known as corticosteroids and play an important role in cardiovascular pathogenesis including cardiac hypertrophy (Mannic et al., 2013; Ren et al., 2012; Tsybouleva et al., 2004), inflammation and cardiac fibrosis (Lin et al., 2012; Rickard et al., 2012; Zhu et al., 2012), left ventricular remodelling post-MI (Hayashi et al., 2001; Weir et al., 2011) and HF (Guder et al., 2007). Corticosteroids are synthesised from cholesterol within the adrenal cortex (as shown in Figure 1.9). Adrenal glomerulosa cells mainly synthesise and secrete the mineralocorticoids, with aldosterone being the major mineralocorticoid, while the adrenal fasciculate cells synthesise and secrete the glucocorticoids (Yanagibashi et al., 1986). This subspeciality is largely due to the complement of biosynthetic enzymes present (Hanukoglu, 1992; Miller and Auchus, 2011).

At physiological levels these hormones are involved in a wide range of physiological processes including immune response, stress response, regulation of inflammation, blood electrolyte levels and behaviour (Gupta and Bhatia, 2008). Mineralocorticoids (aldosterone) maintain water and electrolyte balance by acting upon the distal tubules and collecting ducts of the kidney (Cooper and Hunter, 1994), while glucocorticoids (cortisol) regulate metabolic activity, immune function and behaviour (Munck and Guyre, 1986).

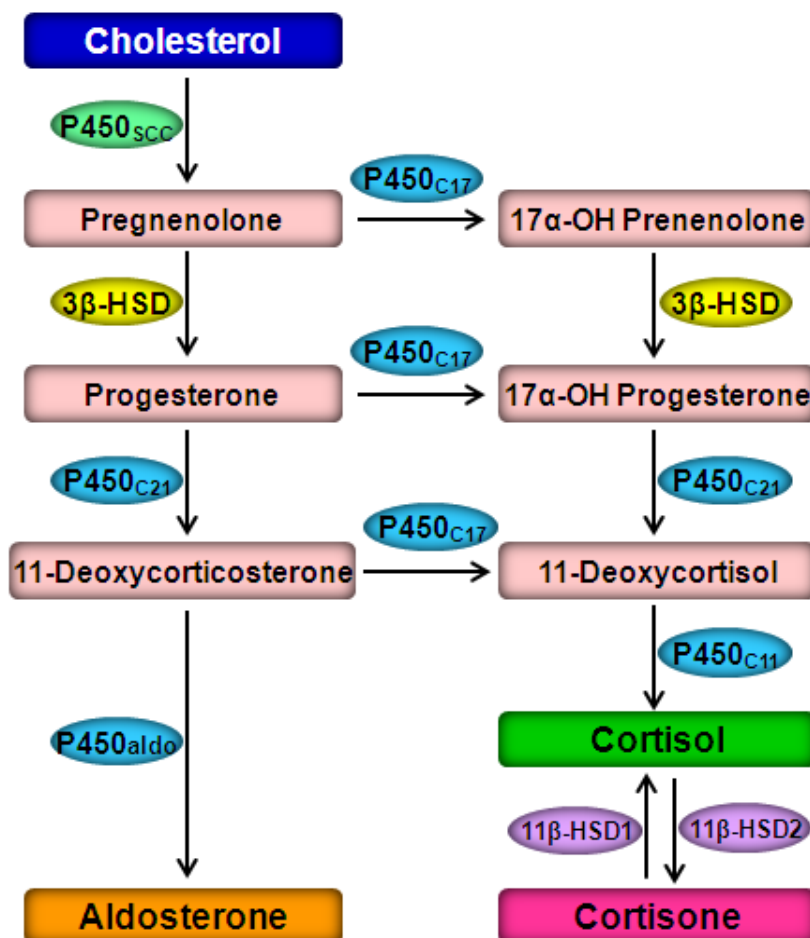


Figure 1.9: Mineralocorticoid (aldosterone) and glucocorticoid (cortisol in human and corticosterone in rodents) synthesis pathway.

Mineralocorticoids and glucocorticoids are synthesised in the adrenal cortex. Adrenal glomerulosa cells mainly synthesise and secrete the mineralocorticoid, while the adrenal fasciculate cells synthesise and secrete the glucocorticoids. All steroid hormones are synthesised from the same precursor, cholesterol. The end product depends on the complement of enzymes present in the cells and tissues. P450, cytochrome P450 oxidation enzyme; P450_{SCC}, side chain cleavage; P450_{C11}, 11-hydroxylase; P450_{C17}, 17- α -hydroxylase; P450_{C21}, 21-hydroxylase; P450_{aldo}, aldosterone synthase; 3 β -HSD, 3 β -hydroxysteroid dehydrogenase; 11 β -HSD, 11 β -hydroxysteroid dehydrogenase.

These hormones exert their biological effects by binding to the mineralocorticoid (MR) and glucocorticoid (GR) receptors (Arriza et al., 1987; Weinberger et al., 1985). MR is a member of the nuclear receptor superfamily in a closely-related subfamily 3, group C, member 2, (NR3C2). MR is closely related to GR/AR/PR (progesterone receptor) within this family of hormone receptors, and MR and GR are the most closely related, sharing several features in common. The ligand binding domain of MR and GR show ~57% amino acid identity, consistent with their ability to bind glucocorticoid hormones. MR and GR are highly homologous in the DNA-binding domain, sharing an amino acid identity of 94%. The N-terminal regions of MR and GR are the most divergent, sharing only 15% amino acid identity. Although MR and GR are closely related, MR displays ~10-fold higher affinity for corticosteroids than GR (0.5 nM vs. 5 nM, respectively for corticosterone), and has been shown to predate the evolution of aldosterone (Kassahn et al., 2011). MR binds aldosterone and the physiologic glucocorticoids with similar affinity (Arriza et al., 1987; Funder et al., 1988; Krozowski and Funder, 1983), but the affinity of GR for aldosterone is very much lower [$K_d = \sim 85$ nM (GR) vs $K_d = \sim 0.6$ nM (MR)], and aldosterone does not appear to act via GR at physiological concentrations (Gaeggeler et al., 2005).

1.6.3 Structural & functional domain of MR

To envisage how these hormones might regulate cardiovascular function we need to understand the structure-function relationships in the receptor through which they exert their effects, the mineralocorticoid receptor (MR). The human MR (hMR) gene (NR3C2) is located on the chromosome 4 in the q31.1 region (Fan et al., 1989). It spans approximately 450 kb (Morrison et al., 1990; Zennaro et al., 1995), and contains 10

exons. The first two exons (1 α & 1 β) are untranslated; the remaining eight exons encode a 984 amino acid protein with molecular weight of 107 kD (Figure 1.10) (Viengchareun et al., 2007). The rat MR (rMR) gene is located on chromosome 19q11 and has three untranslated exons (1 α , 1 β & 1 γ), and the eight translated exons encoding a 981 amino acid protein (Kwak et al., 1993). Similarly, the mMR gene encodes a 978 amino acid protein.

Similar to other nuclear receptors, MR protein contains three main functional domains (shown in Figure 1.10): (i) an N-terminal domain (NTD) important for transcriptional regulation of specific target genes, (ii) a central DNA-binding domain (DBD) that mediates receptor/DNA interactions, and a hinge region linking them to (iii) a carboxy-terminal ligand binding domain (LBD) important for ligand recognition and binding.

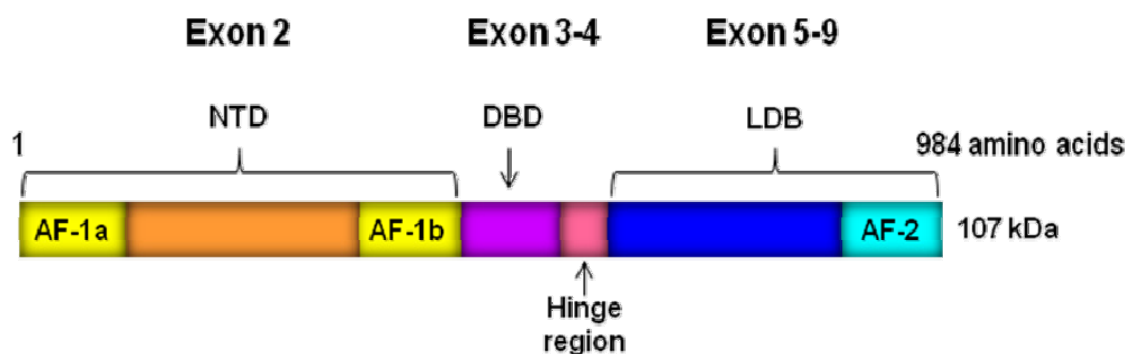


Figure 1.10: Structure of the MR.

The mineralocorticoid receptor consists of three functional domains: (i) N-terminal domain (NTD), exon 2; (ii) DNA binding domain (DBD) and a bipartite nuclear targeting signal within the hinge region, exons 3-4; (iii) The C-terminal region containing the ligand-binding domain (LBD), exons 5-9. AF-1a, activator factor 1a; AF-1b, activator factor 1b; AF-2; activator factor 2.

The NTD of MR is the largest of the steroid receptor family, consisting of 604 amino acids (Zennaro et al., 1995). Structure-function studies have demonstrated that the NTD is important for the regulation of transcription and to interact with transcriptional co-activators (Fischer et al., 2010; Tallec et al., 2003). The NTD contains the first activation function-1 (AF-1, AF-1a and AF-1b) domain. The AF-1 domain is located in the middle of the MR-NTD (residues 328–382) and is important for transactivation (Govindan and Warriar, 1998). Other AF-1 domains are AF-1a and AF-1b which have distinct protein regions (residues 1–167 and 445–602 respectively) (Fuse et al., 2000; Tallec et al., 2003). These activation function domains recruit coregulators important for MR transcriptional activity as well as selectivity (Pascual-Le Tallec and Lombes, 2005). These coactivators act as adapters that recruit CREB-binding protein/p300/SRC-1 complexes and promote transcriptional activity of the receptor (McKenna et al., 1999b).

The DBD is the most highly conserved region across the steroid receptors, with >90% identity with that of GR, AR and PR (Viengchareun et al., 2007), recognising specific target DNA sequences (hormone response elements: HRE). Structurally, it folds into two perpendicular alpha helices and coordinates with two zinc molecules in the classic zinc-finger binding domain fold. The zinc fingers contains the “P box” and “D box” responsible for tight binding to the minor groove on the DNA double helix and involved in receptor homo- and hetero-dimerization (Liu et al., 1995; Pippal and Fuller, 2008). MR, GR, AR and PR are known to bind the AGAACA half site, through this domain, and thereby alter transcription (Pippal and Fuller, 2008). The flexible hinge or D region,

located between DBD and LBD, permits a twist of the DBD relative to the LBD (Pawlak et al., 2012), although the function of this region is not clearly defined.

The LBD of the MR is highly conserved across species (80-97% homology) (Viengchareun et al., 2007) and is similar to that of the GR in that it binds aldosterone and glucocorticoids (cortisol in human and corticosterone in rodents) equally well (Arriza et al., 1987). The C-terminal domain is also important for interactions of the MR with cofactor proteins and chaperones, such as the heat shock proteins. In the basal state, MR are associated with protein chaperones (Hsp90, Hsp70, Hsp40, Hop, p23, FK-binding proteins) (Faresse et al., 2010), the tumor suppressor gene 101 (Tsg101) (Faresse et al., 2012) and the phosphatase calcineurin PP2BA β (Seiferth et al., 2012). Inhibition of Hsp90 with 17-AAG (17-allylamino-17-demethoxygeldanamycin) induced MR degradation in ECs by increasing the association between MR and the ubiquitin-protein ligase CHIP (COOH terminus of Hsp70-interacting protein) (Faresse et al., 2010). It has been shown that aldosterone-modulated the ubiquitylation state of the receptor in ECs by inducing phosphorylation of MR and disruption of MR/Tsg101 association. These events rapid destabilize of MR and regulate its degradation by the ubiquitin proteasome pathway (Faresse et al., 2012). Similarly, treatment with aldosterone decreases hMR protein expression in transfected COS-1 cells (Yokota et al., 2004), effect was blocked by treatment with proteasome inhibitors (ALLnL or MG132).

Other important functions of the LBD include dimerisation and hyper-phosphorylation that induce conformational changes required for transactivation (Couette et al., 1996; Couette et al., 1998). The LBD also contains the C-terminal activation function 2 (AF-

2) domain (Pascual-Le Tallec and Lombes, 2005; Pippal and Fuller, 2008; Viengchareun et al., 2007). The AF-2 is a hydrophobic groove on the surface of the LBD that interacts with coactivators containing an LxxLL motif (Bledsoe et al., 2005; Li et al., 2005; Pippal and Fuller, 2008). Ligand-induced functional synergism between the AF-1 and AF-2 mediates through their interaction with transcriptional coregulators (McKenna et al., 1999a; Rogerson and Fuller, 2003). Although LBD is important for ligand binding, the NTD appears to account for ~40-50% of total transactivation and represents a key determinant of MR specificity (Lim-Tio et al., 1997; Pascual-Le Tallec and Lombes, 2005).

1.6.4 MR expression

MR is expressed in the epithelial target tissues of the kidney and the colon, as well as non-epithelial tissues such as brain and heart (Gomez-Sanchez et al., 2006). In the heart, MR are present in cardiomyocytes (Gomez-Sanchez et al., 2006; Lombes et al., 1992; Pearce and Funder, 1987), fibroblasts (Lothar et al., 2011), VSMCs, ECs (Kornel, 1994; Lombes et al., 1992) and macrophages (Rickard et al., 2009). In epithelial target tissues, such as the kidney, MR regulates sodium balance in response to aldosterone and other factors, including changes in plasma K^+ and Na^+ concentrations. Epithelial MR selectivity for aldosterone is conferred by expression of the enzyme 11 beta-hydroxysteroid dehydrogenase II (11β -HSD2) that converts cortisol to the inactive cortisone which does not bind to MR (Edwards et al., 1988; Funder et al., 1988). However, 11β -HSD2 is not expressed in cardiomyocytes (Sheppard and Autelitano, 2002), therefore endogenous glucocorticoids normally occupy cardiomyocyte MR but do not mimic aldosterone, and normally act as MR antagonists (Gomez-Sanchez et al.,

1990; Sato and Funder, 1996; Young and Funder, 1996).

Under basal conditions, MR are localised to both nuclei and the cytosol of myocytes (both H9c2 cells and sections of rat heart, (Gomez-Sanchez et al., 2006), with even distribution of unliganded receptors between the nucleus and the cytoplasm in a variety of cells (Fejes-Toth et al., 1998; Hernandez-Diaz et al., 2010; Nishi et al., 2001; Walther et al., 2005). In addition, studies using fluorescence resonance energy transfer and co-immunoprecipitation have reported MR can co-localise with EGFR (Grossmann et al., 2010) and caveolin-1 and -3 (Ricchiuti et al., 2011) in the plasma membrane. Moreover, aldosterone binding sites have been detected on the plasma membrane of human endothelial cells by atomic force microscopy (Wildling et al., 2009). However, the characteristics and functional role of such MR membrane sites are not unclear.

MR expression has been found to be upregulated in hearts from patients with congestive HF (Yoshida et al., 2005). Similarly, in animal models of experimental MI, levels of MR protein were increased in the left ventricle after MI (2-4 weeks) (de Resende et al., 2006; Milik et al., 2007; Takeda et al., 2007) and were attenuated by chronic treatment with spironolactone (Takeda et al., 2007). Interestingly, aldosterone also decreases hMR protein expression in transfected COS-1 cells (Yokota et al., 2004), an effect blocked by treatment with proteasome inhibitors (ALLnL or MG132). There have been no studies to determine myocardial MR expression in short-term or acute MI.

1.6.5 Mechanism of action for MR: genomic and non-genomic

The biological effects of aldosterone in cells are mediated by both genomic and non-genomic mechanisms (Figure 1.11; Moura and Worcel, 1984). The genomic action of aldosterone involves aldosterone binding to the cytosolic MR, and nuclear translocation followed by modulation of transcriptional Cytosolic MR are normally attached to multi-protein chaperones (Hsp90, Hsp70, Hsp40, Hop, Hsp90-binding co-chaperone p23) and co-chaperones (FK-binding proteins (FKBP51/52), cyclophilin 40 (Cyp40), serine-threonine protein phosphatase 5 (PP5), Tpr2). These serve to hold the receptor in a conformation that facilitates hormone binding (Echeverria and Picard, 2010). Once aldosterone is bound, a conformational change is induced which allows the chaperone complexes to dissociate from the receptor and activation of the MR. The aldosterone-MR complex translocates to the nucleus, undergoes homodimerization and binds to hormone response elements (HREs) present in the promoter of responsive genes. This results in the complex recruitment of the transcriptional machinery and induces gene transcription into mRNA off the DNA sequence (Fuller and Young, 2005). The expression of a number of genes is regulated by MR, including the epithelial Na⁺ channel (ENaC) (Asher et al., 1996), serum-regulated kinase 1 (Sgk-1) (Chen et al., 1999; Naray-Fejes-Toth and Fejes-Toth, 2000), plasminogen activator inhibitor 1 (PAI-1) (Chun and Pratt, 2005) and Na⁺/K⁺-ATPase (Kolla and Litwack, 2000).

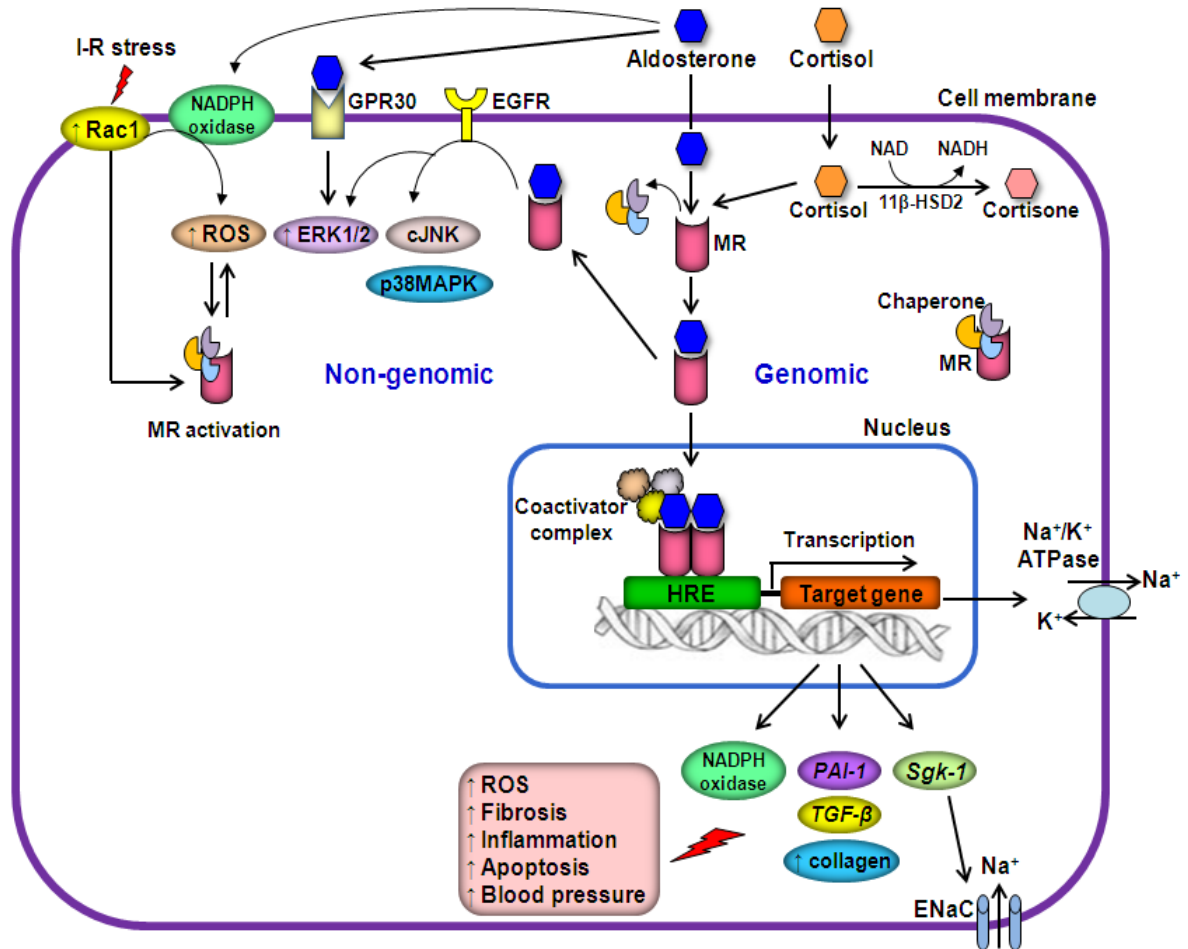


Figure 1.11: Genomic (right) and non-genomic (left) action of aldosterone.

MR, mineralocorticoid receptor; GPR30, G protein-coupled receptor 30; EGFR, epidermal growth factor receptor; HRE, hormone response elements; Sgk-1, serum-regulated kinase 1; PAI-1, plasminogen activator inhibitor 1; ROS, reactive oxygen species; TGF- β , transforming growth factor- β ; ERK1/2, extracellular signal regulated kinase 1/2; cJNK, c-Jun N-terminal kinase; p38MAPK, p38 mitogen-activated protein kinase.

The non-genomic effects of aldosterone occur rapidly after stimulation (seconds to minutes) and include activation of the second messengers protein kinase C (PKC) (Alzamora et al., 2007; Darling et al., 2013; Jennings and Reimer, 1991; Mihailidou et al., 2004), Na⁺/H⁺ exchange (NHE), extracellular signal regulated kinase 1/2 (ERK1/2) (Gekle et al., 2001; Grossmann et al., 2005; Ram and Trivedi, 2012; Surder et al., 2010), and increases intracellular Ca²⁺ and pH (Alzamora et al., 2000; Wehling et al., 1996), and NADPH oxidase-mediated ROS production (Hayashi et al., 2008). Evidence for rapid non-genomic aldosterone effects have been studied in different cells and tissues including VSMC, skin cells from MR-knockout mice, neonatal rat and isolated rabbit cardiomyocytes, trabeculae and coronary arteries. The non-genomic effects of aldosterone are not blocked by inhibitors of transcription and protein synthesis (Hayashi et al., 2008; Mihailidou et al., 2004) and mediated through MR-dependent and MR-independent mechanisms (Barbato et al., 2002; Chai et al., 2005; Michea et al., 2005; Rossol-Haseroth et al., 2004).

Rapid non-genomic aldosterone effects have also observed clinically in healthy subjects was associated with an increase in vascular resistance within first 3-5 minutes (Schmidt et al., 1999; Wehling et al., 1998) and changes in cardiac output and cardiac index after 3 minutes (Wehling et al., 1998). Continuous infusion of aldosterone acutely limits forearm blood flow, between 4 and 8 minutes (Schmidt et al., 2003). Perfusion of the isolated rat heart with aldosterone induces positive inotropic and vasoconstrictor effects within 1-2 minutes which are not blocked by spironolactone (Chai et al., 2005). Similarly, aldosterone rapidly (within 2-5 minutes) increases contractility in rat heart (Barbato et al., 2002), decreases in coronary blood flow, fractional shortening and

lactate extraction rate in non-ischaemic and ischaemic hearts (Fujita et al., 2005). These rapid effects of aldosterone were blocked by PKC inhibition but not spironolactone in dog heart (Fujita et al., 2005).

Investigations into the mechanisms underlying the rapid effects of aldosterone indicate some of these rapid effects are mediated by the G protein-coupled receptor 30 (GPR30 or GPER1) (Gros et al., 2011b; Ji et al., 1998). GPR30 is located at the cell membrane and in the endoplasmic reticulum of transfected cells (Filardo et al., 2007; Revankar et al., 2005; Revankar et al., 2007), and is widely expressed in a variety of tissues including heart, lung, liver and brain (Deschamps and Murphy, 2009; Jessup et al., 2010; O'Dowd et al., 1998), and in freshly isolated cardiac myocytes (Deschamps and Murphy, 2009), vascular smooth muscle and endothelial cells (Ding et al., 2009). Rapid activation of ERK1/2 and apoptosis by aldosterone in vascular smooth muscle cells is GPR30-dependent (Gros et al., 2011b). Conversely, activation of GPR30 improves functional recovery and decreases inflammation during myocardial I-R in the rat (Weil et al., 2010). Although studies suggest GPR30 is a putative membrane receptor mediating MR-independent rapid aldosterone signalling, further studies are required to determine whether GPR30 mediates the direct actions of aldosterone on the heart.

1.6.6 Effects of MR regulation in the cardiovascular system

Substantial evidence has suggested that aldosterone directly exerts adverse effects on the cardiovascular system. MR effects on the heart include oxidative stress, endothelial dysfunction, inflammation, fibrosis and vascular cell apoptosis.

1.6.6.1 Oxidative stress

A number of studies support a specific role of the MR as a mediator of oxidative stress and subsequent inflammation (Sun et al., 2002), fibrosis (Bienvenu et al., 2012), atherosclerosis (Keidar et al., 2004) and apoptosis (Patni et al., 2007). Indeed, aldosterone upregulates various subunits of NADPH oxidase (NOX2, p22phox, p40phox, gp91) and induces ROS generation in various cell types (mononuclear, VSMCs and neonatal cardiomyocytes) (Ahokas et al., 2005; Calo et al., 2004; Hayashi et al., 2008; Schafer et al., 2013; Sun et al., 2002). Aldosterone also decreased G6PD expression and impaired endothelial function (Leopold et al., 2007). These effects of aldosterone on ROS production and G6PD expression were blocked by anti-oxidants or free radical scavenger (tempol), and MR antagonists (Hayashi et al., 2008; Leopold et al., 2007). MR blockade improved impaired endothelial function by decreasing NAD(P)H oxidase subunit p22phox expression, NAD(P)H oxidase activity and superoxide anion generation in chronic HF (Bauersachs et al., 2002) and atherosclerosis (Rajagopalan et al., 2002). A recent study demonstrated that MR blockade prevented ROS production and vascular p22phox upregulation early after MI (Sartorio et al., 2007). Furthermore, MR blockade with spironolactone (50 mg/kg/day) was shown to improve nephropathy in diabetic hypertensive rats by restoring G6PD activity, GSH/GSSG ratio and an overall reduction in oxidative stress (Pessoa et al., 2012)

Although MR are activated during aldosterone excess, they can also be activated in states where aldosterone concentrations are in the low-normal range (Matsui et al., 2008a; Williams et al., 2004). Oxidative stress is recognized as a major contributor to cardiac pathology including reperfusion injury (as reported in section 1.4.1). Several

reports suggest that oxidative stress enhances MR signal transduction. For instance, MR signalling is enhanced in the heart and kidney of obese hypertensive rats with excessive salt intake, whereas the antioxidant Tempol suppressed MR activation and reduced target organ damage (Matsui et al., 2008a; Nagase et al., 2007). The MR-mediated chronotropic, pro-arrhythmogenic response in cultured cardiomyocytes was enhanced by oxidative stress (Rossier et al., 2008). Furthermore, glucocorticoids activate cardiomyocyte MR during experimental MI, a condition with increased oxidant concentrations, and aggravated cardiac damage (Mihailidou et al., 2009). However, the exact mechanisms by which oxidant stress induces MR activation have not been clearly elucidated.

Recent studies identified a ligand-independent pathway of MR activation by Rac1, a Rho family small GTPase, through analysis of RhoGDI α knockout mice (Shibata et al., 2008). The Rac1-mediated MR activation pathway contributes to the pathogenesis of chronic kidney disease (Shibata et al., 2008) and salt-sensitive hypertension (Shibata et al., 2011). RacGTPase is a component of NADPH oxidase (Lambeth, 2004). ROS activates Rac1, which in turn, produces ROS via NADPH oxidase activation, leading to the formation of a feed-forward loop between Rac1 and ROS (Gonzalez-Santiago et al., 2006; Ho et al., 2006). In cultured rat cardiomyocytes (H9c2), BSO-evoked oxidative stress activates Rac1, which, in turn, causes MR activation, as evidenced by enhanced MR-driven transcriptional activity and nuclear accumulation of MR (Nagase et al., 2012). These enhancing effects of BSO were abrogated by two Rac inhibitors, NSC23766 (Shibata et al., 2008) and EHT1864 (Desire et al., 2005), as well as expression of dominant-negative Rac1 construct. The effects of Rac1 on MR are

blocked by spironolactone (Shibata et al., 2008); however, further studies are needed to elucidate the precise mechanisms of MR activation by Rac1.

1.6.6.2 Inflammation, fibrosis and atherosclerosis

Elevated plasma aldosterone are accompanied by a pro-inflammatory and -fibrogenic vascular phenotype (Ahokas et al., 2005; Blasi et al., 2003; Sun et al., 2002) and blocked by both spironolactone and anti-oxidants (Sun et al., 2002). In addition, aldosterone stimulates collagen synthesis in cardiac fibroblasts (Brilla et al., 1994) which ultimately induces cardiac fibrosis (Ahokas et al., 2005). Evidence for aldosterone enhancing plaque formation was demonstrated in an animal model of atherosclerosis. Aldosterone infusion increased overall aortic plaque area with enhanced vascular and macrophage oxidative stress (Keidar et al., 2004). The MR antagonists and aldosterone synthase inhibitors inhibited atherosclerosis and inflammation as well as attenuated macrophage oxidative stress in animal models (Gamliel-Lazarovich et al., 2010; Keidar et al., 2003; Rajagopalan et al., 2002; Suzuki et al., 2006). Furthermore, the role of MR in regulating cardiac fibrosis has been demonstrated in mice with specific monocyte/macrophage MR deletion, which protects against chronic mineralocorticoid/salt-induced cardiac fibrosis and increased systolic blood pressure (Rickard et al., 2009).

1.6.6.3 Apoptosis

Aldosterone is now recognised as an important modulator of myocyte apoptosis (Mano et al., 2004). In cultured adult rat ventricular myocytes (De Silva et al., 2009), human renal proximal tubular (HK2) cells (Patni et al., 2007) and human mesangial cells *in*

vitro and *in vivo* (Mathew et al., 2008) aldosterone promotes apoptosis as indicated by increasing TUNEL positivity, caspase-3 activation and expression of Bax and p53. Moreover, aldosterone decreases Bcl-2 protein expression. Chronic treatment with aldosterone induced caspase-3 activity which was prevented by pre-treatment with spironolactone in heart and skeletal muscle (Burniston et al., 2005). In *in vitro* aldosterone treatment impairs Akt activation in VSMCs (Hitomi et al., 2007), a pro-apoptotic effect inhibited by eplerenone and spironolactone (De Silva et al., 2009; Mathew et al., 2008). Similarly, antioxidants and free radical scavengers attenuated the pro-apoptotic effects of aldosterone (Mihailidou et al., 2009; Patni et al., 2007).

Anti-apoptotic effects of MR blockade have been demonstrated in both *in vitro* and *in vivo* systems. In cultured ECs, spironolactone (10 μ M) inhibits of caspase-3 activity, cytochrome c release and PARP cleavage induced by serum-deprivation, although this effect has been suggested to be mediated by an agonist effect of spironolactone via progesterone receptor (Williams et al., 2006). Similarly, high-dose (200 mg/kg/day) eplerenone attenuated the increase in myocardial expression of the pro-apoptotic BH3 only protein Bax in a model of pressure overload induced by aortic banding (De Silva et al., 2009). Treatment with low dose spironolactone (0.24 mg/day) protects the vasculature from aldosterone-induced apoptosis and structural injury via rescuing Akt activation, independent of blood pressure effects (Wei et al., 2009).

1.6.7 MR regulation during MI: cardiac damage & mechanisms involved

In previous studies from our laboratory, perfusion of rat hearts with corticosteroids exacerbated infarct area and apoptosis during experimental MI, which were prevented by MR but not GR blockade, confirming MR activation aggravates cardiac damage (Mihailidou et al., 2009). These preclinical studies are confirmed clinically, with elevated plasma aldosterone and cortisol levels in patients presenting for primary PCI for ST-segment elevation myocardial infarction (STEMI) and AMI (Beygui et al., 2006; Beygui et al., 2009; Palmer et al., 2008) or chronic HF (Guder et al., 2007) having poor outcomes.

Involvement of MR in MI was also confirmed in cardiomyocyte-specific MR knockout mice which were protected against cardiac remodelling and contractile dysfunction after myocardial infarction (Fraccarollo et al., 2011) and chronic pressure overload (Lothar et al., 2011). In contrast, cardiomyocyte-specific over-expression of MR triggered ROS-mediated endothelial dysfunction (Favre et al., 2011) and induced a transcriptional profile consistent with adverse outcomes in cardiac tissue (Latouche et al., 2010; Messaoudi et al., 2013). Similarly, transgenic mice with over-expression of 11 β -HSD2 (the enzyme that converts cortisol into inactive cortisone allowing aldosterone to selectively activate MR) in the heart display cardiac hypertrophy, fibrosis and HF which can be reversed by eplerenone (Qin et al., 2003).

A role for the cardioprotective effects of MR blockade have been demonstrated in animal models of MI both *in vitro* and *in vivo* (summarised in Table 1.1 and Table 1.2).

Collectively, MR antagonists improved the condition of the heart following MI. MR blockade decreased infarct size and incidence of arrhythmia, whilst simultaneously improving left ventricular pressure recovery and LV function. The reduction in cardiac damage by MR antagonists in these studies vary between 2% to 80% (Table 1.1 and 1.2), with most studies using high doses (μM range) of MR antagonists. Two studies have examined the effect of the lower doses of MR antagonists (Barbato et al., 2002; Mihailidou et al., 2009). Although Barbato et al. (Barbato et al., 2002) did not measure infarct size they reported 10 nM spironolactone markedly increased contractility. In the other study using low dose MR blockade, there was significant reduction in reperfusion-induced infarct size (Mihailidou et al., 2009).

The efficacy of MR blockade to reduce cardiac damage has also been translated clinically with several large clinical trials (summarised in Table 1.3) having shown low-dose MR antagonists, spironolactone and eplerenone, added to standard therapy for HF markedly reduced mortality and hospitalization in severe and mild HF, and HF post-MI (Pitt et al., 2003; Pitt et al., 1999; Zannad et al., 2011). Importantly, the plasma levels of aldosterone in these trials were not elevated but in the physiological range (0.25 – 0.4 nmol/l) (Rousseau et al., 2002), which suggest low levels of MR antagonists have additional actions, although mechanisms were not fully defined. A recent randomised trial has shown a new non-steroidal MR antagonists, BAY 94-8862, is as effective as spironolactone in decreasing levels of B-type natriuretic peptide (BNP) and albuminuria but lower incidence of hyperkalaemia in patients with HF and reduced left ventricular ejection fraction (HFrEF) and moderate chronic kidney disease (CKD) (Pitt et al., 2013).

Animal model	Type & Dose of MR antagonist	Time given treatment	Length of treatment	Effect on infarct size	Other effects	Ref.
Rat <i>Ex vivo</i>	SP 100 nM	15 min before Isch	+ 45 min Isch + 3 h Rep	↓ 34%	↑ LVP recovery	(Chai et al., 2005)
Rat <i>Ex vivo</i>	EPL 1 μM	15 min before Isch	+ 45 min Isch + 3 h Rep	↓ 22%	↑ LVP recovery	(Chai et al., 2006)
Rat <i>Ex vivo</i>	SP 10 nM SP 1000 nM	15 min before Isch	+ 30 min Isch + 2.5 h Rep	↓ 15% (10 nM) ↓ 22% (1000 nM)	↓ apoptosis (TUNEL) with both doses	(Mihailidou et al., 2009)
Rat <i>Ex vivo</i>	EPL 1 μM EPL 10 μM	Hearts subjected to 30 min Isch and treatment given at 5 min before Rep	+ 2 h Rep	↔ (1 μM) ↓ 73% (10 μM)	↑ Akt ↑ ERK1/2	(Schmidt et al., 2010)
Mouse <i>In situ</i>	K-can, 1 mg/kg		+ 2 h Rep	↓ 80%	Underlying mechanisms studies in isolated rat heart	(Schmidt et al., 2010)
Rabbit <i>In situ</i>	K-can, 1 mg/kg		+ 4 or 72 h Rep	↓ 31% (4 h) ↓ 49% (72 h)		

Table 1.1: Animal studies examining effects of MR antagonists on cardiac damage and mechanisms involved during *ex vivo* and *in situ* experimental myocardial ischaemia-reperfusion. SP, spironolactone, EPL, eplerenone; K-can, potassium canrenoate; Isch, ischaemia; Rep, reperfusion; LVP, left ventricular pressure; Akt, also known as protein kinase B (PKB); ERK1/2, extracellular signal-regulated protein kinase 1/2. ↓ decreased, ↑ increased, ↔, no effect

Animal model	Type & Dose of MR antagonist	Time given treatment	Length of treatment	Effect on infarct size	Other effects	Ref.
Rat	SP, 100 mg/kg/d	After MI	2 weeks	↓ 2%	↑ LV function ↓ fibrosis ↓ apoptosis (TUNEL) ↓ MR & 11β-HSD2 mRNAs	(Takeda et al., 2007)
Rat	EPL, 100 mg/kg/d	3 days post MI	4 weeks	↓ 16 % (in male) ↓ 31% (in female)	↑ LV function - Male: restored 4% up-regulated genes - Female: restored 44% up-regulated genes	(Kanashiro-Takeuchi et al., 2009)
Rat	EPL, 150 mg/kg twice daily	24 h after MI	3, 7 or 28 days	↑ 14% (day 3), ↓ 9% (day 7), ↑ 6% (day 28)	↓ fibrosis after 28 days	(Delyani et al., 2001)
Rat	EPL, 100 mg/kg/d	After MI	7 days	↔	↓ thinning & dilatation of infarcted wall ↑ neovessel formation ↑ LV function	(Fraccarollo et al., 2008)
Rat	EPL, 100 mg/kg/d	After MI	4 weeks	↓ 5%	↑ LV haemodynamics ↓ fibrosis ↓ mRNAs: AP-1, NF-κB, MCP-1, PAI-1, ANP, BNP	(Enomoto et al., 2005)
Rat	SP, 100 mg/kg/d	After MI	4 weeks	↑ 11% (SP)	↓ AP-1, NF-κB ↓ mRNAs: collagen I/III, APN, BPN	(Matsumoto et al., 2004)
Rat	SP, 80 mg/kg/d	8 days after MI	7 & 90 days	↓ 2% (day 7) ↑ 2% (day 90)	↑ LV haemodynamics ↓ ROS, collagen density ↓ LV hypertrophy	(Mulder et al., 2008)

Table 1.2: Animal studies examining effects of MR antagonists on cardiac damage and mechanisms involved during *in vivo* experimental myocardial infarction (MI). SP, spironolactone, EPL, eplerenone; LV, left ventricular; AP-1, activator protein 1; NF-κB, nuclear factor κB; MCP-1, monocyte chemoattractant protein 1; PAI-1, plasminogen activator inhibitor 1; ANP, atrial natriuretic peptide; BNP, brain natriuretic peptide; ROS, reactive oxygen species. ↓ decreased, ↑ increased, ↔, no effect

Randomised Controlled Clinical Studies	Injury disease	Standard therapy	Type and dose of MR antagonist	Primary end point	All cause mortality	Hospitalisation for HF	Ref.
RALES	Severe HF	ACE-I, diuretic	Spironolactone 25-50 mg/day	Mortality	↓ 30%	↓ 33%	(Pitt et al., 1999)
EPHESUS	Post-MI, HF	ACE-I/ARB, β-blocker, diuretic	Eplerenone 25-50 mg/day	All cause of CV, or hosp. for HF	↓ 15%	↓ 23%	(Pitt et al., 2003)
EMPHASIS-HF	Mild HF	ACE-I/ARB, β-blocker, diuretic	Eplerenone 25-50 mg/day	CV death or hosp. for HF	↓ 34%	↓ 42%	(Zannad et al., 2011)
Aldo-DHF	Diastolic HF	ACE-I/ARB, β-blocker, diuretic	Spironolactone 25 mg/day	LVD function, peak VO ₂	-	-	(Edelmann et al., 2013)
REMINDER	STEMI	ACE-I/ARB, β-blocker	Eplerenone Up to 50 mg/day	Mortality, or hosp. for HF	Unknown	Unknown	<i>ClinicalTrials.gov</i> ID: NCT01176968
TOPCAT	Clinical HF	ACE-I/ARB, β-blocker, diuretic	Spironolactone 15-45 mg/day	CV death or hosp. for HF	Ongoing study	Ongoing study	<i>ClinicalTrials.gov</i> ID: NCT00094302
ALBATROSS	STEMI or high risk STEMI	ACE-I/ARB, β-blocker, diuretic	Acute bolus of K-canrenoate, then spironolactone 25 mg/day	Death, or worsened HF, or arrhythmias	Ongoing study	Ongoing study	<i>ClinicalTrials.gov</i> ID: NCT01059136

Table 1.3: Clinical MR blockade trials in MI and HF.

RALES, Randomized Aldactone Evaluation Study; EPHESUS, Eplerenone Post acute myocardial infarction Heart failure Efficacy and SURvival Study; EMPHASIS-HF, Eplerenone in Mild Patients Hospitalization And SURvival Study in Heart Failure; Aldo-DHF, Aldosterone Receptor Blockade in Diastolic Heart Failure; REMINDER, Impact of Eplerenone on Cardiovascular Outcomes in Patients Post Myocardial Infarction; TOPCAT, Trial of Aldosterone Antagonist Therapy in Adults with Preserved Ejection Fraction Congestive Heart Failure; ALBATROSS, Aldosterone Lethal Effects Blocked in AMI Treated with or without Reperfusion to Improve Outcome and Survival at Six Months Follow-up; MR, mineralocorticoid receptor; HF, heart failure; MI, myocardial infarction; STEMI, ST-segment elevation MI; CV, cardiovascular; LVD, left ventricular diastolic; peak VO₂, maximal exercise capacity; ACE-I, angiotension converting enzyme inhibitor; ARB, angiotension receptor blocker.

Although mechanisms for the cardioprotective effects of moderate-to-high doses of MR blockade during myocardial I-R are summarised in table 1.1 and 1.2, further studies are required to identify the mechanisms activated by low doses of MR blockade. Oxidative stress and apoptosis have been implicated in the pathogenesis of vascular injury and remodelling after I-R, leading to development of MI, however little is known whether low doses of MR blockade may intercept oxidative stress and apoptosis during I-R.

1.7 Hypotheses and Aims

This chapter provided the currently defined mechanisms of myocardial I-R injury, the role of androgens and oestrogens during I-R injury and the effects of aldosterone and regulation of MR during myocardial I-R damage. Several questions have arisen which have led to the hypothesis for this thesis.

Hypotheses:

Physiological levels of androgens modulate myocardial damage during MI in both males and females and need to be considered in treatment strategies. Targeting MR with low-dose MR antagonists will salvage myocardium by maintaining redox balance, preventing oxidative stress and apoptosis, leading to reduced cardiac damage during myocardial I-R injury.

Specific aims:

- 1. To validate an experimental model of MI and timing of treatment;**

2. **To determine the role of androgens in the sex differences in cardiac damage during MI** by a series of gonadectomy/hormone replacement studies examining mechanisms of reperfusion injury in male and female rat hearts;
3. **To determine the mechanisms involved in MR regulation during MI and the role of low dose MR blockade.**

Chapter 2

General methods

2.1 Animals

Myocardial ischaemia-reperfusion (I-R) experiments were performed using adult male (8-12 weeks, 300-400g) and female (8-12 weeks, 200-300g) Sprague-Dawley (SD) rats. All experiments were approved by the Royal North Shore Hospital Animal Care and Ethics Committee and were conducted in accordance with the Australian Code of Practice for the Care and Use of Animals for Scientific Purposes. Animals were housed in the animal facility under conditions of constant temperature (22°C) and supervised by staff of the Kearns Research Facility. All rats were fed standard diet with access to food and water *ad libitum*.

2.2 Myocardial ischaemia-reperfusion model

Using an animal model allowed us to conduct studies on how I-R injury directly impacts biochemistry, antioxidant enzyme systems, gene expression and protein levels within the myocardium. Rats were weighed before removal from the Kearns facility and anaesthetised using intraperitoneal (IP) injection of Ketamine (60 mg/kg) and Xylazine Hydrochloride (10 mg/kg); administration of IP heparin (250 IU) was used to prevent intravascular blood clots. Once deep anaesthesia was confirmed using suppression of the paw pinch reflex (withdrawal in response to a painful stimulus), a median sternotomy incision was made and the heart quickly removed from the thoracic cavity. The heart was immersed in ice-cold Krebs-Henseleit buffer (KHB, see Appendix for buffer formulation), made fresh on the morning of the experiment, to help clear the blood and reduce injury. After two washes in ice-cold KHB, the aorta was attached to a needle cannula (size 18G) on the Langendorff apparatus and tied in position with a 2.0 silk suture for retrograde perfusion via the aorta with KHB.

KHB perfusate was maintained at 37°C by heating in a water bath and continuously bubbled with carbogen gas (95% O₂ and 5% CO₂; BOC Gas, Australia) to oxygenate the perfusate and maintain the pH at 7.4. Constant flow perfusion was achieved by using a MASTERFLEX pump drive and controller (Cole-Parmer Instrument Co.) to deliver perfusates at a constant rate of 3-4 mL/min. Perfusate was passed through a heating-coil and bubble trap before reaching the isolated heart to ensure the temperature of perfusate in the cannula was at 37°C and to prevent any air bubbles from entering the coronary circulation. The isolated heart was kept warm at 37°C within a water-jacketed organ chamber, connected to the water bath, to ensure the physiological temperature of the heart was maintained.

2.2.1 Induction of regional ischaemia-reperfusion

For regional ischaemia a 6/0 suture was placed around a prominent branch of the left anterior descending (LAD) coronary artery, to occlude flow in the artery. After 10 minutes of stabilisation and 15 minutes KHB perfusion (control or with treatment), the suture was threaded through a 0.5 cm polyethylene tube (OD 2.08 mm) to form a snare. Occlusion was achieved by clamping the epicardial surface with hemostat forceps so that the tube compressed the artery. Regional ischaemia was induced by tightening the snare around the LAD artery for 30 minutes. After release of the snare the heart was reperfused for 150 minutes. Cardiac contraction rate was monitored throughout the experiment. Sham occlusion was achieved by placing the suture around the artery without occluding it.

2.2.2 Collection of heart tissue

At the end of the reperfusion period, the LAD artery was re-occluded. The heart was perfused with 1.5 mL of 0.05% (w/v) Monastral blue dye (Sigma-Aldrich) in KHB to allow identification of the non-ischaemic area. The heart was then removed from the apparatus, immersed in ice-cold KHB and sliced in half. Tissue from mid ventricle to apex (distal part) was immediately frozen at -20°C for infarct size analysis. The proximal part of the heart was quickly fixed in 10% (v/v) neutral buffered formalin for 24 hours and then transferred into 70% (v/v) ethanol until tissue processing (approximately 1-2 weeks). Tissue was embedded in paraffin and sectioned at 5 µm thickness for subsequent immunohistochemical studies. In a separate group of experiments, hearts were removed from the cannula at the end of reperfusion. The left ventricular (LV) free wall tissue was rapidly isolated and washed with ice cold phosphate buffer saline (PBS). Tissue was snap frozen in liquid nitrogen and stored at -80°C for subsequent biochemical and western blot analysis.

2.3 Measurement of infarct size

After being frozen at -20°C for at least 2 hours, the heart was removed and sliced into three cross-sectional pieces (approximately 1.5 mm thickness). Each slice was weighed before staining. The slices were incubated in 1% (w/v) 2,3,5-triphenyl-tetrazolium chloride (TTC) (Sigma-Aldrich) in PBS at 37°C for 20 minutes. TTC reacts with dehydrogenase enzymes and reduced nicotinamide adenine dinucleotide (NADH) in viable tissue, staining it deep red, while infarcted tissue remains unstained or dull yellow (Fishbein et al., 1981). A representative heart slice stained with TTC is shown in Figure 2.1. The area at risk (AAR; ischaemic but viable myocardium) was stained red

by TTC while the infarcted area (IA) remained unstained. Following staining, slices were washed three times in PBS to remove excess reagent on the tissue and then incubated in 10% (v/v) neutral buffer formalin for 7 days to increase contrast between the different zones. Each slice was photographed with a digital camera (COOLPIX 5900, NIKON, Japan) for examination. Computerised planimetry with an image analysis software program (National Institute of Health Image J, NIH Image software) was used to measure IA, AAR and the total area (TA) of each heart slice. Slices were analysed blind by two independent investigators. Calculation of infarct size was as follows:

1. $\text{Infarct weight} = (\text{IA}/\text{AAR}) \times (\text{AAR}/\text{TA}) \times \text{slice weight}$

$$\text{Total Infarct weight} = \sum (\text{Infarct weights of slices 1, 2, 3})$$

2. $\text{AAR weight} = (\text{AAR}/\text{TA}) \times \text{slice weight}$

$$\text{Total AAR weight} = \sum (\text{AAR weights of slices 1, 2, 3})$$

3. $\% \text{ Infarct size relative to AAR} = (\text{Total infarct weight} / \text{Total AAR weight}) \times 100\%$

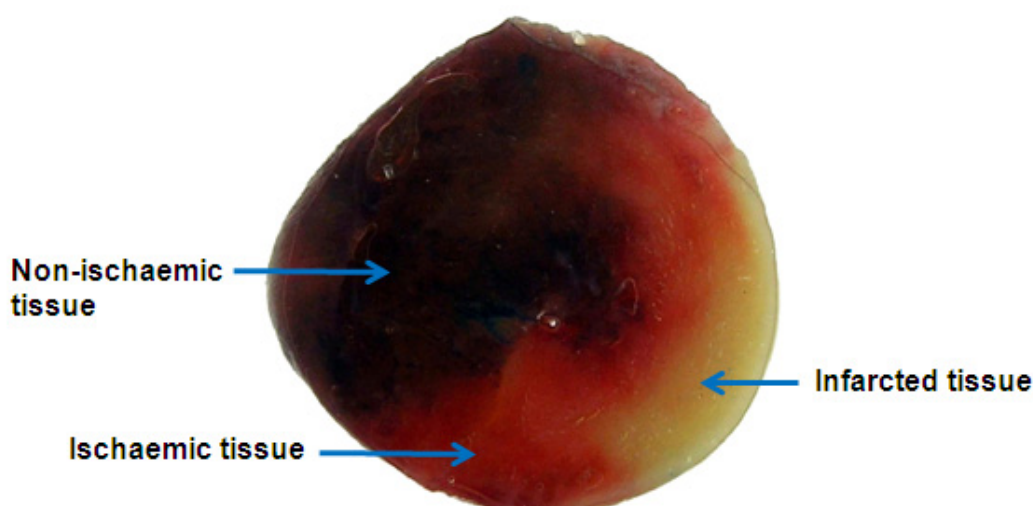


Figure 2.1: Cross-sectional of a heart slice after staining with TTC

2.4 Measurement of apoptosis using *TUNEL* method

Immunohistochemical detection of apoptotic cells was achieved using *In Situ* Cell Death Detection Kit, TMR red (Roche Applied Science), which is based on the terminal deoxynucleotidyl transferase (TdT) – mediated dUTP nick end labeling (TUNEL) method, commonly used for the detection of apoptosis with specific DNA strand breaks (Gold et al., 1994; Gorczyca et al., 1993; Negoescu et al., 1998). The biochemical hallmark of apoptosis involves cleavage of chromosomal DNA into nucleosomal units, resulting in DNA fragmentation (Compton, 1992) which can be labelled by the enzyme TdT. TdT catalyses polymerization of nucleotides to free 3'-OH DNA ends and mediated biotin-16-dUTP nick-end labelling (TUNEL reaction) (Gavrieli et al., 1992; Mochizuki et al., 1994; Portera-Cailliau et al., 1994). Tetramethylrhodamine (TMR, red fluorescence) labels nucleotides, which can be detected by fluorescence microscopy.

Serial sections (5 µm) were cut from paraffin-embedded tissue samples (see Section 2.2.2 for tissue collection). One paraffin section per heart and seven to ten hearts per group were used for analysis. The tissue sections were deparaffinised with xylene (2 x 5 minutes) and rehydrated through serial dilutions of ethanol [absolute (2 x 3 minutes), 95% (v/v) (1 x 3 minutes), 90% (v/v) (1 x 3 minutes), 80% (v/v) (1 x 3 minutes), 70% (v/v) (1 x 5 minutes), diluted in milli-Q water]. Tissue sections were pre-treated with the proteolytic enzyme, Proteinase K (20 µg/ml) (Sigma-Aldrich) for 30 minutes at 37°C. As tissues are fixed in formalin fixative, the enzyme induces conformational changes in antigen molecules by forming intermolecular cross linkages (Fox et al., 1985; French and Edsall, 1945). Proteinase K incubation helps break down the cross-links and thus exposing the antigenic sites (Hilz et al., 1975). Tissue sections were

labelled with the TUNEL reagent for 1.5 hours at 37°C in a humidified chamber, washed three times with 1x PBS and counterstained with 4',6-diamidino-2-phenylindole dihydrochloride (DAPI, 1 µg/mL) for 5 minutes at room temperature. DAPI is a DNA-specific fluorescent dye that binds strongly to A-T rich regions in the minor groove of DNA (Kapuscinski, 1995; Larsen et al., 1989; Williamson and Fennell, 1975) and stains all nuclei in the section. Anti-desmin (1:50 dilution; Abcam) antibody was used to identify cardiomyocytes, and applied to sections and allowed to incubate overnight at 4°C before being counterstained with DAPI reagent. The sections were then washed with 1x PBS and mounted with anti-fade mounting reagent (Invitrogen). Sections were viewed on a fluorescent microscope and images captured at 200x magnification.

An area from the anterior, lateral, septal, posterior and sub-endocardial regions of each section was randomly selected for evaluation. TUNEL positive nuclei and total DAPI nuclei were counted by image analysis software program (National Institute of Health Image J, NIH Image software). The apoptotic index was determined as the ratio of TUNEL-positive myocyte nuclei relative to the total number of DAPI nuclei and expressed as percentage for different regions of the section. Sections were allocated a code and analysed and measurements made by two independent observers.

2.5 Myocardial protein expression

2.5.1 Immunohistochemistry

Protein expression in myocardium was identified using immunostaining on sections from paraffin embedded tissue (5 µm thickness). This technique also allowed us to visualise the localisation of proteins within the tissue. Sections were deparaffinised with

xylene and rehydrated through graded alcohol dilutions as described above (section 2.4). Endogenous peroxidase activity was blocked by 1% (v/v) hydrogen peroxide solution for 30 minutes at room temperature. Heat-induced epitope retrieval was performed by incubating slides in 10 mM sodium citrate buffer (pH 6.0) at 95°C for about 15 minutes. The sections were immunostained with single or dual specific antibodies against proteins of interest (see Table A1, Appendix for details of primary antibodies and concentrations). Following washing with 1 x PBS three times, the sections were incubated with specific secondary antibodies. For bright field microscopy, antibody reactivity was detected with envision+ polymer reagent (DAKO) and 3,3-diaminobenzidine (DAB) used as the chromogen (Sigma-Aldrich) before counterstaining with haematoxylin. For fluorescence staining, antibody reactivity was detected by secondary antibodies conjugated to either Alexa Fluor 488 or Alexa Fluor 594 (1:200 dilution) (Invitrogen) before counterstaining with DAPI reagent. Sections were then washed with 1x PBS and mounted. Images were captured by either bright field or fluorescence microscopy (both conventional and confocal).

2.5.2 Protein extraction from heart tissue

At the end of reperfusion period, LV free wall tissue was snap frozen in liquid nitrogen and stored at -80°C until protein extraction. Frozen myocardium was quickly powdered in a mortar and pestle, and immediately placed into ice cold RIPA buffer (see Appendix for details), at a tissue buffer ratio of 1:4 (w/v). Frozen tissues were homogenised in a glass-teflon homogeniser by 10-20 strokes of the pestle. Tissue homogenates were left on ice for 1 hour before being sonicated (amplitude: 40%, time: 30 sec, pulse: 2.5 sec, rest: 1 sec, temperature: 4°C; SONICS Vibra Cell Amplitude) and centrifuged at

16,000 \times g for 30 minutes at 4°C. The supernatant was collected and stored at -80°C for further study.

The protein concentration of the resulting myocardial lysates was measured by the Bradford Protein Assay (Bradford, 1976), with bovine serum albumin (BSA) as the standard and assayed with all unknown samples on the same microplate (96-well clear microplate). This allows for construction of a standard curve and quantitation of the unknown sample concentrations. The tissue lysates were diluted in milli-Q water at least 1:30 dilution before the protein concentration was determined. Protein concentrations were expressed as $\mu\text{g}/\mu\text{L}$ protein.

2.5.3 Western Blots

SDS-Gel Preparation

Separating gel was made to the desired acrylamide concentration (see Table A2, Appendix). Polymerisation of the separating gel was achieved by addition of ammonium persulfate (AMPS) and N,N,N',N'-tetramethylethylenediamine (TEMED) and the gel mixture poured into an electrophoresis cassette containing 1.5 mm spacers. Separating gel was poured to ~1.5 cm below the level of the glass plates followed by addition of water to achieve an even interface. After polymerization of the separating gel, the unpolymerized gel and water was removed and a 4% stacking gel poured on top of the separating gel. The comb was immediately inserted on top and gel allowed to set.

Sodium dodecyl sulphate - polyacrylamide gel electrophoresis (SDS-PAGE)

Protein from myocardial lysates was separated using SDS-polyacrylamide gel electrophoresis (SDS-PAGE) prior to blotting for protein expression. Gel electrophoresis is a powerful technique which separates the protein content of tissue lysates according to molecular weights. Electrophoresis of samples by SDS-PAGE are separated under denaturing conditions, as SDS is an anionic detergent that binds to, solubilises and partially unfolds proteins, conferring a negative charge on the protein approximately proportional to its length. As such, mobility of proteins in SDS-PAGE is a linear function of the logarithms of their molecular weights (Shapiro et al., 1967). The composition of the gel and its pH are also important for protein molecules to migrate on the gel under the electrical charge. The concentration of acrylamide and its cross-linking determine the pore size of the gel matrix and can be varied between gels depending on the sample being analysed. High concentration gels (12% or higher) were used for low molecular weight proteins (<25 kDa); higher molecular weight proteins (>25 kDa) require a lower percentage gel (<12%). Protein samples containing 30-50 µg of protein were diluted in 2x SDS loading buffer (see Appendix for details), boiled for 5 minutes at 95°C, loaded onto the 7-12% polyacrylamide gels (Laemmli, 1970) and electrophoresed at 100 V in Tris-Glycine running buffer [25 mM Tris, 192 mM glycine and 0.1% (w/v) SDS, pH8.3]. Molecular weight markers (Bio-Rad) were run on the gel with the samples until complete separation of bands was observed.

Protein transfer and immunodetection of protein expression (Western blot)

Proteins separated on acrylamide gels were transferred onto polyvinylidene fluoride (PVDF) membranes (0.45 µm; Millipore) with a Bio-Rad Mini Trans-Blot Cell

Electrophoresis Unit at 24 V [voltage varied depending on how many tanks were being transferred (24 V per tank, 36 V per 2 tanks and 48 V per 3 tanks)] and left overnight at 4°C in transfer buffer [25 mM Tris, 192 mM glycine and 10% (v/v) methanol]. After proteins were transferred, PVDF membranes were incubated in blocking buffer [1x TBS, 0.1% (v/v) Tween-20 and 5% (w/v) non-fat milk powder] for 1 hour at room temperature. Primary antibodies (see Table A1, Appendix) were diluted in blocking buffer and membranes were incubated for either 1 hour at room temperature or overnight at 4°C. Membranes were washed three times for 10 minutes in TBST [1x TBS + 0.1% (w/v) Tween-20] and then incubated with secondary antibody conjugated with horseradish peroxidase (HRP, Dako Cytomation) at 1:3000 dilution in TBST containing 2% (w/v) skim milk. The membranes were washed three times (10 minutes each) in TBST and incubated for 1 minute in Western Lightning Chemiluminescence Reagent Plus (PerkinElmer, Melbourne, Australia). Visualisation of the bands was achieved by digital imaging with LAS4000 (GE Healthcare Life Sciences). Quantitation of band intensities was measured with Image J software Analysis (National Institute of Health Image J, NIH Image software). Data are presented as arbitrary units for each protein analysed.

2.6 Myocardial gene expression

2.6.1 Total RNA extraction from heart tissue

For gene expression studies, total RNA from rat heart tissue was extracted with TRIzol reagent (Sigma-Aldrich), a single step reagent for the isolation of total RNA, DNA or protein from cells or tissues. The reagent is a monophasic solution of phenol and guanidine thiocyanate (Chomczynski and Sacchi, 1987). During sample lysis, the

reagent maintains the integrity of the RNA while disrupting cells and dissolving cell components. Addition of chloroform, followed by centrifugation, separates the solution into an aqueous phase and an organic phase. RNA remains exclusively in the aqueous phase (Chomczynski, 1993; Chomczynski and Mackey, 1995) and is recovered by centrifugation after precipitation with isopropanol.

Total RNA was extracted from individual hearts with TRIzol according to manufacturer's protocol and with RNase free or diethylpyrocarbonate (DEPC)-treated products. Homogenisation of the tissue was performed in the Mixer Mill (Retsch MM301) with the grinding balls (3 mm Tungsten Carbide beads, DEPC-treated) (QIAGEN). Tissue samples were weighed and placed in 2 mL Eppendorff tubes. The two grinding balls were then added to the tube before the addition of TRIzol (1 mL TRIzol reagent per 100 mg tissue). Tissue homogenisation was started immediately following the addition of the TRIzol reagent to prevent degradation of the RNA. The supernatant was left to stand at room temperature for 5 minutes to allow complete dissociation of nucleoprotein complexes before adding chloroform (200 μ L per 1 mL TRIzol above), and the mixture shaken vigorously by hand for 15 seconds. Samples were incubated at room temperature for 5 minutes before separation into phases by centrifugation at 12,000xg for 15 minutes at 4°C. Three layers resulted: an upper clear aqueous phase containing RNA, a white interphase containing DNA, and a lower red organic phenol/choloroform phase containing proteins. The clear aqueous phase (top layer) was transferred to another tube, and RNA precipitated by addition of isopropanol (500 μ L per 1 mL TRIzol), incubation at room temperature for 10 minutes, and centrifugation at 12,000xg for 10 minutes at 4°C. The supernatant was discarded, the

RNA pellet washed with 1 mL of the 75% (v/v) ethanol and recovered by centrifugation at 7,500 \times g for 5 minutes at 4°C. The supernatant was removed, the pellet air-dried until translucent and 30-50 μ L RNase free water added to resuspend the pellet. Total RNA was stored at -80°C until use.

2.6.2 RNA quantitation and determination

The concentration and purity of the samples were assessed using a NanoDrop ND-1000 spectrophotometer (Thermo Scientific) according to the manufacturer's specifications, at 260 nm and 280 nm. The spectral measurement was made on a 2 μ L RNA sample with sample concentration in ng/ μ L based on absorbance at 260 nm. The ratio of absorbance at 260 and 280 nm (A_{260}/A_{280}) is used to assess the purity of RNA. A ratio of ~1.8 – 2.1 is generally accepted as pure for RNA. If the ratio is lower, it indicates the presence of proteins, phenol or other contaminants that absorb strongly at or near 280 nm, or incomplete dissolution of the RNA.

2.6.3 RNA cleanup

This procedure was carried out to purify samples with low A_{260}/A_{280} ratio (<1.8). Total RNA was purified with RNeasy Mini Kit (QIAGEN, cat #217004) as per the manufacturer's instructions. RNA samples were adjusted to a volume of 100 μ L with RNase-free water followed by addition of 350 μ L Buffer RLT. These tubes were mixed well by vortexing before adding in 250 μ L of 96-100% (v/v) ethanol, followed by a subsequent mixing using pipette. Buffer RLT and ethanol added to the sample to create conditions that promote selective binding of RNA to the RNeasy membrane. Each sample (700 μ L) was immediately transferred to an RNeasy Mini column placed in a

supplied 2 mL collection tube. The tube was then closed gently and centrifuged for 15 seconds at 8000xg. The RNeasy mini column contains membrane, which has the binding capacity for RNA and allows contaminants to pass through. After centrifugation, the flow through was discarded, while the collection tube was reused. The column was then washed with 500 μ L of RPE buffer for 15 seconds at 8000xg. After discarding the flow through, the washing step was repeated again for 2 minutes at 8000xg. To eliminate any chance of possible RPE buffer carryover, RNeasy column was placed in a new 2 mL collection tube and centrifuged in a microcentrifuge at full speed for 1 minute. For the elution step, the column was transferred to a new 1.5 mL collection tube and 50 μ L of RNase-free water was added directly onto the column. This was then centrifuged for 1 minute at 8000xg to elute the RNA into the collection tube. The concentration and purity of the samples were assessed as described above (section 2.6.2).

2.6.4 First strand cDNA synthesis from RNA

cDNA was synthesised from 2.5 μ g total RNA by the Superscript III First-Strand Synthesis System and oligo (dT)₂₀ as primer (Invitrogen) according to the manufacturer's protocols. The extracted RNA was added into 0.2 mL PCR tubes, containing 1 μ L of 50 μ M oligo (dT)₂₀ and 1 μ L of annealing buffer. The mixture was made up to a total volume of 8 μ L with RNase free water, and incubated in the thermal cycler at 65°C for 5 minutes, followed by incubation on ice for at least 1 minute. The contents of the tube were then collected by brief centrifugation, followed by addition the reverse transcriptase mix containing 10 μ L of 2X first-strand reaction mix [10 mM MgCl₂ and 1 mM each dNTP] and 2 μ L of SuperScript III/RNaseOUT enzyme mix.

The sample was briefly mixed by vortex and collected by centrifugation. The 20 μ L total reaction was then incubated in the thermal cycler at 50°C for 50 minutes. The reactions were terminated by incubation at 85°C for 5 minutes, and then chilled on ice. Finally, 30 μ L of RNase free water was added to each 20 μ L first strand cDNA synthesis reaction and mixed well prior to storage at -20°C. The diluted cDNA was then used as templates for amplification in reverse transcription polymerase chain reaction (RT-PCR) or quantitative real-time RT-PCR (qRT-PCR) using TaqMan Gene Expression Assays (Applied Biosystems).

2.7 Studies using H9c2 cells

The H9c2 rat cardiomyoblast cell line was used as they have characteristics similar to primary cardiomyocytes (Hescheler et al., 1991) and offer a reproducible model for the study of myocardial hypoxia/reperfusion (Borchi et al., 2009; Granata et al., 2009; Ko et al., 2011; Mizukami et al., 2008). H9c2 cells have also been extensively used in diverse cell culture studies examining the effects of stress on apoptosis, hypertrophy and cardioprotection (Gross et al., 2006; Liu et al., 2008; Qu et al., 2010; Stuck et al., 2008; Watkins et al., 2011).

2.7.1 Culture & passage

H9c2 cells were cultured in Dulbecco's modified Eagle's medium (DMEM) containing 10% (v/v) heat inactivated fetal bovine serum (FBS), 2 mM L-glutamine, 10 U/mL penicillin and 10 μ g/mL streptomycin. This is referred to as complete culture medium. Cells were grown in 10 cm dishes at 37°C in a humidified atmosphere with 5% (v/v) CO₂ and 95% (v/v) air.

At 80-90% confluence cells were washed with 1x PBS and trypsinised with 1 mL TrypLE reagent (Invitrogen) for 5 minutes at 37°C. Complete culture medium was added to each dish and mixed with the trypsinised cells to inactivate trypsin. Cells were resuspended into 9 mL of culture medium and subcultured into 10 cm dishes at 1:5 to 1:10 ratios. Media (7 mL) was replaced routinely every 2-3 days. Experiments were performed at passage 3-10.

2.7.2 Cell quantification and viability by Trypan Blue

To maintain the same cell number between experiments, a haemocytometer was used to count cells. The viable cell density was determined as the number of trypan blue excluding cells in a haemocytometer. The chromopore Trypan Blue is negatively charged and does not enter the cell unless the membrane is damaged (Strober, 2001). Therefore, all the cells which actively exclude the dye were considered as viable. For counting trypsinised cells were suspended in a total of 10 mL and added to trypan blue [0.2% (w/v) in PBS] at a 1:5 dilution followed by gentle mixing and incubation for 2-3 minutes. An aliquot was transferred to the haemocytometer chamber (Weber Scientific International, Teddington, UK) and total live cells counted in four x 1 mm² squares as viewed under the microscope (Magnification 4x; Nikon, Japan). Viable cells appeared as bright dots under microscopy whereas dead cells absorbed the dye and were coloured blue. The viable cell numbers were determined as follows:

Numbers of cell (per mL) = [average count of the four squares] x [dilution factor] x 10⁴

2.7.3 Protein extraction from H9c2 cells

Some conditions (e.g. hypoxia) can weaken the cell's attachment to the plate and therefore the method for collecting cells was modified accordingly. For weakly adherent cells, media and trypsinised cells were collected into 15 mL falcon tubes and centrifuged at 1000xg for 5 minutes. Cells were then washed two times with 5 mL ice cold 1x PBS by centrifugation, and lysed in lysis buffer [50 mM Tris (pH 8.0), 150 mM NaCl, 1% (v/v) Nonidet P-40, 0.02% (w/v) sodium azide, and protease inhibitor cocktail] (300 µL lysis buffer per 100 mm dish or 100 µL lysis buffer per 35 mm dish). For strongly adherent cells, media was removed from the dish and cells were washed two times with 5 mL ice cold 1x PBS (remove PBS as much as possible). Lysis buffer was added to the dish and adherent cells were scraped off the dish with plastic cell scraper and cell suspensions transferred into 1.5 mL Eppendorff tubes. Cell lysates were left on ice for about 30 minutes after being sonicated (duty cycle: 30%, time: 30 sec, output control: 1, pulse, temperature: 4°C; Sonifier Cell Disruptor B-30) and then centrifuged at 16,000xg for 10 minutes at 4°C. The supernatant was collected and stored at -80°C for further study.

2.7.4 Total RNA extraction from H9c2 cells

Cell collection was performed as described above (section 2.7.4). H9c2 cells were lysed in TRIzol reagent (1 mL TRIzol per 100 mm dish or 0.5 mL TRIzol per 60 mm dish) and total RNA was extracted as described in section 2.6.1.

2.8 Statistical analysis

All data were analysed with SigmaStat 3.0 software, with the Kolmogorov-Smirnov test used to confirm normal distribution. Results are presented as the mean \pm standard error of the mean. Statistical comparisons were performed by one-way analysis of variance (ANOVA) followed by the Holm-Sidak correction post-hoc test to adjust for multiple comparisons. In some situations the same control group is used in several comparisons, and Dunnett's test was used as the post-hoc test. Unpaired Student's t-test was used for comparing differences between two treatments. The results were considered significant if $P < 0.05$.

Chapter 3

Validation of the model of myocardial ischaemia-reperfusion injury and timing of treatment

3.1 Introduction

The Langendorff isolated heart preparation has been used extensively to simulate the (patho)physiological of I-R injury (Bell et al., 2011b; Langendorff, 1898; Sievers et al., 1989). The isolated heart preparation by Langendorff is an *ex vivo* model that involves the intact heart removed from the animal and allows measurement of direct mechanisms in the absence of cardiac innervation and other factors that influence the heart in response to ischaemia, using Krebs-Henseleit buffer (KHB, oxygenated solution). Restricted regional flow of blood in a major coronary vessel causes reduction in the oxygen and nutrient supply to myocardial tissues (Liedtke et al., 1975; Neely et al., 1973), representing “myocardial ischaemia”. The most commonly used technique is ligation of the branch of the left anterior descending (LAD) coronary artery (Bredee et al., 1975; Johns and Olson, 1954; Reimer et al., 1981). Most investigators maintain occlusion for 30 minutes (Mersmann et al., 2011). In the Langendorff perfused rodent hearts, infarct size and apoptosis significantly increased in studies using 30 minutes ischaemia followed by 120-240 minutes reperfusion (Mersmann et al., 2011; Redel et al., 2008; Ruixing et al., 2006; Schwarz et al., 2000; Ytrehus et al., 1994), resulting in a consistent infarct size of approximately 42% in the control group (Mersmann et al., 2011; Redel et al., 2008). Previous studies from our laboratory have used this experimental model of MI in both rabbit and rat hearts and found similar changes in infarct size and apoptosis (Mihailidou et al., 2009; Wong et al., 2011).

Since I-R leads to damage of cell membranes, Na^+ and Ca^{2+} overload, generation of ROS, activation of autophagy and cell death (apoptosis and necrosis) processes, the first aim for this thesis was to validate that several of these changes could be detected in our

ex-vivo rat model of I-R. Apoptosis plays an important role in the progression of myocardial damage and left ventricular remodelling following I-R (Ojha et al., 2008). Cardiac apoptosis occurs acutely after I-R in the region of the myocardium with decreased blood flow and oxygen supply, and in the border area around the infarcted myocardium in humans (Olivetti et al., 1996; Saraste et al., 1997) and animals (Fliss and Gattinger, 1996; Gottlieb et al., 1994; Scarabelli et al., 2002; Zhao et al., 2000). Although autophagy at basal level can promote cell survival by removing damaged and toxic cellular components (Rothermel and Hill, 2008), uncontrolled autophagy may lead to cell death (Levine and Yuan, 2005). Autophagy has been shown to be upregulated in response to ischaemia and reperfusion. Previous studies observed induction of autophagy in Langendorff perfused rabbit hearts subjected to I-R (Decker et al., 1980; Decker and Wildenthal, 1980). Further studies described activation of autophagy in the infarct zones of hearts subjected to reperfusion injury (Hamacher-Brady et al., 2007; Hariharan et al., 2011; Matsui et al., 2007). Increased levels of autophagy proteins (such as Beclin-1, Atg5-Atg12 conjugate and LC3-II) indicate that a cell has undergone autophagy processing (Kassiotis et al., 2009). Thus the level of I-R injury can also be estimated by specific markers of autophagy.

Clinical (Pitt et al. 2003) and experimental (Kanashiro-Takeuchi et al., 2009; Schmidt et al., 2010) studies show mineralocorticoid receptor (MR) antagonists significantly reduce myocardial damage during MI. In these studies, MR antagonists were administered post-MI or after ischaemia was established. Early administration (3-7 days post-MI) of MR antagonist eplerenone improved outcomes which were not observed when treatment was started after 7 days (Adamopoulos et al., 2009), similar to other

treatment strategies for MI. In experimental studies using the *ex vivo* rodent I-R model, MR antagonists perfused 15 minutes prior to ischaemia significantly reduced infarct size (Chai et al., 2005; Chai et al., 2006). Therefore part of validating our reperfused rat heart model of MI is to determine the effect of timing of administration of MR antagonists - prior to ischaemia or at reperfusion - on the extent of infarct size.

3.2 Methods

Male Sprague-Dawley rats were used for these studies. Experimental details for *ex vivo* ischaemia-reperfusion of the rat heart, measurement of infarct size, apoptosis (TUNEL), immunohistochemistry and immunoblotting are described in Chapter 2 (sections 2.2-2.5).

3.3 Results

3.3.1 I-R induces increased infarct area

Myocardial infarct size was assessed by measuring the infarct size/area (IA) and area-at-risk (AAR) of the myocardium. Injection of the Evans's Blue dye in the presence of the occlusion delineates the perfused myocardium (PM, blue) from the area at risk. 2-3-5-triphenyl tetrazolium chloride (TTC) stains bright red in the presence of dehydrogenase enzymes in viable tissue. As such, incubation of sections from the infarcted hearts in TTC delineates viable tissue (V) in the area at risk from infarcted tissue, which remains unstained (Figure 3.1A). Minimal damage was observed in hearts subjected to sham I-R, whereas I-R injury caused significant damage to the heart with 42% of the myocardium in the area at risk being non-viable after 150 minutes reperfusion (Figure 3.1B).

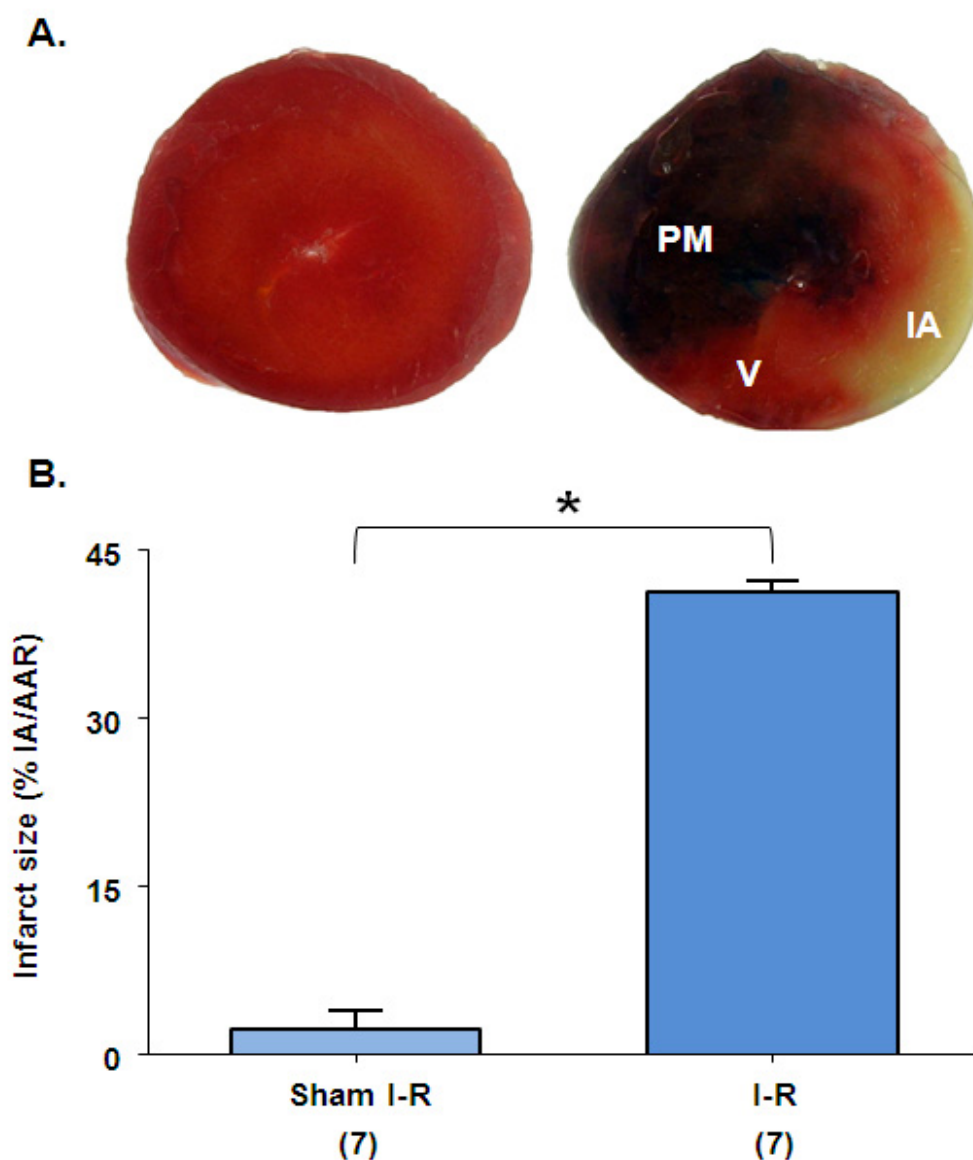
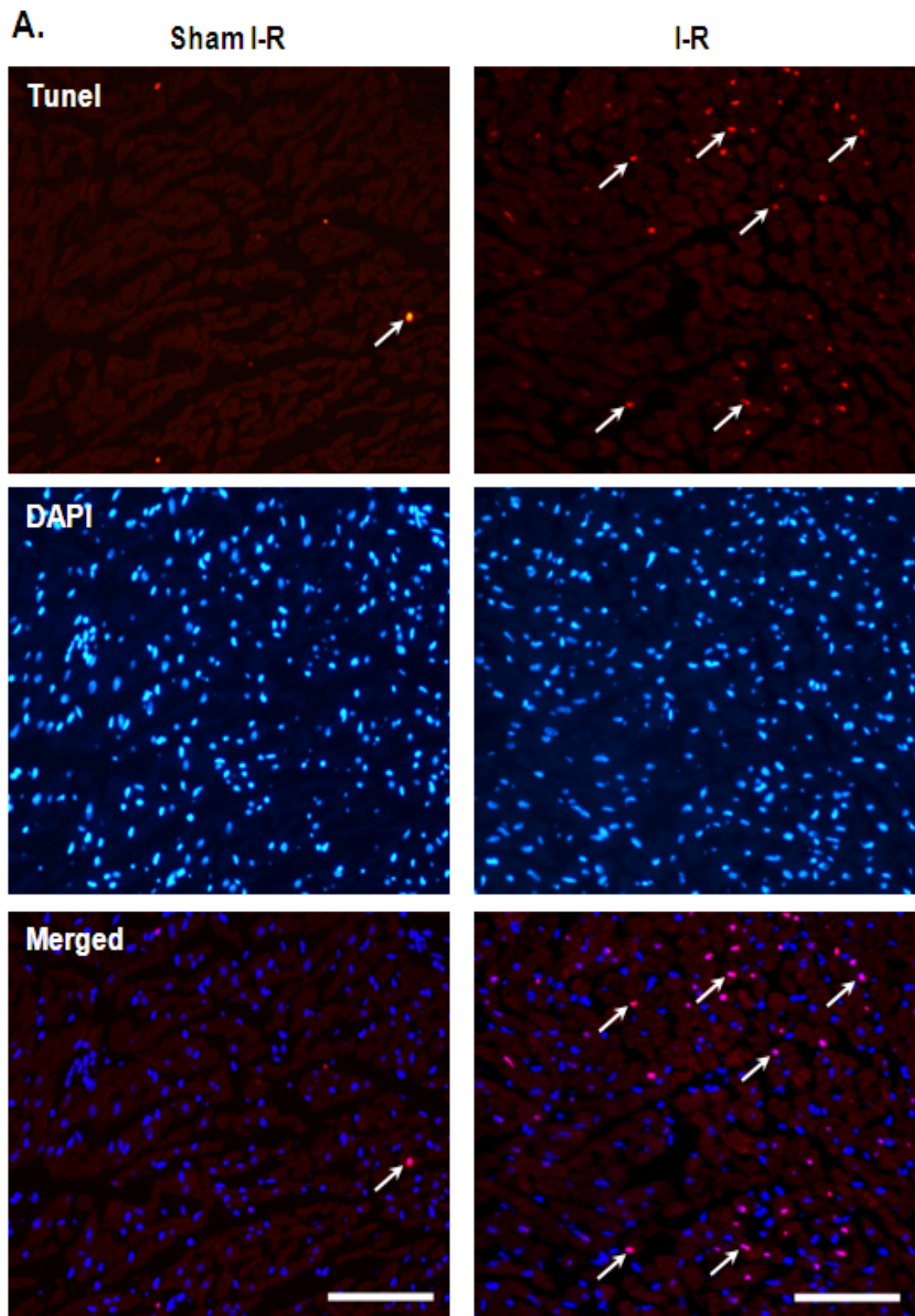


Figure 3.1: Myocardial infarct size in hearts subjected to ischaemia (30 minutes) followed by reperfusion (150 minutes).

(A) Representative cross-sections of the heart stained with 2-3-5-triphenyl tetrazolium chloride (TTC). (B) The effect of I-R injury on infarct size/area (IA) expressed as percentage of area-at-risk (AAR). I-R, ischaemia-reperfusion; PM, perfused myocardium; V, viable tissue; IA, infarcted area. Values expressed as mean \pm SE. Numbers below the bar graph indicate the number of animals in each group; * $P < 0.001$.

3.3.2 I-R induces increased cardiomyocyte apoptosis

Apoptosis in reperfused myocardial tissue samples was detected using terminal deoxynucleotidyl transferase (TdT) mediated nick end labelling (TUNEL) assay which measures DNA fragmentation as DNA strands breaks (Gavrieli et al., 1992). DAPI is a minor groove intercalating dye which stains DNA in all cell nuclei, and is required when calculating the proportion of apoptotic cells. TUNEL negative nuclei appear red, while TUNEL-positive nuclei are bright pink (Figure 3.2A). The apoptotic index (percentage of TUNEL-positive myocyte nuclei relative to the total number of DAPI-stained nuclei) from hearts subjected to sham and I-R injury is shown in Figure 3.2B. Consistent with the effect on infarct size, reperfusion injury significantly increased number of apoptotic myocytes compared with sham-operated hearts.



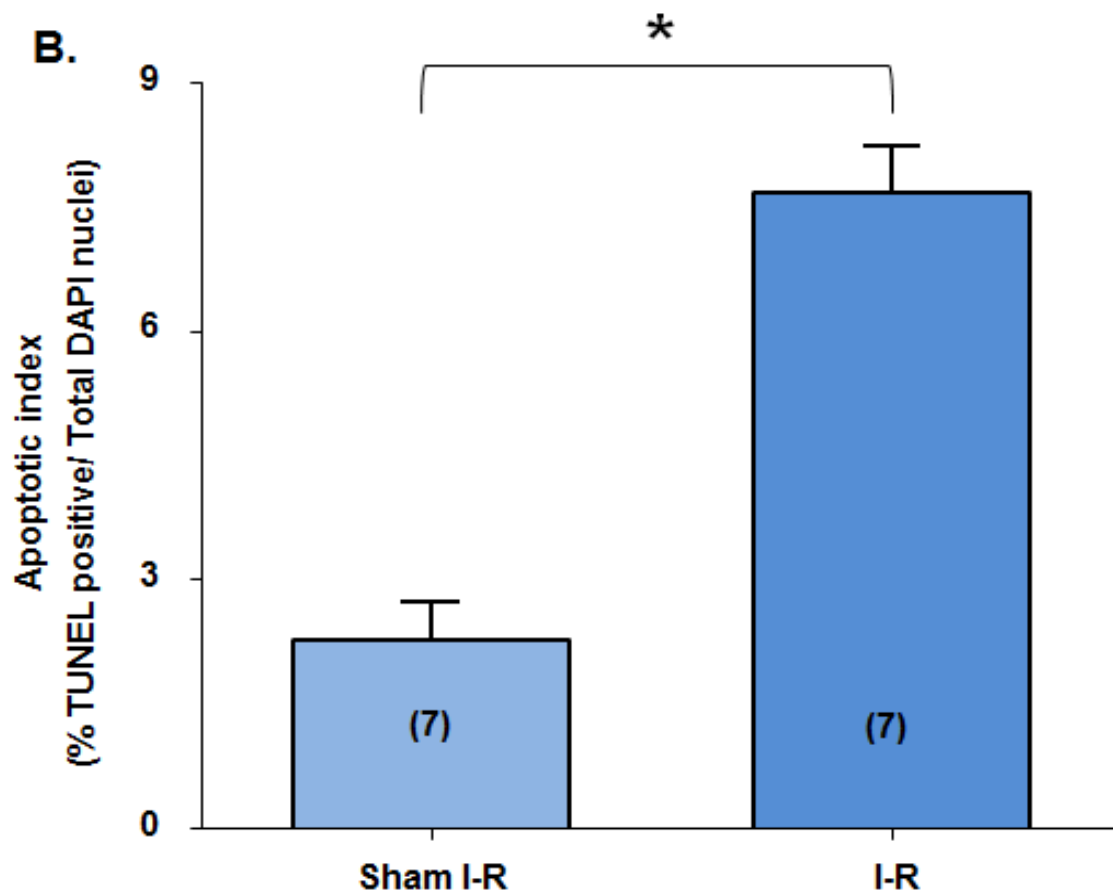


Figure 3.2: Cardiomyocytes apoptosis detected after ischaemia-reperfusion by TUNEL assay.

(A) Representative photomicrographs of ventricular sections show the proportion of TUNEL-positive nuclei (red fluorescence, arrows) relative to DAPI (blue fluorescence) stained nuclei. Arrows indicate apoptotic cardiomyocyte nuclei (pink). Bar = 100 μ m.

(B) Quantification of the apoptotic index in reperfused myocardium. Apoptotic index expressed as a percentage of TUNEL positive nuclei relative to total DAPI nuclei. Apoptotic index quantification was based on average of six fields (anterior, lateral, septal, posterior and sub-endocardial regions) per heart and seven hearts per group. I-R, ischaemia-reperfusion. Values expressed as mean \pm SE. Numbers in parentheses indicate the number of animals in each group; * P <0.01.

3.3.3 Regulation of apoptosis during I-R

Caspase-3 is a primary effector enzyme of the apoptotic pathway, mediating cleavage of nuclear substrates and DNA fragmentation (Liu et al., 1997; Sahara et al., 1999). When activated the intact caspase-3 protein (32 kDa) is cleaved into fragments (17 and 12 kDa) which associate to form a heterotetramer which is the active enzyme (Tawa et al., 2004). The tetrameric holoenzyme can be detected using conformation-specific antibodies that do not bind to the caspase-3 zymogen. In our *ex-vivo* model of I-R, caspase-3 cleavage was observed after 30 minutes ischaemia and 150 minutes reperfusion using an activation specific antibody (Figure 3.3A). Similarly, western blot showed that 32 kDa full-length caspase-3 was cleaved to a 17 kDa fragment during I-R (Figure 3.3B & 3.3C). The anti-apoptotic protein Bcl-2 is known to be regulated in activation of the intrinsic apoptotic pathway (Cory and Adams, 2002). In turn, this protein must be degraded for apoptosis to proceed during myocardial I-R injury. Compared to the sham group, I-R resulted in an approximately 50% decrease in Bcl-2 expression (Figure 3.4). Combined, these data show that I-R induced apoptosis via caspase-3 activation and Bcl-2 suppression correlates with the induction of TUNEL positive nuclei in reperfused tissue.

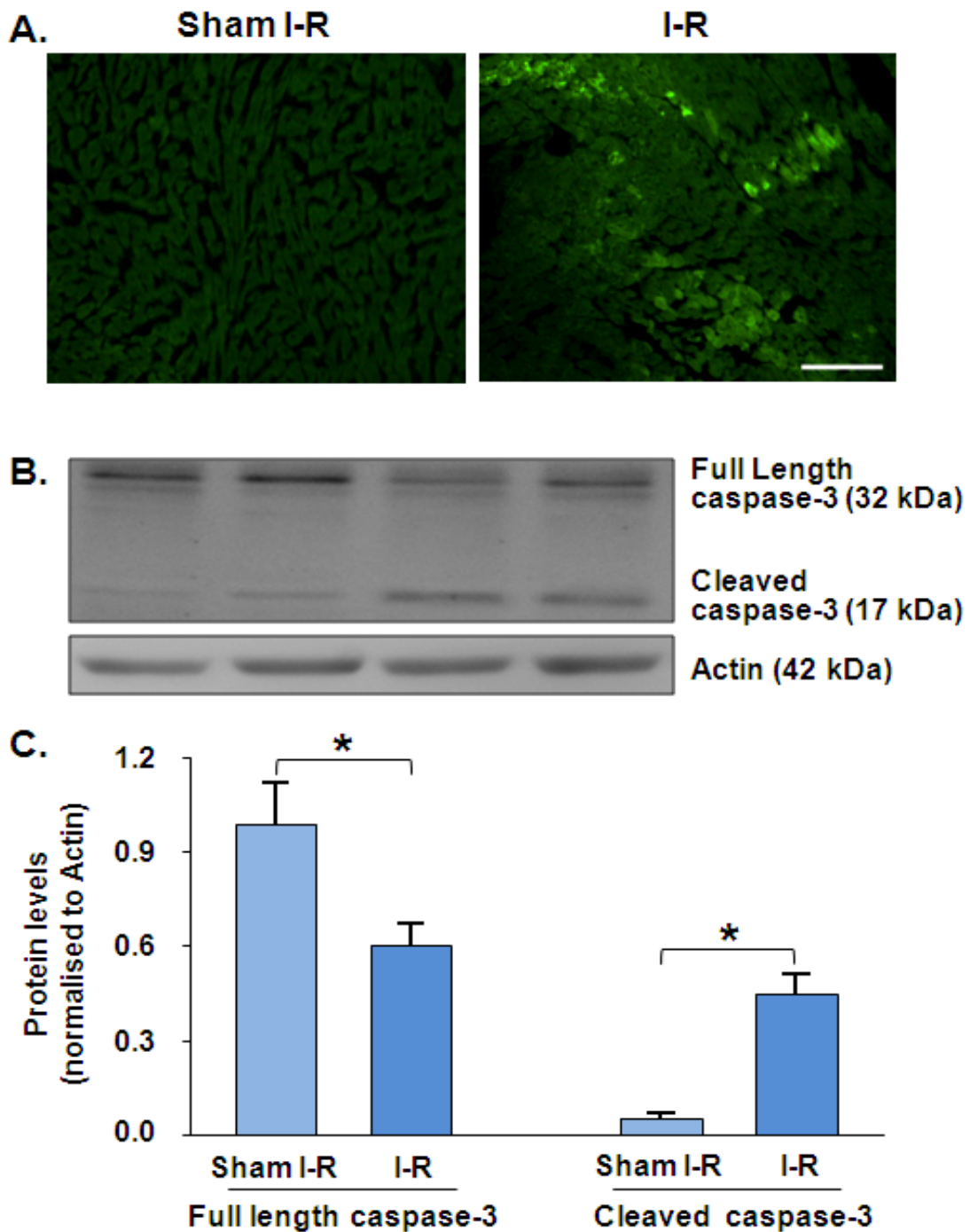


Figure 3.3: Caspase-3 is activated during ischaemia-reperfusion.

(A) Myocardium stained for active caspase-3. Increased green fluorescence indicates cleavage of caspase-3. Bar = 100 μ m. (B) & (C) Representative immunoblots showing processing of pro-caspase-3 in left ventricular free wall homogenates of reperfused hearts. Values expressed as mean \pm SE. N=3-5 per group; * P <0.05.

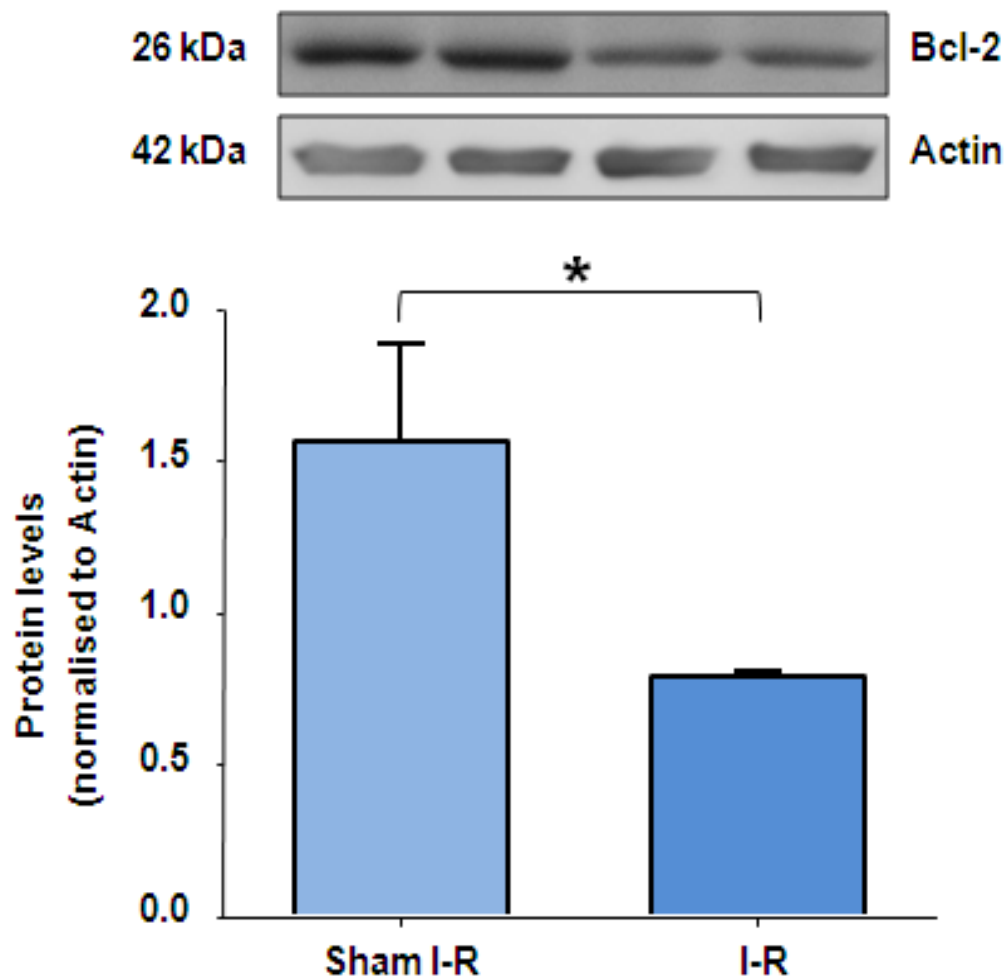


Figure 3.4: Ischaemia-reperfusion induced decreased anti-apoptotic protein Bcl-2.

Expression of the anti-apoptotic protein Bcl-2 in left ventricular free wall homogenates assessed by western blot. *Top:* Representative immunoblots showing protein expression of Bcl-2 in sham and I-R groups. *Below:* Bar graphs show densitometric analysis of Bcl-2 in sham and I-R groups. Values expressed as mean \pm SE. N=3-5 per group; * P <0.05.

3.3.4 Regulation of autophagy during I-R

To determine whether autophagy is regulated in our model of I-R injury, the levels of several autophagy marker proteins were measured (Figure 3.5). Beclin-1 plays a key role in initiating autophagy and forming of autophagosomal membrane (Hamacher-Brady et al., 2006a; Liang et al., 1999; Mizushima et al., 2001). Expression levels of Beclin-1 were increased in response to myocardial I-R (Figure 3.5A), indicating that initiation of autophagy is regulated during myocardial I-R. The process of autophagy also requires autophagy specific genes (Atg), in particular Atg5 and Atg12, to regulate elongation of autophagosomal membrane and formation of autophagic vesicles (Mizushima et al., 2001). Atg5-Atg12 conjugate is required for recruiting LC3-II, a specific marker of autophagosomes (Hamacher-Brady et al., 2006a; Kabeya et al., 2000). The conversion of microtubule-associated protein light chain 3 (LC3)-I into LC3-II (LC3-II/LC3-I ratio) associated with the autophagosome and has been established as indicators of autophagy progression (Kabeya et al., 2000; Klionsky et al., 2008). The expression of Atg5-Atg12 conjugate was up-regulated in the infarcted hearts (Figure 3.5B & 3.5C), which were accompanied by significant increased in LC3-II levels and LC3-II/LC3-I ratio (Figure 3.5C), confirming that progression of autophagy is activated during myocardial I-R.

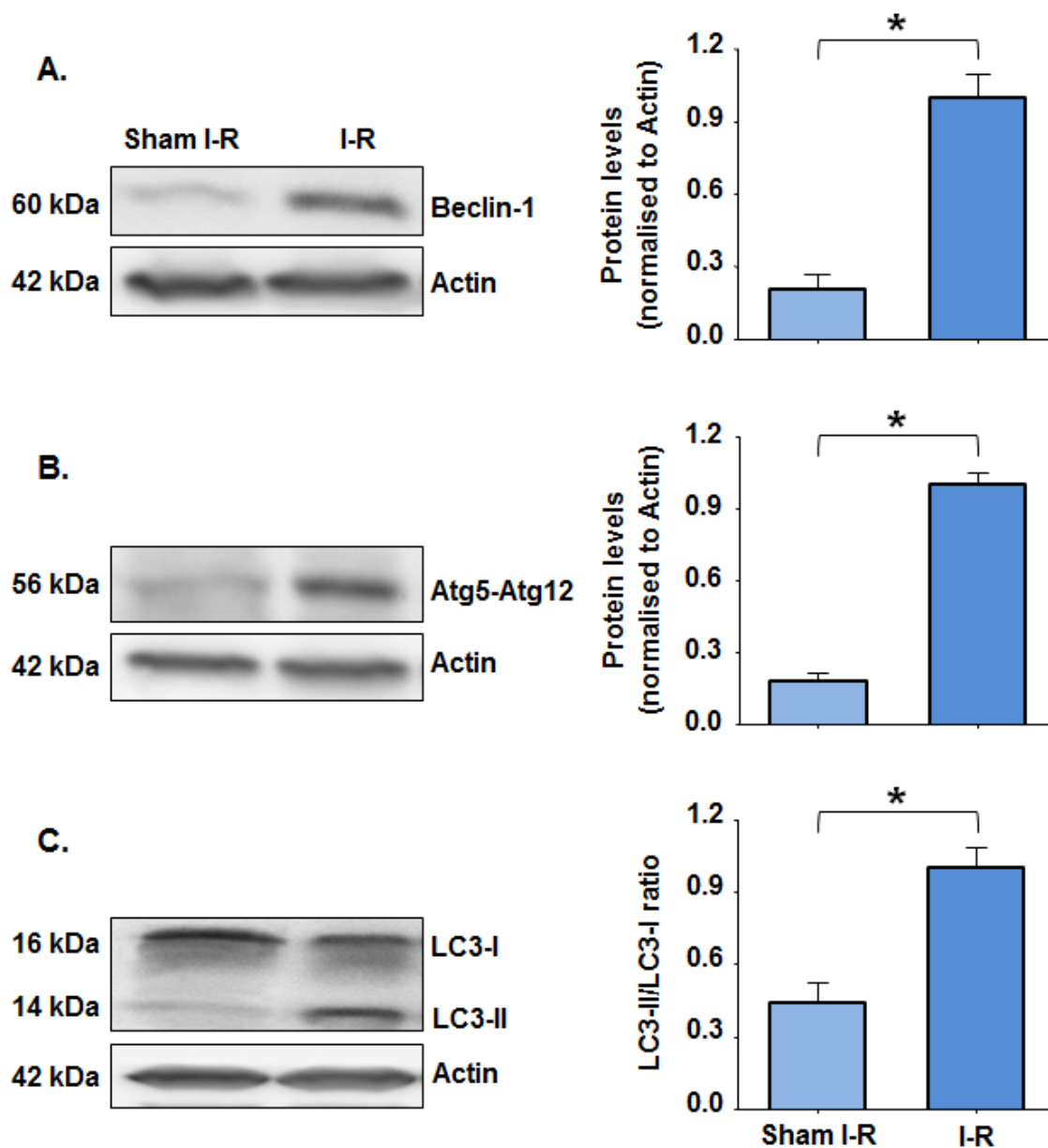


Figure 3.5: Autophagy is activated during myocardial ischaemia-reperfusion.

Expression of autophagy protein markers Beclin-1 (A), Atg5-Atg12 conjugate (B), LC3-I and LC3-II (C) in hearts subjected to ischaemia (30 minutes) followed by reperfusion (150 minutes). *Left:* Representative immunoblots of Beclin-1, Atg5-Atg12 conjugate and LC3 in sham and I-R groups. *Right:* Bar graphs showing densitometric analysis of protein changes and quantification of the ratio of LC3-I to LC3-II conversion. Values expressed as mean \pm SE. N=3-5 per group; * P <0.05.

3.3.5 Mineralocorticoid receptor blockade protects against cardiac damage during myocardial I-R: timing of treatment

Using *ex-vivo* experimental model of I-R, hearts were perfused with the MR antagonist spironolactone (in the absence of other corticosteroids), 15 minutes prior to ischaemia and on reperfusion and measured the effect on extent of infarct size. Figure 6A shows timing of treatment protocols during I-R. We found spironolactone reduced the extent of infarct area whether perfused after ischaemia or on reperfusion (Figure 3.6B).

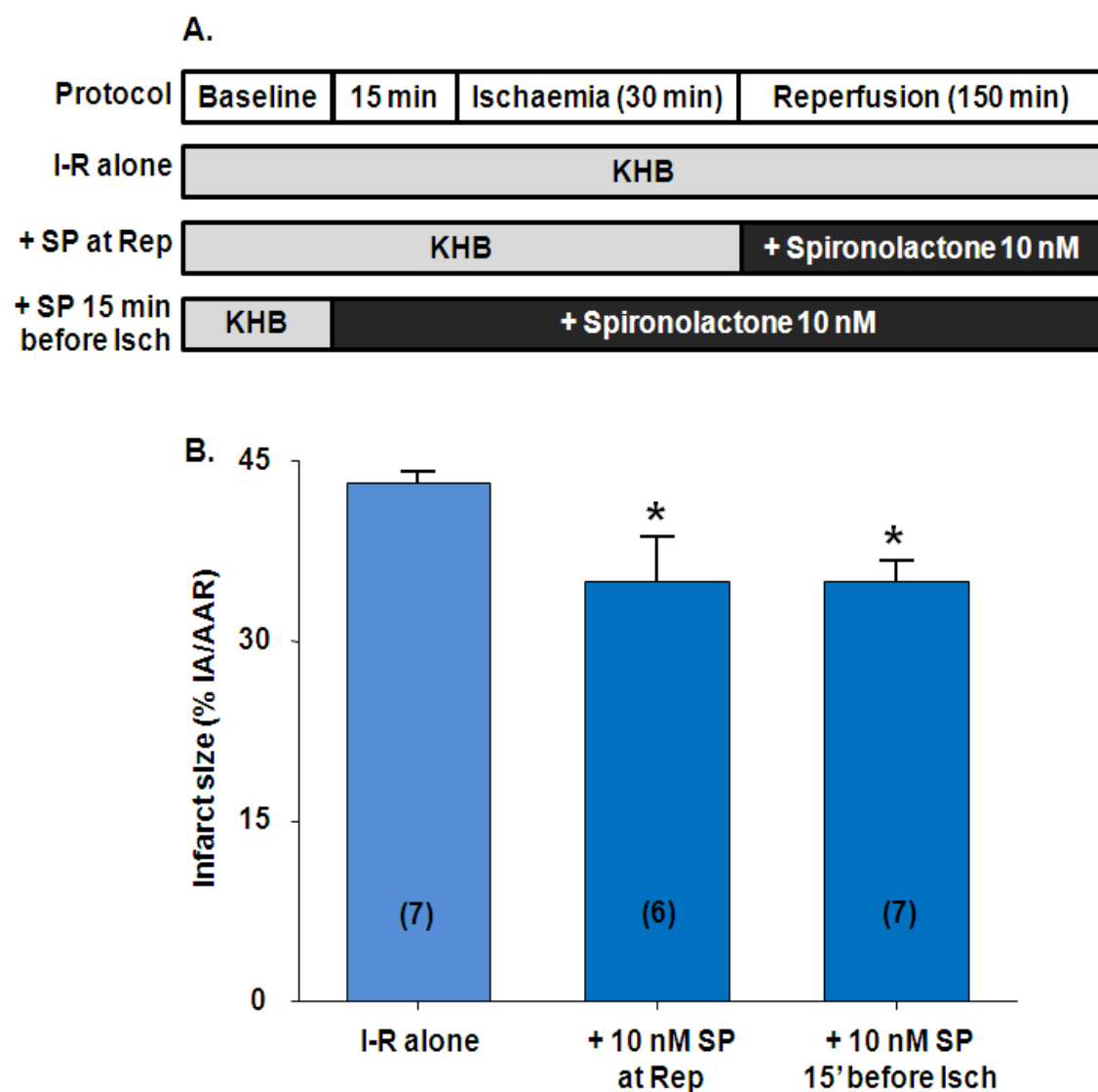


Figure 3.6: Myocardial infarct size during treatment with 10 nM spironolactone, on reperfusion and 15 minutes before ischaemia.

(A) Experimental protocol for myocardial ischaemia-reperfusion and timing of treatment. (B) Bar graph showing myocardial infarct size/area (IA) expressed as percentage of area-at-risk (AAR). Isch, ischaemia; Rep, reperfusion; I-R, ischaemia-reperfusion; KHB, Krebs-Henseleit buffer; SP, spironolactone. Values express as mean \pm SE. Numbers in parentheses indicate the number of animals in each group; * P <0.05 vs I-R alone.

3.4 Discussion

These results validate the *ex-vivo* model of myocardial I-R induced by ligation of LAD coronary artery. Isolated rat hearts subjected to regional ischaemia (30 minutes), followed by reperfusion (150 minutes) showed significant increased cardiomyocyte apoptosis and infarct size. Moreover, the studies in this chapter show that in our rat model of reperfusion injury modulate the cellular pathways that activate the processes of autophagy and apoptosis, as indicated by the increased expression of autophagy proteins (Beclin-1, Atg5-Agt12 conjugate, LC3-II), and by activation of pro-apoptotic protein caspase-3 and suppression of anti-apoptotic protein Bcl-2.

Myocardial infarct size following I-R injury is an important determinant of the extent of myocardial injury. In the current study myocardial injury (% IA/AAR) in response to I-R was approximately 42%, which is consistent with other studies using the *ex-vivo* model of I-R induced myocardial infarction (Brar et al., 2004; Ikeno et al., 2007; Kumar et al., 2012; McIntosh et al., 2010; Mihailidou et al., 2009). Similarly, there have been studies indicating infarct size of 38-46% in animals undergoing myocardial infarction or I-R *in vivo* (Delyani et al., 2001; Enomoto et al., 2005; Holly et al., 1999; Kanashiro-Takeuchi et al., 2009; Schmidt et al., 2010; Takeda et al., 2007), which is comparable to the extent of infarct found in our hands.

Apoptosis and necrosis are two distinct cell death pathways occur during myocardial injury and contribute to myocardial infarct size (McCully et al., 2004). The process of necrosis-induced myocardial cell death mainly takes place during the ischaemia period, in which opening of the mPTP plays an important role (Abdallah et al., 2011;

Nakagawa et al., 2005). In contrast, apoptosis is programmed cell death and controlled by the complex interaction between pro-survival and pro-death molecules. In the current study apoptosis was carefully assessed by histochemical visualisation of nuclear DNA fragments by TUNEL assay and immunoblot of tissue homogenates. Apoptotic index (% TUNEL-positive nuclei/ total DAPI nuclei) was found to increase ~ four-fold after I-R compared with sham (8% vs 2% respectively, Figure 3.2), which is similar to previous studies from our laboratory (Mihailidou et al., 2009) and others (Fisher et al., 2005; Rong et al., 2009; Scarabelli et al., 2001; Scarabelli et al., 1999). Moreover, the semi-quantitative data of the TUNEL staining was confirmed by western blot of apoptotic proteins. Upregulation of the pro-apoptotic protein caspase-3 and downregulation of the anti-apoptotic protein Bcl-2 are known to promote apoptosis in hearts following I-R injury. In the current study, the increase in TUNEL positive cardiomyocytes with I-R injury was associated with an upregulation of caspase-3 and downregulation of Bcl-2, which are comparable to previous studies in different models (Holly et al., 1999; Moudgil et al., 2001).

There is growing interest suggesting autophagy plays a crucial role during myocardial I-R injury. The findings in the current study demonstrate a significant increase in the autophagy proteins Beclin-1 and Atg5-Atg12 conjugate as well as the conversion of LC3-I to LC3-II in left ventricular homogenates from hearts of rat subjected to ischaemia followed by reperfusion and are supported by other studies in different experimental models of myocardial infarction (Kanamori et al., 2011; Matsui et al., 2007; Valentim et al., 2006; Xiao et al., 2011). Moreover, increased levels of Beclin-1, Atg5-Atg12 conjugate and LC3-II indicate cardiomyocytes undergoing autophagy

processing and predict an impaired outcome (Kabeya et al., 2000; Kassiotis et al., 2009; Ma et al., 2012b).

The studies to determine timing of treatment showed that perfusion with low dose (10 nM) spironolactone 15 minutes prior to ischaemia reduces I-R injury which is supported by previous studies showing similar reduction in the extent of infarction (Chai et al., 2005; Chai et al., 2006). Although cardioprotective actions of MR antagonists have been observed when administered at the end of ischaemia (Kanashiro-Takeuchi et al., 2009; Schmidt et al., 2010), our study showed that MR antagonists administered at reperfusion have comparable benefit, which confirm the clinical studies for early administration of MR antagonists .

One of the limitations of the present study was that we did not have the facilities to evaluate contractility, systolic left ventricular pressure, left ventricular end diastolic pressure, cardiac output, echocardiography and heart rate variables, which would provide further information about the effects of myocardial I-R injury. In conclusion, our experimental *ex vivo* model of myocardial infarction is reproducible and consistent with different models reported in the literature and clinical practice. Cardiac apoptosis and autophagy were activated during I-R injury and represent the mechanisms involved in the (patho)physiological of IHD.

Chapter 4

Sex differences in cardiac damage during myocardial infarction

4.1 Introduction

Gender differences have been observed in presentation and outcomes to IHD (Roger et al., 2012). Men have earlier onset and more severe age-specific IHD than women, although women have a greater risk of death after MI (Greenland et al., 1991; Roger et al., 2012). Mechanisms for these differences are not fully defined partly since younger women and older men are insufficiently represented in many studies (Kim et al., 2010), with focus on 17β -oestradiol (E2) actions mediated via oestrogen receptors (E2-R), and less attention on androgen receptor (AR)-mediated androgen action (Vaccarino et al., 2011). There are even fewer studies on androgens and cardiovascular risk in women.

A few conflicting studies have assessed the effects of androgens during MI. Testosterone (T) adversely affects cardiac remodelling and function following MI independent of gender (Bae and Zhang, 2005), whereas dihydrotestosterone (DHT) ameliorated post-I-R recovery via enhanced angiogenesis (Beygui et al., 2009). Male rats have increased infarct area following I-R (Mihailidou et al., 2009; Wang et al., 2005), whereas T replacement to male rats reportedly reduced I-R mediated cardiac injury (Callies et al., 2003). Low circulating T levels are associated with poorer outcomes in HF and decreased survival (Malkin et al., 2010) in men with coronary artery disease (CAD); whether these are cause or effect is yet to be determined.

Reported effects of endogenous E2 similarly vary in females, with reduction (Booth and Lucchesi, 2008) or no difference (Cross et al., 1998) during I-R. Postmenopausal E2 administration also provides conflicting results, with adverse cardiovascular effects in the Women's Health Initiative study, but reduced cardiovascular disease (CVD) risk in

observational trials and the randomised Danish Osteoporosis Prevention Study (Schierbeck et al., 2012). Data on the relationship between E2 and CVD risk in men is limited or unreliable, despite higher E2 levels measured in men with CAD (Phillips et al., 1983). Few studies have examined endogenous T and CAD in women, with either positive (Braunstein, 2007) or no (Barrett-Connor and Goodman-Gruen, 1995) correlation between serum levels and CVD reported; all these studies used immunoassays which provide inaccurate results at low circulating steroid levels (Harwood and Handelsman, 2009).

Myocardial I-R activates release of reactive oxygen species and augmentation of the multi-ligand receptor for advanced glycation end products (RAGE) (Bucciarelli et al., 2006), providing a pro-inflammatory stimulus for cardiac dysfunction. Autophagy, a cell survival pathway (Matsui et al., 2007) is also activated and recent studies indicate autophagy protects cardiomyocytes from apoptosis (Matsui et al., 2007), while in excess it may be detrimental (Ma et al., 2012a). It is not known whether sex steroids regulate autophagy during MI, although apoptosis leads to tissue damage (Saraste et al., 1997). Male rats have increased apoptosis following myocardial I-R (Mihailidou et al., 2009; Wang et al., 2005) and men dying after acute MI have a higher apoptotic rate in the peri-infarct region at autopsy than women (Biondi-Zoccai et al., 2005).

Expression levels of mineralocorticoid receptors (MR) may also contribute to cardiac damage following MI and HF. MR expression levels were upregulated in post-mortem hearts from men with congestive heart failure (Yoshida et al., 2005) and in male animal models of experimental MI, levels of MR protein were increased in the left ventricle 2-

4 weeks post-MI) (de Resende et al., 2006; Milik et al., 2007; Takeda et al., 2007). There are no studies which have examined whether there is sexual dimorphism of MR expression in the heart following myocardial I-R injury. The aim of the current study was to determine how androgens mediate these sex differences in cardiac damage during MI and since the focus of this thesis is regulation of MR during MI, whether there are gender differences in expression levels of MR.

4.2 Methods

Adult age-matched male (300 – 400 g) and female (200 – 300 g) Sprague Dawley rats (N=190) were allocated at random for either no surgery (Intact), bilateral gonadectomy (Gx) or sham operation (Sham Gx) for these studies.

4.2.1 Gonadectomy surgical procedures

For the gonadectomy (Gx) or sham operations (Sham Gx) the rats were anaesthetised with nitrous oxide and oxygen (2:1 v/v, 3 L/min), and 2% (v/v) isoflurane, maintained during the procedures, with additional analgesia provided as required. Female rats were subjected to bilateral ovariectomy which involved placing them prone, both flanks shaved and area disinfected with 70% ethanol followed by a small skin incision (~1 cm) was made in the dorso-lateral area to expose the abdominal muscles and, after ovaries on both sides of the abdomen located, tied off and removed. The skin incisions were closed with michel clips. For orchidectomy, in males, a small mid-line incision (~1 cm) was made in the scrotum, the skin separated and both testes pulled out. The spermatic cord was tied and cut, and the incisions closed with michel clips. Iodine was applied to the incision sites and the rats allowed to recover. In sham operations, the incisions were

made and then closed. Animals were monitored post-operatively during the recovery period to ensure that they did not display any signs of pain and administered temgesic (0.02 mg/kg, i.m.). Rats were then maintained on standard laboratory chow *ad libitum* and monitored daily.

4.2.2 Treatments

Silastic hormone implants were inserted subdermally in gonadectomised animals on the day of surgery and animals monitored for 21 days. Silastic implants have previously been shown to provide sustained, controlled concentrations of steroids (Allan et al., 2010; Meachem et al., 2007). Testosterone and 17 β -oestradiol doses in gonadectomised females were adjusted to compare to those in males by using smaller size implants due to the lower weight of the females. Male animals were divided into the following groups: (1) Sham (N=11), (2) Intact (N=14), (3) Sham Gx (N=6), (4) Gx (N=18), (5) Gx + T (3 cm, N=14), (6) Gx + DHT (1 cm, N=8), (7) Gx + E2 (0.4 cm, N=16). Females were divided into the following groups: (1) Sham (N=16), (2) Intact (N=20), (3) Sham Gx (N=8) (4) Gx (N=15), (5) Gx + T (2.4 cm, N=13) and (6) Gx + E2 (0.3 cm, N=11). Testosterone, 17 β -oestradiol and dihydrotestosterone implants were prepared as previously described (Allan et al., 2010; Meachem et al., 2007). Surgical Gx and steroid replacement were confirmed by measuring serum levels of steroids. Since most steroid hormone immunoassays lack sensitivity, specificity, and accuracy at low plasma levels (Harwood and Handelsman, 2009; Rosner et al., 2013; Stanczyk et al., 2007), especially in rodents (Haisenleder et al., 2011; Handelsman et al., 2011), we used liquid chromatography-tandem mass spectrometry (LC-MS/MS) assay. This assay has

sensitivity and specificity to accurately determine serum androgen levels in rodent samples (Harwood and Handelsman, 2009).

4.2.3 *Ex-vivo* myocardial ischaemia-reperfusion

Following 21 days post gonadectomy and hormone treatment, rats were anaesthetised with intraperitoneal (IP) injection of ketamine (60 mg/kg) and xylazine hydrochloride (10 mg/kg) and then received heparin (250 IU, IP). Hearts rapidly isolated and subjected to regional I-R procedure as described in Chapter 2 (sections 2.2). At the end of reperfusion, infarct size and apoptosis (TUNEL) were measured as described in Chapter 2 (sections 2.3 – 2.4). Infarct size and apoptosis were measured on the same hearts, with a separate group of animals used for protein analysis by immunoblotting.

4.2.4 Western blots

At the end of reperfusion, left ventricular free wall tissue was snap frozen in liquid nitrogen. Protein extraction, SDS-PAGE, electrophoretic transfer of proteins to PVDF membrane and immunoblotting were performed as described in Chapter 2 (section 2.5.2 – 2.5.3). Primary antibodies for Beclin-1 (Cell Signaling), LC3-I/II (Cell Signaling), Atg-5 (Sigma-Aldrich), RAGE (Abcam), mTOR, Phospho-mTOR (Cell Signaling), AMPK, Phospho-AMPK (Cell Signaling), caspase-3/-9 (Cell Signaling), ARC (Apoptosis Repressor with a Caspase recruitment domain, Cayman Chemical), Bcl-xL (B-cell lymphoma-extra large, Santa Cruz), XIAP (X-linked inhibitor of apoptosis protein, (Cell Signaling), rMR 1-18 1D5 (kindly provided by Prof. Celso Gomez-Sanchez), ER α , ER β and AR (Santa Cruz Biotechnology) were used. Bound antibodies were detected with HRP-conjugated secondary antibody (1:3000, Dako Cytomation).

Membranes were exposed to chemiluminescent substrate (Perkin Elmer, Melbourne, Australia) and digital images of the resulting bands captured on a LAS4000 (GE Healthcare Life Sciences).

4.2.5 Statistical analysis

Details for statistical analysis are described in Chapter 2 (sections 2.8).

4.3 Results

Females were approximately 100 grams lighter than male littermates with no differences between intact and sham Gx males or females (Table 4.1). Treatment did not affect body weight except T-treated Gx males were heavier. In females, Gx increased body weight which was restored by E2 but not T administration (Table 4.1). Regional ischaemia-reperfusion produced larger infarct size in male than female hearts (Figure 4.1A), similar to previous reports (Bae and Zhang, 2005), and correlated with increased apoptosis measured by TUNEL staining (Figure 4.1B). In females, smaller infarct size corresponded with less apoptosis (Figure 4.1B).

Treatment	Male Body Weight (g)	Female Body Weight (g)
Intact	350 ± 17	247 ± 5
Sham Gx	360 ± 11	257 ± 9
Gx	373 ± 8	318 ± 7*
Gx + T	397 ± 7*	314 ± 15*
Gx + DHT	380 ± 6	n/a
Gx + E2	362 ± 13	237 ± 8

Table 4.1: Body weights of male and female rats in the various treatment groups.

All values shown are Mean ± SE, N = 8-16 per group; * $P < 0.05$ vs respective sham gonadectomy (Sham Gx); Gx, Gonadectomy; E2, 17 β -oestradiol; T, Testosterone; DHT, Dihydrotestosterone. n/a, not administered

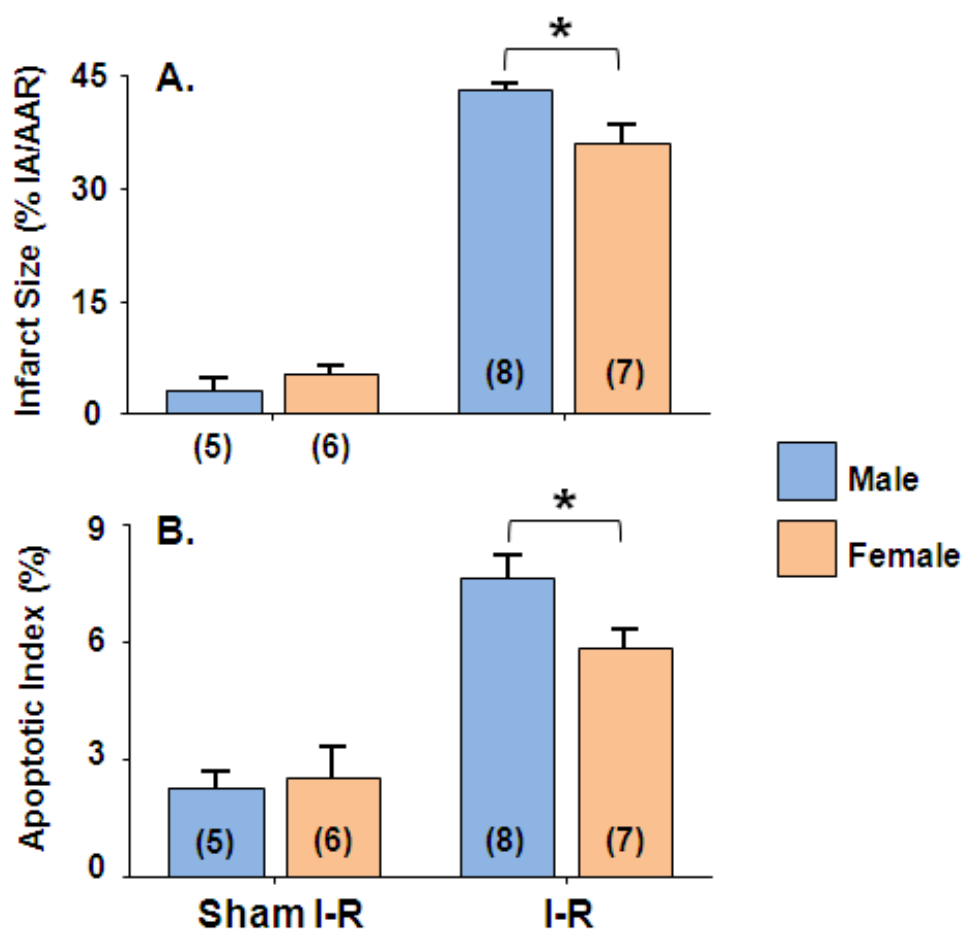


Figure 4.1: Sex differences in left ventricular infarct size and apoptosis.

Myocardial infarct size (**A**) and apoptotic index (**B**) in male and female rat hearts subjected to 30 minutes ischaemia followed by 150 minutes reperfusion (I-R) or sham ischaemia-reperfusion (Sham I-R). Myocardial infarct size/area (IA) is expressed as the percentage of the area-at-risk (AAR). Apoptotic index is expressed as the percentage of TUNEL-positive nuclei relative to DAPI-stained nuclei in the reperfused myocardium. Values expressed as mean \pm SE. Numbers in parentheses indicate the number of animals in each group; * $P < 0.05$.

4.3.1 Role of sex steroids on infarct size

Sham Gx did not influence infarct size in either male [$42 \pm 4\%$ (Sham Gx, N=5) versus $43 \pm 1\%$ (intact, N=6)] or female [$30 \pm 4\%$ (Sham Gx, N=7) versus $36 \pm 3\%$ (intact, N=7)] hearts. Infarct size was reduced in Gx males (Figure 4.2A) but exacerbated in Gx females (Figure 4.2B), with neither having detectable serum T or E2 levels. Treatment with T restored infarct size in Gx males, despite lower serum T levels [1.3 ± 0.2 ng/ml (Gx +T, N=9) versus 2.8 ± 0.8 ng/ml (Sham Gx, N=4), $*P < 0.05$]. To confirm these changes were androgen-specific, we used DHT which unlike T cannot be aromatised to E2. Infarct size was similarly aggravated by DHT (Figure 4.2A) at serum levels below detection limit (< 200 pg/ml). Gx females receiving T had elevated serum T levels [2.1 ± 0.2 ng/ml (Gx+T, N=6) versus 0.04 ± 0.02 ng/ml (sham Gx, N=4), $*P < 0.05$], with no effect on Gx-increased infarct size (Figure 4.2B), whereas E2 reduced infarct size (Figure 4.2B) to Sham Gx levels. Treatment with E2 aggravated infarct size in Gx males (Figure 4.2A) with plasma E2 levels [27.7 ± 7.0 pg/ml, N=10] well above intact male and female levels [E2 < 5 pg/ml].

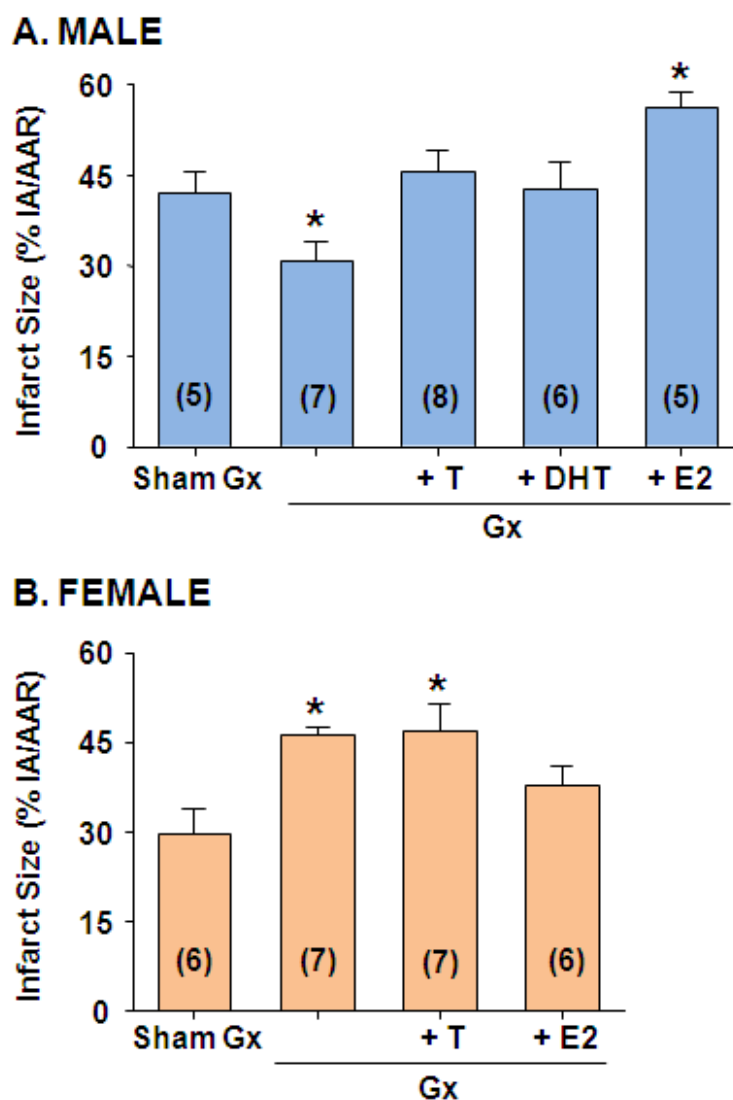


Figure 4.2: Effect of gonadectomy and steroid treatment on left ventricular infarct size in males and females.

Myocardial left ventricular infarct size from gonadectomised male (**A**) and female (**B**) animals (\pm hormones for 21 days) which were subjected to I-R injury. Myocardial infarct size/area (IA) is expressed as the percentage of the area-at-risk (AAR). Sham Gx, sham gonadectomy; Gx, gonadectomised; DHT, dihydrotestosterone; T, testosterone; E2, 17β -oestradiol. Numbers within the columns indicate the number of animals in each group. Values expressed as mean \pm SE; * $P < 0.05$ vs Sham Gx.

4.3.2 Differential regulation of androgen receptor levels during myocardial I-R

Levels of AR, E2-R α and E2-R β were comparable in male and female left ventricular free wall (sham I-R, Figure 4.3B & 4.3D). I-R enhanced AR and E2-R β expression in the infarct area of male (Figure 4.3A & 4.3B) but only E2-R β levels in female (Figure 4.3C & 4.3D) hearts. E2-R α expression did not change with I-R (Figure 4.3B & 4.3D). Myocardial AR levels were decreased in Gx males (Figure 4.3A & 4.3B) but not females (Figure 4.3C & 4.3D) and T treatment restored levels in Gx males (Figure 4.3B) while elevating them in Gx females (Figure 4.3D). E2 had no effect on AR levels in Gx males (Figure 4.3B), but suppressed levels in Gx females (Figure 4.3D). Neither E2-R α nor E2-R β levels in either gender were modified by treatment (Figure 4.3B & 4.3D).

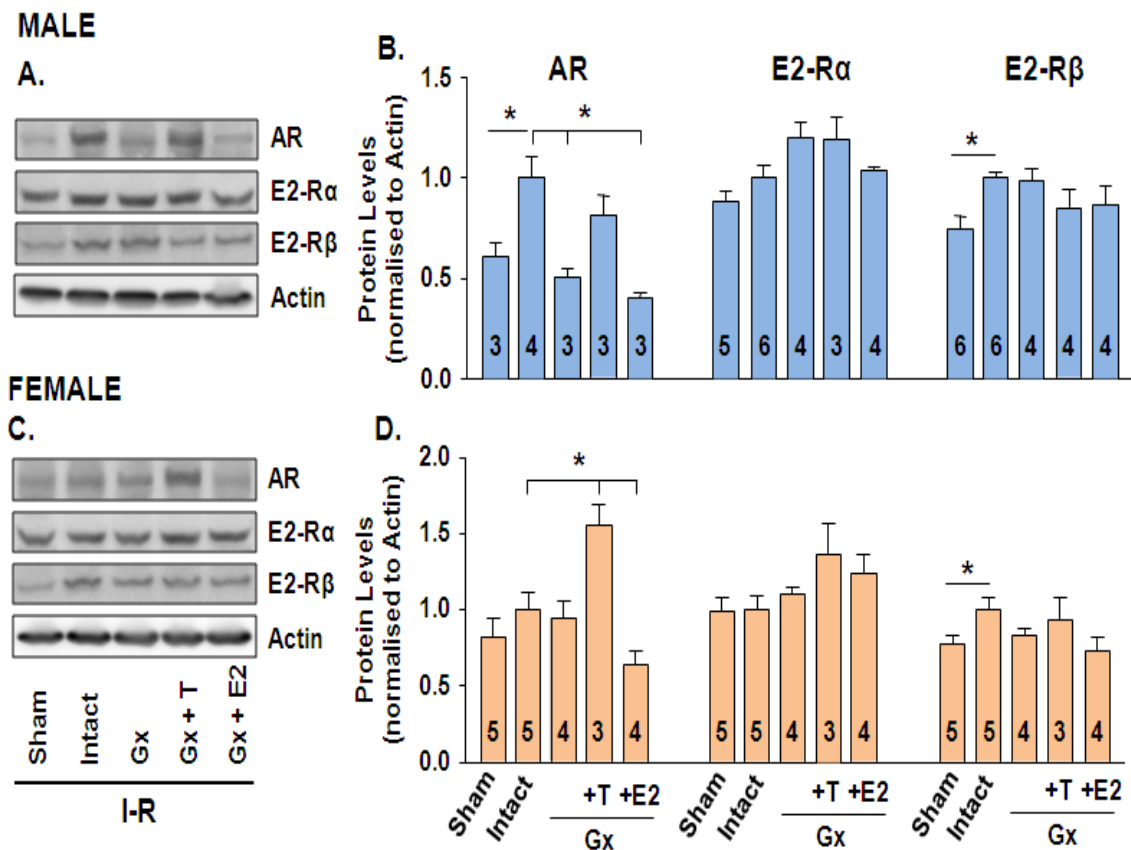


Figure 4.3: Regulation of left ventricular sex steroid receptor expression

Sex steroid receptor expression in the infarcted area from intact and gonadectomised males and females. Representative immunoblots of androgen receptor (AR), oestrogen receptors (E2-R) -alpha (E2-R α) and -beta (E2-R β) in homogenates of male (Panel A) and female (Panel C) left ventricular free wall. Bar graphs show densitometric analysis of protein changes compared to the loading control β -actin for males (Panel B) and females (Panel D). Gx, gonadectomised; T, testosterone; E2, 17 β -oestradiol. Numbers in parentheses indicate number of animals per group; * P <0.05 vs Intact.

4.3.3 Regulation of autophagy by sex steroids during myocardial I-R

I-R activated autophagy signalling kinases (AMP-activated protein kinase (AMPK) and mammalian target of rapamycin (mTOR)) and autophagosome formation initiated by increasing levels of Beclin-1, Atg5-Atg12 conjugate, LC3-II, conversion of LC3-I to LC3-II (LC3-II/LC3-I ratio) in both males and females (Figure 4.4). Activated AMPK activity during I-R was unaffected by Gx (Figure 4.4Ai & 4.4Bi), nor by T or E2 treatment, with a trend ($P=0.045$) for enhanced AMPK activity in Gx females receiving T. This study indicated gender-specific regulation of mTOR activity. Gx had no effect on I-R induced mTOR activation in male hearts (Figure 4.4Aii), but enhanced mTOR activation in female hearts (Figure 4.4Bii). T or E2 treatment had no effect on mTOR activity in Gx males (Figure 4.4Aii & 4.4Bii), whereas both treatments restored mTOR levels in Gx females.

Gx decreased Beclin-1 levels in the infarct area of hearts from males and females (Figure 4.4Aiii & 4.4Biii). There was a trend in restoring Beclin-1 levels in Gx females receiving T or E2 but not Gx males. Formation of autophagic vesicles (denoted by formation of Atg5-Atg12 conjugate) and progression of autophagy (LC3-II/LC3-I ratio) were decreased in the infarct area by Gx in both genders (Figure 4.4Aiv-v & 4.4Biv-v) indicating progression of autophagy was interrupted. T treatment restored Atg5-Atg12 conjugate levels in both genders (Figure 4.4Aiv & 4.4Biv) while E2 treatment only restored Atg5-Atg12 conjugate levels in Gx females (Figure 4.4Biv). Suppressed LC3-II/LC3-I ratios persisted in Gx males despite T or E2 treatment (Figure 4.4Av), indicating autophagy could not progress. In contrast, there was a trend by T and E2 to restore LC3-II/LC3-I ratio in Gx females to levels in intact females, indicating progression of autophagy.

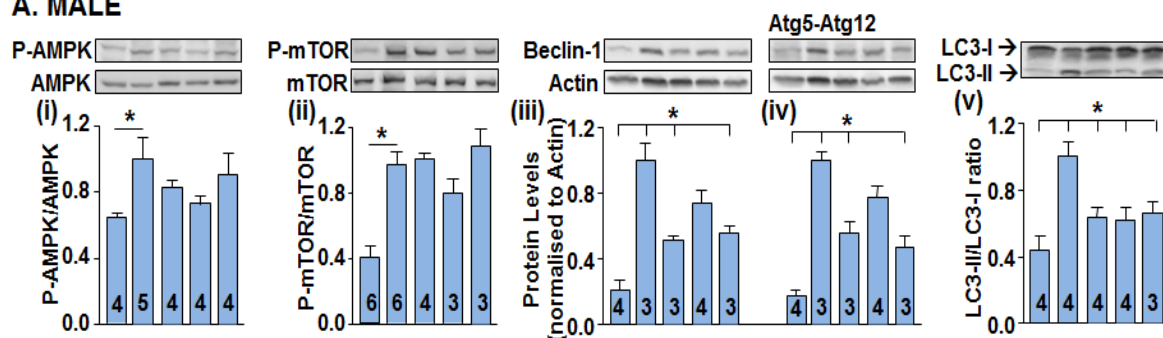
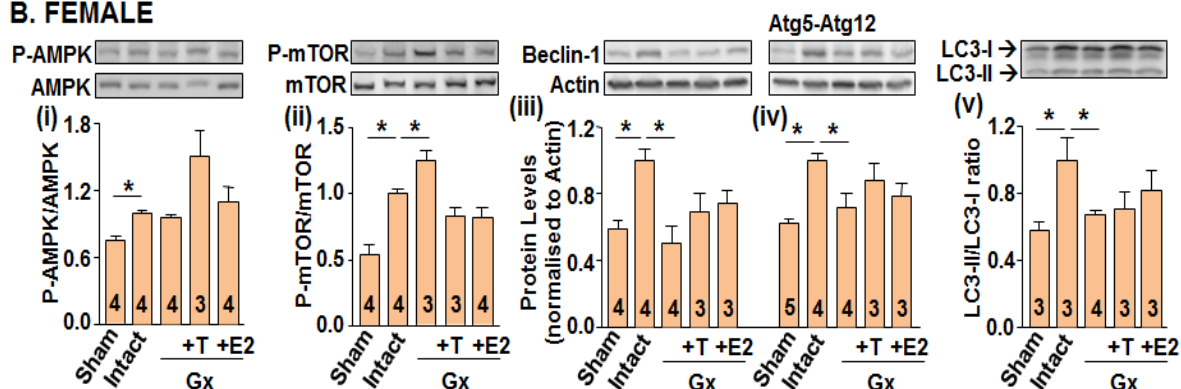
A. MALE**B. FEMALE**

Figure 4.4: Effects of sex steroids on autophagy markers.

I-R induced expression of autophagy markers Beclin-1, Atg5-Atg12 conjugate and LC3-II/I assessed by immunoblotting in homogenates of left ventricular free wall from infarct area of intact and Gx males and females (\pm sex steroids). *Top*: Representative immunoblots of P-AMPK, AMPK, P-mTOR, mTOR, Beclin-1, Atg5-Atg12 conjugate, LC3-I, LC3-II, in males (**A**) and females (**B**). *Below*: Bar graphs are densitometric analysis of the levels of (i) P-AMPK/AMPK ratio, (ii) P-mTOR/mTOR ratio, (iii) Beclin-1, (iv) Atg5-Atg12 conjugate, and (v) ratio of LC3-I to LC3-II conversion. Gx, gonadectomised; T, testosterone; E2, 17β -oestradiol; P-AMPK, phosphorylated AMP-activated protein kinase (AMPK); P-mTOR, phosphorylated mammalian target of rapamycin (mTOR); Atg, autophagy-related gene; Beclin-1, known as Atg6; LC3, microtubule-associated protein light chain 3. Numbers in parentheses indicate number of animals per group; $*P < 0.05$ vs Intact.

4.3.4 Differential regulation of RAGE by sex steroids during myocardial I-R

I-R augmented myocardial RAGE expression in infarcted myocardium from intact males (Figure 4.5A), but not females (Figure 4.5B), while Gx had no effect in either gender (Figure 4.5A & 4.5B). T treatment suppressed RAGE protein levels in Gx males (Figure 4.5A), with the opposite effect in Gx females (increased RAGE levels, Figure 4.5B). E2 treatment had no significant effect in either gender.

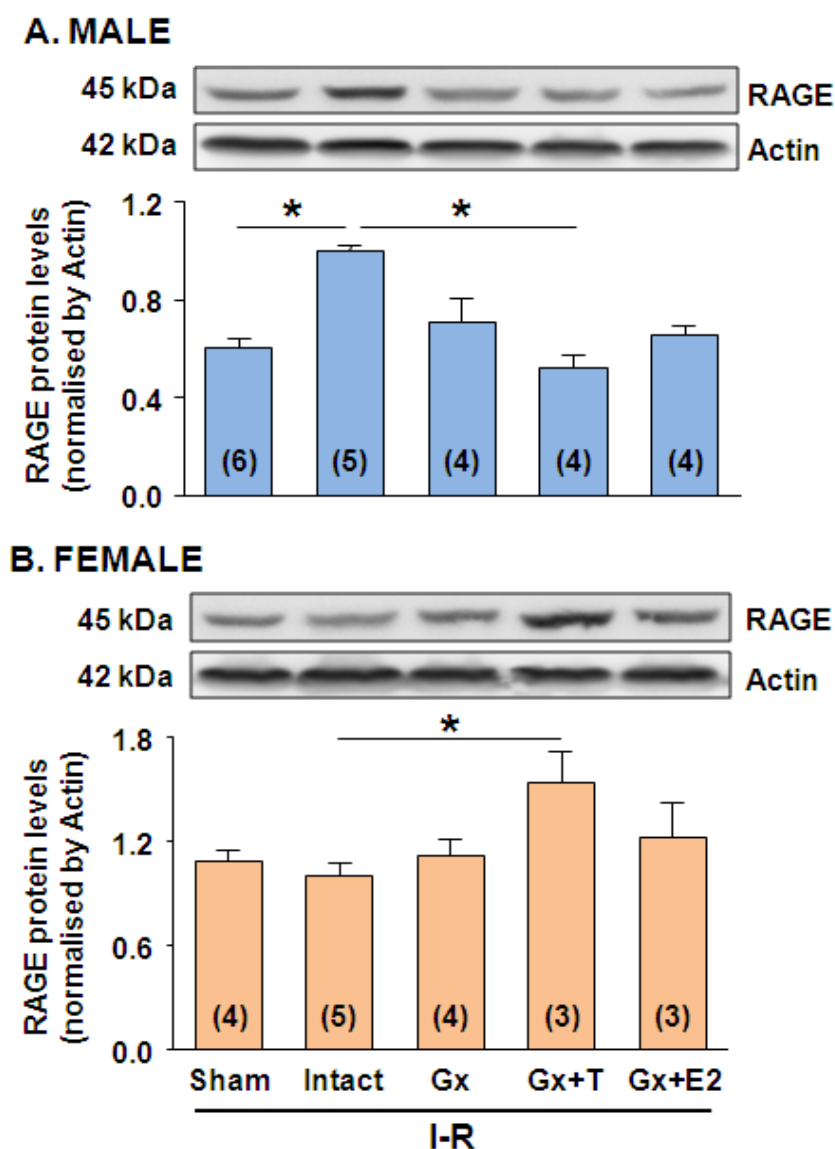


Figure 4.5: Effects of sex steroids on RAGE expression

Expression levels of RAGE in homogenates of left ventricular free wall from the infarct area from intact and gonadectomised (\pm sex steroids) males (**A**) and females (**B**) following I-R. *Top*: Representative immunoblots of RAGE; *Bellow*: Bar graphs show densitometric analysis in the various treatment groups. RAGE, receptor for advanced glycation end products; I-R, ischaemia-reperfusion, Sham, sham I-R; Gx, gonadectomised; T, testosterone; E2, 17β -oestradiol. Numbers in parentheses indicate number of animals per group; $*P < 0.05$ vs Intact.

4.3.5 Sex differences in regulation of apoptosis during myocardial I-R

Caspase-9 and -3 processing are measures of the intrinsic pathway of apoptosis and were activated (presence of cleaved fragments) by I-R in both males and females (Figure 4.6). Consistent with effects on infarct size, Gx suppressed caspase-9 and caspase-3 processing in males (Figure 4.6Ai & 4.6Aii), but augmented caspase cleavage in females (Figure 4.6Bi & 4.6Bii). Treatment with T or E2 restored caspase processing in Gx males (Figure 4.6Ai & 4.6Aii). In females T did not affect Gx-activated caspase processing (Figure 4.6Bi & 4.6Bii), whereas it was reversed by E2.

Expression levels of anti-apoptotic proteins, XIAP, Bcl-X_L and ARC showed dimorphic regulation during I-R. In males, I-R decreased levels of all three anti-apoptotic proteins whereas levels were preserved in females (Figure 4.7). Gx enhanced expression of ARC and Bcl-X_L, but not XIAP, in males which was reversed to levels in intact (non-Gx) males by treatment with T but not E2 (Figure 4.7A and 4.7B). In contrast, expression of XIAP and Bcl-X_L, but not ARC, were suppressed following I-R in Gx females and were restored by E2 but not T (Figure 4.7C & 4.7D).

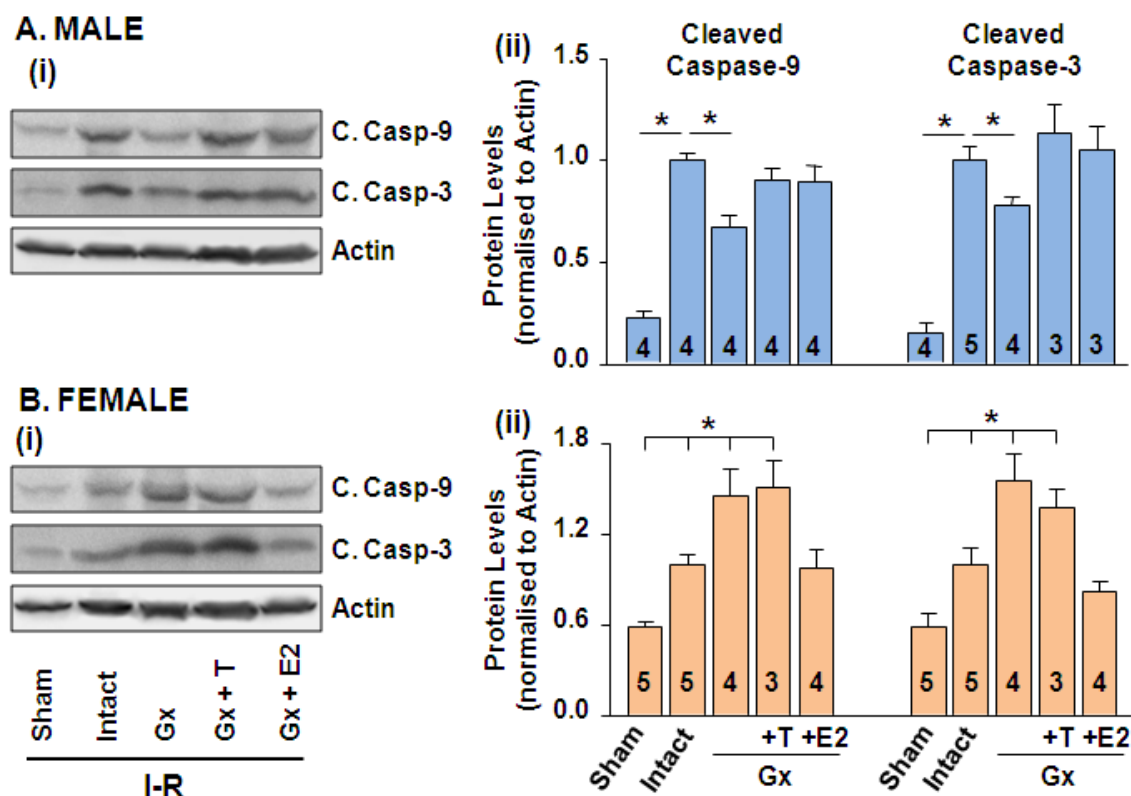


Figure 4.6: Effect of sex steroids on caspase-3 and -9 processing during myocardial ischaemia-reperfusion

Appearance of cleaved fragments represents caspase processing. Representative immunoblots for caspase-3 and -9 cleaved fragments in homogenates of male (A(i)) and female (B(i)) left ventricular free wall from the infarct area during ischaemia-reperfusion (\pm gonadectomy and sex steroids). Bar graphs represent densitometric analysis in males (A(ii)) and females (B(ii)) with β -actin as the loading control. I-R, ischaemia-reperfusion; C.Casp-9, cleaved caspase-9; C.Casp-3, cleaved caspase-3; Gx, gonadectomised; T, testosterone; E2, 17β -oestradiol. Numbers in parentheses indicate number of animals per group; * $P < 0.05$ vs Intact.

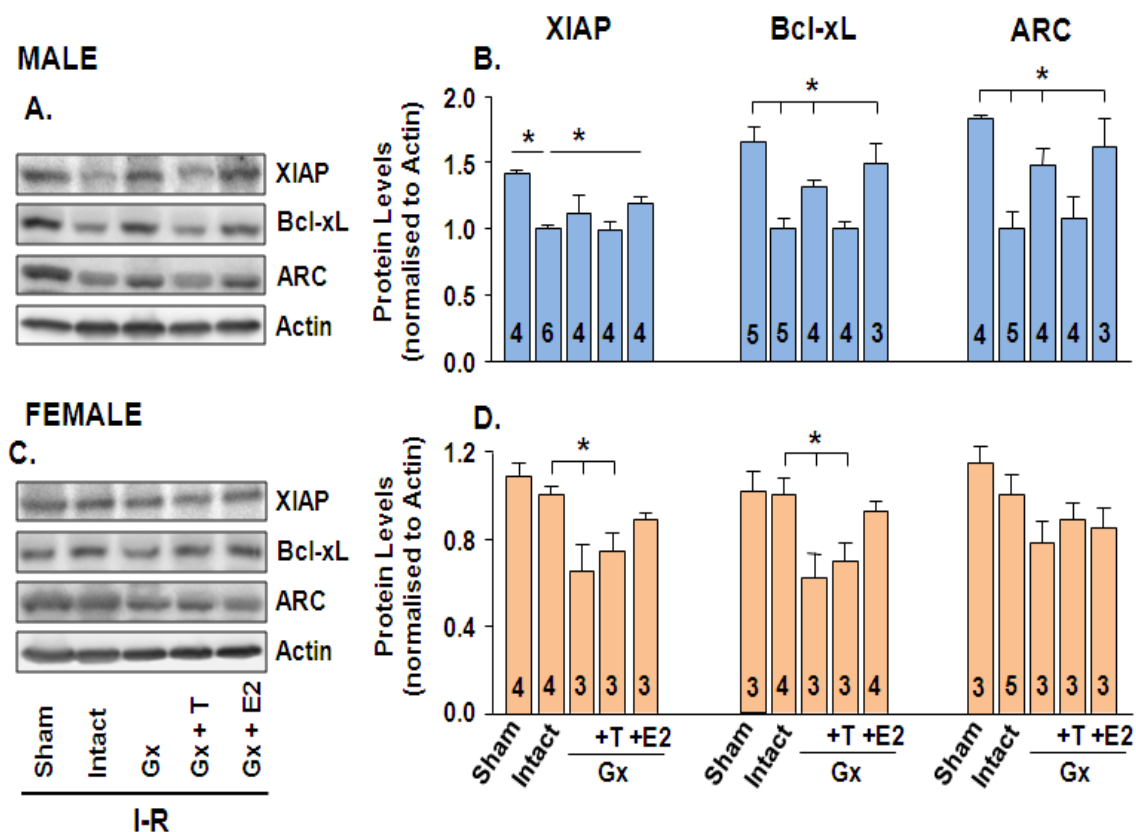


Figure 4.7: Effects of sex steroids on anti-apoptotic regulators of the intrinsic pathway of apoptosis

Left: Representative immunoblots of anti-apoptotic proteins XIAP, Bcl-xL and ARC in homogenates of the left ventricular free wall from infarct area from intact and gonadectomised (\pm sex steroids) males (**A**) and females (**B**). *Right:* Bar graphs show densitometric analysis with loading control β -actin. I-R, ischaemia-reperfusion; Gx, gonadectomised; T, testosterone; E2, 17β -oestradiol; XIAP, X-linked inhibitor of apoptosis protein; Bcl-xL, B-cell lymphoma-extra large; ARC, apoptosis repressor with caspase recruitment domain; Numbers in parentheses indicate number of animals per group; * $P < 0.05$ vs Intact.

4.3.6 Regulation of MR levels by sex steroids during myocardial I-R

MR expression in both male and female hearts is shown in Figure 4.8. Although reperfusion injury showed a trend to decrease levels of MR in male rats, this was not significant. Removal of endogenous sex steroid hormones (androgens or oestrogens) by gonadectomy did not alter the levels of myocardial MR in males or females. Similarly, there was no change in MR expression levels during supplementation with T or E2 (Figure 4.8).

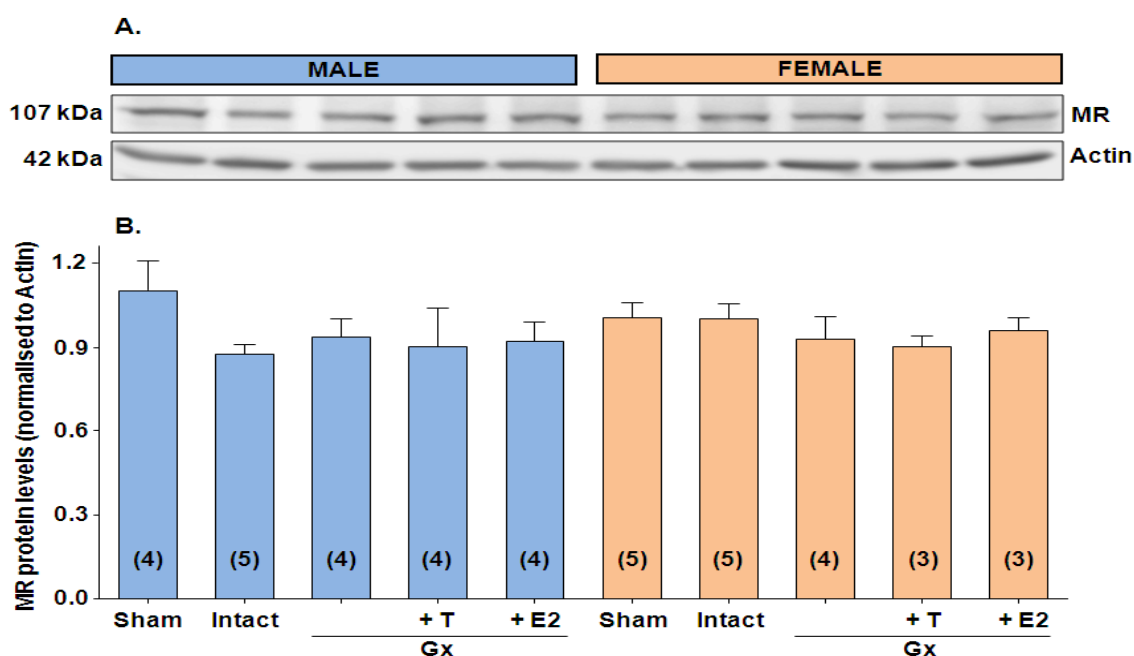


Figure 4.8: Effects of sex steroids on MR protein expression during I-R.

Expression levels of mineralocorticoid receptor in hearts from intact and gonadectomised male and female animals (\pm hormones for 21 days) subjected to ischaemia-reperfusion (I-R). **(A)** Representative immunoblot of MR in left ventricular free wall homogenates of male (left) and female (right) hearts. **(B)** Bar graphs show densitometric analysis of protein changes compared to the loading control β -actin. MR, mineralocorticoid receptor; Gx, gonadectomised; T, testosterone; E2, 17β -oestradiol. Numbers in parentheses indicate the number of animals in each group.

4.4 Discussion

The different sex steroid actions during myocardial I-R involve the androgen receptor, RAGE and an unreported gender dependent shift in the balance between autophagy and apoptosis. Both androgens and E2 aggravated infarct size in males. The current study is one of the few that has shown cardiac actions of low levels of androgens in males. We tried to administer weight adjusted doses of sex steroids, and are unsure why Gx males receiving E2 showed marked elevations in serum levels of E2. The results therefore do not contribute to whether elevated levels of E2 in males are detrimental. This will need to be explored by clinical studies in older men with CAD (Phillips et al., 1983), using LC-MS/MS and not immunoassay to measure serum E2 levels.

The studies in this chapter confirm that T directly aggravates I-R induced cardiac damage in male animals, since Gx reduced infarct size, whereas cardiac damage was restored by T supplementation, despite lower circulating levels, a direct action of T rather than conversion to oestradiol since DHT produced similar effects. Administration of T to Gx females had no effect on infarct size, in agreement with previous reports (Nam et al., 2007a). Increased infarct size following I-R in males may be mediated via elevated AR levels since Gx down-regulated AR levels, which were restored by T treatment in males; T administration to Gx females augmented levels of AR, which has not been previously reported and may be relevant for postmenopausal women receiving treatment with T. E2 administration had no effect on cardiac AR expression in Gx males, whereas cardiac AR levels were down-regulated in Gx females, reducing infarct size and consistent with a previous study (Tivesten et al., 2006).

Autophagy markers were activated by reperfusion injury in both males and females as previously reported for male animals (Matsui et al., 2007); we show for the first time differential gender regulation of mTOR activity. Despite no changes in males, Gx in females enhanced mTOR activity, indicating inhibition of autophagy and correlating with increased infarct size. Beclin-1 is important in regulating balance between autophagy and apoptosis by directly interacting with anti-apoptotic proteins Bcl-2 or Bcl-xL (Hamacher-Brady et al., 2006a). Our data for Beclin-1 and Bcl-xL in the reperfused hearts show an inverse proportional relationship, suggesting this balance as important for regulating autophagy and apoptosis by sex steroids. The autophagy specific gene Atg5 is a rate-limiting protein; in males, T alone regulates expression of Beclin-1 and Atg5-Atg12 to initiate autophagy, whereas in females both T and E2 have a similar effect. This may explain why T given to Gx females did not aggravate infarct size despite increased levels of cardiac AR. Progression of autophagy is indicated by increases in levels of myocardial LC3-II and LC3-II/LC3-I ratio. Although myocardial I-R upregulated LC3-II/LC3-I ratio in intact animals, Gx in both males and females prevented conversion of LC3-I to LC3-II, indicated by the low LC3-II/LC3-I ratio, so autophagy could not proceed; sex steroids did not restore levels in Gx male animals.

Enhanced RAGE expression during myocardial I-R is dependent on circulating T rather than E2 levels in both males and females, differing from a previous report that E2 increases RAGE transcription and protein expression (Tanaka et al., 2000). In the current studies, Gx females receiving T showed enhanced RAGE expression, correlating with increased infarct size. In Gx males supplemented with T but low circulating T levels, RAGE expression was significantly less than intact males. RAGE

stimulation activates pro-apoptotic caspase cascade resulting in cardiomyocyte apoptosis (Essick and Sam, 2010). There were no differences between males and females in activation of pro-apoptotic proteins caspase-3 and -9, confirming terminal apoptotic cell death. Decreased levels of anti-apoptotic proteins XIAP, Bcl-xL and ARC during myocardial I-R in males but not females further promote apoptosis. Although previous studies show sex differences in cardiomyocyte apoptosis following myocardial I-R (Bouma et al., 2010), our study is the first to show androgen-dependent downregulation of Bcl-xL, a key factor for the crosstalk between autophagy and apoptosis.

Although several studies have suggested that MR signalling is gender-specific (Hofmann et al., 2012; Kanashiro-Takeuchi et al., 2009; Kunzel et al., 2012; Rigsby et al., 2007), there have been no studies that determine the effect of sex hormones on MR expression in the heart. In the current study, MR protein levels remain unchanged following ischaemia (30 minutes) and reperfusion (150 minutes) in both male and female hearts (Figure 4.8). Although previous studies have found an upregulation of MR protein levels in left ventricle of animal models of MI, most of these studies were in male animals only and MR levels were measured 2-4 weeks after MI (de Resende et al., 2006; Milik et al., 2007; Takeda et al., 2007). Moreover, the various treatments with sex hormones in our study provided an opportunity to identify differential regulation of MR expression during myocardial I-R in male and female animals which has not been previously reported. There were no significant changes in levels of MR during the various treatments (Figure 4.8); suggesting gonadal steroids do not modify MR expression.

In conclusion, the results in this chapter show novel and key roles for sex steroid action during MI (Figure 4.9). Myocardial I-R in male animals aggravated cardiac damage through increased AR and RAGE expression, with a shift in the balance between autophagy and apoptosis towards increased apoptosis. In contrast, myocardial I-R in females produces less cardiac damage reflecting enhanced autophagy and decreased apoptosis. RAGE is a key regulator of this switch, with T administration to females activating both AR and RAGE expression, which perhaps is relevant for postmenopausal women receiving T. These results therefore provide a platform for new potential treatment strategies for reperfusion injury in both females and males.

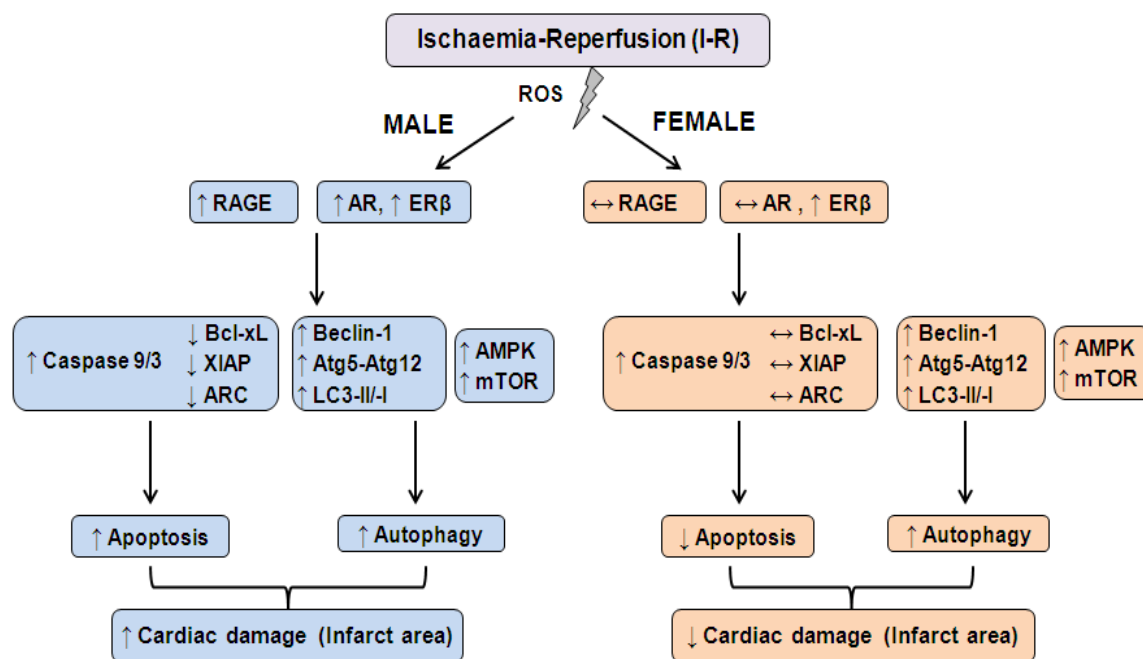


Figure 4.9: Schematic summary of pathways activated during myocardial I-R injury in male and female myocardium.

ROS, reactive oxygen species; RAGE, receptor for advanced glycation end products; AR, androgen receptors; ER, estrogen receptor; Bcl-xL, B-cell lymphoma-extra large; XIAP, X-linked inhibitor of apoptosis protein; ARC, apoptosis repressor with a caspase recruitment domain; Atg, autophagy-related gene; Beclin-1, known as Atg6; LC3, microtubule-associated protein light chain 3; AMPK, AMP-activated protein kinase; mTOR, mammalian target of rapamycin; ↑, increased; ↓, decreased; ↔, no change.

Chapter 5

Cardiac effects of mineralocorticoid receptor activation during myocardial infarction

5.1 Introduction

Similar to other steroid hormones, aldosterone binds to its cognate receptor, the mineralocorticoid receptor (MR), which belongs to the nuclear superfamily of receptors (Griekspoor et al., 2007). Aldosterone and MR activation also have an important role in cardiovascular tissues. Circulating levels of aldosterone have been reported to regulate L-type Ca^{2+} currents in ventricular myocytes (Perrier et al., 2005), regulate intracellular Ca^{2+} movement and activation of the ryanodine receptor (Gomez et al., 2009), while mildly elevated aldosterone levels have been found in patients with essential hypertension (Genest et al., 1956) and elevated levels trigger hypertrophy, fibrosis and remodelling (Brilla et al., 1990; Lin et al., 2012; Tsybouleva et al., 2004; Young et al., 1994).

Elevated plasma levels of aldosterone in patients presenting for primary percutaneous coronary intervention (PCI) for ST-segment elevation myocardial infarction (STEMI) and acute myocardial infarction (AMI) are associated with significantly worse prognosis, including higher death rates, recurrent ischaemia, extended MI and heart failure (Beygui et al., 2006; Beygui et al., 2009; Palmer et al., 2008). Similarly elevated plasma aldosterone levels in patients with coronary artery disease (CAD), independently correlate with long term mortality and increased risk of acute ischaemic events (Ivanov et al., 2012). Whether these pathophysiological actions of aldosterone involve interaction between non-genomic and genomic signalling pathways has not been defined.

The genomic actions of aldosterone involve aldosterone binding to MR followed by

translocation into the nucleus and the hormone-receptor complex modulating transcription of various target genes which include induction of epithelial Na⁺ channel (ENaC) (Asher et al., 1996), serum-regulated kinase 1 (Sgk-1) (Bhargava et al., 2004; Chen et al., 1999; Naray-Fejes-Toth and Fejes-Toth, 2000), Na⁺/K⁺-ATPase (Kolla and Litwack, 2000). These effects normally occur after hours and are blocked by MR antagonists (spironolactone or eplerenone). In contrast, the rapid extranuclear, non-genomic effects of aldosterone are not dependent on transcription. These include activation of signalling pathways such as extracellular signal regulated kinase 1/2 (ERK1/2), c-Jun NH2-terminal kinase 10/2 (JNK1/2) (Gekle et al., 2001; Grossmann et al., 2005; Rossol-Haseroth et al., 2004) and protein kinase C (PKC) (Alzamora et al., 2007; Fujita et al., 2005; Mihailidou et al., 2004), as well as increases in intracellular Ca²⁺, pH (Wehling et al., 1996) and NADPH oxidase-mediated ROS production (Hayashi et al., 2008). The nongenomic effects of aldosterone are not blocked by inhibitors of transcription and protein synthesis, and mediated through MR-dependent and MR-independent mechanisms (Chai et al., 2005; Fujita et al., 2005; Schmidt et al., 1999; Schmidt et al., 2003; Wehling et al., 1998).

Several studies have suggested a potential MR located at the plasma membrane (Grossmann et al., 2010; Ricchiuti et al., 2011; Wildling et al., 2009) to mediate the non-genomic effects, although identifying this receptor has been elusive until recently. Fractionation studies have identified MR in both cytoplasmic and membrane fractions (Ricchiuti et al., 2011), while the G protein-coupled receptor 30 (GPR30 or GPER1) has been shown to mediate non-genomic aldosterone signalling (Gros et al., 2011b) including rapid activation of ERK1/2 and apoptosis in vascular smooth muscle cells

(VSMC) (Gros et al., 2011b) and endothelial cells (Gros et al., 2013) as well as VSMC contraction (Gros et al., 2011a). Although some studies suggest GPR30 is the putative membrane receptor mediating MR-independent rapid aldosterone signalling, the role of GPR30 in the pathophysiological actions of aldosterone in the heart has not been defined. Based on the results from the previous chapter showing significantly greater cardiac damage in males compared with age-matched females following myocardial I-R, the aim of the current study was to determine the interaction of non-genomic with genomic signalling pathways in the cardiac actions of aldosterone in male animals.

5.2 Methods

5.2.1 Reagents

Aldosterone (Ald) and other chemical reagents were purchased from Sigma-Aldrich and cell culture reagents were from Invitrogen. The GPR30 specific agonist G1 and the selective GPR30 antagonist G36 were purchased from Azano Pharmaceuticals, Inc. Aldosterone-3-carboxymethylamine-PEG amine (Aldo-PEG, molecular weight ~40,000) was manufactured by Prof. Celso Gomez-Sanchez as described below. Dose-response studies (0.1-100 nM) were completed from a stock (100 μ M) for Ald and Aldo-PEG.

Chemical synthesis of Aldo-PEG: Aldosterone-3-CMO was prepared by aldosterone (26.5 mg) dissolved in a mixture of methanol (2 mL) and pyrrolidone (13 μ L) for 10 min followed by adding carboxymethylamine hemi hydrochloride (10 mg). The reaction mixture was left overnight at room temperature (~22°C). The methanol was partially evaporated and the product was dissolved in dichloromethane (30 mL), washed

with 1N HCl twice followed by 4 times with water. Complete conversion was checked by thin layer chromatography (TLC) where a single compound was found. The dichloromethane was dried with sodium sulfate, filtered and evaporated. The aldosterone-3-CMO-TFP ester was prepared by dissolving aldosterone-3-CMO in dimethylformamide (2 mL) and tetrafluorophenol (12 mg) and then added diisopropylcarbodiimide (12 μ L). The reaction mixture was left overnight at room temperature and complete conversion was checked by TLC. Coupling of aldosterone-3-CMO-TFP ester to methoxy-PEG was achieved as follows: methoxy-PEG (mw: 40,003 (JenKem, China); 615 mg) dissolved in water (20 mL) were reacted with the aldosterone-3-CMO-TFP ester for overnight. The solution was then dialyzed against 4 L sodium bicarbonate (50 mM) for overnight, then 3 changes of water over 3 days at 4°C. The product was then lyophilized. A small amount was acidified with HCL and extracted, washed and tested by ELISA. No free steroid or free amino groups were demonstrated in the methoxy-PEG- aldo.

5.2.2 Cell culture and treatment

Rat cardiomyoblast, H9c2 cells were used. Experimental details for routine cell culture and passage of H9c2 cells are described in Chapter 2 (sections 2.7.1 – 2.7.2). Before treatment, the cells were washed with PBS and cultured in DMEM containing 10% (v/v) dextran-coated charcoal stripped FBS (DCC-FBS) [2.5% (w/v) Norit-A charcoal and 0.25% (w/v) DextranT-70] for 36 hours to eliminate any steroid source before treatment. H9c2 cells were treated with Ald or Aldo-PEG (0.1, 0.3, 1, 3, 10 and 30 nM) in DMEM/DCC-FBS medium for either 20 minutes (for ERK1/2 activation studies) or 4 hours (for subcellular fractionation and gene expression studies). In a separate

experiment, cells were treated with GPR30 agonist, G1 (10, 100, 1000 and 10000 nM) for 20 minutes for ERK1/2 activation studies. To confirm the specificity of GPR30, the GPR30 antagonist, G36 was used. The suitable dose of G36 was determined by stimulating the cells with a constant dose of G1 and increasing concentrations of G36 (10, 100, 500, 1000 nM) for 20 minutes and protein lysates collected for ERK1/2 activation studies. To examine whether actions of Ald, Aldo-PEG or G1 were mediated via MR or GPR30, H9c2 cells were pre-incubated for 30 minutes with SPIRO (100 nM) or G36 (500 nM) prior to addition of Ald, Aldo-PEG or G1 for ERK1/2 activation studies.

5.2.3 Measurement of superoxide generation

Cardiomyocyte superoxide generation was measured using lucigenin-enhanced chemiluminescence, as previously described (Laskowski et al., 2006; Peshavariya et al., 2007). H9c2 cells were seeded into 6-well plates at a density of 4×10^5 cells/well, serum-deprived overnight and treated with Ald (10 nM) or Aldo-PEG (10 nM) for 4 hours. Stimulated cells were collected in Krebs-HEPES buffer [130 mM NaCl, 5 mM KCl, 1 mM MgCl₂, 1.5 mM CaCl₂, 1 mM K₂HPO₄, 11 mM Glucose and 20 mM HEPES, pH 7.4, with 1 mg/mL bovine serum albumin (BSA)] containing NADPH (100 μM) and lucigenin (5 μM) for chemiluminescence measurements. The cell suspensions were transferred into a 96 well OptiView plates (PerkinElmer, Inc.) and measured using a Veritas Microplate Luminometer (Turner Biosystems, Inc.). Each treatment group was performed in triplicate and the photon emissions were recorded every 30 seconds for up to 20 readings. Background chemiluminescence in buffer containing lucigenin was measured in the absence of cells and subtracted from the average of 20 readings.

5.2.4 Subcellular fractionation

Plasma membrane, cytosolic and nuclear fractions were prepared from 100 mm dishes of confluent H9c2 cells. Plasma membrane and cytoplasmic fractions were prepared at 4°C as previously described (Perez-Reyes et al., 1989) with modifications. Briefly, cells were washed with PBS, which was aspirated, and scraped into 5 mL of PBS containing protease inhibitor cocktail (Roche Applied Science). The cells were pelleted by centrifugation for 5 minutes at 3,000 \times g and resuspended into 1 mL of homogenisation buffer [50 mM Tris (pH 7.2) and 1 mM EDTA with protease inhibitors]. Cells were placed on ice to swell for 5 minutes followed by 20 strokes in a dounce homogeniser and centrifugation of the lysate at 750 \times g for 10 minutes. The supernatant (containing cytoplasmic and membrane fractions) was removed and stored on ice. The pellet was resuspended in 1 mL of homogenisation buffer, homogenised and centrifuged again. The two supernatants were combined and centrifuged at 100,000 \times g for 60 minutes in a Beckman Ti90 rotor. The supernatant from this final centrifugation represents cytoplasmic proteins. The pellet was resuspended in homogenisation buffer and represents the membrane fraction.

For nuclear extraction, cells were resuspended in 400 μ L ice-cold buffer A [10 mM HEPES (pH 7.9), 10 mM KCl, 0.1 mM EDTA, 0.1 mM EGTA, 1 mM DTT and 0.5 mM phenylmethylsulfonyl fluoride (PMSF)] and incubated on ice for 20 minutes. At the conclusion of this incubation, 25 μ L of 10% (v/v) Nonidet P-40 was added, the tube vigorously vortexed (15 seconds) and the homogenate centrifuged at 10,000 \times g for 30 seconds. The nuclear pellet was resuspended in buffer B [20 mM HEPES (pH 7.9), 0.4 mM NaCl, 1 mM EDTA, 1 mM EGTA, 1 mM DTT and 1 mM PMSF]. Lysates of the

nuclear fraction were sonicated and clarified by centrifugation at 10,000xg for 5 minutes.

5.2.5 Immunofluorescence staining

Immunostaining was used to identify and localise proteins in sections of reperfused myocardium using the protocol described in Chapter 2 (section 2.5.1). Sections incubated with anti-MR (1:20) or -GPR30 (1:40) antibodies overnight at 4°C followed by Alexa Fluor 594 conjugated concanavalin A (20 µg/mL; Invitrogen) or anti-IgG conjugated Alexa Fluor 488 antibody (1:200; Invitrogen) for up to 1 hour. Sections were counterstained with DAPI reagent, mounted and analysed using confocal fluorescence microscope (Leica SP5) with a 63x oil objective.

5.2.6 Western blots

Total protein was extracted from rat heart tissue and H9c2 cells as described in Chapter 2 (sections 2.5.2 and 2.7.3). Western blots were performed as described in Chapter 2 (section 2.5.3). The primary antibodies were rMR 1-18 1D5 (kindly donated by Prof. Celso Gomez-Sanchez), GPR30 (Santa Cruz Biotechnology, cat# sc-48524), phospho-(pT²⁰²/pY²⁰⁴) and total p44/42 MAPK (ERK1/2) (Cell Signaling, cat# 9101 & 9102). The proteins aquaporin1 (Santa Cruz, cat# sc-20810), α -tubulin (Santa Cruz, cat# sc-5286) and Histone H1 (clone 1415-1) (NeoMarkers) were used as makers to confirm purity of subcellular fractions as they are exclusive to the membrane, cytoplasm and nucleus, respectively. Antibody binding was detected using HRP-conjugated secondary antibodies (1:3000, Dako Cytomation). Membranes were exposed to chemiluminescent substrate (PerkinElmer, Melbourne, Australia) and digital images captured on a

LAS4000 (GE Healthcare Life Sciences).

5.2.7 Quantitative real-time RT-PCR (qRT-PCR)

Following treatment, total RNA was extracted from H9c2 cells using QIAzol lysis reagent (Qiagen) according to the protocol provided by the manufacturer and described in Chapter 2 (sections 2.6.1 and 2.7.5). The concentration and purity of the RNA samples were assessed using a NanoDrop ND-1000 spectrophotometer (Thermo Scientific). The cDNA was synthesised from 2.5 µg total RNA using the Superscript III First-Strand Synthesis System and oligo (dT)₂₀ as a primer (Invitrogen) according to the manufacturer's protocols (see section 2.6.4 for more details). cDNA samples were stored at -20°C until used for qRT-PCR. The mRNA expression of *serum/glucocorticoid regulated kinase 1 (Sgk-1)* and *plasminogen activator inhibitor type 1 (PAI-1)* were analyzed using TaqMan gene expression assays (Applied Biosystems, [Rn00570285_m1] and [Rn01481341_m1], respectively). *Glyceraldehyde-3-phosphate dehydrogenase (Gapdh)* [Rn99999916_s1] was used as endogenous control. Amplification efficiency curves were performed for all gene expression assays prior to sample analysis, with the sample designated as the calibrator, using six point dilution series (1, 1:10, 1:100, 1:1000, 1:10000, 1:100000 dilutions). The 7900HT Fast Real-Time PCR system (Applied Biosystems) was used to perform qRT-PCR in clear 96 or 384 well plates. Each cDNA sample was run in triplicate and a no template control was included on each plate to check for cross contamination. The qRT-PCR reaction mix consisted of following components:

<i>Components</i>	<i>96 wells plate</i>	<i>384 wells plate</i>
Sterile water (μl)	4	0.5
TaqMan gene expression master mix [2x] (μl)	10	5
TaqMan gene expression assay [20x] (μl)	1	0.5
Diluted cDNA sample [1:5 dilutions] (μl)	5	4
<i>Total reaction volume</i>	<i>20</i>	<i>10</i>

Table 5.1: Preparation of the qRT-PCR reaction cocktail

The real-time PCR program included a holding stage at 50°C for 2 minutes, 95°C for 10 minutes, and cycling 40 times at [95°C for 15 seconds (melting), and 60°C for 1 minute (annealing/extension)]. The Delta–Delta Comparative Threshold ($\Delta\Delta\text{CT}$) method was used to quantify the relative fold change between the samples. Data was analysed using RQ Manager Analysis software, version 1.2.1 (Applied Biosystems).

5.2.8 *Ex vivo* myocardial ischaemia-reperfusion studies

Adult male (300 – 400 g) Sprague Dawley rats (N = 38) were used to avoid any variability associated with fluctuations in female hormonal cycles, and particularly since GPR30 is also a highly avid receptor for estrogen (Ding et al., 2009; Filice et al., 2009). Myocardial I-R injury was performed as described in Chapter 2 (sections 2.2). Briefly, rats were anaesthetised and the hearts rapidly excised and attached to a Langendorff apparatus for regional ischaemia for 30 minutes followed by reperfusion for 150 minutes. At the end of reperfusion, infarct area was determined as per Chapter 2 (section 2.3). Apoptotic cells were visualised by TUNEL staining of paraffin embedded heart sections using In Situ Cell Death Detection Kit described in Chapter 2, section 2.4.

5.2.9 Statistical analysis

Details for statistical analysis are described in Chapter 2 (sections 2.8).

5.3 Results

5.3.1 MR and GPR30 expression in cardiomyocytes

The large molecular size of PEG yields a hybrid molecule that has similar structure to aldosterone (Ald) but is membrane impermeable (Figure 5.1) which allows identification of non-genomic Ald signaling pathways separate to the genomic actions.

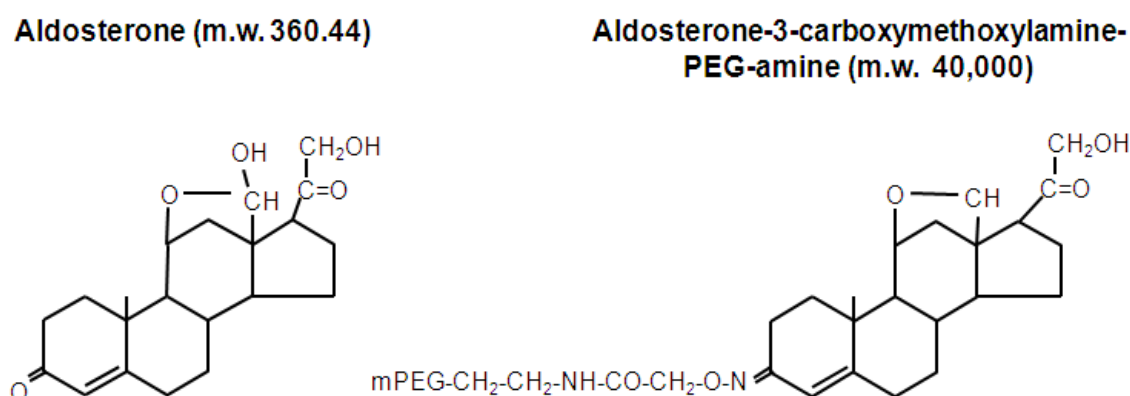


Figure 5.1: Structure of Aldosterone-3-carboxymethoxylamine-PEG-amine (M.W. 40,000) compared to aldosterone (M.W. 360.44).

Immunoblotting confirmed endogenous expression of both MR and GPR30 in H9c2 cardiomyocytes and rat myocardium (Figure 5.2A). Expression of GPR30 was comparable between rat myocardium and H9c2 cells, whereas expression of MR was higher in H9c2 cells than left ventricular myocardium. To determine the profile of potential receptor activation by Ald and Aldo-PEG, we fractionated H9c2 cells and

examined subcellular receptor location. Aquaporin-1, α -tubulin and histone H1 were the plasma membrane, cytoplasmic and nuclear protein markers respectively and clearly demonstrate the integrity of the lysates used.

In untreated H9c2 cells, MR were primarily cytoplasmic ($62 \pm 3\%$, mean \pm SE, N=3) with $38 \pm 3\%$ (N=3) in the nuclear resident pool of MR (even in the presence of DCC-FBS) (Figure 5.2B). Addition of Ald indicated translocation of MR with the proportion of nuclear-resident MR increasing to $77 \pm 6\%$ (Figure 5.2B). In contrast, Aldo-PEG did not mimic the effect of Ald on MR subcellular localisation confirming the inability of Aldo-PEG to enter the cell (Figure 5.2B). GPR30 was localised to the cytoplasmic and membrane fractions of H9c2 cells, consistent with previous reports for GPR30 distribution (Filardo et al., 2007; Revankar et al., 2005; Revankar et al., 2007). In contrast to MR, the level of GPR30 protein was similar in non-stimulated and stimulated cells, with no change in the sub-cellular distribution of the receptor upon addition of Ald or Aldo-PEG (Figure 5.2B).

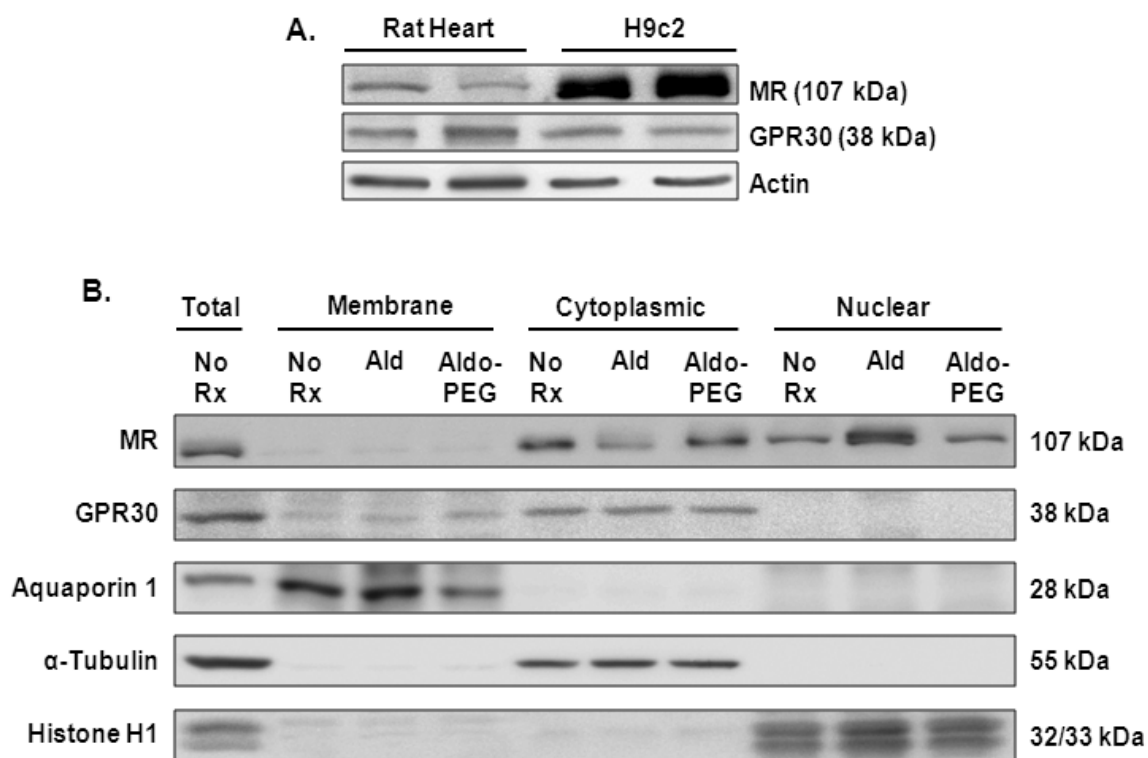


Figure 5.2: Expression and localisation of MR and GPR30 in H9c2 cells

(A) MR and GPR30 expression in H9c2 cells. Western blot of MR and GPR30 total proteins that were extracted from rat heart tissue and H9c2 cardiomyocytes. (B) Subcellular fractions/distribution of MR and GPR30 in H9c2 cells. Total protein, membrane, cytosolic and nuclear protein fractions were extracted and subjected to immunoblot analysis. Aquaporin-1, α -tubulin and histone H1 were used as loading controls for membrane, cytosolic, and nuclear extracts, respectively. Cells were incubated with Ald (10 nM) or Aldo-PEG (10 nM) for 4 hours.

Subcellular distribution of GPR30 and MR was detected by immunostaining in left ventricular myocardial sections from rat hearts subjected to I-R using confocal microscopy (Figure 5.3A), with both MR and GPR30 detected in rat myocardium. For

these studies Concavalin A (Con A), a lectin that specifically binds to α -mannosyl saccharides in the core of integral plasma membrane glycoproteins, was used as a plasma membrane marker (Filardo et al., 2007). Con A staining in tissue sections highlighted the plasma membrane exclusively (Figure 5.3A & 5.3B, *red*). MR displayed a primarily cytosolic localisation, with a small amount in the nucleus and no co-localisation with Con A in rat hearts following reperfusion injury (Figure 5.3A). Consistent with studies in H9c2 cells, there was an increased proportion of MR in the nuclei of injured myocardium exposed to 10 nM Ald but not Aldo-PEG (Figure 5.3A, *arrow*). The overlapping staining of GPR30 and Con A in the membrane shows co-localisation of GPR30 with the plasma membrane marker and its localisation to the cell membrane (Figure 5.3B, *yellow*). Although GPR30 has been reported to localise to the endoplasmic reticulum, which in myocytes is located near and continuous with the outer layer of the nuclear envelope, the current study did not find staining in this location and only detected in the cytoplasm (Figure 5.3B).

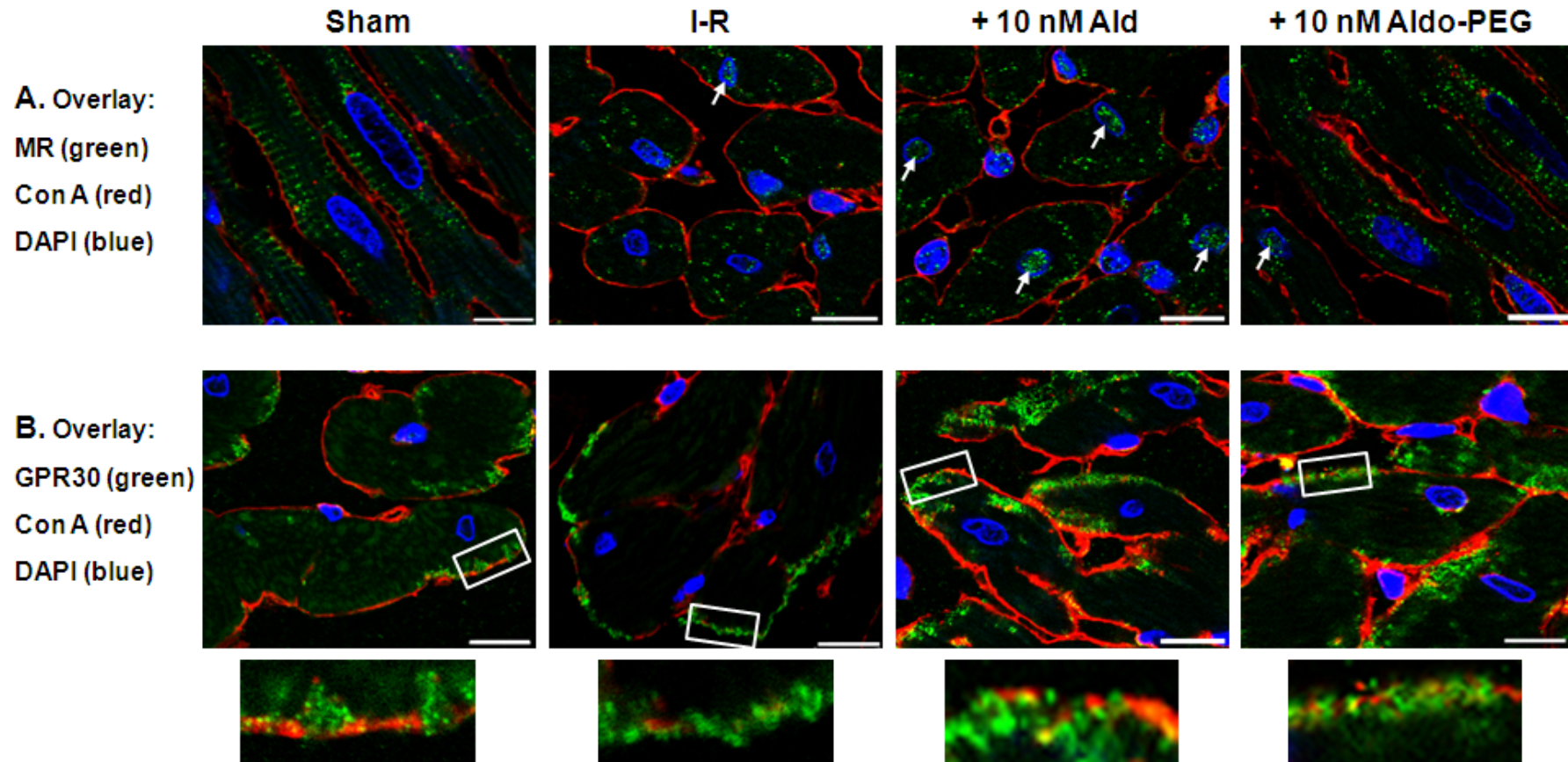


Figure 5.3: Expression and localisation of MR and GPR30 in rat heart

Representative overlay confocal images of ventricular sections from hearts subjected to ischaemia-reperfusion injury. MR (**A**) and GPR30 (**B**) were detected with Alexa 488 (*green*). Tissue sections were co-stained with Alexa 594 conjugate concanavalin A (Con A, *red*), which specifically binds α -mannosyl saccharides in plasma membrane glycoproteins). Nuclei are stained using DAPI (*blue*). Scale bar = 10 μ m.

5.3.2 Aldo-PEG regulates non-genomic signalling pathways similar to aldosterone

Activation of ERK1/2 signalling, a recognised non-genomic signalling pathway for Ald (Gros et al., 2011b; Grossmann et al., 2005) was used to confirm the biological activity of Aldo-PEG. Dose-response studies in H9c2 cardiomyocytes showed that both Ald (Figure 5.4A) and Aldo-PEG (Figure 5.4B) increased phosphorylation of ERK1/2 after 20 minutes incubation, with similar kinetics and potency confirming that the modified compound was as efficacious as Ald when activating non-genomic signalling.

Previous studies suggest that GPR30 is required for MR-independent action of Ald (Gros et al., 2011b). To confirm the involvement of GPR30, we used G1 (GPR30 agonist) and G36 (GPR30 antagonist). Dose-response studies for G1, using concentrations similar to those previously reported (Gros et al., 2013) also increased phosphorylation of ERK1/2, with maximal effect at 100 nM (Figure 5.4C) and this dose was selected for subsequent studies. To confirm GPR30-mediated responses, the GPR30 antagonist G36 was used. Dose-response studies for G36 were completed to find an appropriate dose which would inhibit G1-activated ERK1/2 phosphorylation (Figure 5.5). Cells were stimulated with a constant dose of G1 (100 nM) and increasing concentrations of G36 (10, 100, 500, 1000 nM) were used to identify an optimal dose of G36 at 500 nM (Figure 5.5) and this was selected for subsequent studies.

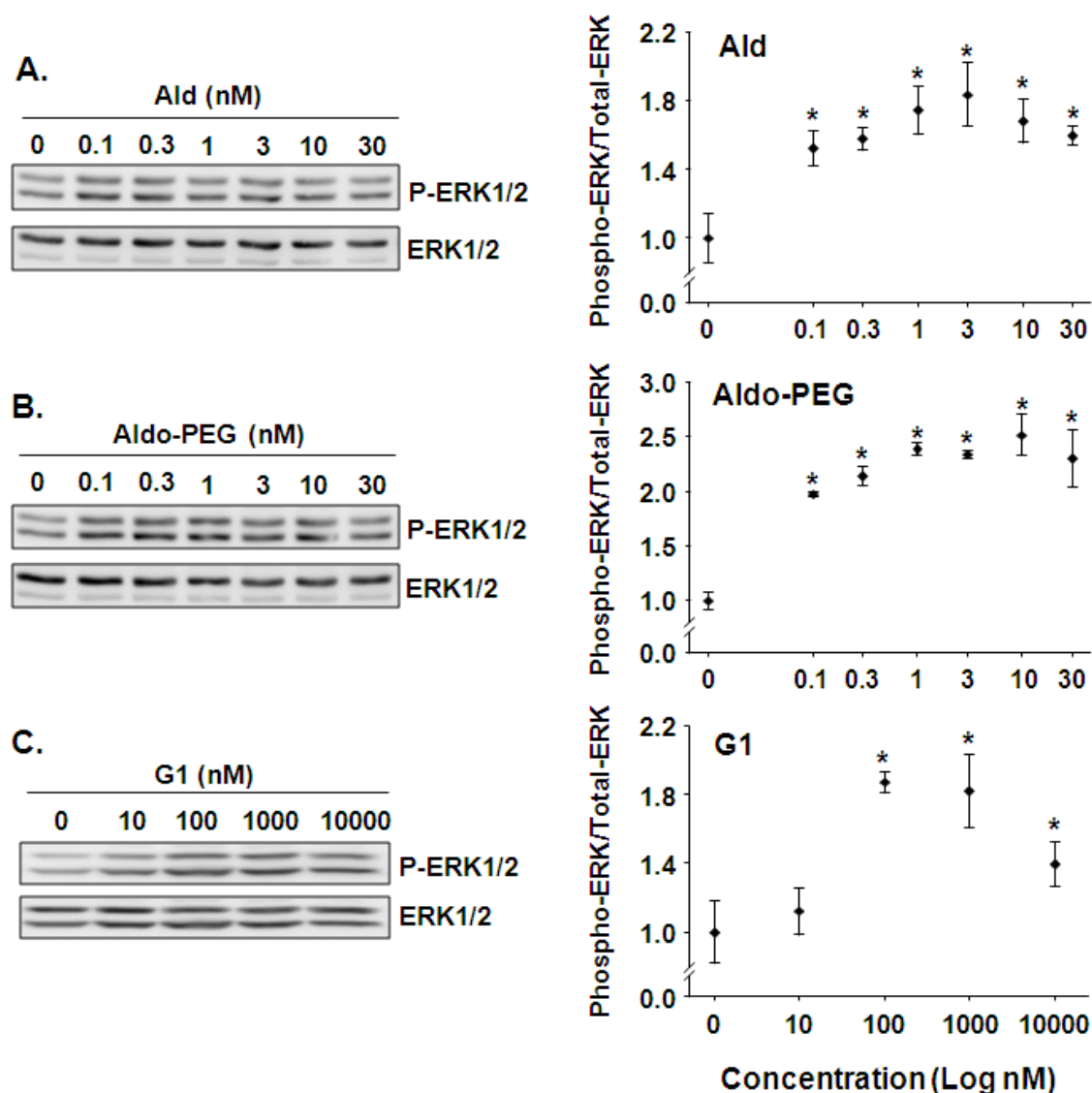


Figure 5.4: Aldo, Aldo-PEG and G1 mediated ERK1/2 phosphorylation

The effects of Aldo (A), Aldo-PEG (B) and G1 (C) on phosphorylation of ERK1/2 in H9c2 cells were measured by western blot. Cells were incubated with indicated concentrations of Aldo, Aldo-PEG or G1 for 20 minutes. *Left*: representative western blot of phosphorylated ERK1/2 and total ERK1/2 images. *Right*: Graphs show quantification of phospho-ERK1/2 to total ERK1/2. Aldo, aldosterone; ERK1/2, extracellular signal-regulated protein kinases 1/2. Values expressed as mean \pm SE from three independent experiments; * $P < 0.05$ vs no treatment.

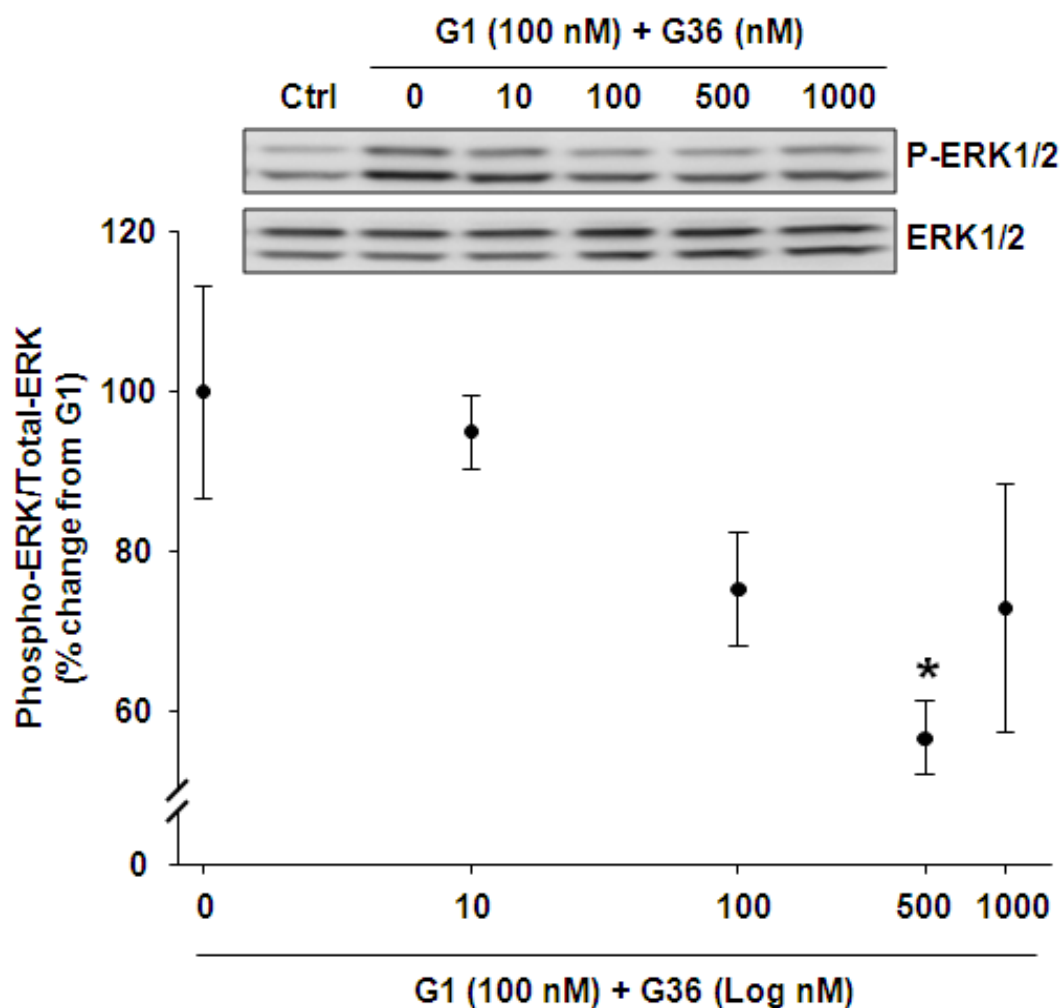


Figure 5.5: Effects of G36 on G1 mediated ERK1/2 phosphorylation.

G1 mediated ERK1/2 phosphorylation is inhibited by increasing concentrations of G36. H9c2 cells were incubated with G36 (10-1000 nM) for 30 minutes prior to G1 (100 nM) addition and protein lysates were collected after 20 minutes. *Top*: representative western blot images of phosphorylated ERK1/2 and total ERK1/2. *Below*: Graph shows quantification of phospho-ERK1/2 to total ERK1/2. ERK1/2, extracellular signal-regulated protein kinases 1/2. Values expressed as means \pm SE from three independent experiments; * $P < 0.05$ vs G1.

To determine whether the rapid responses of Ald and Aldo-PEG were mediated by MR or GPR30, the cells were pretreated with the MR antagonist (SPIRO, 10 nM) or GPR30 antagonist (G36, 500 nM) and assess the effect Ald- and Aldo-PEG-mediated ERK1/2 phosphorylation. Following G36 pre-treatment, Ald, Aldo-PEG and G1 acitvated ERK1/2 phosphorylation were significantly reduced (Figure 5.6), indicating that these actions were mediated by GPR30. In contrast, the effects of Ald, Aldo-PEG and G1 on ERK1/2 activation persisted in the presence of SPIRO indicating that these actions were not mediated by MR. G36 (500 nM) or SPIRO (10 & 100 nM) treatment had no significant effect on baseline ERK1/2 phosphorylation (Figure 5.6).

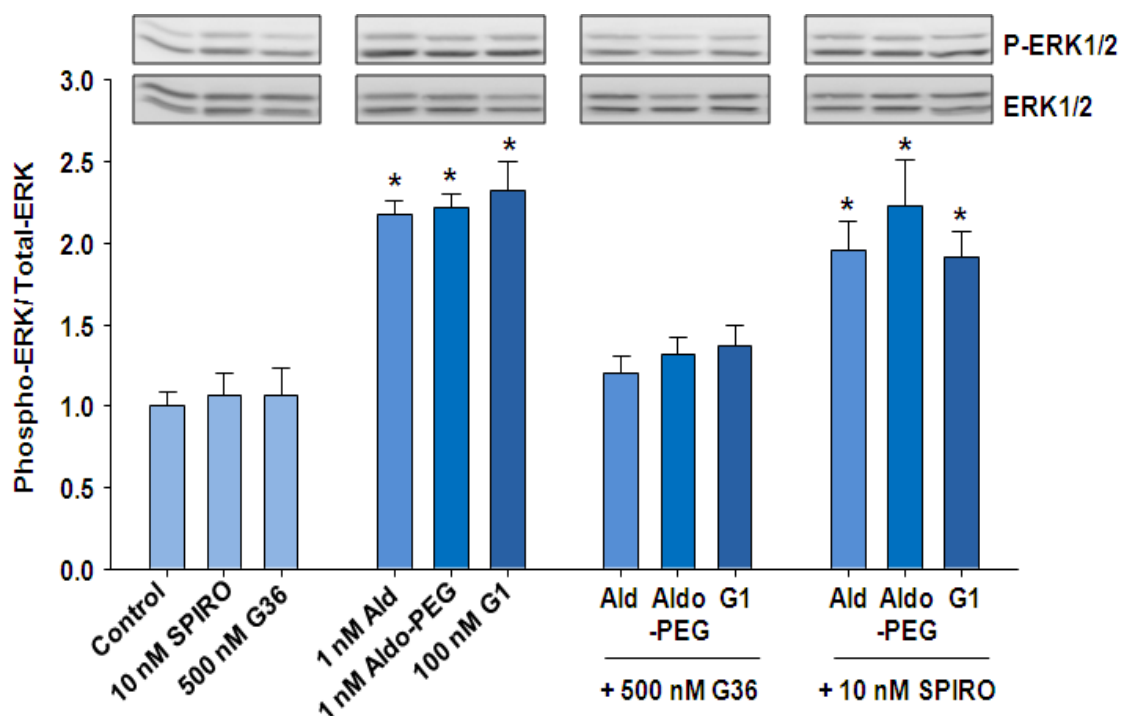


Figure 5.6: Effects of antagonists on Ald, Aldo-PEG and G1 mediated ERK1/2 phosphorylation.

H9c2 cells were incubated with SPIRO (10 nM) or G36 (500 nM) for 30 minutes prior to Ald (1 nM), Aldo-PEG (1 nM) or G1 (100 nM) addition and protein lysates were collect after 20 minutes. *Top*: representative western blot images of phosphorylated ERK1/2 and total ERK1/2. *Below*: Bar graph shows quantification of phospho-ERK1/2 to total ERK1/2. Ald, aldosterone; Aldo-PEG, aldosterone-3-carboxymethoxylamine-PEG amine; SPIRO, spironolactone; ERK1/2, extracellular signal-regulated protein kinases 1/2. Values expressed as mean \pm SE from four independent experiments; * $P < 0.05$ vs control.

One of the actions of aldosterone in the cardiovascular system is generation of oxygen free radicals (Hayashi et al., 2008; Rude et al., 2005) which contributes to the adverse cardiac damage. Generation of superoxide levels was measured in H9c2 cells after exposure to Ald or Aldo-PEG. Superoxide production was significantly increased to equivalent levels in H9c2 cells treated with Ald or Aldo-PEG (Figure 5.7), correlating with the rapid activation of ERK1/2 phosphorylation (Figure 5.7).

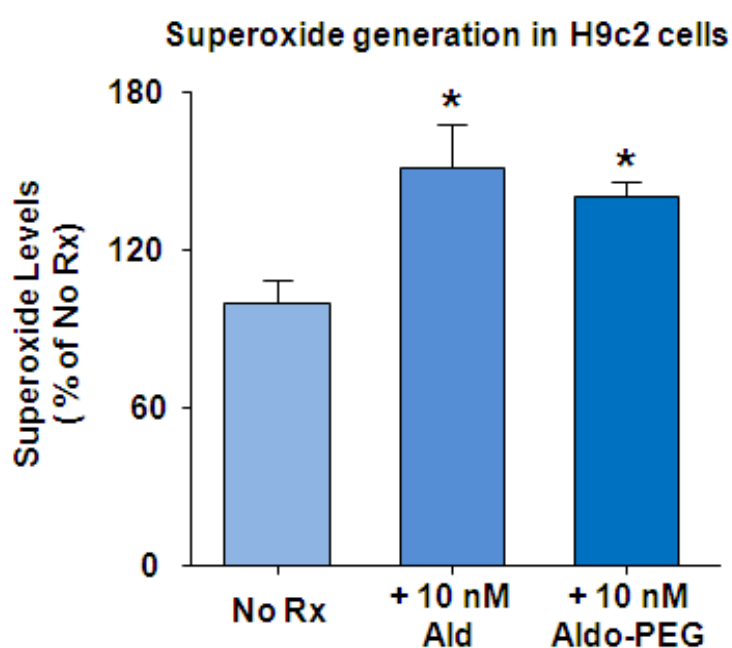


Figure 5.7: Aldosterone and Aldo-PEG mediated superoxide generation

Superoxide generation measured by lucigenin-enhanced chemiluminescence in H9c2 cells following treatment with Ald and Aldo-PEG. Cells were incubated with indicated concentrations of Ald or Aldo-PEG for 4 hours. Bar graphs show quantification of superoxide levels. Ald, aldosterone; Aldo-PEG, aldosterone-3-carboxymethylamine-PEG amine; ERK1/2, extracellular signal-regulated protein kinases 1/2. Values expressed as mean \pm SE from five independent experiments; * P <0.05 vs No Rx.

5.3.3 Aldo-PEG does not activate transcription of aldosterone-responsive genes

The ability of Ald and Aldo-PEG to modulate non-genomic signalling was equivalent (Figure 5.4, 5.6 & 5.7) and next aim therefore examined whether Aldo-PEG may also regulate genomic targets using qRT-PCR from total RNA. Activation of MR results in transcriptional control of a wide variety of genes; the two best characterised MR response genes are Sgk-1 and PAI-1 (Latouche et al., 2010). MR activation in response to treatment with 10 nM Ald for 4 hours significantly increased transcript levels for both Sgk-1 (Figure 5.8A) and PAI-1 (Figure 5.8B) compared to vehicle control. These activities were prevented by co-incubation with SPIRO (10 nM) confirming genomic MR activation. In contrast, Aldo-PEG (1 and 10 nM) had no effect on Sgk-1 and PAI-1 mRNA levels; suggesting genomic MR responses cannot be elicited from a ligand that is cell impermeable. Moreover, these findings discriminate a role for plasma-membrane based receptors (such as GPR30) in non-genomic responses (ERK 1/2 activation) and genomic responses to Ald.

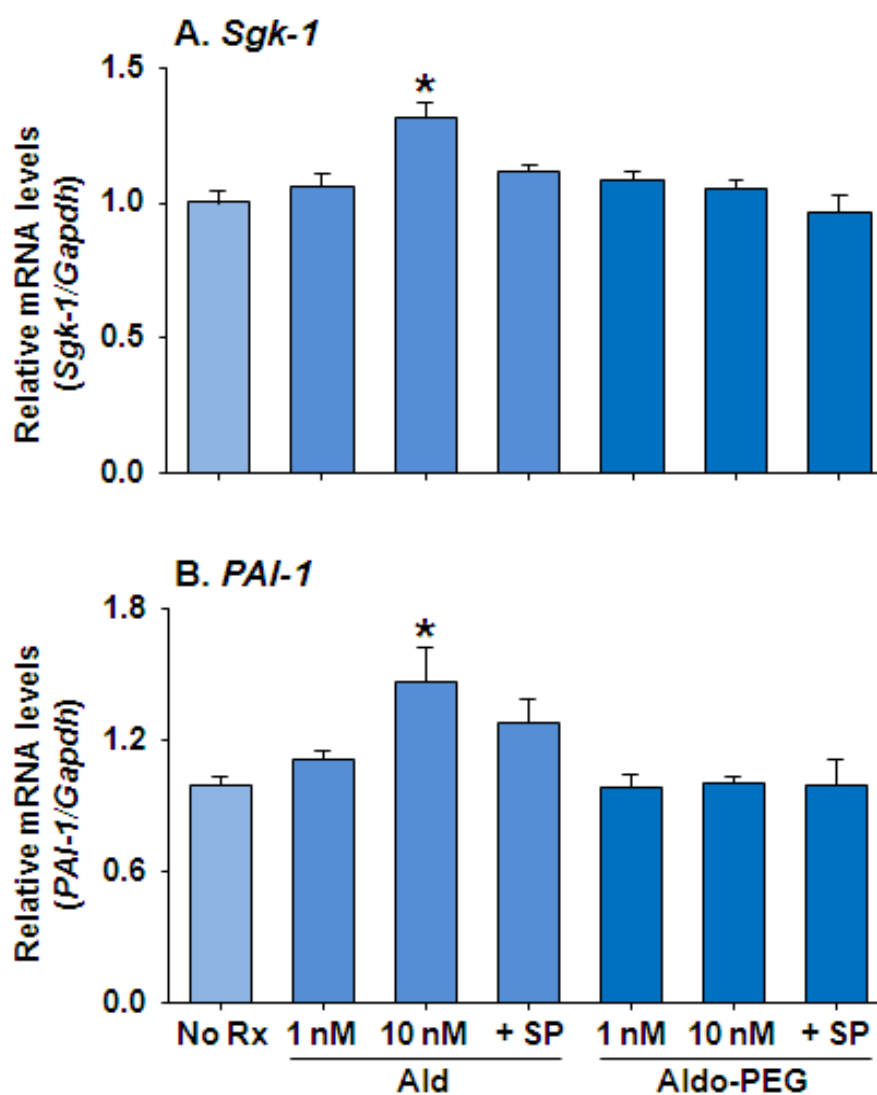


Figure 5.8: MR activation by Ald but not Aldo-PEG regulates Sgk-1 and PAI-1 gene expression

Regulation of Sgk-1 (A) and PAI-1 (B) mRNA expression by Ald and Aldo-PEG (1 and 10 nM) in H9c2 cells was examined by qRT-PCR. H9c2 cells were incubated with indicated concentrations of Ald or Aldo-PEG for 4 hours. Sgk-1, serum/glucocorticoid regulated kinase 1; PAI-1, plasminogen activator inhibitor-1; Ald, aldosterone; Aldo-PEG, aldosterone-3-carboxymethoxylamine-PEG amine; SP, spironolactone. Values expressed as mean \pm SE from four independent experiments; * $P < 0.05$ vs No Rx.

5.3.4 Activation of MR genomic signalling pathways mediate aldosterone-aggravated cardiac damage

The studies in H9c2 cells confirm that the cell impermeable Aldo-PEG elicits non-genomic, but not genomic responses, with equal potency to the classical MR agonist Ald. To determine whether there was a role for MR non-genomic signalling in the pathophysiological action of Ald, *ex vivo* experimental model of myocardial infarction was used. We found that Ald (10 nM) but not Aldo-PEG (10 and 100 nM), increased infarct size (Figure 5.9A) and aggravated myocyte apoptosis (Figure 5.9B). As such, the non-genomic actions of Aldo-PEG (most likely working through GPR30) are insufficient to mediate the cardiac damaging effects of Ald during infarction. These data strongly suggest that the genomic actions downstream of “classical” MR activation drive the aggravation of myocardial I-R injury by Ald (increased infarct size and apoptosis) which complement the sub-cellular localisation (Figure 5.2 & 5.3) and gene expression studies (Figure 5.8).

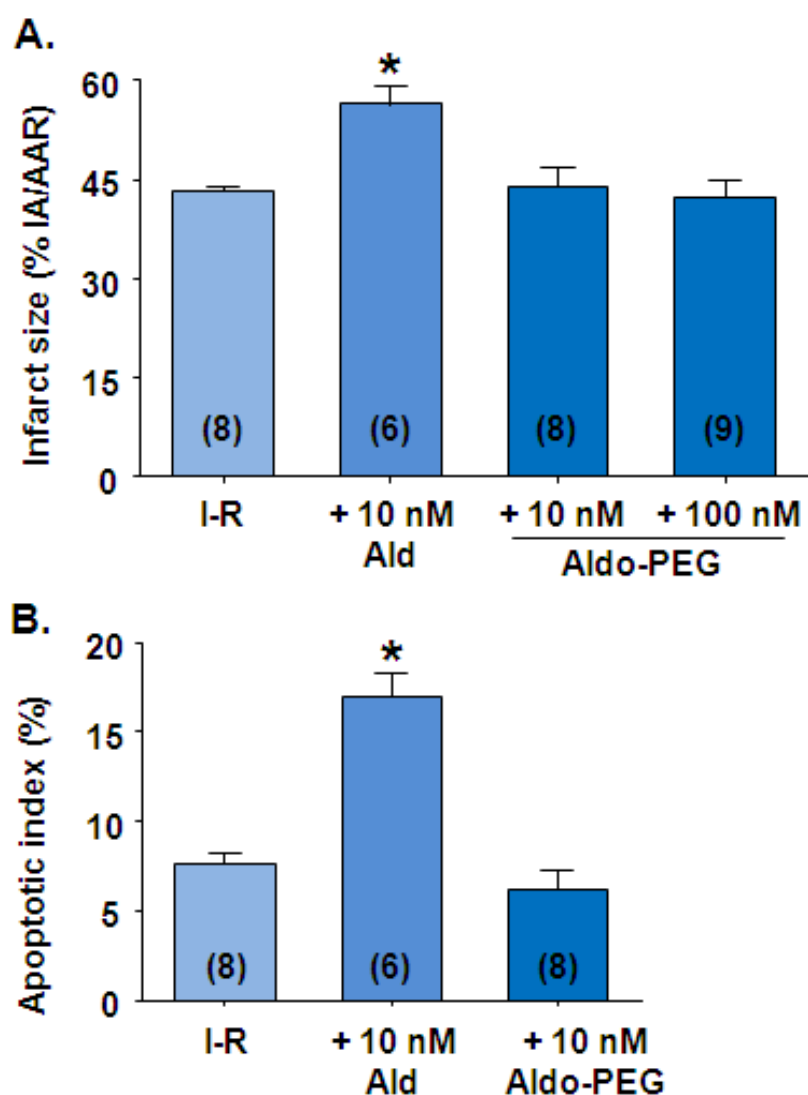


Figure 5.9: Aldo-PEG induces superoxide production but maintains apoptosis and infarct size by preventing MR activation

(A) Myocardial infarct size in hearts subjected to ischaemia followed by reperfusion (I-R) during treatment with Ald and Aldo-PEG. Infarct area/size (IA) is expressed as percentage of area at risk (AAR). (B) Quantification of apoptotic index from treated reperfused myocardium. Apoptotic index is expressed as percentage of TUNEL positive nuclei relative to total nuclei. Numbers of animals in each group are indicated in parentheses within columns. Values expressed as mean \pm SE; * $P < 0.05$ vs I-R alone.

5.4 Discussion

Rapid, non-genomic effects of aldosterone in the cardiovascular system are confirmed (Alzamora et al., 2003; Alzamora et al., 2000; Gros et al., 2011b; Mihailidou et al., 1998; Mihailidou et al., 2004; Schmidt et al., 2005; Wehling et al., 1995), and interaction with the genomic aldosterone effects towards physiological/pathophysiological MR signalling identified, however, how this interaction takes place continues to remain unknown. This is partly due to the lack of a specific tool to delineate the nongenomic from the genomic actions of aldosterone, given that aldosterone activates different signalling pathways. By using the high molecular weight hybrid molecule, Aldo-PEG, that does not cross biological membranes, our findings provide for the first time strong evidence separating the non-genomic aldosterone-responsive signalling pathways from genomic actions in the heart. The current studies show that although non-genomic actions of increased ROS and ERK1/2 phosphorylation, activation of genomic MR signalling is required for the pathophysiological action of aldosterone for aggravated cardiac damage during reperfusion injury.

There has been intense interest in identifying the plasma membrane MR, although the functional role has not been defined. Early studies have used BSA-coupled aldosterone (Gekle et al., 1998; Le Moellic et al., 2004) to identify the MR membrane receptor, although BSA may dissociate from aldosterone, similar to oestrogen-BSA (Hammes and Levin, 2007). Further reports of aldosterone binding sites at the plasma membrane were reported by using atomic force microscopy technology in human endothelial cells (Wildling et al., 2009), or fluorescence resonance energy transfer in a heterologous

expression system using HEK-293 cells (Grossmann et al., 2010), although the exact location of the aldosterone binding sites in the plasma membrane or at the cell surface could not be confirmed.

Subcellular fractionation studies did not detect any levels of MR in the membrane of H9c2 myoblasts or in rat ventricular myocardium by immunofluorescent analysis using a specific MR antibody (kindly donated by Prof Gomez-Sanchez) even though recent studies show MR in membrane fractions of heart tissue (Ricchiuti et al., 2011). Our studies show MR localises in the nucleus and cytoplasm in both H9c2 myoblasts and rat ventricular myocardium, similar to previous reports (Gomez-Sanchez et al., 2006). Using the PEGylated aldosterone (Aldo-PEG), which is polyethyleneglycol (PEG) covalently attached to aldosterone-3-carboxymethoxylamine-TFP ester, provides for the opportunity to separate the rapid, non-genomic signalling at the plasma membrane from the genomic signaling pathways and how these contribute to the pathophysiological cardiac actions of aldosterone. In the absence of ligand, MR were primarily located in the cytoplasm of H9c2 cells (Figure 5.2B). Addition of Ald, but not Aldo-PEG, resulted in increased expression of MR in the nuclei while MR decreased in the cytoplasm, confirming translocation of MR, further confirming that Aldo-PEG was membrane-impermeable.

Recent studies have reported GPR30 mediates the non-genomic actions of aldosterone (Gros et al., 2013; Gros et al., 2011b). GPR30 is ubiquitously expressed (Deschamps and Murphy, 2009; Jessup et al., 2010; O'Dowd et al., 1998) but is particularly prominent in heart tissue and freshly isolated cardiac myocytes (Deschamps and

Murphy, 2009), VSMC and endothelial cells (Ding et al., 2009; Gros et al., 2013). Subcellular localisation of GPR30 is controversial due to the specific GPR30 antibody used, with both expression at the endoplasmic reticulum (Revankar et al., 2005) and plasma membrane reported (Langer et al., 2010). By using subcellular fractionation of H9c2 cells we show GPR30 is located in the plasma membrane (Figure 5.2) and cytoplasm (Figure 5.2) and this was confirmed by immunostaining of cardiomyocytes in rat tissue sections. The lack of immunohistochemical signal near the endoplasmic reticulum in our cardiac tissue sections may be due to recognised limitations of the GPR30 antibodies for immunohistochemistry (Langer et al., 2010).

The results showing that both Aldo-PEG and Ald activate ERK1/2 phosphorylation in the 0.1-1 nM range is in agreement with previous studies in multiple cell types (Ding et al., 2009; Gros et al., 2011b; Grossmann et al., 2005; Maggiolini et al., 2004; Revankar et al., 2005). Similarly, the lack of effect by spironolactone to prevent ERK1/2 phosphorylation, confirms that these are MR-independent actions as previously reported (Gros et al., 2011b). The involvement of GPR30-mediated ERK1/2 phosphorylation by Aldo-PEG and Ald was confirmed by the receptor agonist G1 and antagonist G36 (Figure 5.4-5.6). Conversely, Aldo-PEG and Ald-mediated ERK1/2 activation persisted in the presence of spironolactone. Collectively, these results indicating that GPR30 activation are the major contributor to the rapid non-genomic action of Aldo in these cells.

In contrast, whereas Ald-induced superoxide production has been previously reported (Hayashi et al., 2008; Iwashima et al., 2008; Keidar et al., 2004), the novel finding that

the cell-impermeable Aldo-PEG activated superoxide production with similar efficacy to Ald (Figure 5.7), provides evidence that Ald-induced superoxide production in cardiac myocytes is not only regulated by the traditional intracellular MR. Further experiments on the effects of G36 and G1 on superoxide production would be necessary to confirm the involvement of GPR30 in Ald-induced superoxide production in cardiac myocytes.

Having established that the cell impermeable Aldo-PEG was as efficacious as Ald when activating non-genomic signalling, we examined whether these pathways may interact with genomic signaling such as transcriptional control of two well characterized MR responsive genes Sgk-1 and PAI-1, (Latouche et al., 2010). Exposure to 10 nM Ald for 4 hours significantly increased transcript levels for both Sgk-1 and PAI-1, in agreement with previous reports (Chun and Pratt, 2005; Naray-Fejes-Toth and Fejes-Toth, 2000) and these activities were prevented by co-incubation with spironolactone (10 nM), confirming genomic MR activation. In contrast, Aldo-PEG (1 and 10 nM) had no effect on levels of Sgk-1 and PAI-1 mRNA.

Since aldosterone-induced activation of PAI-1 synthesis has been proposed to mediate myocardial injury (Chun and Pratt, 2005), Aldo-PEG was used to confirm the cross-talk between genomic with non-genomic signalling for aldosterone during experimental MI. Ald but not Aldo-PEG, increased infarct size and aggravated myocyte apoptosis, indicating that although non-genomic aldosterone actions were activated, these were not sufficient alone to aggravate cardiac damage during MI. Previous studies (Weil et al., 2010) show that GPR30 activation, using the GPR30 agonist G-1, improves myocardial

functional recovery and decreases inflammation in the same model of myocardial I-R. Interestingly, GPR30-deficient male mice have impaired left-ventricular cardiac function and enlarged left ventricles (Delbeck et al., 2011), while in separate studies, GPR30-deficient female mice have hyperglycemia and impaired glucose tolerance, reduced body growth and increased blood pressure (Martensson et al., 2009) although these studies did not use MR blockade to determine whether MR-regulated signalling pathways were activated for these adverse effects.

In conclusion, the findings in this chapter provide for the first time the opportunity to examine the non-genomic actions separately from the genomic actions of aldosterone by using the membrane impermeable pegylated aldosterone (Aldo-PEG). This molecule will provide the opportunity to start to identify the contribution of each to the final response. In the heart, activation of GPR30 alone, is not sufficient to trigger the deleterious effects on myocardial reperfusion injury but by raising ROS levels may amplify the MR-mediated actions of aldosterone during myocardial reperfusion injury.

Chapter 6

Cardiac effects of blockade of mineralocorticoid receptors during myocardial infarction

Introduction

Treatment options for IHD include primary PCI, thrombolytic therapy and coronary artery bypass graft surgery (O'Gara et al., 2013); however, additional therapies are required since IHD remains a leading burden of disease (Forouzanfar et al., 2012). Blockade of MR may be a suitable additional treatment based on both experimental and clinical studies. A significant reduction in mortality and hospitalisation was observed when MR antagonists were added to standard treatment in three large randomised trials in severe HF (RALES) (Pitt et al., 1999), mild HF (EMPHASUS-HF) (Zannad et al., 2011) and HF after MI (EPHESUS) (Pitt et al., 2001). Interestingly, patients in these studies had aldosterone levels within the normal range and the doses of MR antagonists were low; however, the mechanisms for this cardioprotection have not been clearly defined. Since apoptosis is activated during I-R injury and involved in LV remodeling post-MI (Baldi et al., 2002; Fliss and Gattinger, 1996), the hypothesis for the current chapter was that MR activation aggravates cell death during I-R injury and that addition of MR blockade will prevent apoptosis, leading to reduced cardiac damage during HF and MI. The findings in the current chapter confirm this hypothesis by demonstrating, for the first time, that activation of MR during I-R injury triggers degradation of the anti-apoptotic protein ARC, aggravating injury and myocyte loss. Further novel findings are that mechanism for the cardioprotective actions of by low concentrations of MR antagonists involve suppression of the intrinsic apoptosis pathway, by preserving the levels of ARC leading to reduced infarct area. This chapter has been published as: Le TYL, Mardini M, Howell VM, Funder JW, Ashton AW, Mihailidou AS. Low-dose spironolactone prevents apoptosis repressor with caspase recruitment domain degradation during myocardial infarction. In *Hypertension*. 2012;59(6):1164-9.

Authorship contribution

Le TYL, Mardini M, Howell VM, Funder JW, Ashton AW, Mihailidou AS. Low-dose spironolactone prevents apoptosis repressor with caspase recruitment domain degradation during myocardial infarction. *Hypertension*. 2012;59(6):1164-9.

The relative contributions of the authors to the paper are listed below:

Thi Yen Loan Le  Date 8/7/2013

- conceived and designed the research
- acquired the data
- analyzed and interpreted the data
- performed statistical analysis
- handled funding and supervision
- drafted the manuscript
- made critical revision of the manuscript for important intellectual content

Mahidi Mardini  Date 27/6/13

- conceived and designed the research
- acquired the data
- analyzed and interpreted the data
- performed statistical analysis
- handled funding and supervision
- drafted the manuscript
- made critical revision of the manuscript for important intellectual content

Vilve M Howell *V.M. Howell* Date 1/8/13

- conceived and designed the research
- acquired the data
- analyzed and interpreted the data — supervision of RNA/PCR
- performed statistical analysis
- handled funding and supervision
- drafted the manuscript
- made critical revision of the manuscript for important intellectual content

John W Funder *J.W. Funder* Date 25/07/2013


- conceived and designed the research
- acquired the data
- analyzed and interpreted the data
- performed statistical analysis
- handled funding and supervision
- drafted the manuscript
- made critical revision of the manuscript for important intellectual content

Anthony W Ashton *Anthony Ashton* Date 1/8/13

- conceived and designed the research
- acquired the data
- analyzed and interpreted the data
- performed statistical analysis
- handled funding and supervision

_____ drafted the manuscript

made critical revision of the manuscript for important intellectual content

Anastasia S Mihailidou  Date 2-8-13

conceived and designed the research

acquired the data

analyzed and interpreted the data

performed statistical analysis

handled funding and supervision

drafted the manuscript

made critical revision of the manuscript for important intellectual content

Low-Dose Spironolactone Prevents Apoptosis Repressor With Caspase Recruitment Domain Degradation During Myocardial Infarction

Thi Yen Loan Le, Mahidi Mardini, Viive M. Howell, John W. Funder, Anthony W. Ashton, Anastasia S. Mihailidou

Abstract—Low-dose mineralocorticoid receptor antagonists reduce morbidity and mortality in patients with heart failure and myocardial infarction, despite normal plasma aldosterone levels. Since apoptosis plays an important role in heart failure and postinfarction left ventricular remodeling, we examined whether low-dose mineralocorticoid receptor antagonists modulate cardiomyocyte death by regulating the apoptosis repressor protein apoptosis repressor with caspase recruitment domain to lessen the extent of apoptosis. Hearts from adult male Sprague-Dawley rats were subjected to regional ischemia followed by reperfusion *ex vivo*, with mineralocorticoid receptor antagonists added to perfusates before ischemia. Low-dose spironolactone (10 nmol/L) or eplerenone (100 nmol/L) significantly reduced infarct size. Spironolactone also prevented cleavage of the apoptotic chromatin condensation inducer in the nucleus and of the inhibitor of caspase-activated DNase induced by ischemia-reperfusion, thereby abolishing chromatin condensation and internucleosomal cleavage. Ischemia-reperfusion–induced activation of caspases 2, 3, and 9, but not caspase 8, was prevented by spironolactone, suggesting targeted regulation of the intrinsic pathway. Low-dose spironolactone and eplerenone prevented loss of the apoptosis repressor with the caspase recruitment domain and reduced myocyte death. In H9c2 cells, mineralocorticoid receptor activation by aldosterone resulted in apoptosis repressor with caspase recruitment domain degradation and enhanced apoptosis; these actions were prevented by coadministration of spironolactone. Using a triple lysine mutant we identified that aldosterone enhances posttranscriptional degradation of the apoptosis repressor with a caspase recruitment domain via the ubiquitin-proteasomal pathway. Our data demonstrate that low-dose mineralocorticoid receptor antagonists reduce infarct size and apoptosis in the reperfused myocardium by preventing the apoptosis repressor with caspase recruitment domain degradation. (*Hypertension*. 2012;59:1164-1169.) • [Online Data Supplement](#)

Key Words: myocardial infarction ■ apoptosis ■ ischemia ■ reperfusion injury ■ heart failure ■ cardiovascular disease

Mortality and morbidity after acute myocardial infarction remain high, despite rapid reperfusion by percutaneous coronary intervention, and additional therapeutic strategies that reduce infarct size are needed.¹ Ischemia alters redox state triggering apoptosis and progressive loss of cardiomyocytes during and after myocardial infarction, which, in turn, contributes to developing congestive cardiac failure.² Low-dose mineralocorticoid receptor (MR) antagonists have been shown clinically to reduce blood pressure,^{3,4} particularly in resistant hypertension, and to substantially increase survival in heart failure,⁵ heart failure after myocardial infarction,⁶ and chronic systolic heart failure with mild symptoms.⁷

Significant benefits follow when eplerenone is administered early (<7 days) after myocardial infarction⁸ and experimentally at reperfusion.^{9,10} Interestingly, MR antagonists added to standard treatment proved effective despite levels of plasma aldosterone in the physiological range. In this regard, we have shown recently that low-dose spironolactone (10 nmol/L) perfused alone is protective during ischemia-reperfusion (I-R) in rats, reducing infarct size and apoptosis, and this protective effect persisted in *ex vivo* I-R studies in hearts from adrenalectomized animals,¹¹ raising interest in defining the mechanism for the cardioprotective action of low-dose MR antagonists.

Received December 25, 2011; first decision January 18, 2012; revision accepted March 20, 2012.

From the Department of Cardiology (T.Y.L.L., M.M., A.S.M.), Royal North Shore Hospital, Sydney, New South Wales, Australia; Cardiovascular and Hormonal Research Laboratory, Cardiology Division (T.Y.L.L., M.M., A.S.M.), Hormone and Cancer Division (V.M.H.), and Division of Perinatal Research (A.W.A.), Kolling Institute of Medical Research, Royal North Shore Hospital and the University of Sydney, Sydney, New South Wales, Australia; Department of Cardiology (M.M.), Westmead Hospital, Sydney, New South Wales, Australia; and Prince Henry's Institute (J.W.F.), Clayton, Victoria, Australia.

Funding bodies had no role in study design, data collection and analysis, decision to publish, or preparation of the article.

A.W.A. and A.S.M. are shared senior authors for this article.

The online-only Data Supplement is available with this article at <http://hyper.ahajournals.org/lookup/suppl/doi:10.1161/HYPERTENSIONAHA.111.190488/-DC1>.

Correspondence to Anastasia S. Mihailidou, Department of Cardiology, Royal North Shore Hospital, Pacific Highway, St Leonards, Sydney, New South Wales, Australia 2065. E-mail anastasia.mihailidou@sydney.edu.au

© 2012 American Heart Association, Inc.

Hypertension is available at <http://hyper.ahajournals.org>

DOI: 10.1161/HYPERTENSIONAHA.111.190488

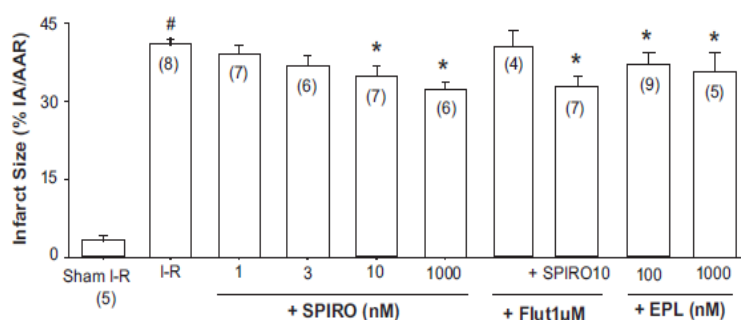


Figure 1. Mineralocorticoid receptor (MR) antagonists reduce myocardial infarct size. Various concentrations of spironolactone (SPIRO) and eplerenone (EPL) treatment on infarct size. Treatment with flutamide (Flut; 1 μ mol/L) on the effect of SPIRO was also investigated. Infarct area/size (IA) is expressed as percentage of area at risk (AAR). I-R indicates ischemia-reperfusion. Numbers of animals in each group are indicated in parentheses. Values are expressed as mean \pm SE. * P < 0.05 vs I-R alone; # P < 0.05 vs sham I-R.

Apoptosis, or programmed cell death, is a tightly regulated process, accounts for a significant part of the infarct size during myocardial I-R, and plays an important role in left ventricular remodeling.¹² The molecular mechanisms in apoptosis involve initiator caspase activation, an integrative phase and an execution phase involving caspases and endonucleases, apoptotic body formation, and cell fragmentation. Activation of effector caspases occurs via the extrinsic (activated by death receptor ligands) or the intrinsic pathway (involving the mitochondria and endoplasmic reticulum).¹³ Each pathway is characterized by a unique signature of caspase activation.¹⁴

Interfering with the apoptotic pathway attenuates myocardial injury.^{15,16} Whether low-dose MR antagonists modulate the onset of apoptosis during reperfusion injury has not been investigated previously. Apoptosis repressor with caspase recruitment domain (ARC) is an endogenous apoptosis repressor protein that is highly expressed in cardiac tissue and is unique in its ability to inhibit both death receptor (extrinsic) and mitochondrial (intrinsic) death pathways.¹⁷ Loss of ARC predisposes cardiac myocytes to undergo apoptosis during myocardial stress,^{17,18} including infarction-induced ventricular remodeling.¹² Decreased ARC expression has been measured in hypertensive animals¹⁹ and myocardium from patients with heart failure.¹⁸ Our aim was to determine whether MR antagonists modulate cardiomyocyte death by regulating apoptosis repressor ARC and preventing the onset of apoptosis.

Methods

Details of materials and methods are provided in the online-only Data Supplement.

Animal Studies

Male Sprague-Dawley rats (N=122; 300–400 g) were used, and study protocols were approved by the Royal North Shore Hospital Animal Care and Ethics Committee. All of the experiments were conducted in accordance with the Australian Code of Practice for the Care and Use of Animals for Scientific Purposes. Details for ex vivo I-R of the rat heart, measurement of apoptosis, immunohistochemistry, and immunoblotting are available in the online-only Data Supplement.

Cell Culture Studies

Rat cardiomyocyte H9c2 cells were used. Details for the cell culture studies, including routine culture, transfection and generation of cell lines with stable expression or knockdown of ARC, simulated ischemia and dose-response studies are available in the online-only Data Supplement.

Statistical Analysis

Results are presented as the mean \pm SE. Statistical comparisons were by unpaired Student *t* test or for comparing differences between treatments, 1-way ANOVA followed by Holm-Sidak post hoc test to adjust for multiple comparisons. Values of P < 0.05 are considered statistically significant.

Results

Low Doses of MR Antagonists Reduce Infarct Size by Preventing Apoptosis

Our dose-response studies confirmed that 10 nmol/L of spironolactone is the lowest dose to significantly reduce infarct size (Figure 1). Although spironolactone is also an androgen receptor antagonist, we found that flutamide (1 μ mol/L) did not prevent the protective effect of spironolactone (Figure 1). The selective MR antagonist eplerenone, at 100 and 1000 nmol/L, also significantly reduced infarct size (Figure 1), confirming an MR-mediated effect of spironolactone on infarct size. Exacerbated reperfusion injury leads to increased apoptosis in the area at risk²⁰; Figure S1A (in the online-only Data Supplement) shows a representative photomicrograph for colocalization of desmin (green) and TUNEL (red) staining, confirming cardiomyocyte apoptosis. Consistent with the effect on infarct size, I-R produced significant myocardial DNA cleavage measured by TUNEL. Both spironolactone and eplerenone attenuated apoptotic index (Figure S1B) in the reperfused myocardium, similar to their effect on infarct size.

Low Doses of MR Antagonists Modify Nuclear Remodeling Substrates

Apoptotic chromatin condensation inducer in the nucleus (ACINUS) and inhibitor of caspase-activated DNase (ICAD) are essential caspase substrates for DNA cleavage and apoptotic chromatin remodeling.^{21,22} Using a dual immunofluorescence assay to monitor ACINUS activation, we found that ACINUS was not processed during sham I-R (Figure S2, equal red [N-terminus ACINUS] and green [cleavable C-terminus] staining); however, during reperfusion, 50% of ACINUS was processed (Figures S2 [loss of green staining] and 2). Low-dose (10 nmol/L) spironolactone prevented ACINUS processing (Figure S2 [equal amounts of red and green staining]) without altering overall ACINUS expression (Figure 2). Similar results were observed with ICAD processing. Reperfusion injury markedly reduced immunoreactivity for full-length ICAD (Figure 2), indicating caspase-mediated

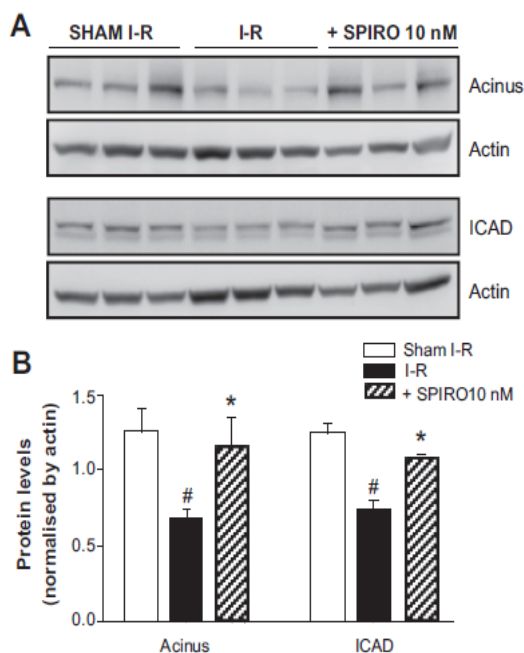


Figure 2. Spironolactone prevents apoptotic chromatin condensation inducer in the nucleus (ACINUS) and inhibitor of caspase-activated DNase (ICAD) processing. **A**, Data show immunoblotting for ACINUS and the inhibitor of caspase-activated DNase, DFF45/ICAD with cleavage-sensitive antibodies. I-R indicates ischemia-reperfusion; SPIRO, spironolactone. **B**, Densitometry was used to quantify expression of ACINUS and ICAD, using actin as the loading control, and values are expressed as mean \pm SE (N=3–6 per group); * P <0.05 vs I-R alone; # P <0.05 vs sham I-R. □, sham I-R; ■, I-R; ▨, + SPIRO 10 nM.

processing; spironolactone (10 nmol/L) prevented ICAD cleavage.

Low-Dose MR Antagonist and Proapoptotic Proteins

Caspase 3 mediates cleavage of nuclear substrates ACINUS and ICAD.^{21,22} During I-R injury, the 32-kDa full-length caspase 3 was cleaved to a 17-kDa fragment shown by staining with a cleavage-specific antibody (Figure S3A) and cleavage of procaspase 3 (Figure S3B). Low-dose (10 nmol/L) spironolactone abolished I-R-induced caspase 3 cleavage (Figure S3A and S3B). Myocardial reperfusion injury also triggered processing of caspase 2 and 9, as indicated by the appearance of the cleaved fragments, and decreased levels of procaspase 2 and 9 proteins (Figure S3C). In contrast, procaspase 8 activity did not change during I-R. Low-dose spironolactone prevented reperfusion-induced activation of procaspase 2 and 9 (Figure S3C).

Low-Dose MR Antagonist Prevents Degradation of Apoptosis Repressor Protein ARC

Antiapoptotic proteins Bcl-2, XIAP, and ARC are known to regulate activation of the intrinsic pathway and the associated apoptosome,^{23,24} and Figure 3A shows representative immunoblots. I-R downregulated Bcl-2 and XIAP by >50%, with neither affected by 10 nmol/L of spironolactone (Figure 3B). In contrast, spironolactone prevented I-R-induced loss of

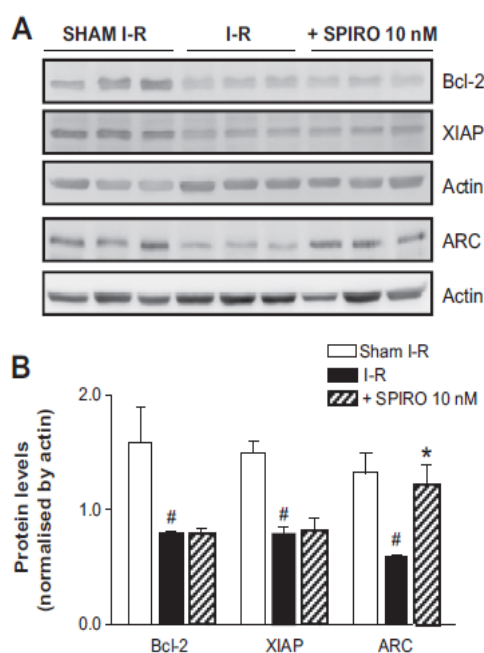


Figure 3. Spironolactone prevents reperfusion-induced ARC degradation. **A**, Representative immunoblots of antiapoptotic proteins, Bcl-2, XIAP, and ARC expression during I-R. **B**, Densitometric analysis of the changes in protein expression illustrated in **A**; actin was used to control for loading. Analysis shows that ARC protein expression decreased during I-R and was prevented by 10 nmol/L of spironolactone (SPIRO). ARC indicates apoptosis repressor with a caspase recruitment domain; I-R, ischemia-reperfusion, (N=3–6 per group). * P <0.05 vs I-R alone; # P <0.05 vs sham I-R. □, sham I-R; ■, I-R; ▨, + SPIRO 10 nM.

ARC expression (\approx 60% to 80%; Figures 3B and S4). Eplerenone produced a similar response to spironolactone, restoring levels of ARC in reperfused hearts (Figure S4). Therefore, low-dose MR antagonists prevent apoptosis during reperfusion injury by maintaining ARC levels, resulting in reduced infarct size.

To investigate whether salvage of ARC expression was essential for the antiapoptotic effects of spironolactone, we transfected H9c2 cells with an ARC knockdown construct (short hairpin RNA). ARC expression was abolished by the ARC short hairpin RNA construct (Figure S5B). Cells were then subjected to simulated ischemia and apoptotic index measured. Simulated ischemia markedly reduced ARC levels (Figure S5C) and increased apoptotic index (Figure S5D); low-dose spironolactone restored ARC levels (Figure S5C) and significantly reversed ischemia-induced apoptosis (Figure S5D). In ARC-short hairpin RNA-transfected cells, ischemia-induced apoptosis was exacerbated (Figure S5D), indicating that residual ARC could not effectively oppose apoptosis. In contrast to nontransfected cells, spironolactone did not salvage the induction of apoptosis because of simulated ischemia in short hairpin RNA-transfected H9c2.

MR Activation Promotes ARC Degradation to Initiate Apoptosis In Vitro

The above data suggest that ARC is targeted for degradation on MR activation during reperfusion. Using H9c2 cells, we

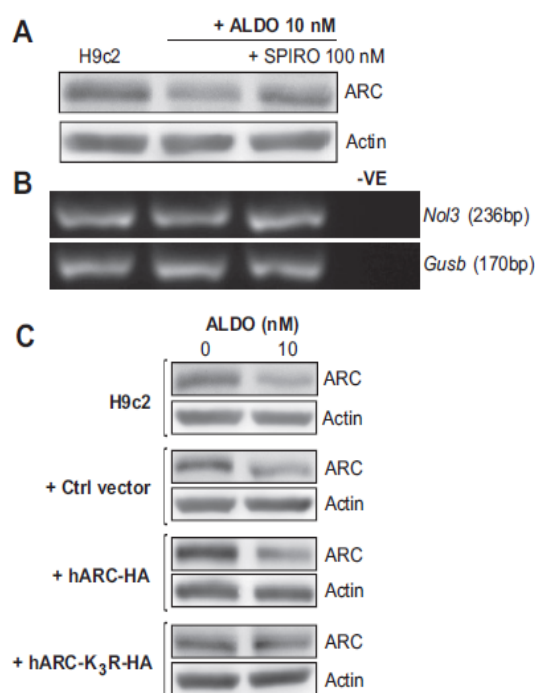


Figure 4. Mineralocorticoid receptor (MR) activation promotes ARC degradation. **A**, Expression of ARC protein levels in ALDO-treated cells and ALDO + SPIRO-treated cells. **B**, Expression of ARC mRNA levels by RT-PCR in ALDO- and ALDO + SPIRO-treated cells and no template control (-VE). **C**, Expression of ARC protein levels in nontransfected H9c2 cells, as well as those transfected with control vector, hARC-HA, and hARC-K₃R-HA. Images are representative of 3 independent experiments. ARC indicates apoptosis repressor with a caspase recruitment domain; *NoI3*, nucleolar protein 3 (*ARC*); *Gusb*, glucuronidase β ; ALDO, aldosterone, SPIRO, spironolactone.

found that MR activation decreased ARC protein levels by $\approx 45\%$ in vitro (Figure 4A; for optimal dose and exposure times see Figure S6). This effect was prevented by spironolactone (Figure 4A), indicating that it was MR mediated. In contrast, ARC transcription measured by RT-PCR remained unchanged during treatment (Figure 4B), indicating post-translational regulation of ARC levels. ARC contains lysines at positions 17, 68, and 163, and expression is regulated by proteosomal degradation. Mutation of all 3, lysine to arginine (ARC-K₃R), renders ARC resistant to degradation,²⁵ providing a ubiquitination-deficient mutant of the ARC protein. H9c2 cells transfected with ARC mutant (ARC-K₃R) were incubated in serum-containing medium (\pm aldosterone, 10 nmol/L). MR activation reduced endogenous ARC protein levels (H9c2 and control vector; Figure 4C) and expression of wild-type human ARC-transfected H9c2 cells. Conversely, ARC-K₃R mutant expression levels did not change (Figure 4C), indicating that MR activation leads to ARC degradation through the ubiquitin-proteosomal pathway.

Discussion

Our study identifies novel mechanisms of action of low-dose MR antagonists on cardiomyocytes during myocardial infarction, preventing degradation of the antiapoptotic protein ARC and processing of the death-promoting proteins, ACINUS and

ICAD. They also provide insight into how MR-regulated signaling during reperfusion injury leads to enhanced myocardial apoptosis and left ventricular remodeling and why low-dose antagonists (eg, spironolactone) may be so effective for the treatment of heart failure and associated conditions where low-level apoptosis drives cardiac damage and remodeling.

Restoration of ARC expression may explain the ability of MR antagonists, such as spironolactone and eplerenone, to regulate activation of the intrinsic pathway during reperfusion injury. Activation of MR during reperfusion injury targets ARC for posttranslational degradation through the ubiquitin-proteosomal pathway. This event is not only critical for apoptosis progression but also an important indicator of the potential effectiveness of MR antagonist treatment. Spironolactone cannot prevent myocyte apoptosis in the absence of ARC expression. Therefore, ongoing suppression of *NoI3* transcription or diminished ARC protein half-life would limit MR antagonists as therapeutic options. Understanding the mechanism by which low-dose MR antagonists prevent ARC degradation provides potential for developing therapeutic regimens in the treatment of heart failure and myocardial infarction. Currently, low doses of MR antagonists are used in both heart failure and heart failure post-MI.

Our ex vivo I-R model results in basal measures of myocardial infarct size comparable to previous studies^{9,16} during in vitro and in vivo I-R. The protective effect of spironolactone persisted in the presence of flutamide, indicating MR-mediated reduction in infarct size. The responses that we observed at the higher doses of MR antagonists are comparable to a previous study,¹⁰ under the same experimental conditions. In contrast, another study⁹ showed no effect of either eplerenone at 1 μ mol/L or canrenoate at 10 μ mol/L, whereas in vivo studies using 80 to 100 mg/kg per day of spironolactone showed only a 1% reduction in infarct size.^{16,26} To our knowledge, there has only been one other study²⁷ that has determined the effect of a low dose of spironolactone (10 nmol/L) during I-R. Although infarct size was not measured in that study, low-dose spironolactone (10 nmol/L) significantly increased contractility.

Increased apoptotic rate during human acute myocardial infarction²⁸ leads to progression of heart failure, and, therefore, alteration of apoptosis pathways may attenuate myocardial injury. Aldosterone induces cardiomyocyte apoptosis,²⁹ although the specific pathway was not identified, with both MR-dependent³⁰ and -independent³¹ pathways proposed. Although Akt and extracellular signal-regulated kinase 1/2 activation have been shown to be molecular targets for higher doses of MR antagonists during I-R,⁹ apoptosis was not measured. Excluding our previous study,¹¹ only 3 other studies explore the effect of MR antagonists on apoptosis. In 1 of these studies apoptosis was assessed only by TUNEL after 100 mg/kg per day of spironolactone.¹⁶ Our studies in H9c2 cardiomyocytes complement our studies in reperfused hearts and show a direct effect of MR activation on steady-state levels of ARC. We used H9c2 cells as a controlled environment to identify whether ARC regulation by low-dose MR antagonists was MR dependent rather than an MR-independent action. Under normoxic conditions and using serum-containing medium, we show that MR activation by

aldosterone decreases ARC protein levels, independent of simulated ischemia. Under similar normoxic conditions, cortisol would be without effect.³² These results are supported by previous studies that propose that the ratio of death inducer to death repressor proteins exerts control over cell survival.³³ Myocardial apoptosis, both at the site of infarction and in the remote zone, correlates with unfavorable postinfarction left ventricular remodeling¹² and progression to heart failure.³⁴ Our results provide that a possible mechanism for the cardioprotective action of low-dose MR antagonists in the clinical studies (Randomized Aldactone Evaluation Study and Eplerenone Post-Acute Myocardial Infarction Heart Failure Efficacy and Survival Study) is to regulate cardiomyocyte ARC and to reduce this ongoing low-grade myocardial apoptosis.

Nuclear remodeling during apoptosis requires activation of cysteinyl-aspartate proteases (caspases), located in the cell as inactive proenzymes (upstream initiator caspases; eg, procaspases 2, 8, 9, 10, and 12) and downstream effector caspases (eg, procaspases 3, 6, and 7)³⁵ mediating unwinding of DNA and subsequent internucleosomal cleavage.^{36,37} Spironolactone attenuating I-R–induced processing of caspase 3 (and subsequent cleavage of nuclear substrates and nuclear fragmentation) is almost certainly a product of inactivation of upstream pathways. In our studies, processing of caspase 2 and 9 (both involved in the intrinsic pathway) was indicated by the appearance of the cleaved fragments and decreased levels of procaspase 2 and 9 proteins (Figure S3C). In contrast, procaspase 8 activity (involved in the extrinsic pathway) did not change during I-R. Low-dose spironolactone prevented activation of procaspase 2 and 9 (Figure S3C) during I-R, confirming that MR antagonists regulate the intrinsic apoptosis pathway.

Our study confirms that antiapoptotic proteins Bcl-2, XIAP, and ARC must be degraded for apoptosis to proceed during myocardial I-R injury.³⁸ MR antagonist-induced stabilization of ARC expression prevents activation of the intrinsic pathway at multiple points. ARC inhibits t-Bid generation³⁹ and caspase 2 processing by the PIDDosome through interaction between the CARD domains of the 2 proteins⁴⁰ and prevents Bax activation in response to I-R injury.^{17,41} There have been discrepant reports for activation of the death receptor (extrinsic) pathway during I-R, with both the absence of caspase 8 processing noted,⁴² confirming our findings, and activation reported by other studies.⁴³

ARC is targeted via ubiquitination to the proteasome^{25,44} and is unique compared with other antiapoptotic proteins that act on only 1 apoptotic pathway. Preserving ARC levels is sufficient to maintain myocyte viability after oxidant stress²⁵ or infarction.⁴¹ Mutation of ubiquitin acceptor sites on ARC prevents degradation and enhances cellular protection,²⁵ confirming the role of decreasing ARC levels as the master controller of cardiomyocyte apoptosis. Regulation of ARC expression during reperfusion is controlled by the expression/activity of the ubiquitin ligase MDM2.^{25,39} MR activation upregulates MDM2, leading to proliferation of vascular smooth muscle cells⁴⁵ and, as shown in our studies, degradation of ARC. MDM2 is also the ligase for p53,⁴⁶ controlling both ubiquitination and degradation of p53.⁴⁴ MR acti-

vation regulates p53, a transcriptional regulator of the proapoptotic protein Bax.⁴⁷ ARC interacts with the C-terminal regulatory domain of Bax, preventing conformational activation and translocation from the cytosol to the mitochondria,²⁵ leading to decreased apoptosis, further confirming that the mitochondrial (or intrinsic) apoptotic pathway is involved.

Perspectives

In conclusion, our findings show that low-dose MR antagonists regulate cardiomyocyte apoptosis repressor protein ARC during I-R. This novel action of MR antagonists provides direct evidence that antagonists have effects beyond denying agonists access to MR, so-called MR blockade. The low doses of spironolactone (and lower affinity of MR-selective antagonist eplerenone) prevented ARC degradation, providing cardioprotection by preventing initiation of apoptosis during myocardial infarction and, by extension, in hypertension, where they are increasingly used. Our studies support early administration of low-dose MR antagonists or addition to drug-eluting stents for protection of the myocardium.

Acknowledgments

We thank Prof Celso Gomez Sanchez for providing the MR antibodies and Prof Richard Kitsis for the K₃R-ARC-HA construct.

Sources of Funding

This study was supported by a project grant from the National Heart Foundation of Australia (A.S.M.). T.Y.L.L. was supported by postgraduate fellowship (633112) and A.W.A. by a Career Development Award (402847) from the National Health and Medical Research Council and V.M.H. by a Cancer Institute New South Wales Fellowship.

Disclosures

J.W.F. is a consultant for Pfizer, Merck, Novo Nordisk, and Allergan, as well as a member of the Board of CBio. All other authors have no conflicts of interests to disclose.

References

- Burns RJ, Gibbons RJ, Yi Q, Roberts RS, Miller TD, Schaefer GL, Anderson JL, Anderson JL, for the CORE Study Investigators. The relationships of left ventricular ejection fraction, end-systolic volume index and infarct size to six-month mortality after hospital discharge following myocardial infarction treated by thrombolysis. *J Am Coll Cardiol*. 2002;39:30–36.
- Kang PM, Izumo S. Apoptosis and heart failure: a critical review of the literature. *Circ Res*. 2000;86:1107–1113.
- Weinberger MH, Roniker B, Krause SL, Weiss RJ. Eplerenone, a selective aldosterone blocker, in mild-to-moderate hypertension. *Am J Hypertens*. 2002;15:709–716.
- Nishizaka MK, Zaman MA, Calhoun DA. Efficacy of low-dose spironolactone in subjects with resistant hypertension. *Am J Hypertens*. 2003;16:925–930.
- Pitt B, Zannad F, Remme WJ, Cody R, Castaigne A, Perez A, Palensky J, Wittes J. The effect of spironolactone on morbidity and mortality in patients with severe heart failure: Randomized Aldactone Evaluation Study investigators. *N Engl J Med*. 1999;341:709–717.
- Pitt B, Remme W, Zannad F, Neaton J, Martinez F, Roniker B, Bittman R, Hurley S, Kleiman J, Galin M, for the Eplerenone Post-Acute Myocardial Infarction Heart Failure Efficacy and Survival Study Investigators. Eplerenone, a selective aldosterone blocker, in patients with left ventricular dysfunction after myocardial infarction. *N Engl J Med*. 2003;348:1309–1321.
- Zannad F, McMurray JJ, Krum H, van Veldhuisen DJ, Swedberg K, Shi H, Vincent J, Pocock SJ, Pitt B, for the EMPHASIS-HF Study Group.

- Eplerenone in patients with systolic heart failure and mild symptoms. *N Engl J Med*. 2011;364:11–21.
8. Adamopoulos C, Ahmed A, Fay R, Angioi M, Filippatos G, Vincent J, Pitt B, Zannad F, for the EPHEsus Investigators. Timing of eplerenone initiation and outcomes in patients with heart failure after acute myocardial infarction complicated by left ventricular systolic dysfunction: insights from the EPHEsus Trial. *Eur J Heart Failure*. 2009;11:1099–1105.
 9. Schmidt K, Tissier R, Ghaleh B, Drogies T, Felix SB, Krieg T. Cardioprotective effects of mineralocorticoid receptor antagonists at reperfusion. *Eur Heart J*. 2010;31:1655–1662.
 10. Chai W, Garrelts IM, de Vries R, Danser AHJ. Cardioprotective effects of eplerenone in the rat heart: interaction with locally synthesized or blood-derived aldosterone? *Hypertension*. 2006;47:665–670.
 11. Mihailidou AS, Le TYL, Mardini M, Funder JW. Glucocorticoids activate cardiac mineralocorticoid receptors during experimental myocardial infarction. *Hypertension*. 2009;54:1306–1312.
 12. Ekhterae D, Hinmon R, Matsuzaki K, Noma M, Zhu W, Xiao R-P, Gorman RC, Gorman JH. Infarction induced myocardial apoptosis and ARC activation. *J Surg Res*. 2011;166:59–67.
 13. Crow MT, Mani K, Mani K, Mani K, Kitsis RN. The mitochondrial death pathway and cardiac myocyte apoptosis. *Circ Res*. 2004;95:957–970.
 14. Slee EA, Adrain C, Martin SJ. Serial killers: ordering caspase activation events in apoptosis. *Cell Death Differ*. 1999;6:1067–1074.
 15. Kuster GM, Kotlyar E, Rude MK, Sitwik DA, Liao R, Colucci WS, Sam F. Mineralocorticoid receptor inhibition ameliorates the transition to myocardial failure and decreases oxidative stress and inflammation in mice with chronic pressure overload. *Circulation*. 2005;111:420–427.
 16. Takeda M, Tatsumi T, Matsunaga S, Hayashi H, Kimata M, Honsho S, Nishikawa S, Manoa A, Shiraishi J, Yamada H, Takahashi T, Matoba S, Kobara M, Matsubara H. Spironolactone modulates expressions of cardiac mineralocorticoid receptor and 11 β -hydroxysteroid dehydrogenase 2 and prevents ventricular remodeling in post-infarct rat hearts. *Hypertens Res*. 2007;30:427–437.
 17. Nam Y-J, Mani K, Ashton AW, Peng C-F, Krishnamurthy B, Hayakawa Y, Lee P, Korsmeyer SJ, Kitsis RN. Inhibition of both the extrinsic and intrinsic death pathways through nonhomotypic death-fold interactions. *Mol Cell*. 2004;15:901–912.
 18. Donath S, Li P, Willenbockel C, Al-Saadi N, Gross V, Willnow T, Bader M, Martin U, Bauersachs J, Wollert KC, Dietz R, von Harsdorf R, for the German Heart Failure Network. Apoptosis repressor with caspase recruitment domain is required for cardioprotection in response to biomechanical and ischemic stress. *Circulation*. 2006;113:1203–1212.
 19. Quadriatero J, Bloemberg D. Apoptosis repressor with caspase recruitment domain is dramatically reduced in cardiac, skeletal, and vascular smooth muscle during hypertension. *Biochem Biophys Res Comm*. 2010;391:1437–1442.
 20. Yellon DM, Hausenloy DJ. Myocardial reperfusion injury. *N Engl J Med*. 2007;357:1121–1135.
 21. Enari M, Sakahira H, Yokoyama H, Okawa K, Iwamatsu A, Nagata S. A caspase-activated dnase that degrades DNA during apoptosis, and its inhibitor ICAD. *Nature*. 1998;391:43–50.
 22. Sahara S, Aoto M, Eguchi Y, Imamoto N, Yoneda Y, Tsujimoto Y. Acinus is a caspase-3-activated protein required for apoptotic chromatin condensation. *Nature*. 1999;401:168–173.
 23. Deveraux QL, Takahashi R, Salvesen GS, Reed JC. X-linked IAP is a direct inhibitor of cell-death proteases. *Nature*. 1997;388:300–304.
 24. Cory S, Adams JM. The Bcl2 family: regulators of the cellular life-or-death switch. *Nat Rev Cancer*. 2002;2:647–656.
 25. Nam Y-J, Mani K, Wu L, Peng C-F, Calvert JW, Foo RS-Y, Krishnamurthy B, Miao W, Ashton AW, Lefer DJ, Kitsis RN. The apoptosis inhibitor ARC undergoes ubiquitin-proteasomal-mediated degradation in response to death stimuli: identification of a degradation-resistant mutant. *J Biol Chem*. 2007;282:5522–5528.
 26. Mulder P, Mellin V, Favre J, Vercauteren M, Remy-Jouet I, Monteil C, Richard V, Renet S, Henry JP, Jeng AY, Webb RL, Thuillez C. Aldosterone synthase inhibition improves cardiovascular function and structure in rats with heart failure: a comparison with spironolactone. *Eur Heart J*. 2008;29:2171–2179.
 27. Barbato JC, Mulrow PJ, Shapiro JL, Franco-Saenz R. Rapid effects of aldosterone and spironolactone in the isolated working rat heart. *Hypertension*. 2002;40:130–135.
 28. Saraste A, Pulkki K, Kallajoki M, Henriksen K, Parvinen M, Voipio-Pulkki L-M. Apoptosis in human acute myocardial infarction. *Circulation*. 1997;95:320–323.
 29. Burniston JG, Saini A, Tan L-B, Goldspink DF. Aldosterone induces myocyte apoptosis in the heart and skeletal muscles of rats in vivo. *J Mol Cell Cardiol*. 2005;39:395–399.
 30. De Angelis N, Fiordaliso F, Latini R, Calvillo L, Funicello M, Gobbi M, Mennini T, Masson S. Appraisal of the role of angiotensin II and aldosterone in ventricular myocyte apoptosis in adult normotensive rat. *J Mol Cell Cardiol*. 2002;34:1655–1665.
 31. Mano A, Tatsumi T, Shiraishi J, Keira N, Nomura T, Takeda M, Nishikawa S, Yamanaka S, Matoba S, Kobara M, Tanaka H, Shirayama T, Takamatsu T, Nozawa Y, Matsubara H. Aldosterone directly induces myocyte apoptosis through calcineurin-independent pathways. *Circulation*. 2004;110:317–323.
 32. Mihailidou AS, Mardini M, Fraser T, Funder JW. Agonist/antagonist activity of cortisol in cardiomyocyte mineralocorticoid receptors is determined by redox state. Presented at the 30th Meeting of the International Aldosterone Conference; June 14–15, 2004; New Orleans, LA.
 33. Almeida OFX, Conde GL, Crochemore C, Demeneix BA, Fischer D, Hassan AHS, Meyer M, Holsboer F, Michaelidis TM. Subtle shifts in the ratio between pro- and antiapoptotic molecules after activation of corticosteroid receptors decide neuronal fate. *FASEB J*. 2000;14:779–790.
 34. Abbate A, Biondi-Zoccai GGL, Bussani R, Dobrina A, Camilot D, Feroce F, Rossiello R, Baldi F, Silvestri F, Biasucci LM, Baldi A. Increased myocardial apoptosis in patients with unfavorable left ventricular remodeling and early symptomatic post-infarction heart failure. *J Am Coll Cardiol*. 2003;41:753–760.
 35. Mani K. Programmed cell death in cardiac myocytes: strategies to maximize post-ischemic salvage. *Heart Fail Rev*. 2008;13:193–209.
 36. Sakahira H, Enari M, Nagata S. Cleavage of CAD inhibitor in CAD activation and DNA degradation during apoptosis. *Nature*. 1998;391:96–99.
 37. Liu X, Li P, Widlak P, Zou H, Luo X, Garrard WT, Wang X. The 40-kDa subunit of DNA fragmentation factor induces DNA fragmentation and chromatin condensation during apoptosis. *Proc Natl Acad Sci USA*. 1998;95:8461–8466.
 38. Misao J, Hayakawa Y, Ohno M, Kato S, Fujiwara T, Fujiwara H. Expression of Bcl-2 protein, an inhibitor of apoptosis, and Bax, an accelerator of apoptosis, in ventricular myocytes of human hearts with myocardial infarction. *Circulation*. 1996;94:1506–1512.
 39. Ludwig-Galezowski A, Flanagan L, Rehm M. Apoptosis repressor with caspase recruitment domain, a multifunctional modulator of cell death. *J Cell Mol Med*. 2011;15:1044–1053.
 40. Zhang YQ, Herman B. ARC protects rat cardiomyocytes against oxidative stress through inhibition of caspase-2 mediated mitochondrial pathway. *J Cell Biochem*. 2006;99:575–588.
 41. Gustafsson AB, Sayen MR, Williams SD, Crow MT, Gottlieb RA. TAT protein transduction into isolated perfused hearts: TAT-apoptosis repressor with caspase recruitment domain is cardioprotective. *Circulation*. 2002;106:735–739.
 42. McCully JD, Wakiyama H, Hsieh YJ, Jones M, Levitsky S. Differential contribution of necrosis and apoptosis in myocardial ischemia-reperfusion injury. *Am J Physiol Heart Circ Physiol*. 2004;286:H1923–H1935.
 43. Scarabelli TM, Stephanou A, Pasini E, Comini L, Raddino R, Knight RA, Latchman DS. Different signaling pathways induce apoptosis in endothelial cells and cardiac myocytes during ischemia/reperfusion injury. *Circ Res*. 2002;90:745–748.
 44. Foo RS-Y, Chan LKW, Kitsis RN, Bennett MR. Ubiquitination and degradation of the anti-apoptotic protein ARC by MDM2. *J Biol Chem*. 2007;282:5529–5535.
 45. Nakamura Y, Suzuki S, Ono K, Miura I, Satoh F, Moriya T, Saito H, Yamada S, Ito S, Sasano H. MDM2: a novel mineralocorticoid-responsive gene involved in aldosterone-induced human vascular structural remodeling. *Am J Pathol*. 2006;169:362–370.
 46. Sohn HJ, Yoo KH, Jang GY, Lee JH, Choi BM, Bae IS, Yim HE, Son CS, Lee JW. Aldosterone modulates cell proliferation and apoptosis in the neonatal rat heart. *J Korean Med Sci*. 2010;25:1296–1304.
 47. McCullers DL, Herman JP. Mineralocorticoid receptors regulate bcl-2 and p53 mRNA expression in hippocampus. *Neuroreport*. 1998;9:3085–3089.

ONLINE SUPPLEMENT

**LOW DOSE SPIRONOLACTONE PREVENTS ARC (APOPTOSIS REPRESSOR
WITH A CASPASE RECRUITMENT DOMAIN) DEGRADATION DURING
MYOCARDIAL INFARCTION**

Le: MR antagonists and ARC

Thi Yen Loan Le^{1,2} BMedSc, Mahidi Mardini^{1,2,3} MBBS FRACP PhD, Viive M Howell^{2,4}
BSc(App) MSc, PhD, John W Funder⁵, MD PhD FRACP, Anthony W Ashton^{2,6} BSc PhD*
and Anastasia S. Mihailidou^{1,2} BSc PhD*

¹Department of Cardiology, Royal North Shore Hospital, ²Kolling Institute of Medical
Research, Royal North Shore Hospital and The University of Sydney; ³Department of
Cardiology, Westmead Hospital, ⁴Hormone and Cancer Division, ⁵Prince Henry's Institute,
Clayton, Victoria, ⁶Division of Perinatal Research, Royal North Shore Hospital, Australia.

Expanded Methods

Materials: Drugs and chemicals were purchased from Sigma–Aldrich unless otherwise specified. Cell culture reagents were from Invitrogen.

Ex vivo ischemia-reperfusion of the rat heart

Rats were anesthetized with intraperitoneal (i.p.) ketamine (60 mg/kg) and xylazine hydrochloride (10 mg/kg), and then received heparin (250 IU, i.p.). Hearts were rapidly isolated and mounted onto a Langendorff apparatus, with regional I-R induced by occluding a branch of the left coronary artery for 30 min and releasing the occlusion to allow reperfusion for 150 min, as previously described [1-3]. MR antagonists, spironolactone (SPIRO, 1, 3, 10 and 1000 nM) or eplerenone (EPL, 100 and 1000 nM) were perfused for 15 minutes prior to ischemia and throughout reperfusion. We used a higher initial dose of eplerenone (100 nM) since affinity of eplerenone *in vitro* is 2-3% that of spironolactone [4]. In separate experiments, the androgen receptor antagonist, flutamide (1 μ M) was administered alone or with spironolactone. At the end of reperfusion, hearts were infused with monastral blue dye to delineate area at risk, and infarct size measured as described previously [3]. Infarct size, apoptosis and immunohistochemistry were measured on the same hearts, with a separate group of animals used for western blot analysis.

Measurement of apoptosis in cardiac tissue

Apoptosis was measured by terminal deoxynucleotide transferase-mediated dUTP nick end labeling (TUNEL) as previously described [3]. Immunostaining for Desmin was used to confirm cardiomyocyte apoptosis [5]. Following TUNEL staining, desmin antibody (10%, Abcam) was applied to sections of reperfused left ventricle and left overnight at 4^oC before counterstaining with DAPI reagent. Images were captured using fluorescence microscopy at 200x magnification.

Immunohistochemistry

Immunostaining for apoptotic mediators was performed using formalin-fixed paraffin embedded sections of reperfused left ventricle (5 μ m thick). Sections were deparaffinised, rehydrated and endogenous peroxidase activity blocked by incubation with 1% hydrogen peroxide for 30 min and epitope retrieval performed in 10 mM citrate buffer (pH 6.0) at 95^oC for 10 min. Sections were immunostained for apoptotic mediators using specific antibodies against ARC (Cayman), active caspase-3 (CM1, Abcam), and by dual immunofluorescence for ACINUS using C- (AnaSpec) and N-(Santa Cruz) terminal and specific secondary antibodies. For caspase-3 and ACINUS staining antibody reactivity was detected using either FITC- or Cy3-labelled secondary antibody (1:200) before counterstaining with DAPI reagent. For all other antibodies reactivity was detected using envision+ polymer reagent (DAKO) with DAB used as the chromogen (Sigma-Aldrich). Images were captured using either bright field or fluorescence microscopy (200x magnification).

SDS-PAGE and Immunoblotting

At the end of reperfusion, left ventricular free wall tissue was snap frozen in liquid nitrogen. For protein extraction, frozen tissue was powdered in a mortar and pestle and homogenized in RIPA buffer (50 mM Tris (pH8.0), 150 mM NaCl, 1% (v/v) Triton x100, 1% (w/v) Na-deoxycholate, 0.1% (w/v) SDS, 1 mM PMSF, and protease inhibitors). Lysates were immediately placed into on ice for 30 minutes at 4^oC followed and clarified by centrifugation at 16,000xg for 10 min. Protein content of lysates was measured by Bradford Protein Assay [6]. Immunoblotting was performed as previously described [7]. Aliquots (30-50 μ g) were

separated by sodium dodecyl sulphate-polyacrylamide gel electrophoresis (SDS-PAGE) on gels of varying acrylamide concentrations (8-15 %). Following transfer to PVDF membranes, primary antibodies including ACINUS (C-terminal), ICAD (N-terminus), caspase-3/-2/-8/-9, ARC, B-cell lymphoma (Bcl)-2 and X-linked inhibitor of Apoptosis (XIAP) were diluted in blocking buffer (TBS-T (10 mM Tris (pH8.0), 150 mM NaCl, 0.1% (v/v) Tween-20) and 5% (w/v) non-fat milk powder) and incubated with membranes overnight at 4 °C. Antibody binding was detected with HRP-conjugated secondary antibodies (1:3000, Dako Cytomation, Dako Australia). Membranes were washed, exposed to chemiluminescent substrate (Perkin Elmer, Melbourne, Australia) and digital images of the resulting bands captured on a LAS4000 (GE Healthcare Life Sciences).

Cell culture studies

To determine whether the mechanism for the cardioprotective action of low dose MR antagonists required regulating ARC processing, we used the rat cardiomyocyte cell line (H9c2) since many of the characteristics of isolated primary cardiomyocytes are retained [8, 9]. H9c2 cells were cultured in Dulbecco's modified Eagle's medium (DMEM) (Invitrogen) which contained 10% fetal bovine serum, L-glutamine (2 mM), penicillin (10 U/mL) and streptomycin (10 µg/mL) at 37°C in a humidified atmosphere with 5% CO₂, and at ~90% confluence were harvested for experiments. Cells were treated with this medium for all studies except during the simulated ischemia protocol.

Simulated ischemia and apoptosis studies in H9c2 cells

Simulated ischemia was achieved by culturing cells in serum free-, glucose free-DMEM in an atmosphere of 1% (v/v) O₂/5% (v/v) CO₂/94% (v/v) N₂ at 37°C for 18 h. For detecting apoptosis, cells were fixed in 4% (w/v) paraformaldehyde in PBS and permeabilized with 0.1% (v/v) Triton X-100 in 0.1% (w/v) sodium citrate, followed by incubation in TUNEL reaction mixture for 60 min at 37°C. After washing, the cells were counterstained with DAPI, mounted and visualised under fluorescence microscope. TUNEL-positive nuclei were calculated in five randomly selected fields for each slide and three independent experiments were used per treatment.

Dose response and time-course studies for aldosterone in H9c2 cells

The cells were plated in 6 well plates and allowed to adhere overnight in complete media. The effective dose (EC₅₀) of aldosterone was determined by treating cells with 1, 2, 5, 10 and 20 nM aldosterone for 24 h prior to harvest. For the time-course study, cells were treated with 10 nM aldosterone and harvested at 6, 12, 18, 24 and 36 h. In separate experiments, optimal conditions for aldosterone stimulation were used to examine the selectivity of MR-activation in the observed effects. H9c2 cells were pre-incubated with 100 nM spironolactone for 30 min prior to aldosterone addition. Cells were then treated with aldosterone ± spironolactone. Treated cells were washed with PBS, trypsinized, and then resuspended in 200 µl of lysis buffer (50 mM Tris (pH8.0), 150 mM NaCl, 1% (v/v) Nonidet P-40, 0.02% (w/v) sodium azide, and protease inhibitors) and protein extracted as described above.

Studies using ARC-knockdown construct

To permanently knockdown ARC, H9c2 cells were transfected with shRNA constructs against ARC and a scramble control (Open Biosystems). Selection was performed using 2 µg/mL puromycin (Sigma Aldrich) and pooled populations used in subsequent experiments. Stably transfected H9c2 cells were screened for ARC expression by immunoblotting to confirm extent of knockdown.

Studies using a ubiquitination-resistant ARC mutant

H9c2 cells were transfected with expression vectors for wild-type (hARC-HA) and a ubiquitination deficient mutant (hARC-K₃R-HA) [10] of ARC using Effectene according to the manufacturer's protocol (Qiagen). An empty vector (pcDNA3.1) was used as a control. Cell lines with stable overexpression were generated using antibiotic selection (150 µg/mL hygromycin) (Sigma Aldrich) for 2 weeks and pooled populations used in subsequent experiments. Expression of the constructs was confirmed by immunoblotting for the HA tag (Santa Cruz). Cells were then incubated with serum and glucose-containing media ± 10 nM aldosterone for 24 h and protein levels were determined by western blot.

Reverse Transcription–Polymerase Chain Reaction (RT-PCR)

Total RNA was extracted from H9c2 cells using Qiazol lysis reagent (Qiagen) and 5 µg was reverse transcribed using the Superscript III First-Strand Synthesis System for RT-PCR kit (Invitrogen) and oligo (dT) according to the manufacturers' protocols. The *Nol3* gene that encodes ARC was amplified with primers: *Nol3*-exon1-F: 5'-CTACTGCTGTTGGTGCAGA-3' and *Nol3*-exon2-R: 5'-GACCTCCGATCTCCTCTTCC-3', resulting in a 236bp product. The endogenous control *Gusb* (*glucuronidase beta*) was amplified with primers: *Gusb*-exon3-F: 5'-GGTGTGGTATGAACGGGAAG-3' and *Gusb*-exon4-R: 5'-TGGTGATGTCAGCCTCAAAG-3', resulting in a 170bp product. Amplification was carried out for 30 cycles in a 50 µL volume with 2 µL cDNA and the products were separated using electrophoresis on 2% (w/v) TAE-agarose gels and visualised, after staining with Gel red solution, using UV light on a gel imaging system (GE Healthcare Life Sciences).

References

1. Schmidt K, Tissier R, Ghaleh B, Drogies T, Felix SB, Krieg T. Cardioprotective effects of mineralocorticoid receptor antagonists at reperfusion. *Eur Heart J*. 2010;31:1655–1662.
2. Chai W, Garrelds IM, de Vries R, Danser AHJ. Cardioprotective effects of eplerenone in the rat heart: Interaction with locally synthesized or blood-derived aldosterone? *Hypertension*. 2006;47:665-670.
3. Mihailidou AS, Le TYL, Mardini M, Funder JW. Glucocorticoids activate cardiac mineralocorticoid receptors during experimental myocardial infarction. *Hypertension*. 2009;54:1306-1312.
4. de Gasparo M, Joss U, Ramjoue S, Whitebread SE, Haenni H, Schenke L, Kraehenbuehl C, Biollaz M, Grob J, Schmidlin J, Wieland P, Wehrli U. Three new epoxy-spiro lactone derivatives: characterization in vivo and in vitro. *J Pharmacol Exp Ther*. 1987;240:650–656.
5. Scarabelli TM, Knight RA, Rayment NB, Cooper TJ, Stephanou A, Brar BK, Lawrence KM, Santilli G, Latchman DS, Baxter GF, Yellon DM. Quantitative assessment of cardiac myocyte apoptosis in tissue sections using the fluorescence-based tunel technique enhanced with counterstains. *J Immunol Methods*. 1999;228:23-28.
6. Bradford MM. A rapid and sensitive method for the quantitation of microgram quantities of protein utilizing the principle of protein-dye binding. *Anal Biochem*. 1976; 72:248-254.
7. Ashton AW, Yokota R, John G, Zhao S, Suadican SO, Spray DC, Ware JA. Inhibition of endothelial cell migration, intercellular communication, and vascular tube formation by thromboxane A(2). *J Biol Chem* 1999;274:35562-35570.

8. Maulik N, Yoshida T, Das DK. Regulation of cardiomyocyte apoptosis in ischemic reperfused mouse heart by glutathione peroxidase. *Mol Cellular Biochem.* 1999;196:13-21.
9. Hescheler J, Meyer R, Plant S, Krautwurst D, Rosenthal W, Schultz G. Morphological, biochemical, and electrophysiological characterization of a clonal cell (H9c2) line from rat heart. *Circ Res.* 1991;69:1476-1486.
10. Nam Y-J, Mani K, Wu L, Peng C-F, Calvert JW, Foo RS-Y, Krishnamurthy B, Miao W, Ashton AW, Lefer DJ, Kitsis RN. The Apoptosis Inhibitor ARC Undergoes Ubiquitin-Proteasomal-mediated Degradation in Response to Death Stimuli. Identification of a degradation-resistant mutant. *J Biol Chem.* 2007;282:5522-5528.

Supplement Figures

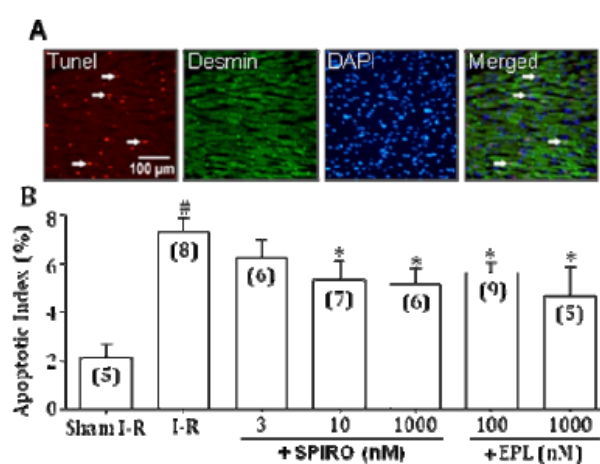


Figure S1. MR antagonists attenuate apoptosis during ischemia-reperfusion.

A. Representative photomicrographs of ventricular sections show proportion of TUNEL-positive nuclei (red fluorescence, arrows) relative to DAPI (blue fluorescence) stained nuclei. Desmin antibody (green fluorescence) indicates cardiomyocytes. Arrows indicate apoptotic cardiomyocyte nuclei (pink). All images are x200 magnification. **B.** Quantification of the apoptotic index from treated reperfused myocardium. I-R, ischemia-reperfusion, SPIRO, spironolactone, EPL, eplerenone. Values express as mean \pm SE. Numbers in parentheses indicate number of animals in group. * $p < 0.05$ vs I-R alone; # $p < 0.05$ vs sham I-R.

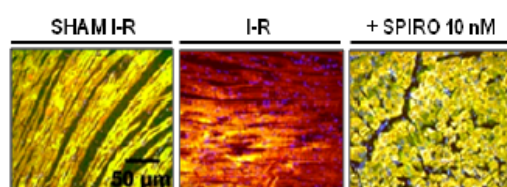


Figure S2: Spironolactone prevents ACINUS processing

A. Dual immunofluorescence staining for ACINUS identifying the non-activation dependent epitope (N-terminus, red) and proteolytically processed C-terminus (green). The two fluorophores co-localize (yellow fluorescence) when ACINUS is inactive. Loss of green fluorescence is observed when ACINUS is cleaved by effector caspases in the reperfused myocardium. Low dose spironolactone (SPIRO 10 nM) prevented ACINUS processing.

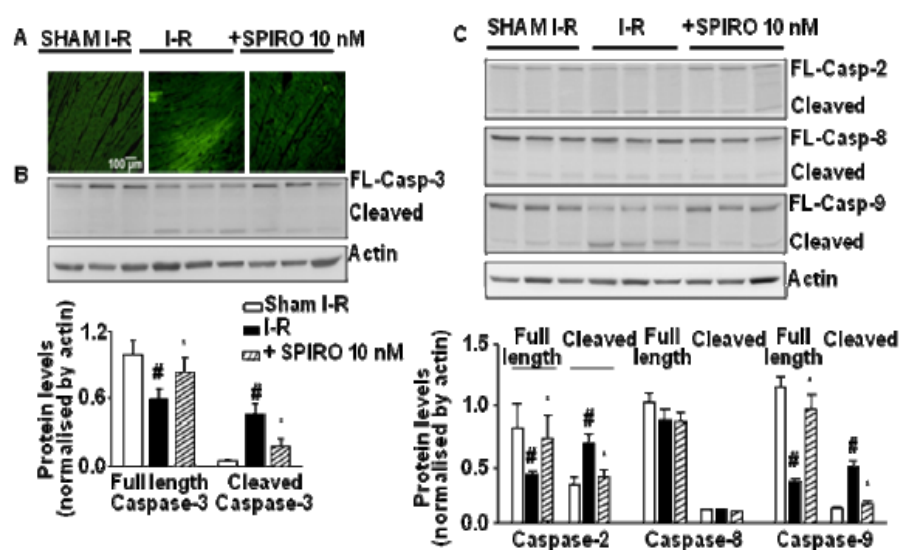


Figure S3. Spironolactone attenuates apoptosis by preventing activation of the intrinsic pathway during IR injury.

A. Myocardial sections stained for active caspase-3. Increased green fluorescence indicates cleavage of caspase-3; spironolactone (SPIRO 10 nM) prevented caspase-3 processing. **B and C.** Representative immunoblots showing processing of pro-caspases-3 (**B**), -2, -8, and -9 (**C**) in lysates from reperfused left ventricular tissue samples compared to sham I-R. SPIRO prevented cleavage of caspases-3, -2 and -9. No changes in pro-caspase-8 protein levels were observed. I-R, Ischemia-reperfusion, FL, full-length, (N=3-6 per group). Changes in **B** and **C** were quantified using densitometric analysis with Actin used as the loading control. * $p < 0.05$ vs I-R alone; # $p < 0.05$ vs sham I-R.

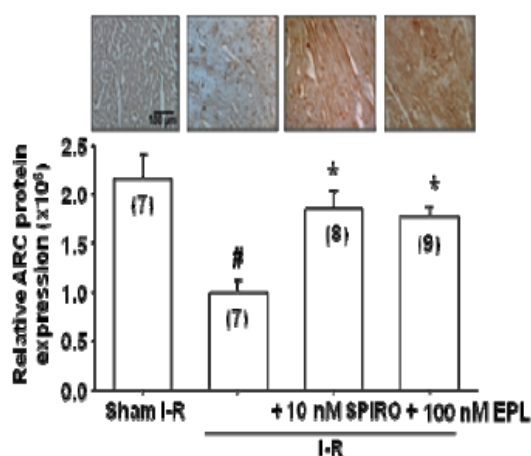


Figure S4. Low dose MR antagonists prevent reperfusion-induced ARC degradation.

Sections of reperfused myocardium were stained for ARC (apoptosis repressor with a caspase recruitment domain) using 3, 3' diaminobenzidine (DAB, brown precipitate). Bar graph shows quantitative analysis of ARC expression. I-R, ischemia-reperfusion, SPIRO, spironolactone, EPL, eplerenone. # $p < 0.05$ vs sham I-R; * $p < 0.05$ vs I-R alone.

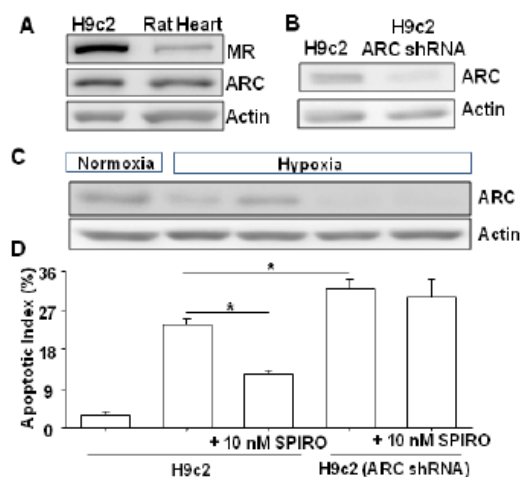


Figure S5. Direct regulation of ARC by low dose spironolactone during simulated ischemia (hypoxia).

A. Both MR and ARC are expressed in H9c2 cells. **B.** ARC expression was abolished by the ARC shRNA construct compared with non-transfected (B) or scrambled shRNA transfected cells (data not shown). **C.** ARC protein expression in normoxic and hypoxic H9c2 cells was determined by western blotting using Actin as the loading control. ARC levels decreased during hypoxia and were restored by low dose spironolactone in H9c2 cells. **D.** Quantification of the apoptotic index during simulated ischemia by TUNEL staining. Low dose spironolactone reversed the effects of simulated ischemia in H9c2 cells with intact ARC levels but not in knockdown cells. MR, mineralocorticoid receptor, ARC, Apoptosis Repressor with a Caspase recruitment domain, SPIRO, spironolactone. Representative gel of three experiments and values expressed as mean \pm SE. * $p < 0.05$ vs hypoxia alone.

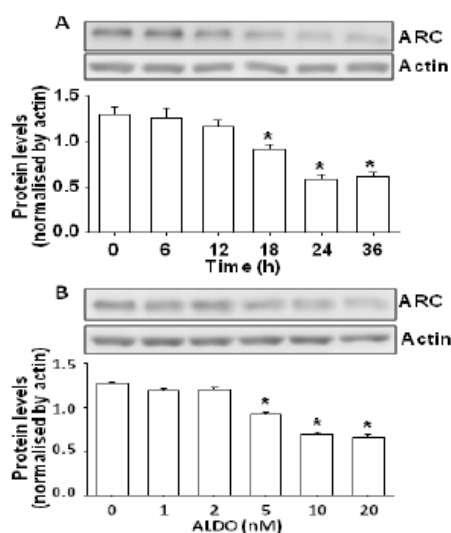


Figure S6: Effect of aldosterone exposure time and dose on ARC expression in H9c2 cells

A. Time course for regulation of ARC expression by 10 nM aldosterone. Processing quantified by densitometry and Actin used to control for loading. Values expressed as mean \pm SE, * $p < 0.05$ vs control ($t=0$). **B.** Varying doses of aldosterone on ARC expression in H9c2 cells. Experiments were performed in triplicate.

The studies presented above demonstrate that ARC is abundant in heart tissue and decreases during I-R injury. Perfusion with low dose MR antagonists (SPIRO 10 nM or EPL 100 nM) restored ARC expression (Figure 3 & S4 in the manuscript). The next aim was to determine the mechanism by which the regulation of ARC stability by MR activation may occur. Interaction of ARC with other proteins causes proteosomal degradation and decreases protein stability (Foo et al., 2007a; Nam et al., 2007b). The hypothesis therefore was that MR may interact with ARC and *in situ* Proximity Ligation Assay (PLA) was used to examine this hypothesis.

Supplemental method: *In situ* Proximity Ligation Assay

Proximity Ligation Assay is a highly specific method for detecting protein-protein interaction in fixed cells or tissue sections using a complementary pair of oligonucleotide-labeled secondary antibodies (PLA probes), which generate a signal only when the two probes hybridise (Soderberg et al., 2006; Soderberg et al., 2008). In this assay, the two primary antibodies (or two proteins) need to be within 40 nm for a signal to be generated. Each interaction site generates a signal which is visualised as an individual fluorescent spot. The number of spots was used as an indicator of the degree of protein-protein or MR-ARC interaction.

The PLA was performed according to the manufacturer's instructions (Duolink II Fluorescence, OLINK Bioscience), using antibodies against MR and ARC. Sections (5 μ m) from reperfused hearts were deparaffinised, rehydrated and subjected to antigen retrieval using the protocol described in Chapter 2 (section 2.5.1). Primary antibodies against MR (MR1-18 1D5, mouse, provided by Prof Celso Gomez-Sanchez) and ARC

(rabbit, Cayman Chemical) were diluted in 1% (w/v) BSA in TBS/T diluent (1:20 and 1:50 respectively) and incubated with sections in a humidified chamber overnight at 4°C. Following three washes in TBS/T, sections were incubated with PLA PLUS anti-mouse and PLA MINUS anti-rabbit probes for 1 hour at 37°C in a humidified chamber. After that, sections were washed in wash buffer A twice for 5 minutes each and exposed to ligation solution for 30 minutes at 37°C. Sections were washed in wash buffer A and incubated with amplification-polymerase solution for 100 minutes at 37°C. The amplification-polymerase solution was then removed, sections washed in wash buffer B and dried at room temperature in the dark. Finally, slides were mounted with Duolink mounting media with DAPI. Negative controls were performed by omitting one of the two primary antibodies. Sections were analyzed using confocal fluorescence microscope (Leica SP5) with a 63x oil objective.

Supplemental result: MR-ARC interact based on *in situ* PLA

Previous studies demonstrated a close correlation between the protein-protein interactions identified by co-immunoprecipitation studies and the *in situ* PLA method (Greenberg et al., 2008; Salmon et al., 2012). Using tissue sections, the interaction between MR and ARC was confirmed in uninjured myocardium (Sham, Figure 6.1, red fluorescent spots). Complex formation is primarily extra-nuclear/cytoplasmic; however, staining patterns do not indicate any specific sub-cellular organelle. This MR-ARC interaction was decreased during myocardial I-R injury (I-R, Figure 6.1), which may be due to the degradation of ARC in these samples (Figure 3 & S4, manuscript), or due to changes in the conformation of MR by oxidative stress during I-R injury. Consistent with SPIRO salvaging ARC levels during I-R injury (Figure 3 and S4) the MR-ARC

complex formation was restored to levels in the sham control by treatment with low dose SPIRO (Figure 6.1). In this case MR-ARC interactions appeared more in the nucleus, although the majority were still cytoplasmic in nature. To our knowledge, these results are the first to show complex formation between MR and ARC proteins within the myocardium.

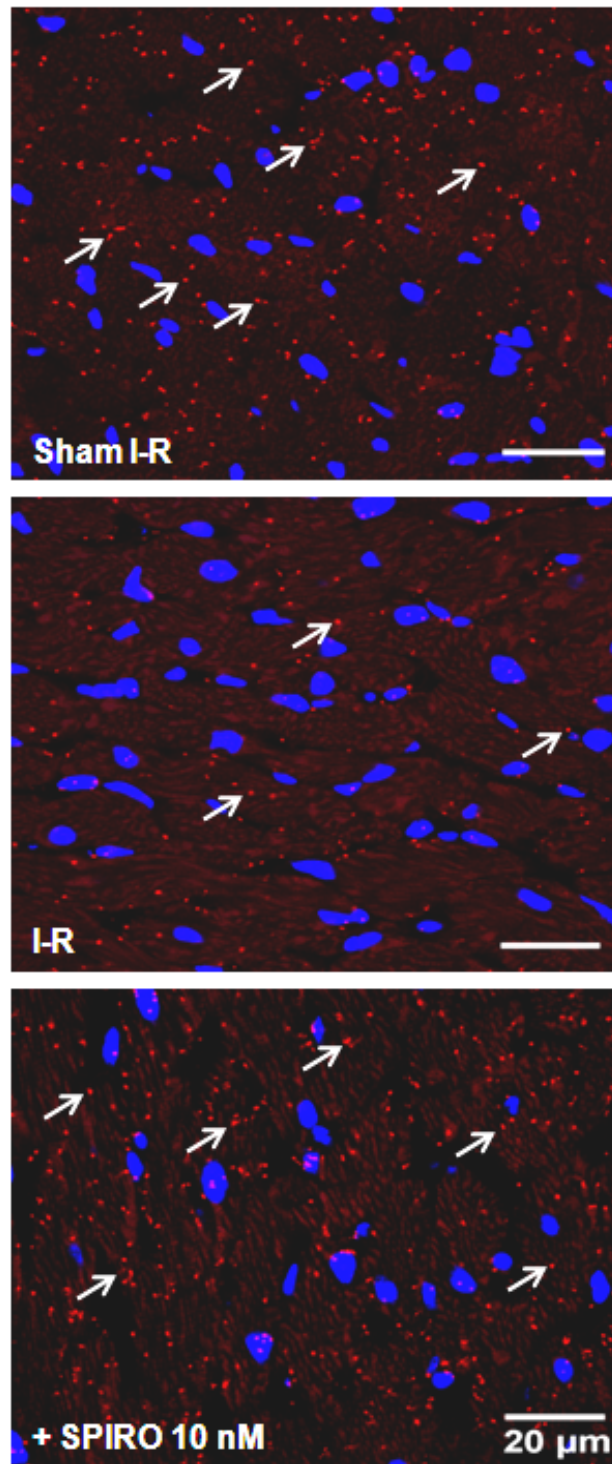


Figure 6.1: Interaction of MR-ARC by *in situ* PLA during myocardial I-R.

Sections of reperfused myocardium were stained with MR and ARC antibodies. Red fluorescent spots (arrows) indicate MR-ARC direct interaction. Nuclei were counterstained with DAPI (blue).

Supplemental discussion

As shown in these studies, there is regulation of ARC by MR agonists and antagonists (Figure 4 and S5, manuscript). ARC is a tissue specific anti-apoptotic repressor protein involved in the intrinsic and extrinsic death pathways. Previous studies have demonstrated direct interaction of ARC with FADD, Fas and Bax which are key to this inhibition (Nam et al., 2004). Similarly, MR-mediated signal transduction requires interactions with multiple protein coregulators, including PGC-1 α , FLASH, RIP140, NF- κ B (summarised in Yang and Fuller, 2012). However, the exact mechanisms and structural basis of the interaction between ARC and MR has not been characterised in such detail.

The key to regulation of ARC expression during MI may be the expression and/or activity of the ubiquitin ligase MDM2 (Foo et al., 2007a). Interestingly, MR activation by aldosterone, induces MDM2 expression, leading to proliferation of human vascular smooth muscle cells (Nakamura et al., 2006) and as shown in the current studies, degradation of ARC (Figure 4, manuscript). MDM2 is also the ligase for p53, controlling both ubiquitination and degradation of p53 (Foo et al., 2007a). MR activation also regulates p53, a transcriptional regulator of the pro-apoptotic protein Bax (McCullers and Herman, 1998). The mechanism by which the regulation of ARC stability by MR during I-R may involve modulation of the ARC/MDM2/p53 signalling pathway or oxidative stress-mediated ARC degradation pathway have yet to be completely defined. Further studies are required for examining the interaction between MR and ARC.

Chapter 7

Other actions of blockade of mineralocorticoid receptors during myocardial infarction

7.1 Introduction

Reperfusion of ischaemic hearts also induces free radical generation, activation of early stress responses in addition to apoptosis (Gottlieb, 2011; Yellon and Hausenloy, 2007), which contribute to the ventricular dysfunction and increased infarct area. In the previous chapter, the mechanism for reduced cardiac damage by treatment with low-dose MR antagonists was shown to involve prevention of mitochondrial apoptotic signaling which led to reduced cardiomyocyte apoptosis during myocardial infarction (MI). One of the triggers for cardiomyocyte apoptosis during MI is increased oxidative stress and depletion of endogenous antioxidants (Kim et al., 2006b; Qin et al., 2007; von Harsdorf et al., 1999).

Oxidative stress is one of the critical mechanisms contributing to ventricular dysfunction following MI (Doerries et al., 2007; Looi et al., 2008; Qin et al., 2007). During MI, the myocardial content of oxidised glutathione (GSSG) is increased, whereas levels of reduced glutathione (GSH) reduced, leading to decreased GSH/GSSG ratio in heart tissue (Hill and Singal, 1996; Lesnefsky et al., 1989; Verbunt et al., 1995). These changes in redox balance are primarily due to an increase in ROS in the myocyte during I-R; in particular, nicotinamide adenine dinucleotide phosphate (NADPH) derived superoxide generation (Talukder et al., 2013). In cardiomyocytes mitochondrial metabolism is the major regulator of the ROS production. Peroxisome proliferator activated receptor (PPAR)- γ coactivator (PGC)-1 α and PGC-1 β are key regulators of mitochondrial biogenesis, oxidative metabolism and ROS generation (Garnier et al., 2003; Huss and Kelly, 2005), with MI suppressing expression of PGC-1 α mRNA reported (Sun et al., 2007).

The imbalance between oxidant and antioxidant triggers a range of physiological, pathological and adaptive responses which ultimately modulate transcriptional outputs and influence cellular processes. I-R injury triggers increased expression number of transcription factors, including heat shock proteins (Hsp27, Hsp40, Hsp70, Hsp72, Hsp90) (Das et al., 1998; Maulik et al., 1993; Nishizawa et al., 1999; Plumier et al., 1996; Schoeniger et al., 1994) and immediate-early genes (*c-fos*, *Egr-1*, *c-jun*, *jun-B*) (Brand et al., 1992; Xu et al., 2008). Heat shock proteins (Hsp) are group of chaperones which protect cells against a variety of stresses including I-R injury (Benjamin and McMillan, 1998; Efthymiou et al., 2004).

In previous studies from our laboratory, activation of MR by aldosterone aggravates the extent of cardiac damage during MI (Mihailidou et al., 2009) and this was prevented by both the free radical scavenger tempol and MR blockade, suggesting a role for myocardial oxidative stress and MR regulation during MI. Indeed MR antagonists (spironolactone or eplerenone) showed attenuation of $O_2^{\bullet-}$ and NADPH oxidase levels in rats with heart failure after MI (Noda et al., 2012; Sartorio et al., 2007) which correlated with improved ventricular function (Noda et al., 2012). Interestingly, even at low levels of aldosterone, increase in oxidative stress or redox imbalance enhances MR signal transduction (Matsui et al., 2008a; Nagase et al., 2012; Rossier et al., 2008), with a ligand-independent pathway of MR activation suggested (Shibata et al., 2008). Cultured rat cardiomyocytes (H9c2), treated with buthionine sulfoximine (BSO), an inhibitor of glutathione synthesis, to simulate increased oxidative stress showed activation of reactive oxygen species (ROS) and Rac1, a small G-protein in the Rho family and regulatory component of the plasma membrane NADPH oxidases

(Lambeth, 2004). This, in turn, resulted in MR activation, indicated by enhanced transcriptional activity and nuclear accumulation (Nagase et al., 2012). Therefore, MR is both a regulator and subject to regulation by oxidative stress in the heart. Therefore the hypothesis tested in this chapter was that reduction of infarct area below basal level by treatment with low-dose MR antagonists involves modulating of redox balance and response or interaction with co-repressors and co-activators which have yet to be completely defined.

7.2 Methods

7.2.1 Protocol for collection of left ventricular tissue following *ex vivo* myocardial I-R

Male Sprague-Dawley rats were used for these studies and experimental details for *ex vivo* I-R of the rat heart are described in Chapter 2 (section 2.2). MR antagonist, spironolactone (SPIRO, 10 nM) was perfused for 15 minutes prior to inducing ischaemia and continued during reperfusion. Since I-R induced ROS peak within the first 15 minutes of reperfusion (Kutala et al., 2006; Petrosillo et al., 2003), left ventricular (LV) free wall tissue was collected after 15 minutes of reperfusion (unless otherwise specified), and snap frozen for measuring free radicals and other biochemical markers.

7.2.2 Measurement of myocardial glutathione levels

Left ventricular free wall tissue collected 15 minutes after reperfusion was homogenised and samples prepared for estimation of oxidised glutathione (GSSG)-to-reduced glutathione (GSH) GSSG:GSH ratio as per the manufacturer's instructions (Cayman

Chemical, GSH Assay Kit, cat# 703002). Tissue was homogenized 1:10 (w/v) in MES buffer, containing 2-(Nnorpholino) ethanesulphonic acid, phosphate, and EDTA. The homogenate was centrifuged twice at 10,000xg for 15 min at 4°C. Supernatant was removed and de-proteinated using meta-phosphoric acid at (5% (w/v) final concentration) and stored at -20°C until assayed (within 6 months). Myocardial concentrations of GSSG and total glutathione (GSSG and GSH) were estimated using the glutathione reductase/5,5'-dithiobis-(2-nitrobenzoic acid) recycling assay. Before analysis, triethanolamine was added to supernatant (final concentration 200 mM) and pH adjusted to pH 7.0. GSSG was measured by derivatizing GSH with 2-vinylpyridine (final concentration of 10 mM) during 60 minutes incubation at room temperature. The assay was quantified using a Synergy Multi-Mode Microplate Reader (BioTek). The absorbance was recorded at 405 nm at 5 minute intervals for 30 minutes. Concentration of GSH was calculated by subtracting oxidized (GSSG) from total (GSH + GSSG) concentrations.

7.2.3 Measurement of I-R triggered superoxide production

Superoxide levels in reperfused myocardium were measured using lucigenin-enhanced chemiluminescence (Noda et al., 2012; Peshavariya et al., 2007). Left ventricular free wall tissue was homogenized in Krebs-HEPES buffer [NaCl (130 mM), KCl (5 mM), MgCl₂ (1 mM), CaCl₂ (1.5 mM), K₂HPO₄ (1 mM), Glucose (11 mM) and HEPES (20 mM), pH 7.4] in a 1:10 (w/v) ratio. NADPH (100 µM) as a substrate, and lucigenin (5 µM) were added to homogenates for chemiluminescence measurements. After stabilisation (10 minutes), the homogenates were transferred into a 96 well OptiView plates (PerkinElmer, Inc.) and the chemiluminescence measured by a Veritas Microplate

Luminometer (Turner Biosystems, Inc.). Samples from each treatment group were assayed in triplicate and the photon emissions were recorded every 30 seconds for up to 10 minutes. Background chemiluminescence in Krebs-HEPES buffer (containing lucigenin and NADPH) was measured in the absence of homogenates and subtracted from the average of 20 readings.

7.2.4 Measurement of myocardial nicotinamide adenine dinucleotide (NAD⁺)

Concentration of NAD⁺ was measured by EnzyChrom NAD⁺/NADH assay (BioAssay Systems, cat# ECND-100), according to manufacturer instruction. Approximately 20 mg tissue was homogenized with 100 μ L NAD extraction buffer, incubated at 60°C for 5 minutes before addition of 20 μ L assay buffer and 100 μ L of the NADH extraction buffer to neutralize the extracts. The homogenate was centrifuged twice at 14,000 \times g for 5 minutes. Supernatant was removed and assayed using the Synergy Multi-Mode Microplate Reader (BioTek). The absorbance was recorded immediately (for optical density at time “zero”, OD_{0min}) at 565 nm and after 15 minutes incubation at room temperature (OD_{15min}). The Δ OD values for standard and sample were calculated by subtracting OD_{0min} from OD_{15min} and used to determine concentration of NAD⁺ in the sample from the standard curve.

7.2.5 Dose-response for BSO \pm SPIRO in H9c2 cells

Rat cardiomyoblast, H9c2 cells were used for these studies. Experimental details for routine cell culture and passage of H9c2 cells are described in Chapter 2 (sections 2.7.1 – 2.7.2). L-Buthionine-(*S,R*)-sulfoximine (BSO), a selective inhibitor of γ -

glutamylcysteine synthetase, was used to induce oxidative stress by depleting GSH. The H9c2 cells were seeded into 60 mm culture plates at a density of $\sim 8 \times 10^5$ cells and serum-deprived overnight. The effective dose (EC_{50}) of BSO was determined by dose-response studies for BSO (0.2 - 1000 μM) for 24 hours prior to harvest. In separate experiments, H9c2 cells were pre-incubated with 10 nM SPIRO for 30 minutes prior to addition of BSO (10 - 1000 μM) and harvested after 24 hours. Following treatment, glutathione levels were measured as described in section 7.2.6.

7.2.6 Measurement of glutathione and superoxide levels in H9c2 cells

Cellular glutathione content was measured using the same Glutathione assay kit listed in section 7.2.2. Following treatment, H9c2 cells were washed twice with PBS and collected in 300 μL of MES buffer. The homogenate was then sonicated and centrifuged at 10,000 $\times g$ for 15 minutes at 4°C. Supernatant was removed, de-proteinated and assayed as described above (section 7.2.2).

Superoxide generation in H9c2 cells was measured using lucigenin-enhanced chemiluminescence, as previously described (Laskowski et al., 2006; Peshavariya et al., 2007). H9c2 cells were seeded into 6-well plates at a density of $\sim 4 \times 10^5$ cells/well, serum-deprived overnight. Cells were then treated with SPIRO (10 & 100 nM) or Tempol (100 μM), either alone or in combination with BSO (5 μM). For co-administration, SPIRO or Tempol was incubated for 30 minutes before BSO addition and harvested after 24 hours. Stimulated cells were collected in Krebs-HEPES buffer [130 mM NaCl, 5 mM KCl, 1 mM MgCl_2 , 1.5 mM CaCl_2 , 1 mM K_2HPO_4 , 11 mM Glucose and 20 mM HEPES, pH 7.4, with 1 mg/mL bovine serum albumin (BSA)]

containing NADPH (100 μ M) and lucigenin (5 μ M) for chemiluminescence measurements. The cell suspensions were transferred into a 96 well OptiView plates (PerkinElmer, Inc.) and measured using a Veritas Microplate Luminometer (Turner Biosystems, Inc.). Samples from each treatment group were assayed in triplicate and the photon emissions were recorded every 30 seconds over a 10 minutes period. Background chemiluminescence in buffer containing lucigenin and NADPH was measured in the absence of cells and subtracted from the average of 20 readings.

7.2.7 qRT-PCR: rat heart tissue and H9c2 cells

Following treatment, total RNA was extracted from rat heart tissue and H9c2 cells using TRIzol lysis reagent (Sigma-Aldrich) according to the protocol provided by the manufacturer and described in Chapter 2 (sections 2.6.1 and 2.7.5). The concentration and purity of the samples were assessed using a NanoDrop ND-1000 spectrophotometer (Thermo Scientific). The cDNA was synthesized from 2.5 μ g total RNA using the Superscript III First-Strand Synthesis System and oligo (dT)₂₀ as a primer (Invitrogen) according to the manufacturer's protocols (see section 2.6.4 for more details). Gene expression was analyzed using TaqMan Gene Expression Assays (Applied Biosystems) as described in Chapter 5 (section 5.2.7). The rat specific assays used were: *c-fos* [Rn02396759_m1], *glucose-6-phosphate dehydrogenase (G6pd)* [Rn00566576_m1], *heat shock protein (Hsp)-27* [Rn00583001_g1], *Hsp40* [Rn01426952_g1], *PGC-1 α* [Rn00580241_m1], *PGC-1 β* [Rn00598552_m1], *PAI-1* [Rn01481341_m1] and *Sgk-1* [Rn00570285_m1]. The endogenous control was *glyceraldehyde-3-phosphate dehydrogenase (Gapdh)* [Rn99999916_s1]. The Delta-Delta Comparative Threshold ($\Delta\Delta$ CT) method was used to quantify the relative fold change between the samples.

Data was analysed using RQ Manager Analysis software, version 1.2.1 (Applied Biosystems).

7.2.8 Western blots: rat heart tissue and H9c2 cells

Total protein was extracted from rat heart tissues and H9c2 cells as described in Chapter 2 (sections 2.5.2 and 2.7.3) and similarly for western blot procedures described in Chapter 2 (section 2.5.3). The primary antibodies were Hsp25/27 (Cayman Chemical, Cat # 12215), Hsp40 (Cell Signaling, cat# 4868), Hsp90 (Cayman Chemical, cat# 19615), c-fos (Abcam, cat# ab7963) and rMR 1-18 1D5 (kindly provided by Prof. Gomez-Sanchez). Antibody binding was detected using HRP-conjugated secondary antibodies (1:3000, Dako Cytomation). Membranes were exposed to chemiluminescent substrate (Perkin Elmer, Melbourne, Australia) and digital images of the resulting bands captured on a LAS4000 (GE Healthcare Life Sciences).

7.2.9 Statistical analysis

Statistical analyses methods similar to those described in Chapter 2 (section 2.8) were used.

7.3 Results

7.3.1 Low-dose SPIRO restores redox balance during I-R

To determine whether the cardioprotective effects of low-dose SPIRO are associated with a reduction in oxidative stress in the reperfused myocardium, both pro-oxidant and antioxidant parameters were measured (Figure 7.1 & 7.2).

SPIRO decreases pro-oxidant superoxide: A burst of ROS generation, in particular superoxide, occurs during the first minutes after reperfusion of ischemic tissue. NADPH oxidase is the major source of pro-oxidant superoxide in cardiomyocytes (Talukder et al., 2013; Tsai et al., 2012). Our results from the lucigenin-enhanced chemiluminescence assay indicate that NADPH-derived superoxide levels were markedly increased in the LV homogenates from the I-R group compared to sham I-R ($100 \pm 7.1\%$ (Sham) vs $165.5 \pm 9.6\%$ (I-R), $P < 0.001$, Figure 7.1A). Treatment with SPIRO prevented the I-R-induced increase in superoxide levels, reducing the levels to those found in sham hearts (Figure 7.1A, $P < 0.005$).

SPIRO maintains antioxidant defense: Further insight into the mechanism by which SPIRO reduces oxidative stress in reperfused myocardium were discovered from assessing the state of anti-oxidant defense, such as changes in glutathione redox status. Under oxidative stress reduced glutathione (GSH) becomes oxidized to the disulfide-bound form (GSSG). Thus, the ratio of GSH/GSSG decreases as a consequence of GSSG accumulation. The GSH/GSSG ratio in LV homogenates was reduced by $53.7 \pm 7.9\%$ in the I-R hearts compared with the Sham I-R group (Figure 7.1B, $P < 0.005$). Similarly, reperfusion injury also significantly reduced NAD^+ levels ($38.8 \pm 7.2\%$; Figure 7.1C, $P < 0.005$), similar to previous reports (Hsu et al., 2009). The loss of NAD^+ may reflect the loss of reduced glutathione levels in reperfused myocardium (Figure 7.1B). Pre-treatment with SPIRO prevented the I-R-induced reduction in the GSH/GSSG ratio (Figure 7.1B, $P < 0.001$) and the loss of NAD^+ levels (Figure 7.1C, $P < 0.05$) and maintained levels equivalent to those observed in sham I-R hearts.

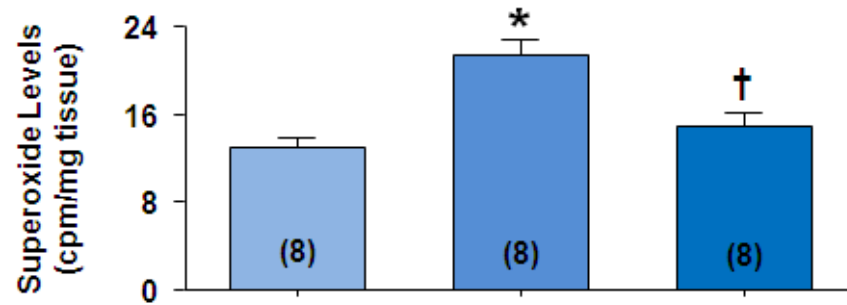
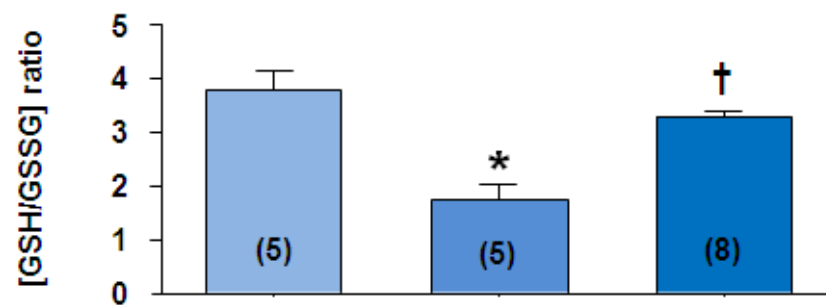
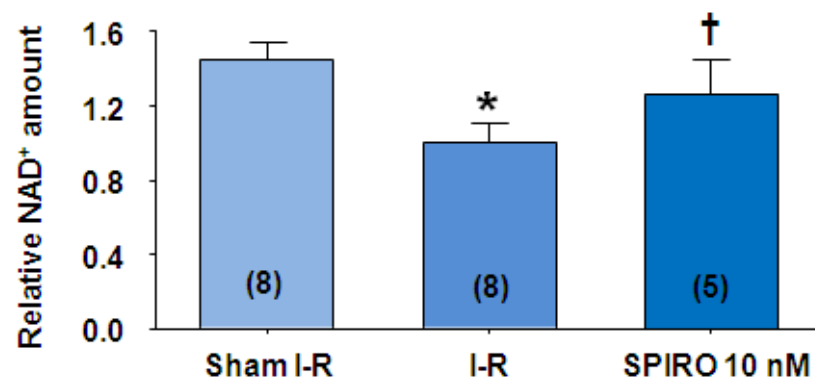
A. NADPH-dependent superoxide generation**B. [GSH/GSSG] ratio****C. NAD⁺**

Figure 7.1: Low-dose SPIRO restores redox balance.

Measurement of (A) superoxide levels, (B) ratio of reduced-to-oxidised glutathione (GSH/GSSG ratio) and (C) NAD⁺ levels in left ventricular free wall homogenates after ischaemia (30 minutes) followed by reperfusion (15 minutes). I-R, ischaemia-reperfusion; SPIRO, spironolactone. Values are means \pm SE; Number in parentheses indicate the number of animals in each group; * P <0.01 vs Sham I-R; † P <0.05 vs I-R.

SPIRO did not modify G6PD gene expression in reperfused myocardium: G6PD is a critical determinant of the intracellular redox state (Leopold et al., 2001). The activity of G6PD has been suggested to be modulated by aldosterone and spironolactone *in vivo* (Leopold et al., 2007). Although, chronic treatment with low-dose SPIRO modulates G6PD activity in kidney nephropathy (Pessoa et al., 2012), we did not observe any changes in G6PD mRNA expression in LV homogenates with neither I-R injury nor SPIRO treatment (Figure 7.2). These data suggest that oxidative stress is rapidly activated in response to reperfusion of ischaemic myocardium, independent of cellular G6PD transcription.

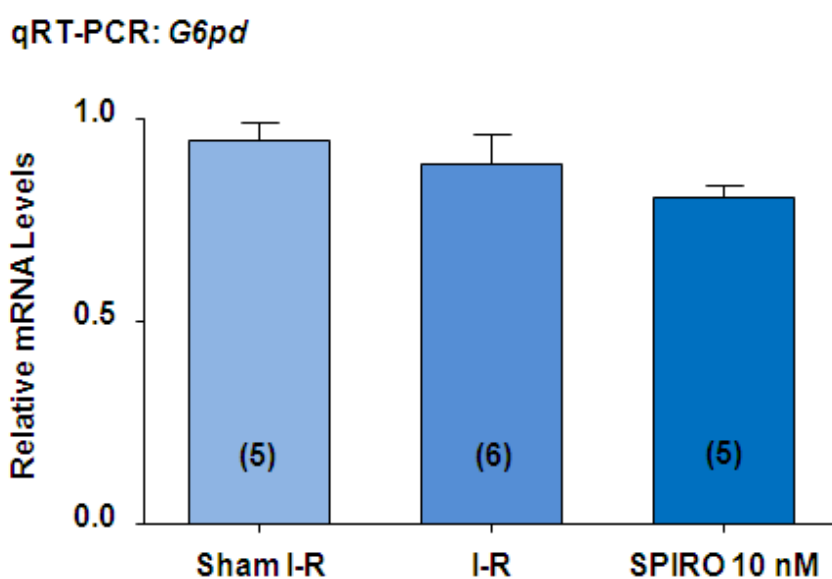


Figure 7.2: Low-dose SPIRO did not modify G6PD gene expression.

mRNA levels of G6PD in left ventricular free wall homogenates of reperfused hearts, analysed by qRT-PCR and normalised by Gapdh level. I-R, ischaemia-reperfusion; SPIRO, spironolactone; G6PD, glucose-6-phosphate dehydrogenase. Values are means \pm SE. Number in parentheses indicate the number of animals in each group.

7.3.2 Low-dose SPIRO restores PGC-1 α and PGC-1 β gene expression

Figure 7.3 shows the mRNA expression of the genes involved in the regulation of mitochondrial biogenesis. PGC-1 α , and its homolog PGC-1 β , with a significant reduction during I-R injury, $39.5 \pm 11.2\%$ and $37.9 \pm 8.6\%$ respectively (Figure 7.3, $P < 0.02$). Perfusion with low-dose SPIRO prevented the loss of PGC-1 α and PGC-1 β mRNA expression in reperfused hearts (Figure 7.3, $P < 0.05$). These alterations are consistent with the increased superoxide generation and reduction in antioxidant enzymes of the infarcted myocardium (Figure 7.1).

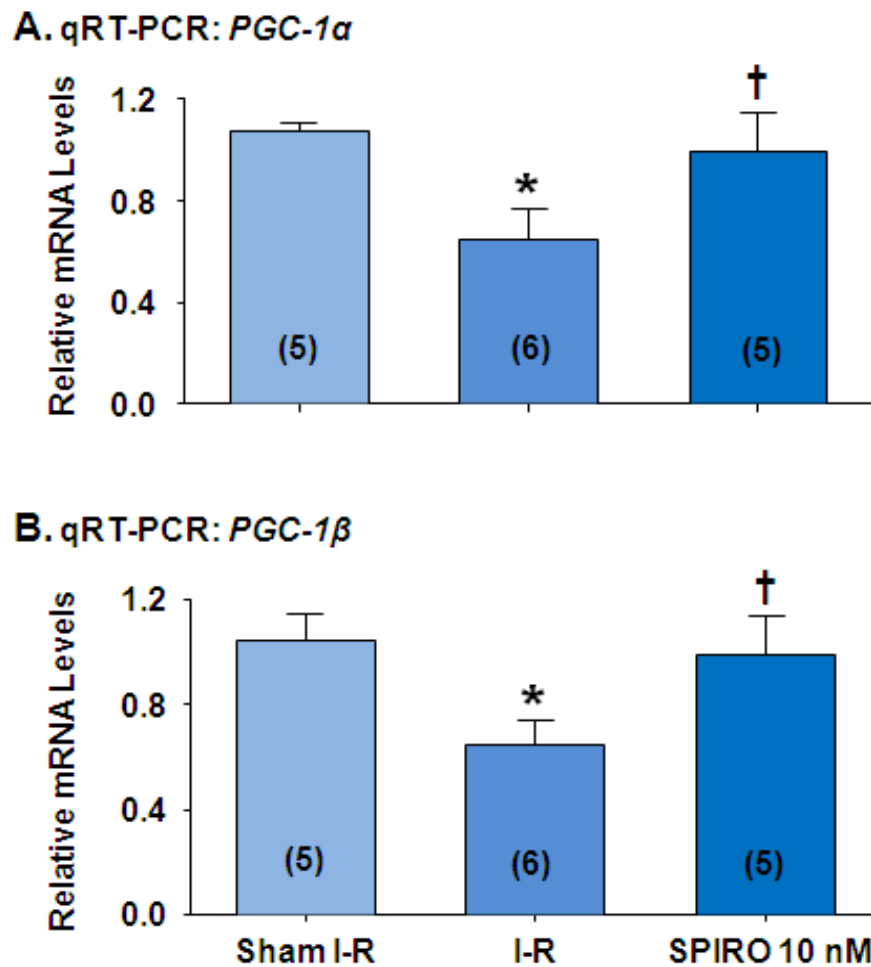


Figure 7.3: Low-dose SPIRO restores PGC-1 α and PGC-1 β gene expression.

mRNA expression of genes involved in mitochondrial biogenesis and ROS production in reperfused hearts. Relative mRNA levels of (A) PGC-1 α and (B) PGC-1 β in left ventricular free wall homogenates analysed by qRT-PCR and normalized by Gapdh level. I-R, ischaemia-reperfusion; SPIRO, spironolactone; PGC-1, peroxisome proliferator-activated receptor- γ coactivator 1. Values are means \pm SE; Number in parentheses indicate the number of animals in each group; * P <0.02 vs Sham I-R; † P <0.05 vs I-R.

7.3.3 Low dose SPIRO prevents the onset of the immediate early gene response in the myocardium after I-R injury

In response to oxidative stress during I-R, heat shock proteins (Hsp) and immediate early response genes are activated (Brand et al., 1992; Webster et al., 1994). We examined the expression of Hsp27, Hsp40, Hsp90 and c-fos mRNA (qRT-PCR) and protein (western blot). qRT-PCR results demonstrated that mRNA of Hsp27, Hsp40 and c-fos were up-regulated in response to I-R injury (2.54 ± 0.32 , 3.02 ± 0.40 and 3.18 ± 0.26 fold changed, respectively; Figure 7.4 A-C, $P < 0.05$, *bar graphs*). Treatment with low-dose SPIRO attenuated the enhanced transcription of these immediate early genes in response to I-R-injury (Figure 7.4 A-C, $P < 0.05$, *bar graphs*). Similarly to qRT-PCR results, the expression of Hsp27, Hsp40 and c-fos encoding protein was significantly up-regulated during I-R and reduced by low-dose SPIRO (Figure 7.4A-C, *immunoblots*). Although, Hsp90 was not examined at transcriptional level, protein levels were markedly up-regulated in response to I-R and SPIRO attenuated this expression (Figure 7.4D). The findings of Hsp and c-fos correlated with changes in oxidative stress early after I-R (Figure 7.1). Taken together, these data implicate Hsp and c-fos rapidly being activated in response to I-R-induced myocardial stress and redox imbalance. Treatment with low-dose (10 nM) SPIRO prior to inducing ischaemia efficiently attenuates oxidative stress and thus, represses immediate genes and their encoding proteins expression in this model.

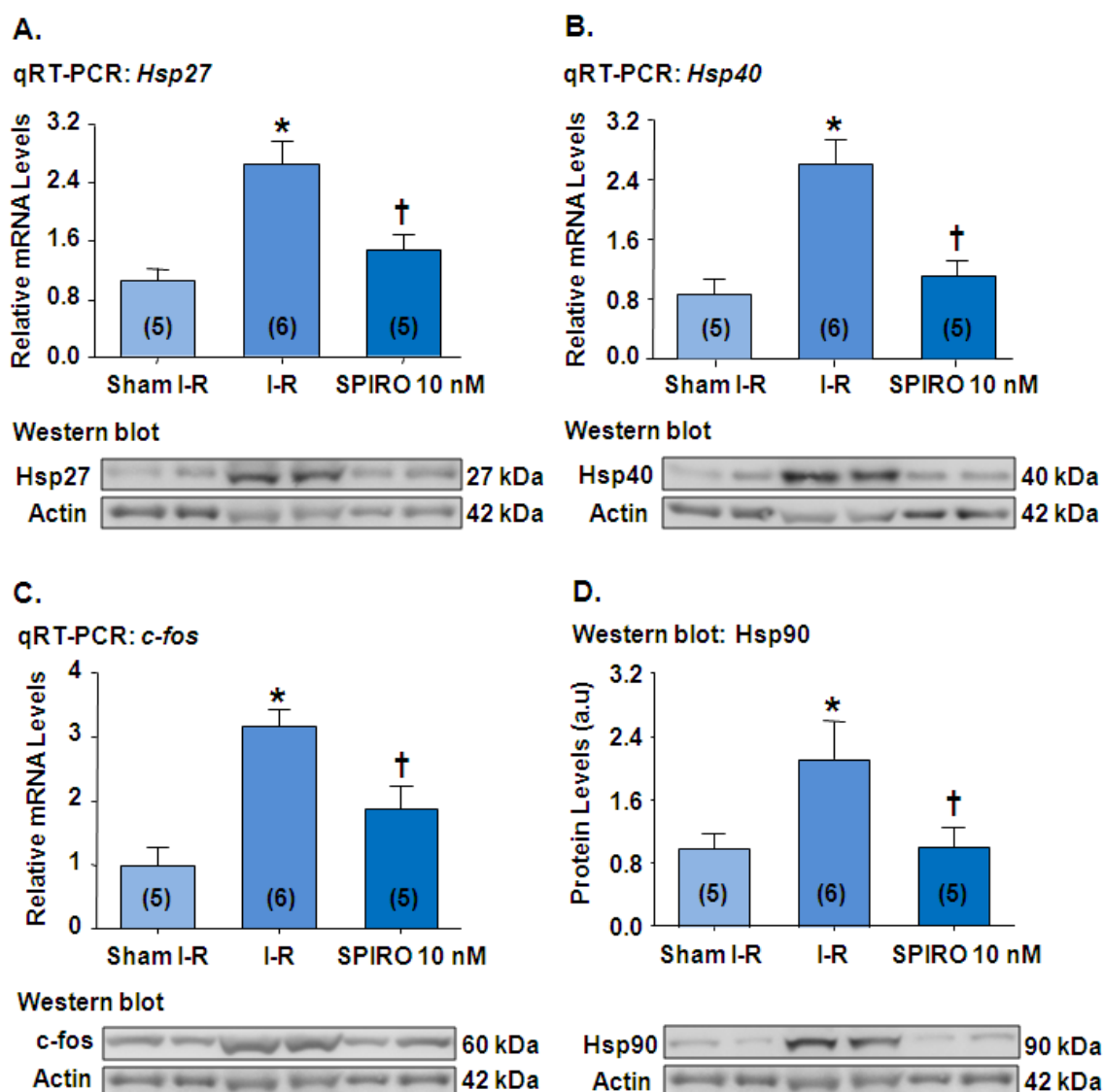


Figure 7.4: Low-dose SPIRO reduces heat shock proteins and immediate early genes and proteins expression.

Top: (A-C) Bar graphs show mRNA expression by qRT-PCR, normalised by Gapdh.

Below: (A-C) Immunoblots of Hsp27, Hsp40, c-fos in left ventricular free wall homogenates. (D) Protein expression of Hsp90 by western blot. I-R, ischaemia-reperfusion; SPIRO, spironolactone; Hsp, heat shock protein. Values are means \pm SE; Number in parentheses indicate the number of animals in each group; * P <0.05 vs Sham I-R; † P <0.05 vs I-R.

7.3.4 Low-dose SPIRO prevents I-R induced MR activation

Sgk-1 and PAI-1 expression in the reperfused myocardium was investigated to determine the role of MR in reperfusion injury-induced oxidative stress (Figure 7.5). Sgk-1 and PAI-1 are MR-targeted transcripts and have been used as an index of MR activation (Latouche et al., 2010). mRNA levels of Sgk-1 and PAI-1 were significantly higher in the I-R hearts compared with sham I-R hearts (1.45 ± 0.08 and 2.17 ± 0.31 fold change, respectively; Figure 7.5A&B, $P < 0.02$), and treatment with low-dose SPIRO attenuated this up-regulation of Sgk-1 (Figure 7.5A&B, $P < 0.05$). The up-regulation of Sgk-1 and PAI-1 activity correlate with increased oxidative stress during I-R (Figure 7.1). These data collectively imply that MR is activated during I-R injury, and that part of the cardioprotective effects of low-dose SPIRO is via preventing oxidative stress, and the associated responses, in the reperfused myocardium. To determine whether I-R induced changes in the level of MR protein, the same lysates from reperfused hearts were immunoblotted for MR protein (Figure 7.5C). There was no modification in protein levels between I-R alone and antagonist-exposed hearts suggesting that MR blockade reduces oxidative stress through mechanisms that involve modulation of MR transcriptional activity but not changes in levels of MR protein nor MR protein synthesis.

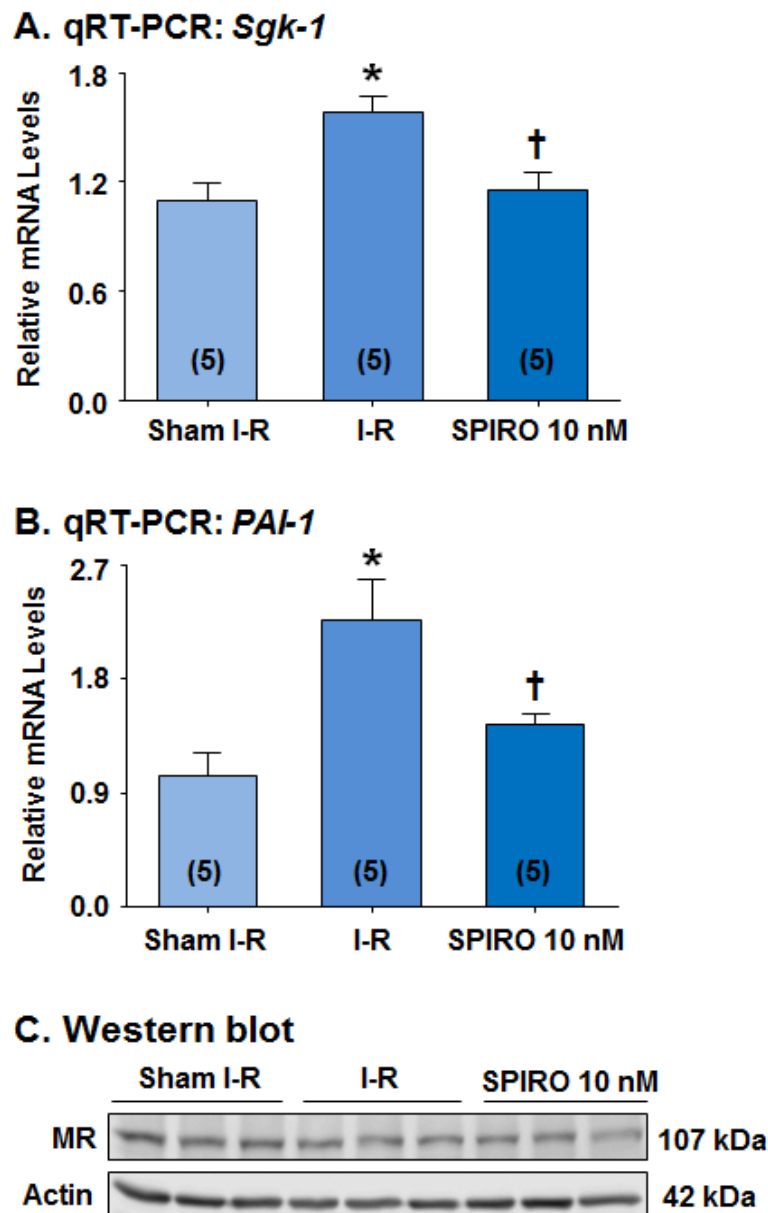


Figure 7.5: Low-dose SPIRO suppresses transcription of MR-responsive genes during I-R.

mRNA expression of *Sgk1* (A) & *PAI-1* (B) by qRT-PCR, normalised by *Gapdh*. (C) MR protein expression by western blot. I-R, ischaemia-reperfusion; SPIRO, spironolactone; *Sgk-1*, serum/glucocorticoid regulated kinase 1; *PAI-1*, plasminogen activator inhibitor-1. Values are means \pm SE; Number in parentheses indicate the number of animals in each group; * $P < 0.02$ vs Sham I-R; † $P < 0.05$ vs I-R.

7.3.5 BSO induced oxidant stress in H9c2 cells

The above results indicate blockade of MR with low-dose SPIRO exhibits antioxidant effects. To further characterise the protective effects of low-dose SPIRO we decided to normalise the oxidant stress to examine whether pathways other than salvage of cellular redox mechanisms were involved in the cardioprotective effects of low-dose SPIRO. Cellular redox state was altered by using BSO, an inhibitor of glutathione synthesis. Dose-response studies in H9c2 cells showed that BSO concentrations above 5 μM significantly decreased GSH levels after 24 hour incubation, with complete depletion of GSH at $[\text{BSO}] \geq 20 \mu\text{M}$ (Figure 7.6). We found that 5 μM BSO depleted GSH levels by $\sim 50\%$ *in vitro* (Figure 7.6), which similar to the reduced levels observed with I-R injury in our *ex vivo* heart model (Figure 7.1B). Consistent with the reduction in glutathione levels, BSO (5 μM) increased ROS production (1.67 ± 0.14 fold change, Figure 7.7, $P < 0.001$), as assessed by NADPH-derived superoxide generation in H9c2 cells. These data indicate that the pro-oxidant effects of the *ex vivo* model could be simulated using BSO *in vitro*.

To determine the concentration of BSO to normalize the anti-oxidant effects of SPIRO we repeated the studies this time in the presence of 10 nM SPIRO (Figure 7.6). Exposure of H9c2 cells to 10 μM BSO for 24 hours in the presence of SPIRO depleted GSH to approximately the same extent as without SPIRO ($\sim 84\%$ decrease, Figure 7.6) indicating the anti-oxidant effects of SPIRO treatment had been normalised by this concentration of BSO. However, we found that the anti-oxidant effects of SPIRO (10 or 100 nM) were quite potent when used on H9c2 cells treated with 5 μM BSO (Figure 7.7), being equivalent to 100 μM tempol (a radical scavenger). These results confirm

the findings with *ex vivo* studies of rat hearts (Figure 7.1). Treatment with SPIRO (10 or 100 nM) or Tempol (100 μ M) alone had no effect on superoxide generation in H9c2 cells (Figure 7.7). Since the pro-oxidant effects of 5 μ M BSO were readily antagonised by 10 nM SPIRO we used an increased concentration of 20 μ M BSO to determine whether the protective effects of SPIRO were independent of anti-oxidant activity as this concentration of BSO removes the anti-oxidant activity of SPIRO.

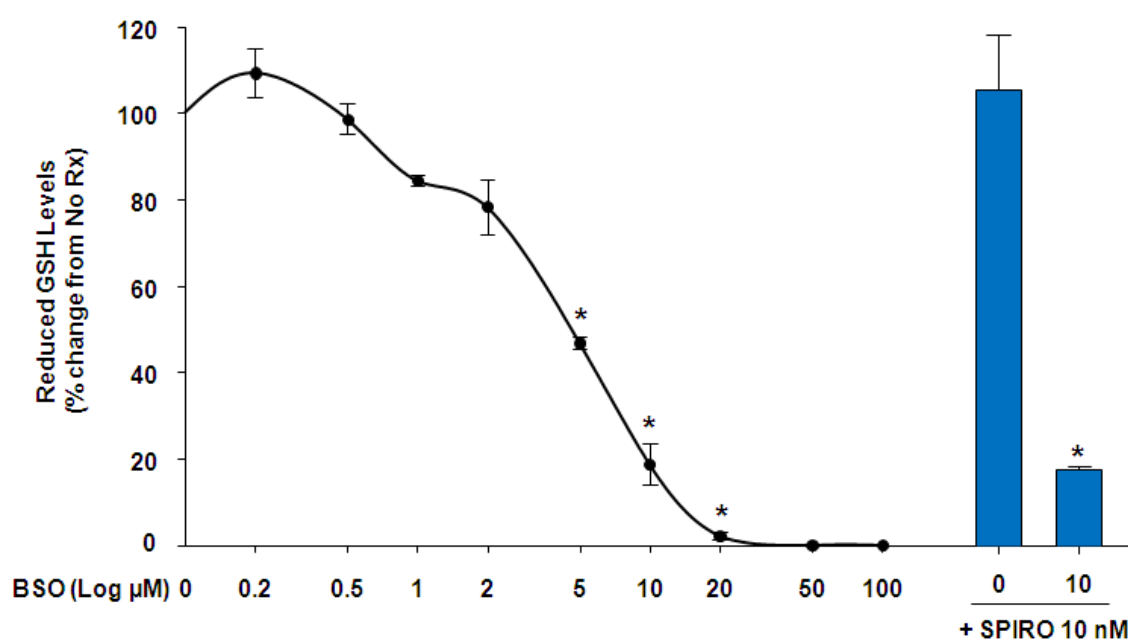


Figure 7.6: Effects of BSO \pm SPIRO (10 nM) exposure on reduced glutathione (GSH) levels in H9c2 cells.

Left: Varying doses of BSO exposure (24 hours) on reduced GSH levels. *Right:* Effects of BSO in the presence of SPIRO (10 nM) on reduced GSH levels. BSO, buthionine sulfoximine; SPIRO, spironolactone. Values expressed as means \pm SE from two independent experiments; * P <0.05 vs No Rx.

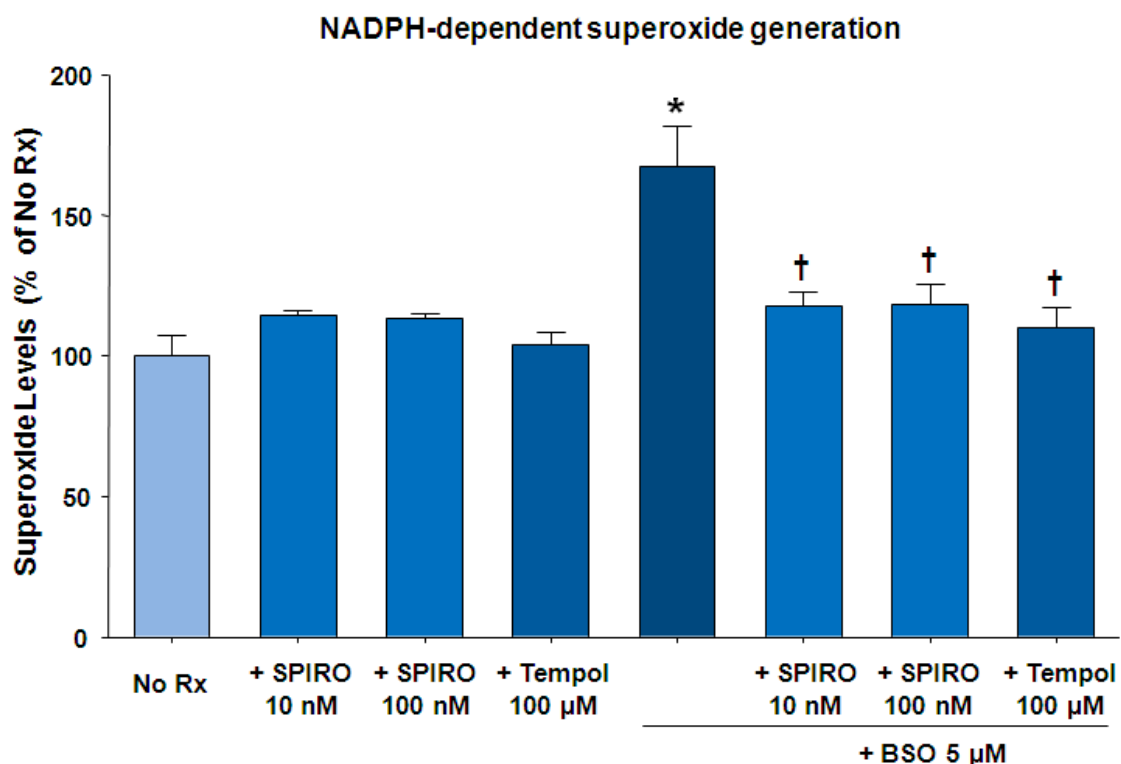


Figure 7.7: Low-dose SPIRO prevents BSO-induced superoxide generation in H9c2 cells.

Superoxide levels in H9c2 cells after exposure to BSO (5 μM) ± SPIRO (10 or 100 nM) or Tempol (100 μM) for 24 hours. BSO, buthionine sulfoximine; SPIRO, spironolactone. Values expressed as means ± SE from five independent experiments; * $P < 0.05$ vs No Rx; † $P < 0.05$ vs BSO 5 μM.

7.3.6 Effects of BSO on SPIRO action in H9c2 cells

The findings with both *ex vivo* (rat hearts) and *in vitro* (H9c2) models indicate that oxidative stress causes MR activation in the absence of ligands. To evaluate whether oxidant stress modulates the action of low-dose SPIRO, we measured mRNA and protein expression of Hsp27, Hsp40, c-fos, PGC-1 α and PGC-1 β . Exposure of H9c2 cells to 20 μ M BSO maintained oxidative stress (indicated by GSH depletion) even in the presence of SPIRO (Figure 7.6). Treatment with BSO (20 μ M) induced up-regulation of the immediate early response genes Hsp27, Hsp40 and c-fos (1.28 ± 0.10 , 1.27 ± 0.04 and 1.42 ± 0.08 fold change, respectively, Figure 7.8). BSO (20 μ M) also induced MR activation, as indicated by increase in Sgk-1 and PAI-1 transcripts (1.59 ± 0.18 and 1.21 ± 0.04 fold change, respectively, Figure 7.8). These increases was prevented by addition of SPIRO (10 nM) even though the anti-oxidant effects had been removed (Figure 7.9). Contrary to the data in heart tissue (Figure 7.3), treatment with BSO up-regulated expression of PGC-1 α and PGC-1 β (1.48 ± 0.09 and 1.64 ± 0.19 fold, respectively), which was reversed with low-dose SPIRO (Figure 7.9). This could be due to the direct effect of oxidative stress alone; however, irrespective of the change (Figure 7.3 & 7.8), SPIRO ablated these changes of PGC-1 α and PGC-1 β (Figure 7.3 & 7.9). Indeed, the change in MR-mediated transcription was, on average, 59.9% of the values obtained with BSO alone (Figure 7.9). These data indicate that only 40% of the protective effect of SPIRO is derived from the anti-oxidant effects and ~60% from other sources, such as direct genomic effects of MR as a transcription factor or possibly through GPR30 activation (See chapter 5).

The changes in gene transcription were also mirrored at the protein level. Treatment with BSO (20 μ M) elevated expression of the proteins encoding for immediate early response genes Hsp27, Hsp40, Hsp90 and c-fos (1.21 ± 0.04 , 1.17 ± 0.06 , 1.24 ± 0.08 and 1.38 ± 0.06 fold change, respectively; Figure 7.10). The inclusion of 10 nM SPIRO ablated the induction by BSO and returned expression of all proteins to levels observed in untreated controls (Figure 7.10). Thus, the effects of SPIRO on protein expression were more complete than that observed on transcription (on average only 60% decrease). This indicates that during oxidative stress the protein and transcriptional control of these proteins may become unlinked; however, SPIRO blockade of MR activation appears to target both aspects of control to bring about normalisation of the myocardial response to reperfusion injury.

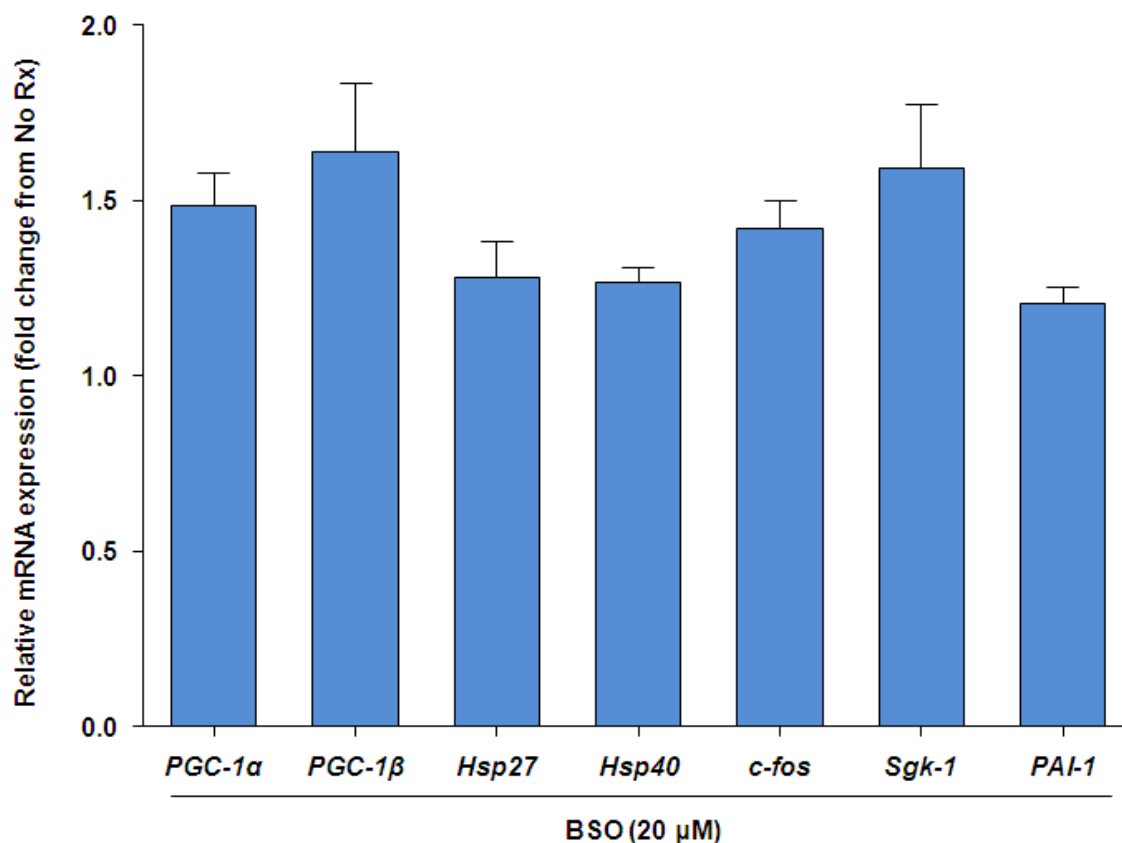


Figure 7.8: BSO-induced various genes expression in H9c2 cells.

mRNA expression of PGC-1 α , PGC-1 β , Hsp27, Hsp40, c-fos, Sgk-1 and PAI-1 in H9c2 cells after stimulation with BSO (20 μ M), analyzed by qRT-PCR and normalised by Gapdh. Bar graphs showing the fold increase of gene expression with [BSO (20 μ M)] treatment compared to No treatment. BSO, buthionine sulfoximine; PGC-1, peroxisome proliferator-activated receptor- γ coactivator-1; Hsp; heat shock protein; Sgk-1, serum/glucocorticoid regulated kinase 1; PAI-1, plasminogen activator inhibitor-1. Values expressed as means \pm SE from five independent experiments.

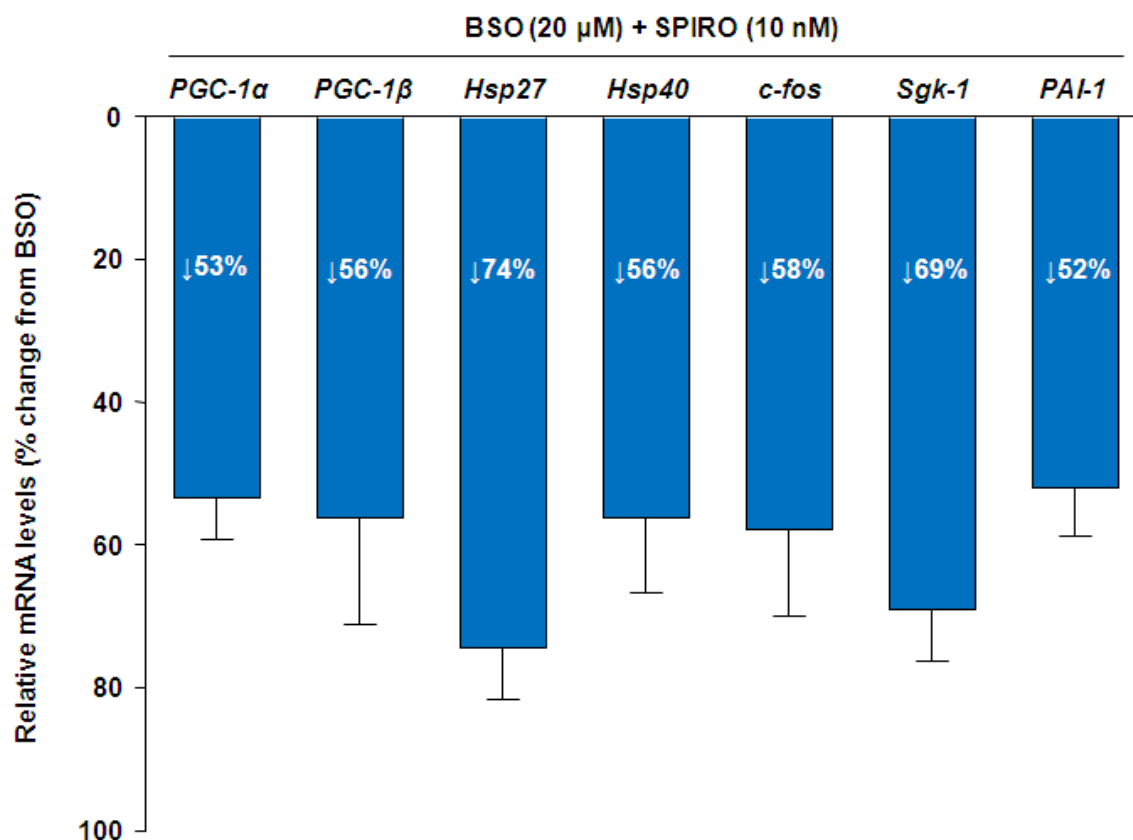


Figure 7.9: Low-dose SPIRO reduces BSO-induced various genes expression in H9c2 cells.

mRNA expression of PGC-1 α , PGC-1 β , Hsp27, Hsp40, c-fos, Sgk-1 and PAI-1 in H9c2 cells after stimulation with BSO (20 μ M) + SP (10 nM), analyzed by qRT-PCR and normalised by Gapdh. Values from [BSO (20 μ M)] and [BSO (20 μ M) + SPIRO (10 nM)] groups were subtracted from [No treatment] group before analysis. Bar graphs showing the percentage reduction of gene expression with [BSO (20 μ M) + SPIRO (10 nM)] treatment compared to BSO (20 μ M) alone. BSO, buthionine sulfoximine; SPIRO, spironolactone; PGC-1, peroxisome proliferator-activated receptor- γ coactivator-1; Hsp; heat shock protein; Sgk-1, serum/glucocorticoid regulated kinase 1; PAI-1, plasminogen activator inhibitor-1. Values expressed as mean \pm SE from five independent experiments.

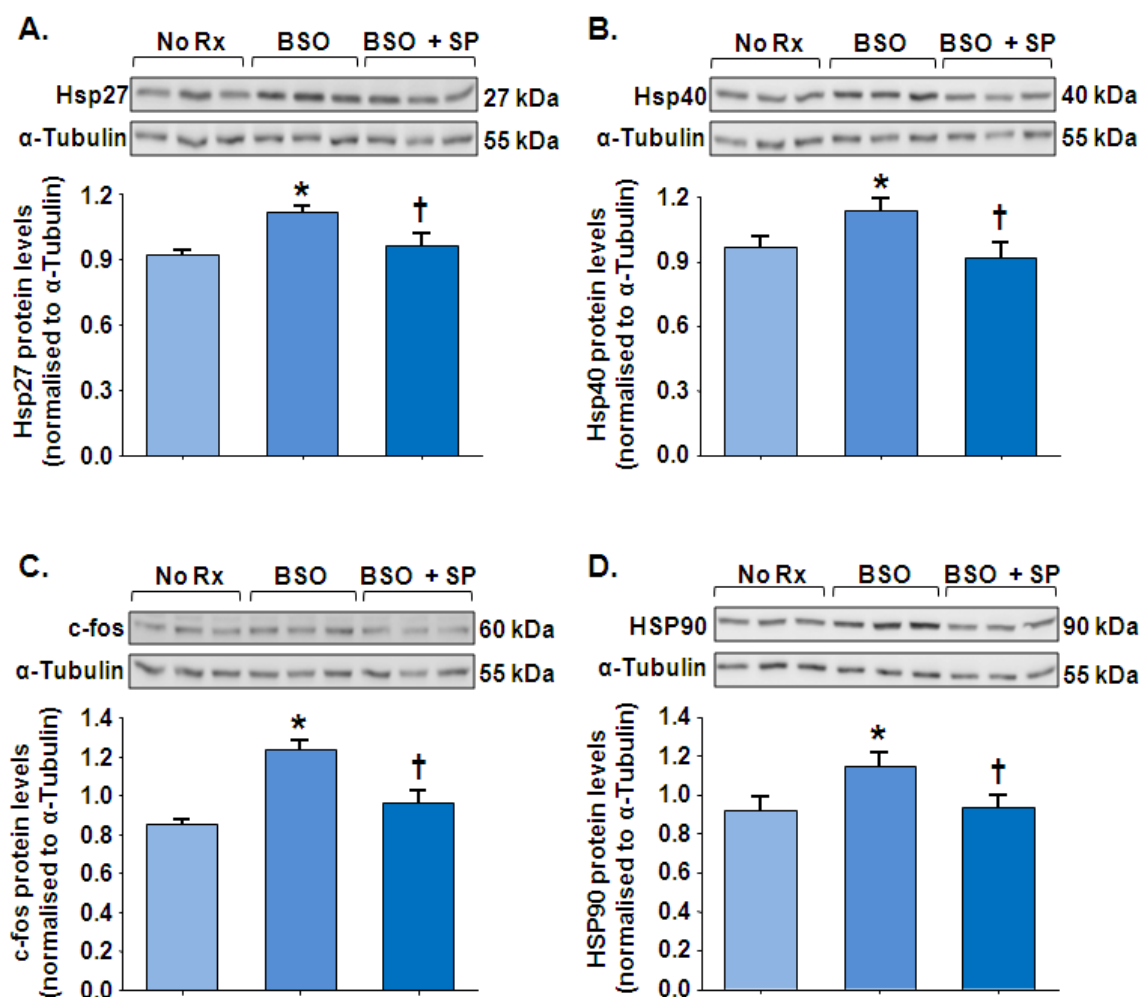


Figure 7.10: Low-dose SPIRO reduces BSO-induced stress responsive protein expression in H9c2 cells.

Protein expression of (A) Hsp27, (B) Hsp40, (C) c-fos and (D) Hsp90 in H9c2 cells after stimulation with BSO (20 μ M) \pm SP (10 nM). *Top*: Representative immunoblots of Hsp27, Hsp40, Hsp90 and c-fos of various treatment groups. *Below*: Bar graphs showing densitometric analysis of protein changes. Values expressed as means \pm SE from five independent experiments. BSO, buthionine sulfoximine; SPIRO, spironolactone; Hsp, heat shock protein. * $P < 0.05$ vs No Rx; † $P < 0.05$ vs BSO.

7.3.7 Low-dose SPIRO regulates MR genomic signaling

The mechanism by which low-dose SPIRO modulates oxidative stress is not known. We have shown that MR blockade with SPIRO modifies oxidant stress (Figure 7.1 & 7.7) and transcription of a number of genes during the myocardial response to reperfusion injury (Figure 7.3-7.5 & 7.9). To link the observed changes in transcription with low-dose SPIRO to the observed regulation of oxidative stress (Figure 7.1) we added actinomycin D (1 μ M) to the perfusate to prevent transcription in response to MR activation. Sgk-1 and PAI-1 mRNA expression were analysed by qRT-PCR from total RNA. Actinomycin D suppressed the induction of Sgk-1 and PAI-1 by reperfusion injury (Figure 7.11), indicating the transcription in response to MR activation had been ablated. The inhibition by actinomycin D was more complete than that of SPIRO alone (combination group, Figure 7.11), suggesting pathways other than MR also regulate these genes. However, under these experimental conditions it is clear that the genomic response to MR activation in these hearts was clearly prevented.

When we examined the levels of cardiac damage following I-R, perfusion of rat hearts with low-dose (10 nM) SPIRO significantly reduced infarct size (Figure 7.12). However, contrary to transcriptional data, actinomycin D did not reverse the protection (reduction in infarct size) established by low-dose SPIRO treatment (Figure 7.12). These data indicate that low-dose SPIRO modifies oxidative stress and cardiac damage through a largely non-genomic signaling pathway. This conclusion is of course tempered by the fact that the inhibition of all gene transcription with actinomycin D may also suppress signalling pathways that occur during I-R that induce detrimental effects.

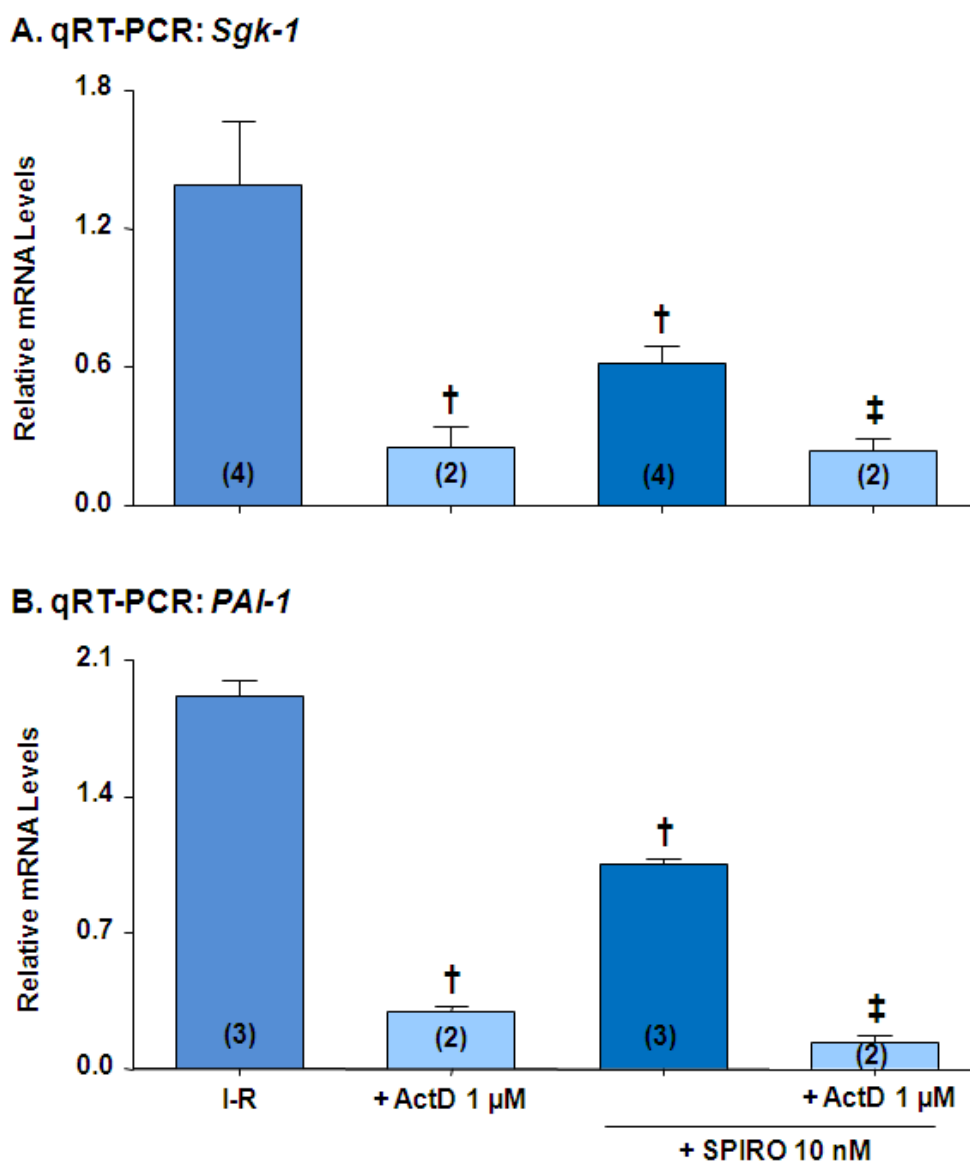


Figure 7.11: Low-dose SPIRO regulates MR genomic signaling.

Transcription inhibitor, actinomycin D (1 μM) perfused 15 minutes prior to SPIRO (10 nM) addition. mRNA expression of (A) *Sgk-1* and (B) *PAI-1* by qRT-PCR, normalized by *Gapdh*. I-R, ischaemia-reperfusion; ActD, actinomycin D; SPIRO, spironolactone; *Sgk-1*, serum/glucocorticoid regulated kinase 1; *PAI-1*, plasminogen activator inhibitor-1. Values are means ± SE; Number in parentheses indicate the number of animals in each group; † $P < 0.05$ vs I-R; ‡ $P < 0.05$ vs SPIRO 10 nM.

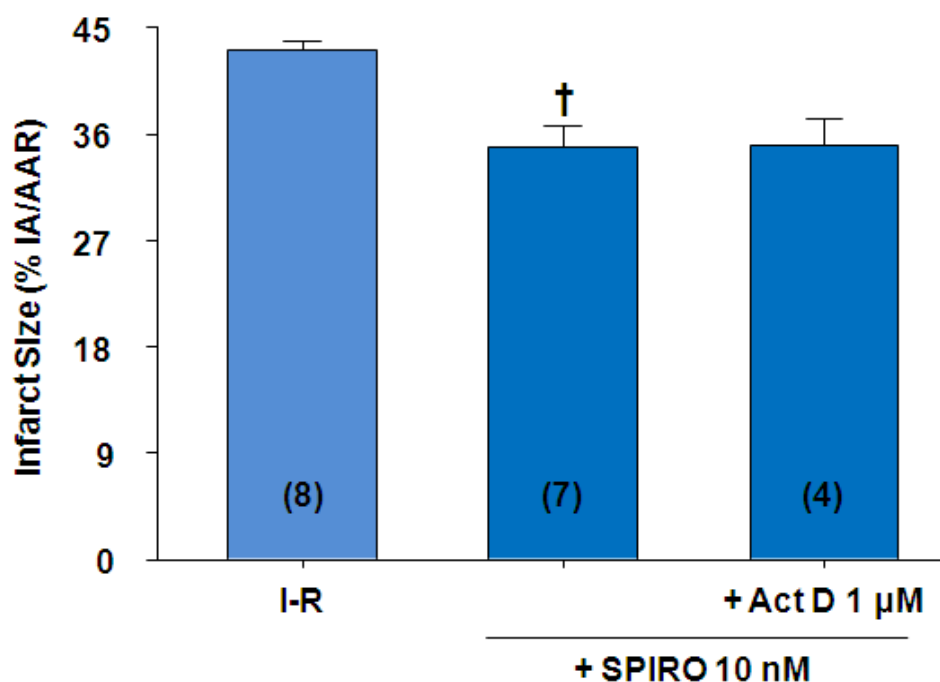


Figure 7.12: Low-dose SPIRO reduces infarct size and persists in the presence of actinomycin D.

Isolated hearts were subjected to regional ischemia (30 minutes) followed by reperfusion (150 minutes). Actinomycin D (1 μM) perfused 15 minutes prior to SPIRO (10 nM) addition and maintained throughout I-R. At the completion of reperfusion, infarct size measured and expressed as the percentage of infarct area (IA) relative to area-at-risk (AAR). I-R, ischaemia-reperfusion; ActD, actinomycin D; SPIRO, spironolactone. Values are means ± SE; Number in parentheses indicate the number of animals in each group; † $P < 0.05$ vs I-R.

7.4 Discussion

Oxidative stress and ROS formation are key cellular events in myocardial reperfusion injury (Raedschelders et al., 2012). Similar to previous reports (Ferrari et al., 1990; Hsu et al., 2009; Singh et al., 1989), we found redox imbalance is an early event during reperfusion of ischemic hearts (Figure 7.1). Perfusion of isolated rat hearts with low-dose SPIRO (10 nM), prior to ischaemia, significantly reduced oxidative stress and maintained redox balance (Figure 7.1). I-R injury also up-regulates expression of immediate-early genes and their encoded proteins (Figure 7.4) (Brand et al., 1992; Plumier et al., 1996). However, no reports have linked MR blockade to the expression of these genes and associated proteins during myocardial I-R injury. Our study showed low-dose (10 nM) SPIRO prevents the up-regulation of immediate-early gene transcription by oxidant stress in both *ex vivo* (Figure 7.4) and *in vitro* (Figure 7.9 & 7.10) models.

The effects of MR antagonism on oxidative stress have been previously studied in animal models of increased tissue renin-angiotension system (RAS) activation and elevated aldosterone levels (Ren2 rats) (Lastra et al., 2008), in diabetic hypertensive rats (Pessoa et al., 2012) and myocardial infarction (Sartorio et al., 2007). These studies examined the chronic impact of MR blockade and found that both low-dose (0.24 mg/day) SPIRO and high-dose (100 mg/kg/d) eplerenone reduce NADPH oxidase activity and superoxide generation (Lastra et al., 2008; Sartorio et al., 2007). Similarly, chronic treatment with SPIRO (50 mg/kg/d) for eight weeks reduces NADPH-mediated superoxide generation, maintains glutathione redox balance and increases of G6PD activity in diabetic nephropathy tissue (Pessoa et al., 2012). No studies have examined

the direct effects of low-dose MR blockade on vascular oxidative stress in the early phase post-MI. Our results are novel and show low-dose (10 nM) SPIRO, in the absence of other steroids, modifies oxidative stress by attenuating NADPH-mediated superoxide generation, reducing NAD^+ levels and restoring redox balance (GSH/GSSG ratio) during reperfusion injury (Figure 7.1). Contrary to previous studies that have shown SPIRO enhances G6PD activity in aorta tissue (Leopold et al., 2007) and in diabetic nephropathy (Pessoa et al., 2012), we did not observe any changes with G6PD transcripts neither during I-R nor with SPIRO treatment (Figure 7.2). This could be due to differences in experimental conditions and tissue-specific effects of G6PD. Other reason may be that SPIRO regulated activity of G6PD (Leopold et al., 2007; Pessoa et al., 2012) but did not alter its transcription expression as shown in our current studies.

The mechanisms by which treatment with SPIRO restores redox balance are not fully identified, however, it likely involves the restoration of key regulators of mitochondrial biogenesis such as PGC-1 α and PGC-1 β and ROS generation. Levels of PGC-1 α and PGC-1 β are usually highly expressed in tissues with abundant mitochondria and oxidative metabolism, such as the heart and believed to contribute significantly to maintaining baseline mitochondrial and cardiac contractile function in congestive heart failure (Garnier et al., 2003) and pressure overload hypertrophy (Riehle et al., 2011). Acute MI substantially decreases expression of PGC-1 α mRNA (Chen et al., 2012b; Sun et al., 2007). Similarly, we found mRNA levels of PGC-1 α and PGC-1 β rapidly decrease in reperfused myocardial tissue which was prevented with low-dose SPIRO treatment (Figure 7.3). Our finding is of interest in that low-dose SPIRO can reverse the process through an up-regulation of PGC-1 α and PGC-1 β expression very rapidly

during MI and have not been previously examined. Our results imply that SPIRO directly modulates PGC-1 α and PGC-1 β expression, reducing ROS formation and oxidative stress through a mitochondrial pathway. This correlates with our findings in the previous chapter, in which, low-dose SPIRO also prevents apoptosis by inhibiting mitochondrial apoptotic pathway (see chapter 6). Furthermore, MR blockade with SPIRO may impact on the modulation of oxidative stress because PGC-1 α and PGC-1 β are coactivators of MR (Knutti et al., 2000). Additional studies are required to clarify the role of MR coactivators PGC-1 α and -1 β interact with oxidative stress during MI.

Expression of immediate-early genes, and their encoded proteins, play important roles in regulating cell survival or death through activating/inhibiting inflammation and apoptosis after MI (Dybdahl et al., 2005; Efthymiou et al., 2004; Schenkel et al., 2010; Zhang et al., 2013). Immediate redox-sensitive genes are rapidly activated in response to oxidative stress-induced by I-R. Similar to previous reports (Nelson et al., 2002; Plumier et al., 1996; Zhang et al., 2013), we found I-R injury significantly increased expression of Hsp and c-fos genes, which translated to increased protein levels; in particular Hsp27, Hsp40, Hsp90 and c-fos. Interestingly, Hsp40 and Hsp90 are co-chaperones for MR and also involved in regulation of ROS production and apoptosis (Chen et al., 2011; Lanneau et al., 2008) while Hsp27 has multiple actions, including protection against I-R injury by regulating redox state and mitochondrial-mediated apoptosis (Arrigo, 2001; Efthymiou et al., 2004; Tan et al., 2009). Similarly, c-fos is a key transcriptional factor involved in regulation of apoptosis or cell survival in MI (Gidh-Jain et al., 1998; Preston et al., 1996; Zhang et al., 2013). MR antagonism, with low-dose SPIRO, inhibited the effect of oxidative stress on expression of these redox-

sensitive genes (Figure 7.4). This effect of low-dose SPIRO are maintained under high oxidant stress-induced by BSO (Figure 7.9 & 7.10), confirming MR blockade directly modulates these redox-sensitive molecules. To our knowledge, no reports have shown MR to regulate these immediate redox-sensitive genes in association with I-R stress.

We also found up-regulation of MR-responsive transcripts (Sgk-1 and PAI-1) induced by I-R in isolated rat hearts (Figure 7.5) and BSO treatment in H9c2 cells (Figure 7.8). What is interesting about these results is that MR activation occurred in the absence of ligand since these perfusates (heart) or culture media (H9c2 cells) contain no added steroids. MR antagonism with SPIRO blocked the effects of both I-R and BSO suggesting MR activation is mediated by oxidative stress and independent of ligand binding. Our studies, indicating BSO-induced oxidative stress mediates MR activation are supported by previous reports (Nagase et al., 2012). Furthermore, our findings suggest that during tissue damage, such as I-R injury, increased oxidative stress (or accumulation of ROS) activates MR which, in turn, promotes further ROS generation and aggravates tissue damage. Blockade of the receptor with antagonists prevented MR activation and thus reduced ROS formation or damage. In support of this hypothesis MR antagonism with SPIRO alone significantly reduced apoptosis and tissue damage induced by I-R, whereas, the free radical scavenger tempol did not affect apoptosis and infarction (Mihailidou et al., 2009). However, both SPIRO and tempol prevent aldosterone and cortisol aggravated cell death and tissue damage following I-R (Mihailidou et al., 2009), implicating MR signal transduction enhanced by oxidative stress. Taken together, this suggests that the cardioprotective effects of SPIRO involve both a reduction in ROS formation as well as blockade of MR activation.

MR signaling is often linked to the pathogenesis of multiple diseases, including hypertension, inflammation and fibrosis. Interestingly, oxidative stress has numerous regulatory targets in these same processes (including apoptosis). Therefore it is important to further explore the target network of oxidative stress and MR signaling. Our findings in the previous chapter showing that the anti-apoptotic protein ARC is a target of MR regulation and SPIRO prevents activation of mitochondrial (intrinsic) apoptosis signaling pathway during I-R through preservation of ARC expression (chapter 6) is a new target network. ARC degradation is promoted by oxidative stress (Nam et al., 2007) leading to myocyte death (Ekhterae et al., 1999; Nam et al., 2007b; Zhang and Herman, 2006). The exact mechanisms of how low-dose SPIRO prevents loss of ARC during I-R is not known; however, we propose the cardioprotective mechanism by which low-dose MR blockade protects against reperfusion injury is due to both prevention of ROS formation (restoration of redox balance through maintaining mitochondrial biogenesis and preventing MR activation) and direct transcriptional control over myocardial programming. This, in turn, prevents ARC degradation and myocytes apoptosis, leading to reduction in cardiac damage following I-R.

Furthermore, our results indicate an approximately 40% of the protective effect by low-dose SPIRO is derived from the anti-oxidant effects and ~60% from other sources, such as direct genomic effects of MR-mediated transcription (Figure 7.3-7.5, 7.9) or through non-genomic effects (ROS, ERK1/2 activation) manifest through different receptors such as GPR30 (see chapter 5). The genomic response of SPIRO-mediated MR signaling in the *ex vivo* hearts was suppressed by actinomycin D (Figure 7.11).

However, contrary to transcriptional data, actinomycin D did not reverse the protection of low-dose SPIRO treatment on cardiac damage (Figure 7.12), suggesting that low-dose SPIRO protects against reperfusion injury via other pathways than just MR genomic signaling. Previous studies have demonstrated that MR-induced superoxide production by the non-genomic activation of NADPH oxidase and Rac1 in endothelial cells and cardiomyocytes (Iwashima et al., 2008; Nagase et al., 2012). In addition, our results in chapter 5 showed non-genomic effects of aldosterone via a membrane receptor, GPR30, resulting in ERK1/2 phosphorylation and ROS production. Increased ROS production, in turn, induces MR activation and signal transduction. Importantly, we demonstrated that MR genomic signalling is required for mediating cardiac damage during MI (see chapter 5). Taken together, these data indicate that the cardioprotective action of low-dose SPIRO is mediated through the balance of both non-genomic and genomic signaling, by modifying oxidative stress, and controlling transcription and protein synthesis, leading to reduced cardiac damage.

Chapter 8

Summary and future perspectives

Advances in treatment strategies have decreased heart disease; however, it still remains the leading cause of death globally. Myocardial infarction (MI) is the primary contributor to this mortality. Using an experimental model of MI, several novel findings have been reported in this thesis, including gender dependent shift in the balance between autophagy and apoptosis, leading to cardiomyocyte death and aggravated cardiac damage in males compared to age-matched females. Treatment with low dose mineralocorticoid receptor (MR) antagonists significantly reduced cardiac damage following MI. The findings in this thesis identify novel mechanisms of action for low dose MR antagonists during MI by modulating redox balance and immediate early gene transcription, preventing degradation of the anti-apoptotic protein ARC, leading to decreased apoptosis and reduce reperfusion damage. These novel mechanisms may explain the ability of low dose MR antagonists such as spironolactone and eplerenone to reduce mortality observed with clinical studies in patients with heart failure and heart failure post-MI (Pitt et al., 2003; Pitt et al., 1999; Zannad et al., 2011).

Our studies to examine the role of androgens in sex differences in cardiac damage during MI are novel since they have demonstrated for the first time that sex steroids, specifically testosterone, influence the balance between autophagy and apoptosis in the heart. These data imply that endogenous testosterone levels represent a critical risk factor for IHD in adult males and support previous studies (Bener et al., 2013; Papakonstantinou et al., 2013; Tunstall-Pedoe, 1998; Wingard et al., 1983) which show higher death rates due to IHD in men than age-matched women. Thus serum testosterone levels play an important role in the development of coronary heart disease and levels should be monitored. In addition, our results suggest that the severity of IHD

should be judged by different markers in males compared to females. Our data highlight the importance for future development of new therapies that address male and female differences in response to IHD. Moreover, clinical trials should incorporate a higher percentage of female patients so that they become sufficiently powered to determine the gender differences in treatment.

Increasing evidence suggests that hormones such as mineralocorticoids play significant role in regulating the adverse outcomes of MI. As such, elevated serum aldosterone levels have been associated with adverse outcomes following AMI (Beygui et al., 2006; Beygui et al., 2009; Milliez et al., 2005; Napoli et al., 1999; Palmer et al., 2008). Although the mechanisms by which aldosterone promotes adverse outcomes of acute MI have been well documented, the contribution of aldosterone-mediated non-genomic signalling to the enhanced cardiac damage following MI is not known. In chapter 5, we demonstrated that the aggravation of cardiac damage by aldosterone during I-R occurs via activation of a MR-mediated genomic response.

The physiological role of GPR30 in cardiovascular disease is unclear by the fact that multiple ligands activate this receptor. GPR30 is also a membrane-bound oestrogen receptor (Prossnitz et al., 2007; Revankar et al., 2005) with low affinity for oestrogen (10^{-7} M). However, this concentration of oestradiol is higher than any concentration seen *in vivo*; thus, GPR30 cannot be a functional physiological receptor for oestrogen. Female GPR30 knockout mice display elevated blood pressure resulting in the hypothesis that GPR30 mediates the effect on blood pressures (Martensson et al., 2009). However, aldosterone promotes hypertension and the data from the GPR30 mice offer

an interesting concept of the physiological role of GPR30. Control of blood pressure by aldosterone is thought to occur through MR activation by its ligand. Thus, if GPR30 acted as a physiological receptor for extracellular aldosterone this would create an environment where less aldosterone was available for MR activation. In the GPR30 null mice this mechanism would be abolished due to deletion of GPR30, raising free aldosterone levels and resulting essential hypertension as observed in these mice (Martensson et al., 2009). Clearly further experiments are required to validate this hypothesis.

Our results showing treatment with low-dose MR antagonists protects the heart during MI which correlate with the large randomised trials where low levels of MR antagonists added to standard therapy significantly reduced morbidity and mortality in patients with progressive heart failure and heart failure post-MI. What is interesting about these clinical studies is that the cardioprotective action of MR antagonists occurred in the absence of other steroids, with plasma levels of aldosterone in the low-normal physiological range (0.25 – 0.4 nmol/l) (Rousseau et al., 2002) similar to our studies described in chapter 6 & 7. The studies in chapter 6 & 7 of this thesis identified molecular mechanisms of how low-dose MR blockade protect the heart during MI.

Chapter 6 addressed the effects of MR blockade on apoptosis during MI and we discovered a novel mechanism of cardioprotective action of low dose MR antagonists to regulate ARC stability and therefore modulate the initiation/inhibition of apoptosis during myocardial I-R injury. This is a direct effect of MR interacting with the anti-apoptotic protein ARC. Hence when levels of aldosterone are elevated, MR activation

aggravates cardiac damage and faster progression to failure due to degradation of ARC and myocyte loss.

The physiological significance of ARC in MR signalling is unclear, especially in the heart where ARC is expressed predominantly in the cardiomyocytes, while MR is basally occupied by endogenous glucocorticoids in cardiac myocytes, due to the absence of the 11β -HSD2 enzyme. Under normal condition, there is no signalling and MR-ARC complex formation is high. Thus, association with ARC may prevent binding of other MR co-activators or prevent MR translocation to the nucleus. The second hypothesis is that in the SPIRO treatment group, more MR-ARC complexes were observed in the nucleus and this would correlate with inhibition of MR transcriptional activity and nuclear export. It is possible that a change in the conformational of MR through the effects of oxidative stress may promote loss of the binding site for ARC. Thus, the hypothesis is that the high level of ARC expression in cardiac tissue may prevent basal MR signalling providing a novel level of regulation by which the damaging influence of MR activation in the heart is removed; however, further studies are required to examine this hypothesis.

Concurrently in chapter 7, we examined whether treatment with low-dose MR antagonists modify oxidative stress and immediate early gene transcription during MI. In line with effects on apoptosis, perfusion of isolated rat hearts with low-dose (10 nM) spironolactone significantly attenuated activation of immediate transcription factors and maintained redox balance. Importantly, spironolactone prevented the I-R induced activation of PGC-1 α and PGC-1 β , key regulators of mitochondrial biogenesis and ROS

generation. In addition, MR activation was promoted in response to I-R, as indicated by increased expression of Sgk-1 and PAI-1 transcripts, even in the absence of exogenous ligands. These results suggest that MR are activated by oxidative stress or redox imbalance during I-R, and support previous studies (Nagase et al., 2012; Shibata et al., 2008) which indicate a ligand-independent pathway of MR activation. This pathway involves the activation of the NADPH oxidase subunit Rac1 by oxidative stress. The effects of Rac1 on MR are blocked by MR antagonists. Future studies are needed to elucidate the precise mechanisms of how MR is regulated by Rac1 during MI.

Increasing evidence suggests that autophagy plays an important role in controlling cell survival during reperfusion injury. Given apoptosis and oxidative stress (mechanisms activated during I-R) are regulated by aldosterone (see chapter 5), and protected by low-dose MR antagonists treatment (see chapter 6 & 7), it would be important to document whether the protective action of low-dose MR antagonists is also mediated by alteration in autophagy during I-R injury. Currently the effects of MR activation on autophagy during I-R are unexplored.

Although the findings in this thesis have defined the mechanisms for cardioprotective action by low-dose MR antagonists, these studies were performed only in males (chapter 6 & 7). As outlined in chapter 4, there is gender disparity in the modulation of cardiac damage during I-R. Therefore, it is important to examine the mechanisms for low-dose MR blockade in females, to further our understanding of control mechanisms and treatment strategies for IHD in both genders.

Another extension of this thesis will be to examine the cardioprotective mechanism(s) and novel pathways of low-dose MR antagonists using *in vivo* models of MI. First, the *in vivo* MI models may include other steroids or factors in the blood that may alter the efficacy of low-dose MR antagonists. Since the enzyme 11 β -HSD2, which converts cortisol into inactive cortisone is not expressed in cardiomyocytes (Sheppard and Autelitano, 2002), MR are normally occupied by endogenous glucocorticoids (cortisol in human and corticosterone in rodent) which act as MR antagonists (Gomez-Sanchez et al., 1990; Sato and Funder, 1996; Young and Funder, 1996). In tissue damage where there is increased in oxidative stress or ROS formation, cortisol has similar action to aldosterone to aggravate tissue damage (Mihailidou et al., 2009), although the mechanisms have not been defined. Future studies need to investigate the mechanisms for regulation of cortisol action during MI since clinically elevated levels of cortisol have been detected in patients with MI.

An important approach is to determine whether the physiological MR antagonist progesterone and the synthetic progestin/potent MR antagonist drosperinone, as well as, the potent non-steroidal MR antagonists SM-368229 and BAY 94-8862, show protective responses similar to that of spironolactone and eplerenone during MI. Examining the protective mechanism(s) of various MR antagonists offer therapeutic options for the treatment of hypertension, acute myocardial infarction and heart failure.

Overall, the findings from this thesis provide valuable insights into the molecular mechanisms of myocardial I-R injury and beneficial effects of treatment with low-dose MR antagonists during MI. The translation from this work is that guidelines recommend

MR antagonists are administered to patients with heart failure with or without myocardial infarction. Given the novel findings in this thesis, MR antagonists may be extended to other disease states (such as hypertension, obesity and diabetes) where there is increased oxidative stress, decreased ARC protein levels and increased apoptosis.

Appendices

Buffer formulations

Krebs-Henseleit Buffer

- 118.0 mM NaCl
- 4.7 mM KCl
- 1.5 mM CaCl₂.H₂O
- 1.2 mM KH₂PO₄
- 1.6 mM MgSO₄.7H₂O
- 24.9 mM NaHCO₃
- 11.1 mM glucose

10x PBS (Phosphate Buffer Saline)

- NaCl 80 g
- KCl 2 g
- Na₂HPO₄ 14.4 g
- K₂HPO₄ 2.4 g
- Make up to 1 L with milli-Q water
- Check pH 7.6

10X TBS (Tris Buffer Saline)

- Tris Base 24.2 g
- NaCl 80 g
- pH 7.6 with HCl
- Make up to 1 L with milli-Q water

RIPA Buffer

- 50 mM Tris (pH 8.0)
- 150 mM NaCl
- 1% (v/v) TritonX-100
- 1% (w/v) Na deoxycholate
- 0.1% (w/v) sodium dodecyl sulphate (SDS)
- 1 mM phenylmethyl sulfonyl fluoride (PMSF)
- Protease inhibitor cocktail (Roche Applied Science)

2x SDS Loading Buffer

Prepare loading buffer in milli-Q containing the following:

- 125 mM Tris (pH 6.8)
- 4% (w/v) SDS
- 20% (v/v) Glycerol
- 10% (v/v) 2-mercaptoethanol
- 0.01% (w/v) Bromophenol Blue

5x SDS (sodium dodecyl sulphate) Loading Buffer

Prepare loading buffer in milli-Q containing the following:

- 312.5 mM Tris (pH 6.8)
- 10% (w/v) SDS
- 50% (v/v) Glycerol
- 25% (v/v) 2-mercaptoethanol
- 0.05% (w/v) Bromophenol Blue

Tris-Glycine running buffer

- 25 mM Tris
- 192 mM Glycine
- 0.1 % (w/v) SDS
- pH 8.3

Tris-Glycine transfer buffer

- 25 mM Tris
- 192 mM Glycine
- 10 % (v/v) Methanol

TBST Washing Buffer

- 1x TBS
- 0.1% (w/v) Tween-20

Blocking buffer

- 1x TBS
- 0.1% (w/v) Tween-20
- 5% (w/v) non-fat milk powder

Coomassie Blue staining for SDS-PAGE Gels

Prepare staining solution in milli-Q water containing the following:

- 0.25% (w/v) Coomassie Brilliant Blue R250
- 40% (v/v) Methanol
- 10% (v/v) Glacial Acetic Acid

Coomassie Blue destain solution

Prepare destain solution in milli-Q water containing the following:

- 40% (v/v) Methanol
- 10% (v/v) Glacial Acetic Acid

Stripping Buffer (for reprobing western blots)

- 10% SDS 20 ml
- 0.5 M Tris (pH 6.8) 12.5 ml
- β -mecaptoethanol 0.8 ml
- Milli-Q water 67.5 ml
- Incubate membrane at 50°C for up to 45 minutes with some agitation

50x TAE (Tris-acetate)

- Tris Base 242 g
- Glacial acetic acid 57.1 ml
- 0.5 M EDTA (pH 8.0) 100 ml

Table A1: Details of primary antibodies and concentrations used in western blots (WB) and immunohistochemistry (IHC)

Primary Antibody	Manufacturer	Cat #	Dilution (IHC)	Dilution (WB)
α -Tubulin	Santa Cruz Biotechnology	Sc-5286	-	1:1000
Actin	Sigma	A3853	-	1:2000
Acinus p23 (NT)	Santa Cruz Biotechnology	Sc-5430	1:50	-
Acinus (CT)	AnaSpec	53206	1:50	1:500
Annexin V	Abcam	Ab14196	1:50	-
ARC	Cayman Chemical	160737	1:100	1:1000
AR	Santa Cruz Biotechnology	Sc-816	-	1:500
Atg5-Atg12	Sigma-Aldrich	A2859	-	1:1000
Bcl-2	Santa Cruz Biotechnology	Sc-7382	-	1:1000
Bcl-xL	Santa Cruz Biotechnology	Sc-634	-	1:1000
Beclin-1	Cell Signaling	3738	-	1:1000
Caspase-2	Abcam	Ab18737	-	1:500
Caspase-3 (active)	Abcam	Ab2302	1:50	-
Caspase-3	Cell Signaling	9662	-	1:500
Capase-8	Abcam	Ab15552	-	1:200
Caspase-9	Cell Signaling	9506	-	1:500
c-fos	Abcam	Ab7963	1:50	1:1000
Desmin	Abcam	Ab8592	1:50	-
ER α	Santa Cruz Biotechnology	Sc-542	-	1:500
ER β	Santa Cruz Biotechnology	Sc-8974	-	1:500
ERK1/2	Cell Signaling	9102	-	1:1000
Phospho-ERK1/2 (Thr202/Tyr204)	Cell Signaling	9101	-	1:1000

GPR30	Santa Cruz Biotechnology	Sc-48524	-	1:500
HSP25/27	Cayman Chemical	12215	-	1:5000
HSP40	Cell Signaling	4868	-	1:1000
HSP90	Cayman Chemical	19615	-	1:1000
ICAD (CT)	Santa Cruz Biotechnology	Sc-6866	-	-
ICAD (NT)	AnaSpec	28043	-	1:500
LC3A/B	Cell Signaling	4108	-	1:1000
MR	Santa Cruz Biotechnology	Sc-11412	-	1:500
MR1-18 1D5	Prof. Gomez-Sanchez's Lab	-	1:20	1:100
MR1-18 6G1	Prof. Gomez-Sanchez's Lab	-	1:20	1:100
mTOR	Cell Signaling	2972	-	1:500
Phospho-mTOR (Ser2448)	Cell Signaling	2971	-	1:500
RAGE	Abcam	Ab3611	1:100	1:1000
XIAP	Cell Signaling	2042	-	1:500

Table A2: Formulation for sodium dodecyl sulphate (SDS) - separating and stacking gels

Components	Separating gel			Stacking gel
	7 %	10 %	12 %	4 %
30% Acrylamide:bis (29:1)	5.83 mL	8.3 mL	10 mL	1.3 mL
1.5 M Tris, pH 8.8	6.25 mL	6.25 mL	6.25 mL	-
1.0 M Tris, pH 6.8	-	-	-	2.5 mL
10% (w/v) SDS	0.25 mL	0.25 mL	0.25 mL	0.1 mL
MilliQ Water	12.53 mL	10.01 mL	8.36 mL	6.04 mL
10% (w/v) AMPS	125 µL	125 µL	125 µL	50 µL
TEMED	12.5 µL	12.5 µL	12.5 µL	10 µL
Total Volume	25 mL	25 mL	25 mL	10 mL

Bibliography

1. Abdallah Y, Kasseckert SA, Iraqi W, et al. 2011. Interplay between Ca²⁺ cycling and mitochondrial permeability transition pores promotes reperfusion-induced injury of cardiac myocytes. *J Cell Mol Med.* 15:2478-2485.
2. Adamopoulos C, Ahmed A, Fay R, et al. 2009. Timing of eplerenone initiation and outcomes in patients with heart failure after acute myocardial infarction complicated by left ventricular systolic dysfunction: insights from the EPHESUS trial. *Eur J Heart Fail.* 11:1099-1105.
3. Ago T, Kitazono T, Ooboshi H, et al. 2004. Nox4 as the major catalytic component of an endothelial NAD(P)H oxidase. *Circulation.* 109:227-233.
4. Ahokas RA, Sun Y, Bhattacharya SK, et al. 2005. Aldosteronism and a proinflammatory vascular phenotype: role of Mg²⁺, Ca²⁺, and H₂O₂ in peripheral blood mononuclear cells. *Circulation.* 111:51-57.
5. AIHW. 2011. Australian Institute of Health and Welfare 2011. Cardiovascular disease: Australian facts 2011. Cardiovascular disease series. Cat. no. CVD 53. Canberra: AIHW.
6. Akishita M, Hashimoto M, Ohike Y, et al. 2010. Low testosterone level as a predictor of cardiovascular events in Japanese men with coronary risk factors. *Atherosclerosis.* 210:232-236.
7. Albertine KH, Weyrich AS, Ma XL, et al. 1994. Quantification of neutrophil migration following myocardial ischemia and reperfusion in cats and dogs. *J Leukoc Biol.* 55:557-566.
8. Allan CM, Couse JF, Simanainen U, et al. 2010. Estradiol induction of spermatogenesis is mediated via an estrogen receptor- α mechanism involving neuroendocrine activation of follicle-stimulating hormone secretion. *Endocrinology.* 151:2800-2810.
9. Alnemri ES, Livingston DJ, Nicholson DW, et al. 1996. Human ICE/CED-3 protease nomenclature. *Cell.* 87:171.
10. Alvarez RJ, Gips SJ, Moldovan N, et al. 1997. 17 β -estradiol inhibits apoptosis of endothelial cells. *Biochem Biophys Res Commun.* 237:372-381.
11. Alzamora R, Brown LR, and Harvey BJ. 2007. Direct binding and activation of protein kinase C isoforms by aldosterone and 17 β -estradiol. *Mol Endocrinol.* 21:2637-2650.
12. Alzamora R, Marusic ET, Gonzalez M, et al. 2003. Nongenomic effect of aldosterone on Na⁺,K⁺-adenosine triphosphatase in arterial vessels. *Endocrinology.* 144:1266-1272.
13. Alzamora R, Michea L, and Marusic ET. 2000. Role of 11 β -hydroxysteroid dehydrogenase in nongenomic aldosterone effects in human arteries. *Hypertension.* 35:1099-1104.

14. Ambrosio G, Flaherty JT, Duilio C, et al. 1991a. Oxygen radicals generated at reflow induce peroxidation of membrane lipids in reperfused hearts. *J Clin Invest.* 87:2056-2066.
15. Ambrosio G, Zweier JL, and Flaherty JT. 1991b. The relationship between oxygen radical generation and impairment of myocardial energy metabolism following post-ischemic reperfusion. *J Mol Cell Cardiol.* 23:1359-1374.
16. An J, Li P, Li J, et al. 2009. ARC is a critical cardiomyocyte survival switch in doxorubicin cardiotoxicity. *J Mol Med (Berl).* 87:401-410.
17. Anand SS, Islam S, Rosengren A, et al. 2008. Risk factors for myocardial infarction in women and men: insights from the INTERHEART study. *Eur Heart J.* 29:932-940.
18. Anderson PG, Digerness SB, Sklar JL, et al. 1990. Use of the isolated perfused heart for evaluation of cardiac toxicity. *Toxicol Pathol.* 18:497-510.
19. Angelos MG, Kutala VK, Torres CA, et al. 2006. Hypoxic reperfusion of the ischemic heart and oxygen radical generation. *Am J Physiol Heart Circ Physiol.* 290:H341-347.
20. Angerer P, Stork S, Kothny W, et al. 2001. Effect of oral postmenopausal hormone replacement on progression of atherosclerosis : a randomized, controlled trial. *Arterioscler Thromb Vasc Biol.* 21:262-268.
21. Antignani A, and Youle RJ. 2006. How do Bax and Bak lead to permeabilization of the outer mitochondrial membrane? *Curr Opin Cell Biol.* 18:685-689.
22. Anversa P, Beghi C, Kikkawa Y, et al. 1985. Myocardial response to infarction in the rat. Morphometric measurement of infarct size and myocyte cellular hypertrophy. *Am J Pathol.* 118:484-492.
23. Anversa P, Beghi C, Kikkawa Y, et al. 1986. Myocardial infarction in rats. Infarct size, myocyte hypertrophy, and capillary growth. *Circ Res.* 58:26-37.
24. Anversa P, Beghi C, McDonald SL, et al. 1984. Morphometry of right ventricular hypertrophy induced by myocardial infarction in the rat. *Am J Pathol.* 116:504-513.
25. Arbustini E, Brega A, and Narula J. 2008. Ultrastructural definition of apoptosis in heart failure. *Heart Fail Rev.* 13:121-135.
26. Arnoult D, Gaume B, Karbowski M, et al. 2003. Mitochondrial release of AIF and EndoG requires caspase activation downstream of Bax/Bak-mediated permeabilization. *Embo J.* 22:4385-4399.
27. Arrigo AP. 2001. Hsp27: novel regulator of intracellular redox state. *IUBMB life.* 52:303-307.
28. Arriza JL, Weinberger C, Cerelli G, et al. 1987. Cloning of human mineralocorticoid receptor complementary DNA: structural and functional kinship with the glucocorticoid receptor. *Science.* 237:268-275.
29. Asher C, Wald H, Rossier BC, et al. 1996. Aldosterone-induced increase in the abundance of Na⁺ channel subunits. *Am J Physiol.* 271:C605-611.

30. Assaly R, de Tassigny A, Paradis S, et al. 2012. Oxidative stress, mitochondrial permeability transition pore opening and cell death during hypoxia-reoxygenation in adult cardiomyocytes. *Eur J Pharmacol.* 675:6-14.
31. Assmus B, Rolf A, Erbs S, et al. 2010. Clinical outcome 2 years after intracoronary administration of bone marrow-derived progenitor cells in acute myocardial infarction. *Circ Heart Fail.* 3:89-96.
32. Bae S, and Zhang L. 2005. Gender differences in cardioprotection against ischemia/reperfusion injury in adult rat hearts: focus on Akt and protein kinase C signaling. *J Pharmacol Exp Ther.* 315:1125-1135.
33. Baines CP. 2010. The cardiac mitochondrion: nexus of stress. *Annu Rev Physiol.* 72:61-80.
34. Baines CP, Kaiser RA, Purcell NH, et al. 2005. Loss of cyclophilin D reveals a critical role for mitochondrial permeability transition in cell death. *Nature.* 434:658-662.
35. Baker L, Meldrum KK, Wang M, et al. 2003. The role of estrogen in cardiovascular disease. *J Surg Res.* 115:325-344.
36. Baldi A, Abbate A, Bussani R, et al. 2002. Apoptosis and post-infarction left ventricular remodeling. *J Mol Cell Cardiol.* 34:165-174.
37. Barbato JC, Mulrow PJ, Shapiro JI, et al. 2002. Rapid effects of aldosterone and spironolactone in the isolated working rat heart. *Hypertension.* 40:130-135.
38. Barrett-Connor E, and Goodman-Gruen D. 1995. Prospective study of endogenous sex hormones and fatal cardiovascular disease in postmenopausal women. *Bmj.* 311:1193-1196.
39. Bauersachs J, Heck M, Fraccarollo D, et al. 2002. Addition of spironolactone to angiotensin-converting enzyme inhibition in heart failure improves endothelial vasomotor dysfunction: role of vascular superoxide anion formation and endothelial nitric oxide synthase expression. *J Am Coll Cardiol.* 39:351-358.
40. Becker LB. 2004. New concepts in reactive oxygen species and cardiovascular reperfusion physiology. *Cardiovasc Res.* 61:461-470.
41. Bedard K, and Krause KH. 2007. The NOX family of ROS-generating NADPH oxidases: physiology and pathophysiology. *Physiol Rev.* 87:245-313.
42. BelAiba RS, Djordjevic T, Petry A, et al. 2007. NOX5 variants are functionally active in endothelial cells. *Free Radic Biol Med.* 42:446-459.
43. Belenky P, Bogan KL, and Brenner C. 2007. NAD⁺ metabolism in health and disease. *Trends Biochem Sci.* 32:12-19.
44. Bell JR, Mellor KM, Wollermann AC, et al. 2011a. Aromatase deficiency confers paradoxical postischemic cardioprotection. *Endocrinology.* 152:4937-4947.
45. Bell RM, Mocanu MM, and Yellon DM. 2011b. Retrograde heart perfusion: the Langendorff technique of isolated heart perfusion. *J Mol Cell Cardiol.* 50:940-950.

46. Bendall JK, Cave AC, Heymes C, et al. 2002. Pivotal role of a gp91(phox)-containing NADPH oxidase in angiotensin II-induced cardiac hypertrophy in mice. *Circulation*. 105:293-296.
47. Bener A, Zirie MA, Kim EJ, et al. 2013. Measuring burden of diseases in a rapidly developing economy: state of Qatar. *Glob J Health Sci*. 5:134-144.
48. Benjamin IJ, and McMillan DR. 1998. Stress (heat shock) proteins: molecular chaperones in cardiovascular biology and disease. *Circ Res*. 83:117-132.
49. Berger F, Ramirez-Hernandez MH, and Ziegler M. 2004. The new life of a centenarian: signalling functions of NAD(P). *Trends Biochem Sci*. 29:111-118.
50. Beygui F, Collet JP, Benoliel JJ, et al. 2006. High plasma aldosterone levels on admission are associated with death in patients presenting with acute ST-elevation myocardial infarction. *Circulation*. 114:2604-2610.
51. Beygui F, Montalescot G, Vicaut E, et al. 2009. Aldosterone and long-term outcome after myocardial infarction: A substudy of the french nationwide Observatoire sur la Prise en charge hospitaliere, l'Evolution a un an et les caRacteristiques de patients presentant un infArctus du myocarde avec ou sans onde Q (OPERA) study. *Am Heart J*. 157:680-687.
52. Bhargava A, Wang J, and Pearce D. 2004. Regulation of epithelial ion transport by aldosterone through changes in gene expression. *Mol Cell Endocrinol*. 217:189-196.
53. Bhatt DL. 2013. Timely PCI for STEMI - Still the Treatment of Choice. *N Engl J Med*.
54. Bhuiyan MS, and Fukunaga K. 2008. Activation of HtrA2, a mitochondrial serine protease mediates apoptosis: current knowledge on HtrA2 mediated myocardial ischemia/reperfusion injury. *Cardiovasc Ther*. 26:224-232.
55. Bienvenu LA, Morgan J, Rickard AJ, et al. 2012. Macrophage mineralocorticoid receptor signaling plays a key role in aldosterone-independent cardiac fibrosis. *Endocrinology*. 153:3416-3425.
56. Billen LP, Kokoski CL, Lovell JF, et al. 2008. Bcl-XL inhibits membrane permeabilization by competing with Bax. *PLoS Biol*. 6:e147.
57. Bindoli A, Fukuto JM, and Forman HJ. 2008. Thiol chemistry in peroxidase catalysis and redox signaling. *Antioxid Redox Signal*. 10:1549-1564.
58. Bing RJ, Gudbjarnason S, Tschopp H, et al. 1969. Molecular changes in myocardial infarction in heart muscle. *Ann N Y Acad Sci*. 156:583-593.
59. Biondi-Zoccai GG, Abate A, Bussani R, et al. 2005. Reduced post-infarction myocardial apoptosis in women: a clue to their different clinical course? *Heart*. 91:99-101.
60. Birnbaum Y, Hale SL, and Kloner RA. 1997. Differences in reperfusion length following 30 minutes of ischemia in the rabbit influence infarct size, as measured by triphenyltetrazolium chloride staining. *J Mol Cell Cardiol*. 29:657-666.

61. Bjorkoy G, Lamark T, Brech A, et al. 2005. p62/SQSTM1 forms protein aggregates degraded by autophagy and has a protective effect on huntingtin-induced cell death. *J Cell Biol.* 171:603-614.
62. Blasi ER, Rocha R, Rudolph AE, et al. 2003. Aldosterone/salt induces renal inflammation and fibrosis in hypertensive rats. *Kidney Int.* 63:1791-1800.
63. Bledsoe RK, Madauss KP, Holt JA, et al. 2005. A ligand-mediated hydrogen bond network required for the activation of the mineralocorticoid receptor. *J Biol Chem.* 280:31283-31293.
64. Boden WE, Lansky A, and Angiolillo DJ. 2013. Refining the role of antiplatelet therapy in medically managed patients with acute coronary syndrome. *Am J Cardiol.* 111:439-444.
65. Boengler K, Hilfiker-Kleiner D, Heusch G, et al. 2010. Inhibition of permeability transition pore opening by mitochondrial STAT3 and its role in myocardial ischemia/reperfusion. *Basic Res Cardiol.* 105:771-785.
66. Bolli R, and Marban E. 1999. Molecular and cellular mechanisms of myocardial stunning. *Physiol Rev.* 79:609-634.
67. Bologna CG, Revankar CM, Young SM, et al. 2006. Virtual and biomolecular screening converge on a selective agonist for GPR30. *Nat Chem Biol.* 2:207-212.
68. Booth EA, and Lucchesi BR. 2008. Estrogen-mediated protection in myocardial ischemia-reperfusion injury. *Cardiovasc Toxicol.* 8:101-113.
69. Booth EA, Marchesi M, Kilbourne EJ, et al. 2003. 17Beta-estradiol as a receptor-mediated cardioprotective agent. *J Pharmacol Exp Ther.* 307:395-401.
70. Booth EA, Marchesi M, Knittel AK, et al. 2007. The pathway-selective estrogen receptor ligand WAY-169916 reduces infarct size after myocardial ischemia and reperfusion by an estrogen receptor dependent mechanism. *J Cardiovasc Pharmacol.* 49:401-407.
71. Booth EA, Obeid NR, and Lucchesi BR. 2005. Activation of estrogen receptor-alpha protects the in vivo rabbit heart from ischemia-reperfusion injury. *Am J Physiol Heart Circ Physiol.* 289:H2039-2047.
72. Borch E, Parri M, Papucci L, et al. 2009. Role of NADPH oxidase in H9c2 cardiac muscle cells exposed to simulated ischaemia-reperfusion. *J Cell Mol Med.* 13:2724-2735.
73. Borden WB, Fennessy MM, O'Connor AM, et al. 2012. Quality improvement in the door-to-balloon times for ST-elevation myocardial infarction patients presenting without chest pain. *Catheter Cardiovasc Interv.* 79:851-858.
74. Borghi C, Boschi S, Ambrosioni E, et al. 1993. Evidence of a partial escape of renin-angiotensin-aldosterone blockade in patients with acute myocardial infarction treated with ACE inhibitors. *Journal of clinical pharmacology.* 33:40-45.
75. Bouma W, Noma M, Kanemoto S, et al. 2010. Sex-related resistance to myocardial ischemia-reperfusion injury is associated with high constitutive ARC expression. *Am J Physiol Heart Circ Physiol.* 298:H1510-1517.

76. Bowles DK, Maddali KK, Dhulipala VC, et al. 2007. PKCdelta mediates anti-proliferative, pro-apoptotic effects of testosterone on coronary smooth muscle. *Am J Physiol Cell Physiol.* 293:C805-813.
77. Bozdag-Turan I, Turan RG, Ludovicy S, et al. 2012. Intra coronary freshly isolated bone marrow cells transplantation improve cardiac function in patients with ischemic heart disease. *BMC Res Notes.* 5:195.
78. Bradford MM. 1976. A rapid and sensitive method for the quantitation of microgram quantities of protein utilizing the principle of protein-dye binding. *Anal Biochem.* 72:248-254.
79. Bradley EH, Curry L, Horwitz LI, et al. 2012. Contemporary evidence about hospital strategies for reducing 30-day readmissions: a national study. *J Am Coll Cardiol.* 60:607-614.
80. Brand T, Sharma HS, Fleischmann KE, et al. 1992. Proto-oncogene expression in porcine myocardium subjected to ischemia and reperfusion. *Circ Res.* 71:1351-1360.
81. Brar BK, Jonassen AK, Egorina EM, et al. 2004. Urocortin-II and urocortin-III are cardioprotective against ischemia reperfusion injury: an essential endogenous cardioprotective role for corticotropin releasing factor receptor type 2 in the murine heart. *Endocrinology.* 145:24-35; discussion 21-23.
82. Bratton SB, Lewis J, Butterworth M, et al. 2002. XIAP inhibition of caspase-3 preserves its association with the Apaf-1 apoptosome and prevents CD95- and Bax-induced apoptosis. *Cell Death Differ.* 9:881-892.
83. Braunersreuther V, and Jaquet V. 2012. Reactive oxygen species in myocardial reperfusion injury: from physiopathology to therapeutic approaches. *Curr Pharm Biotechnol.* 13:97-114.
84. Braunstein GD. 2007. Management of female sexual dysfunction in postmenopausal women by testosterone administration: safety issues and controversies. *J Sex Med.* 4:859-866.
85. Braunwald E. 1989. Myocardial reperfusion, limitation of infarct size, reduction of left ventricular dysfunction, and improved survival. Should the paradigm be expanded? *Circulation.* 79:441-444.
86. Bredee JJ, Blickman JR, Holman van der Heide JN, et al. 1975. Standardized induction of myocardial ischaemia in the dog. *Eur Surg Res.* 7:269-286.
87. Brilla CG, Pick R, Tan LB, et al. 1990. Remodeling of the rat right and left ventricles in experimental hypertension. *Circ Res.* 67:1355-1364.
88. Brilla CG, Zhou G, Matsubara L, et al. 1994. Collagen metabolism in cultured adult rat cardiac fibroblasts: response to angiotensin II and aldosterone. *J Mol Cell Cardiol.* 26:809-820.
89. Bucciarelli LG, Kaneko M, Ananthakrishnan R, et al. 2006. Receptor for advanced-glycation end products: key modulator of myocardial ischemic injury. *Circulation.* 113:1226-1234.

90. Budoff MJ, Young R, Lopez VA, et al. 2013. Progression of Coronary Calcium and Incident Coronary Heart Disease Events: The Multi-Ethnic Study of Atherosclerosis. *J Am Coll Cardiol.* 61:1231-1239.
91. Burniston JG, Saini A, Tan LB, et al. 2005. Aldosterone induces myocyte apoptosis in the heart and skeletal muscles of rats in vivo. *J Mol Cell Cardiol.* 39:395-399.
92. Byrne JA, Grieve DJ, Bendall JK, et al. 2003. Contrasting roles of NADPH oxidase isoforms in pressure-overload versus angiotensin II-induced cardiac hypertrophy. *Circ Res.* 93:802-805.
93. Callies F, Stromer H, Schwinger RH, et al. 2003. Administration of testosterone is associated with a reduced susceptibility to myocardial ischemia. *Endocrinology.* 144:4478-4483.
94. Calo LA, Zaghetto F, Pagnin E, et al. 2004. Effect of aldosterone and glycyrrhetic acid on the protein expression of PAI-1 and p22(phox) in human mononuclear leukocytes. *J Clin Endocrinol Metab.* 89:1973-1976.
95. Camper-Kirby D, Welch S, Walker A, et al. 2001. Myocardial Akt activation and gender: increased nuclear activity in females versus males. *Circ Res.* 88:1020-1027.
96. Cattabiani C, Basaria S, Ceda GP, et al. 2012. Relationship between testosterone deficiency and cardiovascular risk and mortality in adult men. *J Endocrinol Invest.* 35:104-120.
97. Cavaşin MA, Sankey SS, Yu AL, et al. 2003. Estrogen and testosterone have opposing effects on chronic cardiac remodeling and function in mice with myocardial infarction. *Am J Physiol Heart Circ Physiol.* 284:H1560-1569.
98. Cavaşin MA, Tao ZY, Yu AL, et al. 2006. Testosterone enhances early cardiac remodeling after myocardial infarction, causing rupture and degrading cardiac function. *Am J Physiol Heart Circ Physiol.* 290:H2043-2050.
99. Ceconi C, Bernocchi P, Boraso A, et al. 2000. New insights on myocardial pyridine nucleotides and thiol redox state in ischemia and reperfusion damage. *Cardiovasc Res.* 47:586-594.
100. Chai W, Garrelds IM, Arulmani U, et al. 2005. Genomic and nongenomic effects of aldosterone in the rat heart: why is spironolactone cardioprotective? *Br J Pharmacol.* 145:664-671.
101. Chai W, Garrelds IM, de Vries R, et al. 2006. Cardioprotective effects of eplerenone in the rat heart: interaction with locally synthesized or blood-derived aldosterone? *Hypertension.* 47:665-670.
102. Chandrasekar B, Smith JB, and Freeman GL. 2001. Ischemia-reperfusion of rat myocardium activates nuclear factor-KappaB and induces neutrophil infiltration via lipopolysaccharide-induced CXC chemokine. *Circulation.* 103:2296-2302.
103. Chandrashekhar Y, Sen S, Anway R, et al. 2004. Long-term caspase inhibition ameliorates apoptosis, reduces myocardial troponin-I cleavage, protects left ventricular function, and attenuates remodeling in rats with myocardial infarction. *J Am Coll Cardiol.* 43:295-301.

104. Chen F, Pandey D, Chadli A, et al. 2011. Hsp90 regulates NADPH oxidase activity and is necessary for superoxide but not hydrogen peroxide production. *Antioxid Redox Signal*. 14:2107-2119.
105. Chen J, Petranka J, Yamamura K, et al. 2003a. Gender differences in sarcoplasmic reticulum calcium loading after isoproterenol. *Am J Physiol Heart Circ Physiol*. 285:H2657-2662.
106. Chen JQ, Cammarata PR, Baines CP, et al. 2009. Regulation of mitochondrial respiratory chain biogenesis by estrogens/estrogen receptors and physiological, pathological and pharmacological implications. *Biochim Biophys Acta*. 1793:1540-1570.
107. Chen Q, Moghaddas S, Hoppel CL, et al. 2006. Reversible blockade of electron transport during ischemia protects mitochondria and decreases myocardial injury following reperfusion. *J Pharmacol Exp Ther*. 319:1405-1412.
108. Chen Q, Moghaddas S, Hoppel CL, et al. 2008. Ischemic defects in the electron transport chain increase the production of reactive oxygen species from isolated rat heart mitochondria. *Am J Physiol Cell Physiol*. 294:C460-466.
109. Chen Q, Vazquez EJ, Moghaddas S, et al. 2003b. Production of reactive oxygen species by mitochondria: central role of complex III. *J Biol Chem*. 278:36027-36031.
110. Chen S, and Li S. 2012. The Na⁽⁺⁾/Ca⁽²⁺⁾ exchanger in cardiac ischemia/reperfusion injury. *Med Sci Monit*. 18:RA161-165.
111. Chen SY, Bhargava A, Mastroberardino L, et al. 1999. Epithelial sodium channel regulated by aldosterone-induced protein sgk. *Proc Natl Acad Sci U S A*. 96:2514-2519.
112. Chen Y, Fu L, Han Y, et al. 2012a. Testosterone replacement therapy promotes angiogenesis after acute myocardial infarction by enhancing expression of cytokines HIF-1 α , SDF-1 α and VEGF. *Eur J Pharmacol*. 684:116-124.
113. Chen Y, Wang Y, Chen J, et al. 2012b. Roles of transcriptional corepressor RIP140 and coactivator PGC-1 α in energy state of chronically infarcted rat hearts and mitochondrial function of cardiomyocytes. *Mol Cell Endocrinol*. 362:11-18.
114. Chen Z, Chua CC, Ho YS, et al. 2001. Overexpression of Bcl-2 attenuates apoptosis and protects against myocardial I/R injury in transgenic mice. *Am J Physiol Heart Circ Physiol*. 280:H2313-2320.
115. Cheng EH, Wei MC, Weiler S, et al. 2001. BCL-2, BCL-X(L) sequester BH3 domain-only molecules preventing BAX- and BAK-mediated mitochondrial apoptosis. *Mol Cell*. 8:705-711.
116. Cheng P, Ni Z, Dai X, et al. 2013. The novel BH-3 mimetic apogossypolone induces Beclin-1- and ROS-mediated autophagy in human hepatocellular cells. *Cell Death Dis*. 4:e489.
117. Cho YS, Challa S, Moquin D, et al. 2009. Phosphorylation-driven assembly of the RIP1-RIP3 complex regulates programmed necrosis and virus-induced inflammation. *Cell*. 137:1112-1123.

118. Chomczynski P. 1993. A reagent for the single-step simultaneous isolation of RNA, DNA and proteins from cell and tissue samples. *Biotechniques*. 15:532-534, 536-537.
119. Chomczynski P, and Mackey K. 1995. Substitution of chloroform by bromochloropropane in the single-step method of RNA isolation. *Anal Biochem*. 225:163-164.
120. Chomczynski P, and Sacchi N. 1987. Single-step method of RNA isolation by acid guanidinium thiocyanate-phenol-chloroform extraction. *Anal Biochem*. 162:156-159.
121. Christakou C, and Diamanti-Kandarakis E. 2013. Pcos and Cardiovascular Risk Factors. *Curr Pharm Des*.
122. Christian RC, Dumesic DA, Behrenbeck T, et al. 2003. Prevalence and predictors of coronary artery calcification in women with polycystic ovary syndrome. *J Clin Endocrinol Metab*. 88:2562-2568.
123. Chun TY, and Pratt JH. 2005. Aldosterone increases plasminogen activator inhibitor-1 synthesis in rat cardiomyocytes. *Mol Cell Endocrinol*. 239:55-61.
124. Cocco P, Todde P, Fornera S, et al. 1998. Mortality in a cohort of men expressing the glucose-6-phosphate dehydrogenase deficiency. *Blood*. 91:706-709.
125. Compton MM. 1992. A biochemical hallmark of apoptosis: internucleosomal degradation of the genome. *Cancer Metastasis Rev*. 11:105-119.
126. Contreras JL, Vilatoba M, Eckstein C, et al. 2004. Caspase-8 and caspase-3 small interfering RNA decreases ischemia/reperfusion injury to the liver in mice. *Surgery*. 136:390-400.
127. Cooper GJ, and Hunter M. 1994. Na(+)-H+ exchange in frog early distal tubule: effect of aldosterone on the set-point. *J Physiol*. 479 (Pt 3):423-432.
128. Cortassa S, O'Rourke B, Winslow RL, et al. 2009. Control and regulation of mitochondrial energetics in an integrated model of cardiomyocyte function. *Biophys J*. 96:2466-2478.
129. Cory S, and Adams JM. 2002. The Bcl2 family: regulators of the cellular life-or-death switch. *Nat Rev Cancer*. 2:647-656.
130. Couette B, Fagart J, Jalaguier S, et al. 1996. Ligand-induced conformational change in the human mineralocorticoid receptor occurs within its hetero-oligomeric structure. *Biochem J*. 315 (Pt 2):421-427.
131. Couette B, Jalaguier S, Hellal-Levy C, et al. 1998. Folding requirements of the ligand-binding domain of the human mineralocorticoid receptor. *Mol Endocrinol*. 12:855-863.
132. Crisostomo PR, Wang M, Wairiuko GM, et al. 2006. Brief exposure to exogenous testosterone increases death signaling and adversely affects myocardial function after ischemia. *Am J Physiol Regul Integr Comp Physiol*. 290:R1168-1174.
133. Cross HR, Lu L, Steenbergen C, et al. 1998. Overexpression of the cardiac Na⁺/Ca²⁺ exchanger increases susceptibility to ischemia/reperfusion injury in male, but not female, transgenic mice. *Circ Res*. 83:1215-1223.

134. Cross HR, Murphy E, and Steenbergen C. 2002. Ca(2+) loading and adrenergic stimulation reveal male/female differences in susceptibility to ischemia-reperfusion injury. *Am J Physiol Heart Circ Physiol.* 283:H481-489.
135. Crow MT, Mani K, Nam YJ, et al. 2004. The mitochondrial death pathway and cardiac myocyte apoptosis. *Circ Res.* 95:957-970.
136. Cucoranu I, Clempus R, Dikalova A, et al. 2005. NAD(P)H oxidase 4 mediates transforming growth factor-beta1-induced differentiation of cardiac fibroblasts into myofibroblasts. *Circ Res.* 97:900-907.
137. Curello S, Ceconi C, de Giuli F, et al. 1995. Oxidative stress during reperfusion of human hearts: potential sources of oxygen free radicals. *Cardiovasc Res.* 29:118-125.
138. Cushman M, Legault C, Barrett-Connor E, et al. 1999. Effect of postmenopausal hormones on inflammation-sensitive proteins: the Postmenopausal Estrogen/Progestin Interventions (PEPI) Study. *Circulation.* 100:717-722.
139. Daemen MA, van 't Veer C, Denecker G, et al. 1999. Inhibition of apoptosis induced by ischemia-reperfusion prevents inflammation. *J Clin Invest.* 104:541-549.
140. Dai DF, and Rabinovitch P. 2011. Mitochondrial oxidative stress mediates induction of autophagy and hypertrophy in angiotensin-II treated mouse hearts. *Autophagy.* 7:917-918.
141. Dai W, Li Y, and Zheng H. 2012. Estradiol/Testosterone Imbalance: Impact on Coronary Heart Disease Risk Factors in Postmenopausal Women. *Cardiology.* 121:249-254.
142. Danial NN, and Korsmeyer SJ. 2004. Cell death: critical control points. *Cell.* 116:205-219.
143. Darley-USmar VM, O'Leary V, and Stone D. 1989. The glutathione status of perfused rat hearts subjected to hypoxia and reoxygenation: the oxygen paradox. *Free Radic Res Commun.* 6:261-267.
144. Darling CE, Smith CS, Sun JE, et al. 2013. Cost reductions associated with a quality improvement initiative for patients with ST-elevation myocardial infarction. *Jt Comm J Qual Patient Saf.* 39:16-21.
145. Das B, and Sarkar C. 2006. Similarities between ischemic preconditioning and 17beta-estradiol mediated cardiomyocyte KATP channel activation leading to cardioprotective and antiarrhythmic effects during ischemia/reperfusion in the intact rabbit heart. *J Cardiovasc Pharmacol.* 47:277-286.
146. Das DK, Maulik N, Engelman RM, et al. 1998. Signal transduction pathway leading to Hsp27 and Hsp70 gene expression during myocardial adaptation to stress. *Ann N Y Acad Sci.* 851:129-138.
147. Das DK, Maulik N, and Moraru, II. 1995. Gene expression in acute myocardial stress. Induction by hypoxia, ischemia, reperfusion, hyperthermia and oxidative stress. *J Mol Cell Cardiol.* 27:181-193.

148. De Meyer GR, and Martinet W. 2009. Autophagy in the cardiovascular system. *Biochim Biophys Acta*. 1793:1485-1495.
149. de Resende MM, Kauser K, and Mill JG. 2006. Regulation of cardiac and renal mineralocorticoid receptor expression by captopril following myocardial infarction in rats. *Life Sci*. 78:3066-3073.
150. De Silva DS, Wilson RM, Hutchinson C, et al. 2009. Fenofibrate inhibits aldosterone-induced apoptosis in adult rat ventricular myocytes via stress-activated kinase-dependent mechanisms. *Am J Physiol Heart Circ Physiol*. 296:H1983-1993.
151. Death AK, McGrath KC, Sader MA, et al. 2004. Dihydrotestosterone promotes vascular cell adhesion molecule-1 expression in male human endothelial cells via a nuclear factor-kappaB-dependent pathway. *Endocrinology*. 145:1889-1897.
152. Decker RS, Poole AR, Crie JS, et al. 1980. Lysosomal alterations in hypoxic and reoxygenated hearts. II. Immunohistochemical and biochemical changes in cathepsin D. *Am J Pathol*. 98:445-456.
153. Decker RS, and Wildenthal K. 1980. Lysosomal alterations in hypoxic and reoxygenated hearts. I. Ultrastructural and cytochemical changes. *Am J Pathol*. 98:425-444.
154. Degtarev A, Huang Z, Boyce M, et al. 2005. Chemical inhibitor of nonapoptotic cell death with therapeutic potential for ischemic brain injury. *Nat Chem Biol*. 1:112-119.
155. Delbeck M, Golz S, Vonk R, et al. 2011. Impaired left-ventricular cardiac function in male GPR30-deficient mice. *Mol Med Rep*. 4:37-40.
156. Delyani JA, Robinson EL, and Rudolph AE. 2001. Effect of a selective aldosterone receptor antagonist in myocardial infarction. *Am J Physiol Heart Circ Physiol*. 281:H647-654.
157. Deschamps AM, and Murphy E. 2009. Activation of a novel estrogen receptor, GPER, is cardioprotective in male and female rats. *Am J Physiol Heart Circ Physiol*. 297:H1806-1813.
158. Desire L, Bourdin J, Loiseau N, et al. 2005. RAC1 inhibition targets amyloid precursor protein processing by gamma-secretase and decreases Abeta production in vitro and in vivo. *J Biol Chem*. 280:37516-37525.
159. Devalaraja-Narashimha K, Diener AM, and Padanilam BJ. 2009. Cyclophilin D gene ablation protects mice from ischemic renal injury. *Am J Physiol Renal Physiol*. 297:F749-759.
160. Deveraux QL, Roy N, Stennicke HR, et al. 1998. IAPs block apoptotic events induced by caspase-8 and cytochrome c by direct inhibition of distinct caspases. *Embo J*. 17:2215-2223.
161. Deveraux QL, Takahashi R, Salvesen GS, et al. 1997. X-linked IAP is a direct inhibitor of cell-death proteases. *Nature*. 388:300-304.
162. Di Lisa F, Menabo R, Canton M, et al. 2001. Opening of the mitochondrial permeability transition pore causes depletion of mitochondrial and cytosolic

- NAD⁺ and is a causative event in the death of myocytes in postischemic reperfusion of the heart. *J Biol Chem.* 276:2571-2575.
163. Diano S, Horvath TL, Mor G, et al. 1999. Aromatase and estrogen receptor immunoreactivity in the coronary arteries of monkeys and human subjects. *Menopause.* 6:21-28.
 164. Dickens LS, Boyd RS, Jukes-Jones R, et al. 2012. A death effector domain chain DISC model reveals a crucial role for caspase-8 chain assembly in mediating apoptotic cell death. *Mol Cell.* 47:291-305.
 165. Dickinson DA, and Forman HJ. 2002. Glutathione in defense and signaling: lessons from a small thiol. *Ann N Y Acad Sci.* 973:488-504.
 166. Dill T, Schachinger V, Rolf A, et al. 2009. Intracoronary administration of bone marrow-derived progenitor cells improves left ventricular function in patients at risk for adverse remodeling after acute ST-segment elevation myocardial infarction: results of the Reinfusion of Enriched Progenitor cells And Infarct Remodeling in Acute Myocardial Infarction study (REPAIR-AMI) cardiac magnetic resonance imaging substudy. *Am Heart J.* 157:541-547.
 167. Ding Q, Gros R, Limbird LE, et al. 2009. Estradiol-mediated ERK phosphorylation and apoptosis in vascular smooth muscle cells requires GPR 30. *Am J Physiol Cell Physiol.* 297:C1178-1187.
 168. Diwan A, Krenz M, Syed FM, et al. 2007. Inhibition of ischemic cardiomyocyte apoptosis through targeted ablation of Bnip3 restrains postinfarction remodeling in mice. *J Clin Invest.* 117:2825-2833.
 169. Dixon IM, Kaneko M, Hata T, et al. 1990. Alterations in cardiac membrane Ca²⁺ transport during oxidative stress. *Mol Cell Biochem.* 99:125-133.
 170. Doerries C, Grote K, Hilfiker-Kleiner D, et al. 2007. Critical role of the NAD(P)H oxidase subunit p47phox for left ventricular remodeling/dysfunction and survival after myocardial infarction. *Circ Res.* 100:894-903.
 171. Doggrell SA. 2013. Percutaneous coronary intervention with drug-eluting stents or coronary artery bypass surgery in subjects with type 2 diabetes. *Expert Opin Pharmacother.* 14:1269-1273.
 172. Donath S, Li P, Willenbockel C, et al. 2006. Apoptosis repressor with caspase recruitment domain is required for cardioprotection in response to biomechanical and ischemic stress. *Circulation.* 113:1203-1212.
 173. Dong Y, Undyala VV, Gottlieb RA, et al. 2010. Autophagy: definition, molecular machinery, and potential role in myocardial ischemia-reperfusion injury. *J Cardiovasc Pharmacol Ther.* 15:220-230.
 174. Döring HJ, and Dehnert H. 1988. The Isolated Perfused Warm-blooded Heart According to Langendorff: Biomesstechnik-Verl.
 175. Dosenko VE, Nagibin VS, Tumanovska LV, et al. 2006. Protective effect of autophagy in anoxia-reoxygenation of isolated cardiomyocyte? *Autophagy.* 2:305-306.

176. Drose S, Bleier L, and Brandt U. 2011. A common mechanism links differently acting complex II inhibitors to cardioprotection: modulation of mitochondrial reactive oxygen species production. *Mol Pharmacol*. 79:814-822.
177. Dubey RK, Imthurn B, Barton M, et al. 2005. Vascular consequences of menopause and hormone therapy: importance of timing of treatment and type of estrogen. *Cardiovasc Res*. 66:295-306.
178. Dunlay SM, and Roger VL. 2012. Gender differences in the pathophysiology, clinical presentation, and outcomes of ischemic heart failure. *Curr Heart Fail Rep*. 9:267-276.
179. Dutta D, Xu J, Kim JS, et al. 2013. Upregulated autophagy protects cardiomyocytes from oxidative stress-induced toxicity. *Autophagy*. 9:328-344.
180. Dwivedi S, Pandey D, Khandoga AL, et al. 2010. Rac1-mediated signaling plays a central role in secretion-dependent platelet aggregation in human blood stimulated by atherosclerotic plaque. *J Transl Med*. 8:128.
181. Dybdahl B, Slordahl SA, Waage A, et al. 2005. Myocardial ischaemia and the inflammatory response: release of heat shock protein 70 after myocardial infarction. *Heart*. 91:299-304.
182. Echeverria PC, and Picard D. 2010. Molecular chaperones, essential partners of steroid hormone receptors for activity and mobility. *Biochim Biophys Acta*. 1803:641-649.
183. Edelmann F, Tomaschitz A, Wachter R, et al. 2012. Serum aldosterone and its relationship to left ventricular structure and geometry in patients with preserved left ventricular ejection fraction. *Eur Heart J*. 33:203-212.
184. Edelmann F, Wachter R, Schmidt AG, et al. 2013. Effect of spironolactone on diastolic function and exercise capacity in patients with heart failure with preserved ejection fraction: the Aldo-DHF randomized controlled trial. *Jama*. 309:781-791.
185. Edwards CR, Stewart PM, Burt D, et al. 1988. Localisation of 11 beta-hydroxysteroid dehydrogenase--tissue specific protector of the mineralocorticoid receptor. *Lancet*. 2:986-989.
186. Efthymiou CA, Mocanu MM, de Belloche J, et al. 2004. Heat shock protein 27 protects the heart against myocardial infarction. *Basic Res Cardiol*. 99:392-394.
187. Ekhterae D, Lin Z, Lundberg MS, et al. 1999. ARC inhibits cytochrome c release from mitochondria and protects against hypoxia-induced apoptosis in heart-derived H9c2 cells. *Circ Res*. 85:e70-77.
188. Elsasser A, Vogt AM, Nef H, et al. 2004. Human hibernating myocardium is jeopardized by apoptotic and autophagic cell death. *J Am Coll Cardiol*. 43:2191-2199.
189. Enari M, Sakahira H, Yokoyama H, et al. 1998. A caspase-activated DNase that degrades DNA during apoptosis, and its inhibitor ICAD. *Nature*. 391:43-50.

190. Enomoto S, Yoshiyama M, Omura T, et al. 2005. Effects of eplerenone on transcriptional factors and mRNA expression related to cardiac remodelling after myocardial infarction. *Heart*. 91:1595-1600.
191. Essick EE, and Sam F. 2010. Oxidative stress and autophagy in cardiac disease, neurological disorders, aging and cancer. *Oxid Med Cell Longev*. 3:168-177.
192. Esumi K, Nishida M, Shaw D, et al. 1991. NADH measurements in adult rat myocytes during simulated ischemia. *Am J Physiol*. 260:H1743-1752.
193. Fan M, Rhee J, St-Pierre J, et al. 2004. Suppression of mitochondrial respiration through recruitment of p160 myb binding protein to PGC-1alpha: modulation by p38 MAPK. *Genes Dev*. 18:278-289.
194. Fan YS, Eddy RL, Byers MG, et al. 1989. The human mineralocorticoid receptor gene (MLR) is located on chromosome 4 at q31.2. *Cytogenet Cell Genet*. 52:83-84.
195. Faresse N, Ruffieux-Daidie D, Salamin M, et al. 2010. Mineralocorticoid receptor degradation is promoted by Hsp90 inhibition and the ubiquitin-protein ligase CHIP. *Am J Physiol Renal Physiol*. 299:F1462-1472.
196. Faresse N, Vitagliano JJ, and Staub O. 2012. Differential ubiquitylation of the mineralocorticoid receptor is regulated by phosphorylation. *Faseb J*. 26:4373-4382.
197. Fauconnier J, Meli AC, Thireau J, et al. 2011. Ryanodine receptor leak mediated by caspase-8 activation leads to left ventricular injury after myocardial ischemia-reperfusion. *Proc Natl Acad Sci U S A*. 108:13258-13263.
198. Favre J, Gao J, Zhang AD, et al. 2011. Coronary endothelial dysfunction after cardiomyocyte-specific mineralocorticoid receptor overexpression. *Am J Physiol Heart Circ Physiol*. 300:H2035-2043.
199. Feissner RF, Skalska J, Gaum WE, et al. 2009. Crosstalk signaling between mitochondrial Ca²⁺ and ROS. *Front Biosci*. 14:1197-1218.
200. Fejes-Toth G, Pearce D, and Naray-Fejes-Toth A. 1998. Subcellular localization of mineralocorticoid receptors in living cells: effects of receptor agonists and antagonists. *Proc Natl Acad Sci U S A*. 95:2973-2978.
201. Ferdinandy P, Panas D, and Schulz R. 1999. Peroxynitrite contributes to spontaneous loss of cardiac efficiency in isolated working rat hearts. *Am J Physiol*. 276:H1861-1867.
202. Fernandes AP, and Holmgren A. 2004. Glutaredoxins: glutathione-dependent redox enzymes with functions far beyond a simple thioredoxin backup system. *Antioxid Redox Signal*. 6:63-74.
203. Ferrari R, Alfieri O, Curello S, et al. 1990. Occurrence of oxidative stress during reperfusion of the human heart. *Circulation*. 81:201-211.
204. Ferrari R, Ceconi C, Curello S, et al. 1991. Oxygen free radicals and myocardial damage: protective role of thiol-containing agents. *Am J Med*. 91:95S-105S.

205. Ferrari R, Ceconi C, Curello S, et al. 1985. Oxygen-mediated myocardial damage during ischaemia and reperfusion: role of the cellular defences against oxygen toxicity. *J Mol Cell Cardiol.* 17:937-945.
206. Ferrera R, Benhabbouche S, Bopassa JC, et al. 2009. One hour reperfusion is enough to assess function and infarct size with TTC staining in Langendorff rat model. *Cardiovasc Drugs Ther.* 23:327-331.
207. Filardo E, Quinn J, Pang Y, et al. 2007. Activation of the novel estrogen receptor G protein-coupled receptor 30 (GPR30) at the plasma membrane. *Endocrinology.* 148:3236-3245.
208. Filardo EJ. 2002. Epidermal growth factor receptor (EGFR) transactivation by estrogen via the G-protein-coupled receptor, GPR30: a novel signaling pathway with potential significance for breast cancer. *J Steroid Biochem Mol Biol.* 80:231-238.
209. Filardo EJ, and Thomas P. 2005. GPR30: a seven-transmembrane-spanning estrogen receptor that triggers EGF release. *Trends Endocrinol Metab.* 16:362-367.
210. Filice E, Recchia AG, Pellegrino D, et al. 2009. A new membrane G protein-coupled receptor (GPR30) is involved in the cardiac effects of 17beta-estradiol in the male rat. *J Physiol Pharmacol.* 60:3-10.
211. Fischer K, Kelly SM, Watt K, et al. 2010. Conformation of the mineralocorticoid receptor N-terminal domain: evidence for induced and stable structure. *Mol Endocrinol.* 24:1935-1948.
212. Fishbein MC, Maclean D, and Maroko PR. 1978. Experimental myocardial infarction in the rat: qualitative and quantitative changes during pathologic evolution. *Am J Pathol.* 90:57-70.
213. Fishbein MC, Meerbaum S, Rit J, et al. 1981. Early phase acute myocardial infarct size quantification: validation of the triphenyl tetrazolium chloride tissue enzyme staining technique. *Am Heart J.* 101:593-600.
214. Fisher PW, Salloum F, Das A, et al. 2005. Phosphodiesterase-5 inhibition with sildenafil attenuates cardiomyocyte apoptosis and left ventricular dysfunction in a chronic model of doxorubicin cardiotoxicity. *Circulation.* 111:1601-1610.
215. Fliss H, and Gattinger D. 1996. Apoptosis in ischemic and reperfused rat myocardium. *Circ Res.* 79:949-956.
216. Florian M, and Magder S. 2008. Estrogen decreases TNF-alpha and oxidized LDL induced apoptosis in endothelial cells. *Steroids.* 73:47-58.
217. Foo RS, Chan LK, Kitsis RN, et al. 2007a. Ubiquitination and degradation of the anti-apoptotic protein ARC by MDM2. *J Biol Chem.* 282:5529-5535.
218. Foo RS, Nam YJ, Ostreicher MJ, et al. 2007b. Regulation of p53 tetramerization and nuclear export by ARC. *Proc Natl Acad Sci U S A.* 104:20826-20831.
219. Forouzanfar MH, Moran AE, Flaxman AD, et al. 2012. Assessing the global burden of ischemic heart disease, part 2: analytic methods and estimates of the global epidemiology of ischemic heart disease in 2010. *Glob Heart.* 7:331-342.

220. Fox CH, Johnson FB, Whiting J, et al. 1985. Formaldehyde fixation. *J Histochem Cytochem.* 33:845-853.
221. Fraccarollo D, Berger S, Galuppo P, et al. 2011. Deletion of cardiomyocyte mineralocorticoid receptor ameliorates adverse remodeling after myocardial infarction. *Circulation.* 123:400-408.
222. Fraccarollo D, Galuppo P, Schraut S, et al. 2008. Immediate mineralocorticoid receptor blockade improves myocardial infarct healing by modulation of the inflammatory response. *Hypertension.* 51:905-914.
223. Frederiks WM, Kummerlin IP, Bosch KS, et al. 2007. NADPH production by the pentose phosphate pathway in the zona fasciculata of rat adrenal gland. *J Histochem Cytochem.* 55:975-980.
224. French D, and Edsall JT. 1945. The reaction of formaldehyde with amino acids and proteins. *Adv. Protein Chem.* 2:277-335.
225. Fujita M, Minamino T, Asanuma H, et al. 2005. Aldosterone nongenomically worsens ischemia via protein kinase C-dependent pathways in hypoperfused canine hearts. *Hypertension.* 46:113-117.
226. Fukui T, Yoshiyama M, Hanatani A, et al. 2001. Expression of p22-phox and gp91-phox, essential components of NADPH oxidase, increases after myocardial infarction. *Biochem Biophys Res Commun.* 281:1200-1206.
227. Fuller PJ, and Young MJ. 2005. Mechanisms of mineralocorticoid action. *Hypertension.* 46:1227-1235.
228. Funder JW, Pearce PT, Smith R, et al. 1988. Mineralocorticoid action: target tissue specificity is enzyme, not receptor, mediated. *Science.* 242:583-585.
229. Fuse H, Kitagawa H, and Kato S. 2000. Characterization of transactivational property and coactivator mediation of rat mineralocorticoid receptor activation function-1 (AF-1). *Mol Endocrinol.* 14:889-899.
230. Gabel SA, Walker VR, London RE, et al. 2005. Estrogen receptor beta mediates gender differences in ischemia/reperfusion injury. *J Mol Cell Cardiol.* 38:289-297.
231. Gaeggeler HP, Gonzalez-Rodriguez E, Jaeger NF, et al. 2005. Mineralocorticoid versus glucocorticoid receptor occupancy mediating aldosterone-stimulated sodium transport in a novel renal cell line. *J Am Soc Nephrol.* 16:878-891.
232. Gajarsa JJ, and Kloner RA. 2011. Left ventricular remodeling in the post-infarction heart: a review of cellular, molecular mechanisms, and therapeutic modalities. *Heart Fail Rev.* 16:13-21.
233. Gamliel-Lazarovich A, Gantman A, Coleman R, et al. 2010. FAD286, an aldosterone synthase inhibitor, reduced atherosclerosis and inflammation in apolipoprotein E-deficient mice. *J Hypertens.* 28:1900-1907.
234. Gao F, Yao CL, Gao E, et al. 2002. Enhancement of glutathione cardioprotection by ascorbic acid in myocardial reperfusion injury. *J Pharmacol Exp Ther.* 301:543-550.

235. Garnier A, Fortin D, Delomenie C, et al. 2003. Depressed mitochondrial transcription factors and oxidative capacity in rat failing cardiac and skeletal muscles. *J Physiol*. 551:491-501.
236. Gavrieli Y, Sherman Y, and Ben-Sasson SA. 1992. Identification of programmed cell death in situ via specific labeling of nuclear DNA fragmentation. *J Cell Biol*. 119:493-501.
237. Gekle M, Freudinger R, Mildenerger S, et al. 2001. Rapid activation of Na⁺/H⁺-exchange in MDCK cells by aldosterone involves MAP-kinase ERK1/2. *Pflugers Arch*. 441:781-786.
238. Gekle M, Silbernagl S, and Wunsch S. 1998. Non-genomic action of the mineralocorticoid aldosterone on cytosolic sodium in cultured kidney cells. *J Physiol*. 511 (Pt 1):255-263.
239. Genest J, Lemieux G, Davignon A, et al. 1956. Human arterial hypertension: a state of mild chronic hyperaldosteronism? *Science*. 123:503-505.
240. Ghaffari S, Kazemi B, Toluey M, et al. 2012. The Effect of Pre-thrombolytic Cyclosporine-A Injection on Clinical Outcome of Acute Anterior ST-Elevation Myocardial Infarction. *Cardiovasc Ther*.
241. Gidh-Jain M, Huang B, Jain P, et al. 1998. Alterations in cardiac gene expression during ventricular remodeling following experimental myocardial infarction. *J Mol Cell Cardiol*. 30:627-637.
242. Gold R, Schmied M, Giegerich G, et al. 1994. Differentiation between cellular apoptosis and necrosis by the combined use of in situ tailing and nick translation techniques. *Lab Invest*. 71:219-225.
243. Goldman S, and Raya TE. 1995. Rat infarct model of myocardial infarction and heart failure. *J Card Fail*. 1:169-177.
244. Gomez-Sanchez CE, de Rodriguez AF, Romero DG, et al. 2006. Development of a panel of monoclonal antibodies against the mineralocorticoid receptor. *Endocrinology*. 147:1343-1348.
245. Gomez-Sanchez EP, Venkataraman MT, Thwaites D, et al. 1990. ICV infusion of corticosterone antagonizes ICV-aldosterone hypertension. *Am J Physiol*. 258:E649-653.
246. Gomez AM, Rueda A, Sainte-Marie Y, et al. 2009. Mineralocorticoid modulation of cardiac ryanodine receptor activity is associated with downregulation of FK506-binding proteins. *Circulation*. 119:2179-2187.
247. Gonzalez-Santiago L, Suarez Y, Zarich N, et al. 2006. Aplidin induces JNK-dependent apoptosis in human breast cancer cells via alteration of glutathione homeostasis, Rac1 GTPase activation, and MKP-1 phosphatase downregulation. *Cell Death Differ*. 13:1968-1981.
248. Gorczyca W, Gong J, and Darzynkiewicz Z. 1993. Detection of DNA strand breaks in individual apoptotic cells by the in situ terminal deoxynucleotidyl transferase and nick translation assays. *Cancer Res*. 53:1945-1951.

249. Gorenkova N, Robinson E, Grieve D, et al. 2013. Conformational change of mitochondrial complex I increases ROS sensitivity during ischaemia. *Antioxid Redox Signal*.
250. Gorlach A, Brandes RP, Nguyen K, et al. 2000. A gp91phox containing NADPH oxidase selectively expressed in endothelial cells is a major source of oxygen radical generation in the arterial wall. *Circ Res*. 87:26-32.
251. Gottlieb RA. 2011. Cell death pathways in acute ischemia/reperfusion injury. *J Cardiovasc Pharmacol Ther*. 16:233-238.
252. Gottlieb RA, Burleson KO, Kloner RA, et al. 1994. Reperfusion injury induces apoptosis in rabbit cardiomyocytes. *J Clin Invest*. 94:1621-1628.
253. Gottlieb RA, and Mentzer RM. 2010. Autophagy during cardiac stress: joys and frustrations of autophagy. *Annu Rev Physiol*. 72:45-59.
254. Govindan MV, and Warriar N. 1998. Reconstitution of the N-terminal transcription activation function of human mineralocorticoid receptor in a defective human glucocorticoid receptor. *J Biol Chem*. 273:24439-24447.
255. Granata R, Trovato L, Gallo MP, et al. 2009. Growth hormone-releasing hormone promotes survival of cardiac myocytes in vitro and protects against ischaemia-reperfusion injury in rat heart. *Cardiovasc Res*. 83:303-312.
256. Greenberg JI, Shields DJ, Barillas SG, et al. 2008. A role for VEGF as a negative regulator of pericyte function and vessel maturation. *Nature*. 456:809-813.
257. Greenland P, Reicher-Reiss H, Goldbourt U, et al. 1991. In-hospital and 1-year mortality in 1,524 women after myocardial infarction. Comparison with 4,315 men. *Circulation*. 83:484-491.
258. Griekspoor A, Zwart W, Neefjes J, et al. 2007. Visualizing the action of steroid hormone receptors in living cells. *Nucl Recept Signal*. 5:e003.
259. Gros R, Ding Q, Davis M, et al. 2011a. Delineating the receptor mechanisms underlying the rapid vascular contractile effects of aldosterone and estradiol. *Can J Physiol Pharmacol*. 89:655-663.
260. Gros R, Ding Q, Liu B, et al. 2013. Aldosterone mediates its rapid effects in vascular endothelial cells through GPER activation. *Am J Physiol Cell Physiol*. 304:C532-540.
261. Gros R, Ding Q, Sklar LA, et al. 2011b. GPR30 expression is required for the mineralocorticoid receptor-independent rapid vascular effects of aldosterone. *Hypertension*. 57:442-451.
262. Gross ER, Hsu AK, and Gross GJ. 2006. The JAK/STAT pathway is essential for opioid-induced cardioprotection: JAK2 as a mediator of STAT3, Akt, and GSK-3 beta. *Am J Physiol Heart Circ Physiol*. 291:H827-834.
263. Grossmann C, Benesic A, Krug AW, et al. 2005. Human mineralocorticoid receptor expression renders cells responsive for nongenotropic aldosterone actions. *Mol Endocrinol*. 19:1697-1710.

264. Grossmann C, Husse B, Mildenerger S, et al. 2010. Colocalization of mineralocorticoid and EGF receptor at the plasma membrane. *Biochim Biophys Acta*. 1803:584-590.
265. Guder G, Bauersachs J, Frantz S, et al. 2007. Complementary and incremental mortality risk prediction by cortisol and aldosterone in chronic heart failure. *Circulation*. 115:1754-1761.
266. Guerra S, Leri A, Wang X, et al. 1999. Myocyte death in the failing human heart is gender dependent. *Circ Res*. 85:856-866.
267. Gupta P, and Bhatia V. 2008. Corticosteroid physiology and principles of therapy. *Indian journal of pediatrics*. 75:1039-1044.
268. Gupte RS, Vijay V, Marks B, et al. 2007. Upregulation of glucose-6-phosphate dehydrogenase and NAD(P)H oxidase activity increases oxidative stress in failing human heart. *J Card Fail*. 13:497-506.
269. Gupte SA, Levine RJ, Gupte RS, et al. 2006. Glucose-6-phosphate dehydrogenase-derived NADPH fuels superoxide production in the failing heart. *J Mol Cell Cardiol*. 41:340-349.
270. Gurusamy N, and Das DK. 2009. Is autophagy a double-edged sword for the heart? *Acta Physiol Hung*. 96:267-276.
271. Gurusamy N, Lekli I, Gherghiceanu M, et al. 2009. BAG-1 induces autophagy for cardiac cell survival. *Autophagy*. 5:120-121.
272. Gurusamy N, Lekli I, Mukherjee S, et al. 2010. Cardioprotection by resveratrol: a novel mechanism via autophagy involving the mTORC2 pathway. *Cardiovasc Res*. 86:103-112.
273. Gustafsson AB, Sayen MR, Williams SD, et al. 2002. TAT protein transduction into isolated perfused hearts: TAT-apoptosis repressor with caspase recruitment domain is cardioprotective. *Circulation*. 106:735-739.
274. Gustafsson AB, Tsai JG, Logue SE, et al. 2004. Apoptosis repressor with caspase recruitment domain protects against cell death by interfering with Bax activation. *J Biol Chem*. 279:21233-21238.
275. Guzick DS, Talbott EO, Sutton-Tyrrell K, et al. 1996. Carotid atherosclerosis in women with polycystic ovary syndrome: initial results from a case-control study. *Am J Obstet Gynecol*. 174:1224-1229; discussion 1229-1232.
276. Haisenleder DJ, Schoenfelder AH, Marcinko ES, et al. 2011. Estimation of estradiol in mouse serum samples: evaluation of commercial estradiol immunoassays. *Endocrinology*. 152:4443-4447.
277. Hak AE, Wittman JC, de Jong FH, et al. 2002. Low levels of endogenous androgens increase the risk of atherosclerosis in elderly men: the Rotterdam study. *J Clin Endocrinol Metab*. 87:3632-3639.
278. Hale SL, Birnbaum Y, and Kloner RA. 1997. Estradiol, Administered Acutely, Protects Ischemic Myocardium in Both Female and Male Rabbits. *J Cardiovasc Pharmacol Ther*. 2:47-52.

279. Halestrap AP, Clarke SJ, and Javadov SA. 2004. Mitochondrial permeability transition pore opening during myocardial reperfusion--a target for cardioprotection. *Cardiovasc Res.* 61:372-385.
280. Halliwell B, and Cross CE. 1994. Oxygen-derived species: their relation to human disease and environmental stress. *Environ Health Perspect.* 102 Suppl 10:5-12.
281. Hamacher-Brady A, Brady NR, and Gottlieb RA. 2006a. Enhancing macroautophagy protects against ischemia/reperfusion injury in cardiac myocytes. *J Biol Chem.* 281:29776-29787.
282. Hamacher-Brady A, Brady NR, and Gottlieb RA. 2006b. The interplay between pro-death and pro-survival signaling pathways in myocardial ischemia/reperfusion injury: apoptosis meets autophagy. *Cardiovasc Drugs Ther.* 20:445-462.
283. Hamacher-Brady A, Brady NR, Gottlieb RA, et al. 2006c. Autophagy as a protective response to Bnip3-mediated apoptotic signaling in the heart. *Autophagy.* 2:307-309.
284. Hamacher-Brady A, Brady NR, Logue SE, et al. 2007. Response to myocardial ischemia/reperfusion injury involves Bnip3 and autophagy. *Cell Death Differ.* 14:146-157.
285. Hammes SR, and Levin ER. 2007. Extranuclear steroid receptors: nature and actions. *Endocr Rev.* 28:726-741.
286. Handelsman DJ, Simanainen U, Walters KA, et al. 2011. Estradiol Immunoassays for Mice: Not Fit for Purpose. *Letter to Editor of Endocrinology*:1501.
287. Hanukoglu I. 1992. Steroidogenic enzymes: structure, function, and role in regulation of steroid hormone biosynthesis. *J Steroid Biochem Mol Biol.* 43:779-804.
288. Hariharan N, Zhai P, and Sadoshima J. 2011. Oxidative stress stimulates autophagic flux during ischemia/reperfusion. *Antioxid Redox Signal.* 14:2179-2190.
289. Hartgens F, Cheriex EC, and Kuipers H. 2003. Prospective echocardiographic assessment of androgenic-anabolic steroids effects on cardiac structure and function in strength athletes. *Int J Sports Med.* 24:344-351.
290. Harwood DT, and Handelsman DJ. 2009. Development and validation of a sensitive liquid chromatography-tandem mass spectrometry assay to simultaneously measure androgens and estrogens in serum without derivatization. *Clin Chim Acta.* 409:78-84.
291. Hassan NA, Salem MF, and Sayed MA. 2009. Doping and effects of anabolic androgenic steroids on the heart: histological, ultrastructural, and echocardiographic assessment in strength athletes. *Hum Exp Toxicol.* 28:273-283.
292. Hausenloy DJ, Boston-Griffiths EA, and Yellon DM. 2012. Cyclosporin A and cardioprotection: from investigative tool to therapeutic agent. *Br J Pharmacol.* 165:1235-1245.

293. Hausenloy DJ, Duchon MR, and Yellon DM. 2003. Inhibiting mitochondrial permeability transition pore opening at reperfusion protects against ischaemia-reperfusion injury. *Cardiovasc Res*. 60:617-625.
294. Hausenloy DJ, and Yellon DM. 2013. Myocardial ischemia-reperfusion injury: a neglected therapeutic target. *J Clin Invest*. 123:92-100.
295. Hayashi H, Kobara M, Abe M, et al. 2008. Aldosterone nongenomically produces NADPH oxidase-dependent reactive oxygen species and induces myocyte apoptosis. *Hypertens Res*. 31:363-375.
296. Hayashi M, Tsutamoto T, Wada A, et al. 2001. Relationship between transcatheter extraction of aldosterone and left ventricular remodeling in patients with first acute myocardial infarction: extracting aldosterone through the heart promotes ventricular remodeling after acute myocardial infarction. *J Am Coll Cardiol*. 38:1375-1382.
297. Haynes MP, Li L, Russell KS, et al. 2002. Rapid vascular cell responses to estrogen and membrane receptors. *Vascul Pharmacol*. 38:99-108.
298. Haynes MP, Sinha D, Russell KS, et al. 2000. Membrane estrogen receptor engagement activates endothelial nitric oxide synthase via the PI3-kinase-Akt pathway in human endothelial cells. *Circ Res*. 87:677-682.
299. He C, and Klionsky DJ. 2009. Regulation mechanisms and signaling pathways of autophagy. *Annu Rev Genet*. 43:67-93.
300. He H, Yang F, Liu X, et al. 2007. Sex hormone ratio changes in men and postmenopausal women with coronary artery disease. *Menopause*. 14:385-390.
301. Hecker PA, Leopold JA, Gupte SA, et al. 2013a. Impact of glucose-6-phosphate dehydrogenase deficiency on the pathophysiology of cardiovascular disease. *Am J Physiol Heart Circ Physiol*. 304:H491-500.
302. Hecker PA, Lionetti V, Ribeiro RF, Jr., et al. 2013b. Glucose 6-phosphate dehydrogenase deficiency increases redox stress and moderately accelerates the development of heart failure. *Circ Heart Fail*. 6:118-126.
303. Heer T, Schiele R, Schneider S, et al. 2002. Gender differences in acute myocardial infarction in the era of reperfusion (the MITRA registry). *Am J Cardiol*. 89:511-517.
304. Heitzler VN, Babic Z, Milicic D, et al. 2012. Evaluation of importance of door-to-balloon time and total ischemic time in acute myocardial infarction with ST-elevation treated with primary percutaneous coronary intervention. *Acta Clin Croat*. 51:387-395.
305. Henry TD, Archer SL, Nelson D, et al. 1990. Enhanced chemiluminescence as a measure of oxygen-derived free radical generation during ischemia and reperfusion. *Circ Res*. 67:1453-1461.
306. Hernandez-Diaz I, Giraldez T, Arnau MR, et al. 2010. The mineralocorticoid receptor is a constitutive nuclear factor in cardiomyocytes due to hyperactive nuclear localization signals. *Endocrinology*. 151:3888-3899.

307. Herrington DM, and Klein KP. 2001. Cardiovascular trials of estrogen replacement therapy. *Ann N Y Acad Sci.* 949:153-162.
308. Hescheler J, Meyer R, Plant S, et al. 1991. Morphological, biochemical, and electrophysiological characterization of a clonal cell (H9c2) line from rat heart. *Circ Res.* 69:1476-1486.
309. Hilenski LL, Clempus RE, Quinn MT, et al. 2004. Distinct subcellular localizations of Nox1 and Nox4 in vascular smooth muscle cells. *Arterioscler Thromb Vasc Biol.* 24:677-683.
310. Hill MF, and Singal PK. 1996. Antioxidant and oxidative stress changes during heart failure subsequent to myocardial infarction in rats. *Am J Pathol.* 148:291-300.
311. Hilz H, Wieggers U, and Adamietz P. 1975. Stimulation of proteinase K action by denaturing agents: application to the isolation of nucleic acids and the degradation of 'masked' proteins. *Eur J Biochem.* 56:103-108.
312. Hingtgen SD, Tian X, Yang J, et al. 2006. Nox2-containing NADPH oxidase and Akt activation play a key role in angiotensin II-induced cardiomyocyte hypertrophy. *Physiol Genomics.* 26:180-191.
313. Hitomi H, Kiyomoto H, Nishiyama A, et al. 2007. Aldosterone suppresses insulin signaling via the downregulation of insulin receptor substrate-1 in vascular smooth muscle cells. *Hypertension.* 50:750-755.
314. Ho HY, Cheng ML, Chen CM, et al. 2008. Oxidative damage markers and antioxidants in patients with acute myocardial infarction and their clinical significance. *Biofactors.* 34:135-145.
315. Ho TC, Yang YC, Cheng HC, et al. 2006. Activation of mitogen-activated protein kinases is essential for hydrogen peroxide -induced apoptosis in retinal pigment epithelial cells. *Apoptosis.* 11:1899-1908.
316. Hochhauser E, Kivity S, Offen D, et al. 2003. Bax ablation protects against myocardial ischemia-reperfusion injury in transgenic mice. *Am J Physiol Heart Circ Physiol.* 284:H2351-2359.
317. Hodis HN, Mack WJ, Azen SP, et al. 2003. Hormone therapy and the progression of coronary-artery atherosclerosis in postmenopausal women. *N Engl J Med.* 349:535-545.
318. Hodis HN, Mack WJ, Lobo RA, et al. 2001. Estrogen in the prevention of atherosclerosis. A randomized, double-blind, placebo-controlled trial. *Ann Intern Med.* 135:939-953.
319. Hofmann PJ, Michaelis M, Gotz F, et al. 2012. Flutamide increases aldosterone levels in gonadectomized male but not female Wistar rats. *Am J Hypertens.* 25:697-703.
320. Hofstra L, Liem IH, Dumont EA, et al. 2000. Visualisation of cell death in vivo in patients with acute myocardial infarction. *Lancet.* 356:209-212.

321. Holly TA, Drincic A, Byun Y, et al. 1999. Caspase inhibition reduces myocyte cell death induced by myocardial ischemia and reperfusion in vivo. *J Mol Cell Cardiol.* 31:1709-1715.
322. Hsu CP, Oka S, Shao D, et al. 2009. Nicotinamide phosphoribosyltransferase regulates cell survival through NAD⁺ synthesis in cardiac myocytes. *Circ Res.* 105:481-491.
323. Hu Y, Benedict MA, Ding L, et al. 1999. Role of cytochrome c and dATP/ATP hydrolysis in Apaf-1-mediated caspase-9 activation and apoptosis. *Embo J.* 18:3586-3595.
324. Huang C, Gu H, Zhang W, et al. 2010. Testosterone-down-regulated Akt pathway during cardiac ischemia/reperfusion: a mechanism involving BAD, Bcl-2 and FOXO3a. *J Surg Res.* 164:e1-11.
325. Huang J, Ito Y, Morikawa M, et al. 2003. Bcl-xL gene transfer protects the heart against ischemia/reperfusion injury. *Biochem Biophys Res Commun.* 311:64-70.
326. Huggins CE, Domenighetti AA, Pedrazzini T, et al. 2003. Elevated intracardiac angiotensin II leads to cardiac hypertrophy and mechanical dysfunction in normotensive mice. *J Renin Angiotensin Aldosterone Syst.* 4:186-190.
327. Hulley S, Grady D, Bush T, et al. 1998. Randomized trial of estrogen plus progestin for secondary prevention of coronary heart disease in postmenopausal women. Heart and Estrogen/progestin Replacement Study (HERS) Research Group. *Jama.* 280:605-613.
328. Huss JM, and Kelly DP. 2004. Nuclear receptor signaling and cardiac energetics. *Circ Res.* 95:568-578.
329. Huss JM, and Kelly DP. 2005. Mitochondrial energy metabolism in heart failure: a question of balance. *J Clin Invest.* 115:547-555.
330. Ichimura Y, Kominami E, Tanaka K, et al. 2008. Selective turnover of p62/A170/SQSTM1 by autophagy. *Autophagy.* 4:1063-1066.
331. Ide T, Tsutsui H, Kinugawa S, et al. 1999. Mitochondrial electron transport complex I is a potential source of oxygen free radicals in the failing myocardium. *Circ Res.* 85:357-363.
332. Ikeno F, Inagaki K, Rezaee M, et al. 2007. Impaired perfusion after myocardial infarction is due to reperfusion-induced deltaPKC-mediated myocardial damage. *Cardiovasc Res.* 73:699-709.
333. Inafuku H, Kuniyoshi Y, Yamashiro S, et al. 2012. Determination of Oxidative Stress and Cardiac Dysfunction after Ischemia/Reperfusion Injury in Isolated Rat Hearts. *Ann Thorac Cardiovasc Surg.*
334. Isaksson RM, Jansson JH, Lundblad D, et al. 2011. Better long-term survival in young and middle-aged women than in men after a first myocardial infarction between 1985 and 2006. An analysis of 8630 patients in the northern Sweden MONICA study. *BMC Cardiovasc Disord.* 11:1.

335. Isik T, Ayhan E, Uyarel H, et al. 2012. A comparison of direct versus conventional stenting in patients undergoing primary angioplasty for ST-elevation myocardial infarction. *Coron Artery Dis.* 23:348-353.
336. Ivanes F, Susen S, Mouquet F, et al. 2012. Aldosterone, mortality, and acute ischaemic events in coronary artery disease patients outside the setting of acute myocardial infarction or heart failure. *Eur Heart J.* 33:191-202.
337. Iwashima F, Yoshimoto T, Minami I, et al. 2008. Aldosterone induces superoxide generation via Rac1 activation in endothelial cells. *Endocrinology.* 149:1009-1014.
338. Jacobs AK. 2009. Coronary intervention in 2009: are women no different than men? *Circ Cardiovasc Interv.* 2:69-78.
339. Jain M, Brenner DA, Cui L, et al. 2003. Glucose-6-phosphate dehydrogenase modulates cytosolic redox status and contractile phenotype in adult cardiomyocytes. *Circ Res.* 93:e9-16.
340. Jain M, Cui L, Brenner DA, et al. 2004. Increased myocardial dysfunction after ischemia-reperfusion in mice lacking glucose-6-phosphate dehydrogenase. *Circulation.* 109:898-903.
341. Janicke RU, Ng P, Sprengart ML, et al. 1998. Caspase-3 is required for alpha-fodrin cleavage but dispensable for cleavage of other death substrates in apoptosis. *J Biol Chem.* 273:15540-15545.
342. Jay DB, Papaharalambus CA, Seidel-Rogol B, et al. 2008. Nox5 mediates PDGF-induced proliferation in human aortic smooth muscle cells. *Free Radic Biol Med.* 45:329-335.
343. Jennings RB, Hawkins HK, Lowe JE, et al. 1978. Relation between high energy phosphate and lethal injury in myocardial ischemia in the dog. *Am J Pathol.* 92:187-214.
344. Jennings RB, and Reimer KA. 1991. The cell biology of acute myocardial ischemia. *Annu Rev Med.* 42:225-246.
345. Jeremias I, Kupatt C, Martin-Villalba A, et al. 2000. Involvement of CD95/Apo1/Fas in cell death after myocardial ischemia. *Circulation.* 102:915-920.
346. Jessup JA, Lindsey SH, Wang H, et al. 2010. Attenuation of salt-induced cardiac remodeling and diastolic dysfunction by the GPER agonist G-1 in female mRen2.Lewis rats. *PLoS One.* 5:e15433.
347. Ji TH, Grossmann M, and Ji I. 1998. G protein-coupled receptors. I. Diversity of receptor-ligand interactions. *J Biol Chem.* 273:17299-17302.
348. Jiang M, Liu K, Luo J, et al. 2010. Autophagy is a renoprotective mechanism during in vitro hypoxia and in vivo ischemia-reperfusion injury. *Am J Pathol.* 176:1181-1192.
349. Jo DG, Jun JI, Chang JW, et al. 2004. Calcium binding of ARC mediates regulation of caspase 8 and cell death. *Mol Cell Biol.* 24:9763-9770.

350. Johns TN, and Olson BJ. 1954. Experimental myocardial infarction. I. A method of coronary occlusion in small animals. *Ann Surg.* 140:675-682.
351. Johnson MS, Moore RL, and Brown DA. 2006. Sex differences in myocardial infarct size are abolished by sarcolemmal KATP channel blockade in rat. *Am J Physiol Heart Circ Physiol.* 290:H2644-2647.
352. Joselin AP, Schulze-Osthoff K, and Schwerk C. 2006. Loss of Acinus inhibits oligonucleosomal DNA fragmentation but not chromatin condensation during apoptosis. *J Biol Chem.* 281:12475-12484.
353. Jovanovic S, Jovanovic A, Shen WK, et al. 2000. Low concentrations of 17beta-estradiol protect single cardiac cells against metabolic stress-induced Ca²⁺ loading. *J Am Coll Cardiol.* 36:948-952.
354. Juarez-Herrera U, and Jerjes-Sanchez C. 2013. Risk Factors, Therapeutic Approaches, and In-Hospital Outcomes in Mexicans With ST-Elevation Acute Myocardial Infarction: The RENASICA II Multicenter Registry. *Clin Cardiol.*
355. Kabeya Y, Mizushima N, Ueno T, et al. 2000. LC3, a mammalian homologue of yeast Apg8p, is localized in autophagosome membranes after processing. *Embo J.* 19:5720-5728.
356. Kahles H, Gebhard MM, Mezger VA, et al. 1979. The role of ATP and lactic acid for mitochondrial function during myocardial ischemia. *Basic Res Cardiol.* 74:611-620.
357. Kajstura J, Cheng W, Sarangarajan R, et al. 1996. Necrotic and apoptotic myocyte cell death in the aging heart of Fischer 344 rats. *Am J Physiol.* 271:H1215-1228.
358. Kalin MF, and Zumoff B. 1990. Sex hormones and coronary disease: a review of the clinical studies. *Steroids.* 55:330-352.
359. Kalogeris T, Baines CP, Krenz M, et al. 2012. Cell biology of ischemia/reperfusion injury. *Int Rev Cell Mol Biol.* 298:229-317.
360. Kam KW, Qi JS, Chen M, et al. 2004. Estrogen reduces cardiac injury and expression of beta1-adrenoceptor upon ischemic insult in the rat heart. *J Pharmacol Exp Ther.* 309:8-15.
361. Kaminski KA, Bonda TA, Korecki J, et al. 2002. Oxidative stress and neutrophil activation--the two keystones of ischemia/reperfusion injury. *Int J Cardiol.* 86:41-59.
362. Kanamori H, Takemura G, Goto K, et al. 2011. The role of autophagy emerging in postinfarction cardiac remodelling. *Cardiovasc Res.* 91:330-339.
363. Kanashiro-Takeuchi RM, Heidecker B, Lamirault G, et al. 2009. Sex-specific impact of aldosterone receptor antagonism on ventricular remodeling and gene expression after myocardial infarction. *Clin Transl Sci.* 2:134-142.
364. Kandel ES, and Hay N. 1999. The regulation and activities of the multifunctional serine/threonine kinase Akt/PKB. *Exp Cell Res.* 253:210-229.
365. Kapuscinski J. 1995. DAPI: a DNA-specific fluorescent probe. *Biotech Histochem.* 70:220-233.

366. Kassahn KS, Ragan MA, and Funder JW. 2011. Mineralocorticoid receptors: evolutionary and pathophysiological considerations. *Endocrinology*. 152:1883-1890.
367. Kassiotis C, Ballal K, Wellnitz K, et al. 2009. Markers of autophagy are downregulated in failing human heart after mechanical unloading. *Circulation*. 120:S191-197.
368. Kawaguchi M, Takahashi M, Hata T, et al. 2011. Inflammasome activation of cardiac fibroblasts is essential for myocardial ischemia/reperfusion injury. *Circulation*. 123:594-604.
369. Keidar S, Hayek T, Kaplan M, et al. 2003. Effect of eplerenone, a selective aldosterone blocker, on blood pressure, serum and macrophage oxidative stress, and atherosclerosis in apolipoprotein E-deficient mice. *J Cardiovasc Pharmacol*. 41:955-963.
370. Keidar S, Kaplan M, Pavlotzky E, et al. 2004. Aldosterone administration to mice stimulates macrophage NADPH oxidase and increases atherosclerosis development: a possible role for angiotensin-converting enzyme and the receptors for angiotensin II and aldosterone. *Circulation*. 109:2213-2220.
371. Kerr JF, Wyllie AH, and Currie AR. 1972. Apoptosis: a basic biological phenomenon with wide-ranging implications in tissue kinetics. *Br J Cancer*. 26:239-257.
372. Kim AM, Tingen CM, and Woodruff TK. 2010. Sex bias in trials and treatment must end. *Nature*. 465:688-689.
373. Kim H, Tu HC, Ren D, et al. 2009. Stepwise activation of BAX and BAK by tBID, BIM, and PUMA initiates mitochondrial apoptosis. *Mol Cell*. 36:487-499.
374. Kim JK, Pedram A, Razandi M, et al. 2006a. Estrogen prevents cardiomyocyte apoptosis through inhibition of reactive oxygen species and differential regulation of p38 kinase isoforms. *J Biol Chem*. 281:6760-6767.
375. Kim JS, Jin Y, and Lemasters JJ. 2006b. Reactive oxygen species, but not Ca²⁺ overloading, trigger pH- and mitochondrial permeability transition-dependent death of adult rat myocytes after ischemia-reperfusion. *Am J Physiol Heart Circ Physiol*. 290:H2024-2034.
376. Kim JW, Choi EJ, and Joe CO. 2000. Activation of death-inducing signaling complex (DISC) by pro-apoptotic C-terminal fragment of RIP. *Oncogene*. 19:4491-4499.
377. Kim SJ, Kuklov A, and Crystal GJ. 2011. In vivo gene delivery of XIAP protects against myocardial apoptosis and infarction following ischemia/reperfusion in conscious rabbits. *Life Sci*. 88:572-577.
378. Kim YS, Morgan MJ, Choksi S, et al. 2007. TNF-induced activation of the Nox1 NADPH oxidase and its role in the induction of necrotic cell death. *Mol Cell*. 26:675-687.
379. Klionsky DJ, Abeliovich H, Agostinis P, et al. 2008. Guidelines for the use and interpretation of assays for monitoring autophagy in higher eukaryotes. *Autophagy*. 4:151-175.

380. Knutti D, Kaul A, and Kralli A. 2000. A tissue-specific coactivator of steroid receptors, identified in a functional genetic screen. *Mol Cell Biol.* 20:2411-2422.
381. Ko YE, Lee IH, So HM, et al. 2011. Mechanism of glutathione depletion during simulated ischemia-reperfusion of H9c2 cardiac myocytes. *Free Radic Res.* 45:1074-1082.
382. Kobayashi A, Imamura H, Isobe M, et al. 2001. Mac-1 (CD11b/CD18) and intercellular adhesion molecule-1 in ischemia-reperfusion injury of rat liver. *Am J Physiol Gastrointest Liver Physiol.* 281:G577-585.
383. Kocoska-Maras L, Hirschberg AL, Bystrom B, et al. 2009. Testosterone addition to estrogen therapy - effects on inflammatory markers for cardiovascular disease. *Gynecol Endocrinol.* 25:823-827.
384. Kohno H, Takahashi N, Shinohara T, et al. 2007. Receptor-mediated suppression of cardiac heat-shock protein 72 expression by testosterone in male rat heart. *Endocrinology.* 148:3148-3155.
385. Kolla V, and Litwack G. 2000. Transcriptional regulation of the human Na/K ATPase via the human mineralocorticoid receptor. *Mol Cell Biochem.* 204:35-40.
386. Kornel L. 1994. Colocalization of 11 beta-hydroxysteroid dehydrogenase and mineralocorticoid receptors in cultured vascular smooth muscle cells. *Am J Hypertens.* 7:100-103.
387. Korsmeyer SJ, Wei MC, Saito M, et al. 2000. Pro-apoptotic cascade activates BID, which oligomerizes BAK or BAX into pores that result in the release of cytochrome c. *Cell Death Differ.* 7:1166-1173.
388. Koseki T, Inohara N, Chen S, et al. 1998. ARC, an inhibitor of apoptosis expressed in skeletal muscle and heart that interacts selectively with caspases. *Proc Natl Acad Sci U S A.* 95:5156-5160.
389. Kostapanos MS, Florentin M, and Elisaf MS. 2013. Gender differences in the epidemiology, clinical presentation, prevention, and prognosis of acute coronary syndromes. *Angiology.* 64:5-8.
390. Kosuge M, Kimura K, Ishikawa T, et al. 2006. Differences between men and women in terms of clinical features of ST-segment elevation acute myocardial infarction. *Circ J.* 70:222-226.
391. Krieg M, Smith K, and Bartsch W. 1978. Demonstration of a specific androgen receptor in rat heart muscle: relationship between binding, metabolism, and tissue levels of androgens. *Endocrinology.* 103:1686-1694.
392. Krijnen PA, Meischl C, Hack CE, et al. 2003. Increased Nox2 expression in human cardiomyocytes after acute myocardial infarction. *J Clin Pathol.* 56:194-199.
393. Krijnen PA, Nijmeijer R, Meijer CJ, et al. 2002. Apoptosis in myocardial ischaemia and infarction. *J Clin Pathol.* 55:801-811.
394. Kroemer G, Galluzzi L, and Brenner C. 2007. Mitochondrial membrane permeabilization in cell death. *Physiol Rev.* 87:99-163.

395. Krown KA, Page MT, Nguyen C, et al. 1996. Tumor necrosis factor alpha-induced apoptosis in cardiac myocytes. Involvement of the sphingolipid signaling cascade in cardiac cell death. *J Clin Invest.* 98:2854-2865.
396. Krozowski ZS, and Funder JW. 1983. Renal mineralocorticoid receptors and hippocampal corticosterone-binding species have identical intrinsic steroid specificity. *Proc Natl Acad Sci U S A.* 80:6056-6060.
397. Kuhar P, Lunder M, and Drevensek G. 2007. The role of gender and sex hormones in ischemic-reperfusion injury in isolated rat hearts. *Eur J Pharmacol.* 561:151-159.
398. Kuiper GG, Lemmen JG, Carlsson B, et al. 1998. Interaction of estrogenic chemicals and phytoestrogens with estrogen receptor beta. *Endocrinology.* 139:4252-4263.
399. Kuller LH. 2003. Hormone replacement therapy and risk of cardiovascular disease: implications of the results of the Women's Health Initiative. *Arterioscler Thromb Vasc Biol.* 23:11-16.
400. Kumar A, Taliyan R, and Sharma PL. 2012. Evaluation of thyroid hormone induced pharmacological preconditioning on cardiomyocyte protection against ischemic-reperfusion injury. *Indian J Pharmacol.* 44:68-72.
401. Kunzel HE, Apostolopoulou K, Pallauf A, et al. 2012. Quality of life in patients with primary aldosteronism: gender differences in untreated and long-term treated patients and associations with treatment and aldosterone. *J Psychiatr Res.* 46:1650-1654.
402. Kutala VK, Khan M, Mandal R, et al. 2006. Attenuation of myocardial ischemia-reperfusion injury by trimetazidine derivatives functionalized with antioxidant properties. *J Pharmacol Exp Ther.* 317:921-928.
403. Kwak SP, Patel PD, Thompson RC, et al. 1993. 5'-Heterogeneity of the mineralocorticoid receptor messenger ribonucleic acid: differential expression and regulation of splice variants within the rat hippocampus. *Endocrinology.* 133:2344-2350.
404. Laemmli UK. 1970. Cleavage of structural proteins during the assembly of the head of bacteriophage T4. *Nature.* 227:680-685.
405. Lambeth JD. 2004. NOX enzymes and the biology of reactive oxygen. *Nat Rev Immunol.* 4:181-189.
406. Langendorff O. 1898. O. Langendorff, Untersuchungen am überlebenden Säugetierherzen. *Pflügers Archiv.* 61:291-332.
407. Langer G, Bader B, Meoli L, et al. 2010. A critical review of fundamental controversies in the field of GPR30 research. *Steroids.* 75:603-610.
408. Lanneau D, Brunet M, Frisan E, et al. 2008. Heat shock proteins: essential proteins for apoptosis regulation. *J Cell Mol Med.* 12:743-761.
409. Larsen TA, Goodsell DS, Cascio D, et al. 1989. The structure of DAPI bound to DNA. *J Biomol Struct Dyn.* 7:477-491.

410. Laskowski A, Woodman OL, Cao AH, et al. 2006. Antioxidant actions contribute to the antihypertrophic effects of atrial natriuretic peptide in neonatal rat cardiomyocytes. *Cardiovasc Res.* 72:112-123.
411. Lassegue B, Sorescu D, Szocs K, et al. 2001. Novel gp91(phox) homologues in vascular smooth muscle cells : nox1 mediates angiotensin II-induced superoxide formation and redox-sensitive signaling pathways. *Circ Res.* 88:888-894.
412. Lastra G, Whaley-Connell A, Manrique C, et al. 2008. Low-dose spironolactone reduces reactive oxygen species generation and improves insulin-stimulated glucose transport in skeletal muscle in the TG(mRen2)27 rat. *Am J Physiol Endocrinol Metab.* 295:E110-116.
413. Latouche C, Sainte-Marie Y, Steenman M, et al. 2010. Molecular signature of mineralocorticoid receptor signaling in cardiomyocytes: from cultured cells to mouse heart. *Endocrinology.* 151:4467-4476.
414. Laughlin GA, Barrett-Connor E, and Bergstrom J. 2008. Low serum testosterone and mortality in older men. *J Clin Endocrinol Metab.* 93:68-75.
415. Lazou A, Iliodromitis EK, Cieslak D, et al. 2006. Ischemic but not mechanical preconditioning attenuates ischemia/reperfusion induced myocardial apoptosis in anaesthetized rabbits: the role of Bcl-2 family proteins and ERK1/2. *Apoptosis.* 11:2195-2204.
416. Le Moellic C, Ouvrard-Pascaud A, Capurro C, et al. 2004. Early nongenomic events in aldosterone action in renal collecting duct cells: PKCalpha activation, mineralocorticoid receptor phosphorylation, and cross-talk with the genomic response. *J Am Soc Nephrol.* 15:1145-1160.
417. Lee HL, Chen CL, Yeh ST, et al. 2012. Biphasic modulation of the mitochondrial electron transport chain in myocardial ischemia and reperfusion. *Am J Physiol Heart Circ Physiol.* 302:H1410-1422.
418. Lee TM, Lin MS, Chou TF, et al. 2004. Adjunctive 17beta-estradiol administration reduces infarct size by altered expression of canine myocardial connexin43 protein. *Cardiovasc Res.* 63:109-117.
419. Lehman JJ, and Kelly DP. 2002. Transcriptional activation of energy metabolic switches in the developing and hypertrophied heart. *Clin Exp Pharmacol Physiol.* 29:339-345.
420. Leichtweis S, and Ji LL. 2001. Glutathione deficiency intensifies ischaemia-reperfusion induced cardiac dysfunction and oxidative stress. *Acta Physiol Scand.* 172:1-10.
421. Leopold JA, Cap A, Scribner AW, et al. 2001. Glucose-6-phosphate dehydrogenase deficiency promotes endothelial oxidant stress and decreases endothelial nitric oxide bioavailability. *Faseb J.* 15:1771-1773.
422. Leopold JA, Dam A, Maron BA, et al. 2007. Aldosterone impairs vascular reactivity by decreasing glucose-6-phosphate dehydrogenase activity. *Nat Med.* 13:189-197.

423. Leopold JA, Zhang YY, Scribner AW, et al. 2003. Glucose-6-phosphate dehydrogenase overexpression decreases endothelial cell oxidant stress and increases bioavailable nitric oxide. *Arterioscler Thromb Vasc Biol.* 23:411-417.
424. Lesnefsky EJ, Repine JE, and Horwitz LD. 1989. Oxidation and release of glutathione from myocardium during early reperfusion. *Free Radic Biol Med.* 7:31-35.
425. Leto TL, Morand S, Hurt D, et al. 2009. Targeting and regulation of reactive oxygen species generation by Nox family NADPH oxidases. *Antioxid Redox Signal.* 11:2607-2619.
426. Levin ER. 2009. Plasma membrane estrogen receptors. *Trends Endocrinol Metab.* 20:477-482.
427. Levine B, and Kroemer G. 2008. Autophagy in the pathogenesis of disease. *Cell.* 132:27-42.
428. Levine B, and Yuan J. 2005. Autophagy in cell death: an innocent convict? *J Clin Invest.* 115:2679-2688.
429. Li H, Zhu H, Xu CJ, et al. 1998. Cleavage of BID by caspase 8 mediates the mitochondrial damage in the Fas pathway of apoptosis. *Cell.* 94:491-501.
430. Li J, Stouffs M, Serrander L, et al. 2006. The NADPH oxidase NOX4 drives cardiac differentiation: Role in regulating cardiac transcription factors and MAP kinase activation. *Mol Biol Cell.* 17:3978-3988.
431. Li JM, and Shah AM. 2002. Intracellular localization and preassembly of the NADPH oxidase complex in cultured endothelial cells. *J Biol Chem.* 277:19952-19960.
432. Li PF, Li J, Muller EC, et al. 2002. Phosphorylation by protein kinase CK2: a signaling switch for the caspase-inhibiting protein ARC. *Mol Cell.* 10:247-258.
433. Li Y, and Kloner RA. 1995. Is There a Gender Difference in Infarct Size and Arrhythmias Following Experimental Coronary Occlusion and Reperfusion? *J Thromb Thrombolysis.* 2:221-225.
434. Li Y, Suino K, Daugherty J, et al. 2005. Structural and biochemical mechanisms for the specificity of hormone binding and coactivator assembly by mineralocorticoid receptor. *Mol Cell.* 19:367-380.
435. Li YZ, Lu DY, Tan WQ, et al. 2008. p53 initiates apoptosis by transcriptionally targeting the antiapoptotic protein ARC. *Mol Cell Biol.* 28:564-574.
436. Liang XH, Jackson S, Seaman M, et al. 1999. Induction of autophagy and inhibition of tumorigenesis by beclin 1. *Nature.* 402:672-676.
437. Liedtke AJ, Hughes HC, and Neely JR. 1975. Metabolic responses to varying restrictions of coronary blood flow in swine. *Am J Physiol.* 228:655-662.
438. Lim-Tio SS, Keightley MC, and Fuller PJ. 1997. Determinants of specificity of transactivation by the mineralocorticoid or glucocorticoid receptor. *Endocrinology.* 138:2537-2543.

439. Lim SY, Hausenloy DJ, Arjun S, et al. 2011. Mitochondrial cyclophilin-D as a potential therapeutic target for post-myocardial infarction heart failure. *J Cell Mol Med.* 15:2443-2451.
440. Lin J, Tarr PT, Yang R, et al. 2003. PGC-1beta in the regulation of hepatic glucose and energy metabolism. *J Biol Chem.* 278:30843-30848.
441. Lin YH, Wu XM, Lee HH, et al. 2012. Adrenalectomy reverses myocardial fibrosis in patients with primary aldosteronism. *J Hypertens.* 30:1606-1613.
442. Ling S, Zhou L, Li H, et al. 2006. Effects of 17beta-estradiol on growth and apoptosis in human vascular endothelial cells: influence of mechanical strain and tumor necrosis factor-alpha. *Steroids.* 71:799-808.
443. Linkermann A, Brasen JH, Himmerkus N, et al. 2012. Rip1 (receptor-interacting protein kinase 1) mediates necroptosis and contributes to renal ischemia/reperfusion injury. *Kidney Int.* 81:751-761.
444. Lippi G, Franchini M, and Cervellin G. 2013. Diagnosis and management of ischemic heart disease. *Semin Thromb Hemost.* 39:202-213.
445. Liu A, Gao L, Kang S, et al. 2012. Testosterone enhances estradiol's cardioprotection in ovariectomized rats. *J Endocrinol.* 212:61-69.
446. Liu HR, Gao E, Hu A, et al. 2005a. Role of Omi/HtrA2 in apoptotic cell death after myocardial ischemia and reperfusion. *Circulation.* 111:90-96.
447. Liu J, Mao W, Ding B, et al. 2008. ERKs/p53 signal transduction pathway is involved in doxorubicin-induced apoptosis in H9c2 cells and cardiomyocytes. *Am J Physiol Heart Circ Physiol.* 295:H1956-1965.
448. Liu PY, Christian RC, Ruan M, et al. 2005b. Correlating androgen and estrogen steroid receptor expression with coronary calcification and atherosclerosis in men without known coronary artery disease. *J Clin Endocrinol Metab.* 90:1041-1046.
449. Liu W, Wang J, Sauter NK, et al. 1995. Steroid receptor heterodimerization demonstrated in vitro and in vivo. *Proc Natl Acad Sci U S A.* 92:12480-12484.
450. Liu X, Zou H, Slaughter C, et al. 1997. DFF, a heterodimeric protein that functions downstream of caspase-3 to trigger DNA fragmentation during apoptosis. *Cell.* 89:175-184.
451. Lizotte E, Grandy SA, Tremblay A, et al. 2009. Expression, distribution and regulation of sex steroid hormone receptors in mouse heart. *Cell Physiol Biochem.* 23:75-86.
452. Lombes M, Oblin ME, Gasc JM, et al. 1992. Immunohistochemical and biochemical evidence for a cardiovascular mineralocorticoid receptor. *Circ Res.* 71:503-510.
453. Looi YH, Grieve DJ, Siva A, et al. 2008. Involvement of Nox2 NADPH oxidase in adverse cardiac remodeling after myocardial infarction. *Hypertension.* 51:319-325.
454. Loor G, Kondapalli J, Iwase H, et al. 2011. Mitochondrial oxidant stress triggers cell death in simulated ischemia-reperfusion. *Biochim Biophys Acta.* 1813:1382-1394.

455. Lothar A, Berger S, Gilsbach R, et al. 2011. Ablation of mineralocorticoid receptors in myocytes but not in fibroblasts preserves cardiac function. *Hypertension*. 57:746-754.
456. Lu A, Frink M, Choudhry MA, et al. 2007. Mitochondria play an important role in 17beta-estradiol attenuation of H(2)O(2)-induced rat endothelial cell apoptosis. *Am J Physiol Endocrinol Metab*. 292:E585-593.
457. Lu D, Liu J, Jiao J, et al. 2013. Transcription factor Foxo3a prevents apoptosis by regulating calcium through the apoptosis repressor with caspase recruitment domain. *J Biol Chem*. 288:8491-8504.
458. Luo S, and Rubinsztein DC. 2010. Apoptosis blocks Beclin 1-dependent autophagosome synthesis: an effect rescued by Bcl-xL. *Cell Death Differ*. 17:268-277.
459. Lyn D, Bao S, Bennett NA, et al. 2002. Ischemia elicits a coordinated expression of pro-survival proteins in mouse myocardium. *ScientificWorldJournal*. 2:997-1003.
460. Ma X, Liu H, Foyil SR, et al. 2012a. Autophagy is impaired in cardiac ischemia-reperfusion injury. *Autophagy*. 8:1394-1396.
461. Ma X, Liu H, Foyil SR, et al. 2012b. Impaired autophagosome clearance contributes to cardiomyocyte death in ischemia/reperfusion injury. *Circulation*. 125:3170-3181.
462. Maack C, Kartes T, Kilter H, et al. 2003. Oxygen free radical release in human failing myocardium is associated with increased activity of rac1-GTPase and represents a target for statin treatment. *Circulation*. 108:1567-1574.
463. Machens K, and Schmidt-Gollwitzer K. 2003. Issues to debate on the Women's Health Initiative (WHI) study. Hormone replacement therapy: an epidemiological dilemma? *Hum Reprod*. 18:1992-1999.
464. Madesh M, Antonsson B, Srinivasula SM, et al. 2002. Rapid kinetics of tBid-induced cytochrome c and Smac/DIABLO release and mitochondrial depolarization. *J Biol Chem*. 277:5651-5659.
465. Maggiolini M, Vivacqua A, Fasanella G, et al. 2004. The G protein-coupled receptor GPR30 mediates c-fos up-regulation by 17beta-estradiol and phytoestrogens in breast cancer cells. *J Biol Chem*. 279:27008-27016.
466. Maiuri MC, Le Toumelin G, Criollo A, et al. 2007. Functional and physical interaction between Bcl-X(L) and a BH3-like domain in Beclin-1. *Embo J*. 26:2527-2539.
467. Malkin CJ, Pugh PJ, Morris PD, et al. 2010. Low serum testosterone and increased mortality in men with coronary heart disease. *Heart*. 96:1821-1825.
468. Mallat Z, Fornes P, Costagliola R, et al. 2001. Age and gender effects on cardiomyocyte apoptosis in the normal human heart. *J Gerontol A Biol Sci Med Sci*. 56:M719-723.

469. Manfroi WC, Peukert C, Berti CB, et al. 2002. Acute myocardial infarction: the first manifestation of ischemic heart disease and relation to risk factors. *Arq Bras Cardiol.* 78:392-395.
470. Mangelsdorf DJ, Thummel C, Beato M, et al. 1995. The nuclear receptor superfamily: the second decade. *Cell.* 83:835-839.
471. Mannic T, Mouffok M, Python M, et al. 2013. DHEA prevents mineralo- and glucocorticoid receptor-induced chronotropic and hypertrophic actions in isolated rat cardiomyocytes. *Endocrinology.* 154:1271-1281.
472. Mano A, Tatsumi T, Shiraishi J, et al. 2004. Aldosterone directly induces myocyte apoptosis through calcineurin-dependent pathways. *Circulation.* 110:317-323.
473. Marino M, Ascenzi P, and Acconcia F. 2006. S-palmitoylation modulates estrogen receptor alpha localization and functions. *Steroids.* 71:298-303.
474. Marsh JD, Lehmann MH, Ritchie RH, et al. 1998. Androgen receptors mediate hypertrophy in cardiac myocytes. *Circulation.* 98:256-261.
475. Martensson UE, Salehi SA, Windahl S, et al. 2009. Deletion of the G protein-coupled receptor 30 impairs glucose tolerance, reduces bone growth, increases blood pressure, and eliminates estradiol-stimulated insulin release in female mice. *Endocrinology.* 150:687-698.
476. Maselli A, Matarrese P, Straface E, et al. 2009. Cell sex: a new look at cell fate studies. *Faseb J.* 23:978-984.
477. Mathers CD, and Loncar D. 2006. Projections of global mortality and burden of disease from 2002 to 2030. *PLoS Med.* 3:e442.
478. Mathew JT, Patni H, Chaudhary AN, et al. 2008. Aldosterone induces mesangial cell apoptosis both in vivo and in vitro. *Am J Physiol Renal Physiol.* 295:F73-81.
479. Mathur R, and Braunstein GD. 2010. Androgen deficiency and therapy in women. *Curr Opin Endocrinol Diabetes Obes.* 17:342-349.
480. Matsubara T, and Dhalla NS. 1996. Relationship between mechanical dysfunction and depression of sarcolemmal Ca(2+)-pump activity in hearts perfused with oxygen free radicals. *Mol Cell Biochem.* 160-161:179-185.
481. Matsui H, Ando K, Kawarazaki H, et al. 2008a. Salt excess causes left ventricular diastolic dysfunction in rats with metabolic disorder. *Hypertension.* 52:287-294.
482. Matsui R, Xu S, Maitland KA, et al. 2006. Glucose-6-phosphate dehydrogenase deficiency decreases vascular superoxide and atherosclerotic lesions in apolipoprotein E(-/-) mice. *Arterioscler Thromb Vasc Biol.* 26:910-916.
483. Matsui Y, Kyo S, Takagi H, et al. 2008b. Molecular mechanisms and physiological significance of autophagy during myocardial ischemia and reperfusion. *Autophagy.* 4:409-415.
484. Matsui Y, Takagi H, Qu X, et al. 2007. Distinct roles of autophagy in the heart during ischemia and reperfusion: roles of AMP-activated protein kinase and Beclin 1 in mediating autophagy. *Circ Res.* 100:914-922.

485. Matsumoto R, Yoshiyama M, Omura T, et al. 2004. Effects of aldosterone receptor antagonist and angiotensin II type I receptor blocker on cardiac transcriptional factors and mRNA expression in rats with myocardial infarction. *Circ J*. 68:376-382.
486. Maulik N, Engelman RM, Rousou JA, et al. 1999. Ischemic preconditioning reduces apoptosis by upregulating anti-death gene Bcl-2. *Circulation*. 100:II369-375.
487. Maulik N, Engelman RM, Wei Z, et al. 1993. Interleukin-1 alpha preconditioning reduces myocardial ischemia reperfusion injury. *Circulation*. 88:II387-394.
488. McCormick J, Suleman N, Scarabelli TM, et al. 2012. STAT1 deficiency in the heart protects against myocardial infarction by enhancing autophagy. *J Cell Mol Med*. 16:386-393.
489. McCrohon JA, Death AK, Nakhla S, et al. 2000. Androgen receptor expression is greater in macrophages from male than from female donors. A sex difference with implications for atherogenesis. *Circulation*. 101:224-226.
490. McCullers DL, and Herman JP. 1998. Mineralocorticoid receptors regulate bcl-2 and p53 mRNA expression in hippocampus. *Neuroreport*. 9:3085-3089.
491. McCully JD, Wakiyama H, Hsieh YJ, et al. 2004. Differential contribution of necrosis and apoptosis in myocardial ischemia-reperfusion injury. *Am J Physiol Heart Circ Physiol*. 286:H1923-1935.
492. McIntosh R, Lee S, Ghio AJ, et al. 2010. The critical role of intracellular zinc in adenosine A(2) receptor activation induced cardioprotection against reperfusion injury. *J Mol Cell Cardiol*. 49:41-47.
493. McKenna NJ, Lanz RB, and O'Malley BW. 1999a. Nuclear receptor coregulators: cellular and molecular biology. *Endocr Rev*. 20:321-344.
494. McKenna NJ, Xu J, Nawaz Z, et al. 1999b. Nuclear receptor coactivators: multiple enzymes, multiple complexes, multiple functions. *J Steroid Biochem Mol Biol*. 69:3-12.
495. Meachem SJ, Schlatt S, Ruwanpura SM, et al. 2007. The effect of testosterone, dihydrotestosterone and oestradiol on the re-initiation of spermatogenesis in the adult photoinhibited Djungarian hamster. *J Endocrinol*. 192:553-561.
496. Mehilli J, Ndrepepa G, Kastrati A, et al. 2005. Gender and myocardial salvage after reperfusion treatment in acute myocardial infarction. *J Am Coll Cardiol*. 45:828-831.
497. Meirhaeghe A, Crowley V, Lenaghan C, et al. 2003. Characterization of the human, mouse and rat PGC1 beta (peroxisome-proliferator-activated receptor-gamma co-activator 1 beta) gene in vitro and in vivo. *Biochem J*. 373:155-165.
498. Meloni L, Manca MR, Loddo I, et al. 2008. Glucose-6-phosphate dehydrogenase deficiency protects against coronary heart disease. *J Inherit Metab Dis*. 31:412-417.
499. Mendelsohn ME. 2000. Mechanisms of estrogen action in the cardiovascular system. *J Steroid Biochem Mol Biol*. 74:337-343.

500. Mendelsohn ME, and Karas RH. 1999. The protective effects of estrogen on the cardiovascular system. *N Engl J Med.* 340:1801-1811.
501. Meng X, Dai X, Liao TD, et al. 2011. Dose-dependent toxic effects of high-dose estrogen on renal and cardiac injury in surgically postmenopausal mice. *Life Sci.* 88:178-186.
502. Mentz RJ, Bakris GL, Waeber B, et al. 2012. The past, present and future of renin-angiotensin aldosterone system inhibition. *Int J Cardiol.*
503. Merrill DC, Ebert TJ, Skelton MM, et al. 1989. Effect of plasma sodium on aldosterone secretion during angiotensin II stimulation in normal humans. *Hypertension.* 14:164-169.
504. Mersmann J, Latsch K, Habeck K, et al. 2011. Measure for measure-determination of infarct size in murine models of myocardial ischemia and reperfusion: a systematic review. *Shock.* 35:449-455.
505. Messaoudi S, Gravez B, Tarjus A, et al. 2013. Aldosterone-specific activation of cardiomyocyte mineralocorticoid receptor in vivo. *Hypertension.* 61:361-367.
506. Michea L, Delpiano AM, Hitschfeld C, et al. 2005. Eplerenone blocks nongenomic effects of aldosterone on the Na⁺/H⁺ exchanger, intracellular Ca²⁺ levels, and vasoconstriction in mesenteric resistance vessels. *Endocrinology.* 146:973-980.
507. Mieyal JJ, Gallogly MM, Qanungo S, et al. 2008. Molecular mechanisms and clinical implications of reversible protein S-glutathionylation. *Antioxid Redox Signal.* 10:1941-1988.
508. Migliaresi P, Celentano A, Palmieri V, et al. 2007. Knowledge of cardiovascular risk factors and awareness of non-pharmacological approach for risk prevention in young survivors of acute myocardial infarction. The cardiovascular risk prevention project "Help Your Heart Stay Young". *Nutr Metab Cardiovasc Dis.* 17:468-472.
509. Mihailidou AS, Buhagiar KA, and Rasmussen HH. 1998. Na⁺ influx and Na(+)-K⁺ pump activation during short-term exposure of cardiac myocytes to aldosterone. *Am J Physiol.* 274:C175-181.
510. Mihailidou AS, Loan Le TY, Mardini M, et al. 2009. Glucocorticoids activate cardiac mineralocorticoid receptors during experimental myocardial infarction. *Hypertension.* 54:1306-1312.
511. Mihailidou AS, Mardini M, and Funder JW. 2004. Rapid, nongenomic effects of aldosterone in the heart mediated by epsilon protein kinase C. *Endocrinology.* 145:773-780.
512. Mikhailov V, Mikhailova M, Degenhardt K, et al. 2003. Association of Bax and Bak homo-oligomers in mitochondria. Bax requirement for Bak reorganization and cytochrome c release. *J Biol Chem.* 278:5367-5376.
513. Milik E, Szczepanska-Sadowska E, Maslinski W, et al. 2007. Enhanced expression of mineralocorticoid receptors in the heart after the myocardial infarct in rats. *J Physiol Pharmacol.* 58:745-755.

514. Miller KK. 2001. Androgen deficiency in women. *J Clin Endocrinol Metab.* 86:2395-2401.
515. Miller VM, and Duckles SP. 2008. Vascular actions of estrogens: functional implications. *Pharmacol Rev.* 60:210-241.
516. Miller WL, and Auchus RJ. 2011. The molecular biology, biochemistry, and physiology of human steroidogenesis and its disorders. *Endocr Rev.* 32:81-151.
517. Milliez P, Girerd X, Plouin PF, et al. 2005. Evidence for an increased rate of cardiovascular events in patients with primary aldosteronism. *J Am Coll Cardiol.* 45:1243-1248.
518. Miura H, Kiuchi K, Nejima J, et al. 2002. Limitation of infarct size and ventricular remodeling in patients with completely reperfused anterior acute myocardial infarction--the potential role of ischemia time. *Clin Cardiol.* 25:566-571.
519. Miura M, Matsu-oka H, Saito T, et al. 1991. The pathophysiology of myocardial stunning: reversibility, accumulation and continuity of the ischemic myocardial damage after reperfusion. *Jpn Circ J.* 55:868-877.
520. Miura T, Nishihara M, and Miki T. 2009. Drug development targeting the glycogen synthase kinase-3beta (GSK-3beta)-mediated signal transduction pathway: role of GSK-3beta in myocardial protection against ischemia/reperfusion injury. *J Pharmacol Sci.* 109:162-167.
521. Mizukami Y, Ono K, Du CK, et al. 2008. Identification and physiological activity of survival factor released from cardiomyocytes during ischaemia and reperfusion. *Cardiovasc Res.* 79:589-599.
522. Mizushima N, Yamamoto A, Hatano M, et al. 2001. Dissection of autophagosome formation using Apg5-deficient mouse embryonic stem cells. *J Cell Biol.* 152:657-668.
523. Mochizuki H, Nakamura N, Nishi K, et al. 1994. Apoptosis is induced by 1-methyl-4-phenylpyridinium ion (MPP+) in ventral mesencephalic-striatal co-culture in rat. *Neurosci Lett.* 170:191-194.
524. Moquin D, and Chan FK. 2010. The molecular regulation of programmed necrotic cell injury. *Trends Biochem Sci.* 35:434-441.
525. Morel O, Perret T, Delarche N, et al. 2012. Pharmacological approaches to reperfusion therapy. *Cardiovasc Res.* 94:246-252.
526. Moreno-Sanchez R, Hernandez-Esquivel L, Rivero-Segura NA, et al. 2013. Reactive oxygen species are generated by the respiratory complex II--evidence for lack of contribution of the reverse electron flow in complex I. *Febs J.* 280:927-938.
527. Mori-Abe A, Tsutsumi S, Takahashi K, et al. 2003. Estrogen and raloxifene induce apoptosis by activating p38 mitogen-activated protein kinase cascade in synthetic vascular smooth muscle cells. *J Endocrinol.* 178:417-426.
528. Moriarty K, Kim KH, and Bender JR. 2006. Minireview: estrogen receptor-mediated rapid signaling. *Endocrinology.* 147:5557-5563.

529. Morrison N, Harrap SB, Arriza JL, et al. 1990. Regional chromosomal assignment of the human mineralocorticoid receptor gene to 4q31.1. *Hum Genet.* 85:130-132.
530. Mosca L. 2000. The role of hormone replacement therapy in the prevention of postmenopausal heart disease. *Arch Intern Med.* 160:2263-2272.
531. Moudgil R, Menon V, Xu Y, et al. 2001. Postischemic apoptosis and functional recovery after angiotensin II type 1 receptor blockade in isolated working rat hearts. *J Hypertens.* 19:1121-1129.
532. Moura AM, and Worcel M. 1984. Direct action of aldosterone on transmembrane ^{22}Na efflux from arterial smooth muscle. Rapid and delayed effects. *Hypertension.* 6:425-430.
533. Mourmoura E, Leguen M, Dubouchaud H, et al. 2011. Middle age aggravates myocardial ischemia through surprising upholding of complex II activity, oxidative stress, and reduced coronary perfusion. *Age (Dordr).* 33:321-336.
534. Mulder P, Mellin V, Favre J, et al. 2008. Aldosterone synthase inhibition improves cardiovascular function and structure in rats with heart failure: a comparison with spironolactone. *Eur Heart J.* 29:2171-2179.
535. Mulrow PJ. 1999. Angiotensin II and aldosterone regulation. *Regul Pept.* 80:27-32.
536. Munck A, and Guyre PM. 1986. Glucocorticoid physiology, pharmacology and stress. *Adv Exp Med Biol.* 196:81-96.
537. Murphy E, and Steenbergen C. 2008. Ion transport and energetics during cell death and protection. *Physiology (Bethesda).* 23:115-123.
538. Murtaza I, Wang HX, Feng X, et al. 2008. Down-regulation of catalase and oxidative modification of protein kinase CK2 lead to the failure of apoptosis repressor with caspase recruitment domain to inhibit cardiomyocyte hypertrophy. *J Biol Chem.* 283:5996-6004.
539. Nagase M, Ayuzawa N, Kawarazaki W, et al. 2012. Oxidative stress causes mineralocorticoid receptor activation in rat cardiomyocytes: role of small GTPase Rac1. *Hypertension.* 59:500-506.
540. Nagase M, Matsui H, Shibata S, et al. 2007. Salt-induced nephropathy in obese spontaneously hypertensive rats via paradoxical activation of the mineralocorticoid receptor: role of oxidative stress. *Hypertension.* 50:877-883.
541. Nakagawa T, Shimizu S, Watanabe T, et al. 2005. Cyclophilin D-dependent mitochondrial permeability transition regulates some necrotic but not apoptotic cell death. *Nature.* 434:652-658.
542. Nakamura Y, Suzuki S, Suzuki T, et al. 2006. MDM2: a novel mineralocorticoid-responsive gene involved in aldosterone-induced human vascular structural remodeling. *Am J Pathol.* 169:362-371.
543. Nam UH, Wang M, Crisostomo PR, et al. 2007a. The effect of chronic exogenous androgen on myocardial function following acute ischemia-reperfusion in hosts with different baseline levels of sex steroids. *J Surg Res.* 142:113-118.

544. Nam YJ, Mani K, Ashton AW, et al. 2004. Inhibition of both the extrinsic and intrinsic death pathways through nonhomotypic death-fold interactions. *Mol Cell*. 15:901-912.
545. Nam YJ, Mani K, Wu L, et al. 2007b. The apoptosis inhibitor ARC undergoes ubiquitin-proteasomal-mediated degradation in response to death stimuli: identification of a degradation-resistant mutant. *J Biol Chem*. 282:5522-5528.
546. Napoli C, Di Gregorio F, Leccese M, et al. 1999. Evidence of exercise-induced myocardial ischemia in patients with primary aldosteronism: the Cross-sectional Primary Aldosteronism and Heart Italian Multicenter Study. *J Investig Med*. 47:212-221.
547. Naray-Fejes-Toth A, and Fejes-Toth G. 2000. The *sgk*, an aldosterone-induced gene in mineralocorticoid target cells, regulates the epithelial sodium channel. *Kidney Int*. 57:1290-1294.
548. Ndrepepa G, Mehilli J, Tiroch K, et al. 2010. Myocardial perfusion grade, myocardial salvage indices and long-term mortality in patients with acute myocardial infarction and full restoration of epicardial blood flow after primary percutaneous coronary intervention. *Rev Esp Cardiol*. 63:770-778.
549. Nechushtan A, Smith CL, Hsu YT, et al. 1999. Conformation of the Bax C-terminus regulates subcellular location and cell death. *Embo J*. 18:2330-2341.
550. Neely JR, Rovetto MJ, Whitmer JT, et al. 1973. Effects of ischemia on function and metabolism of the isolated working rat heart. *Am J Physiol*. 225:651-658.
551. Negoescu A, Guillermet C, Lorimier P, et al. 1998. Importance of DNA fragmentation in apoptosis with regard to TUNEL specificity. *Biomed Pharmacother*. 52:252-258.
552. Nelson DP, Wechsler SB, Miura T, et al. 2002. Myocardial immediate early gene activation after cardiopulmonary bypass with cardiac ischemia-reperfusion. *Ann Thorac Surg*. 73:156-162.
553. Neuss M, Monticone R, Lundberg MS, et al. 2001. The apoptotic regulatory protein ARC (apoptosis repressor with caspase recruitment domain) prevents oxidant stress-mediated cell death by preserving mitochondrial function. *J Biol Chem*. 276:33915-33922.
554. Nicholson DW, Ali A, Thornberry NA, et al. 1995. Identification and inhibition of the ICE/CED-3 protease necessary for mammalian apoptosis. *Nature*. 376:37-43.
555. Niles NW, Conley SM, Yang RC, et al. 2010. Primary percutaneous coronary intervention for patients presenting with ST-segment elevation myocardial infarction: process improvement in a rural ST-segment elevation myocardial infarction receiving center. *Prog Cardiovasc Dis*. 53:202-209.
556. Nishi M, Ogawa H, Ito T, et al. 2001. Dynamic changes in subcellular localization of mineralocorticoid receptor in living cells: in comparison with glucocorticoid receptor using dual-color labeling with green fluorescent protein spectral variants. *Mol Endocrinol*. 15:1077-1092.

557. Nishizawa J, Nakai A, Matsuda K, et al. 1999. Reactive oxygen species play an important role in the activation of heat shock factor 1 in ischemic-reperfused heart. *Circulation*. 99:934-941.
558. Noda K, Kobara M, Hamada J, et al. 2012. Additive amelioration of oxidative stress and cardiac function by combined mineralocorticoid and angiotensin receptor blockers in postinfarct failing hearts. *J Cardiovasc Pharmacol*. 60:140-149.
559. Nordlie MA, Wold LE, and Kloner RA. 2005. Genetic contributors toward increased risk for ischemic heart disease. *J Mol Cell Cardiol*. 39:667-679.
560. Nordmeyer J, Eder S, Mahmoodzadeh S, et al. 2004. Upregulation of myocardial estrogen receptors in human aortic stenosis. *Circulation*. 110:3270-3275.
561. Notarangelo MF, Coppini L, Guidorossi A, et al. 2012. [Genetic basis of ischemic heart disease. Do women have distinctive characteristics?]. *G Ital Cardiol (Rome)*. 13:386-395.
562. Nuutinen EM. 1984. Subcellular origin of the surface fluorescence of reduced nicotinamide nucleotides in the isolated perfused rat heart. *Basic Res Cardiol*. 79:49-58.
563. O'Brien MA, Moravec RA, and Riss TL. 2001. Poly (ADP-ribose) polymerase cleavage monitored in situ in apoptotic cells. *Biotechniques*. 30:886-891.
564. O'Dowd BF, Nguyen T, Marchese A, et al. 1998. Discovery of three novel G-protein-coupled receptor genes. *Genomics*. 47:310-313.
565. O'Gara PT, Kushner FG, Ascheim DD, et al. 2013. 2013 ACCF/AHA guideline for the management of ST-elevation myocardial infarction: a report of the American College of Cardiology Foundation/American Heart Association Task Force on Practice Guidelines. *J Am Coll Cardiol*. 61:e78-140.
566. Oberstein A, Jeffrey PD, and Shi Y. 2007. Crystal structure of the Bcl-XL-Bcl-1 peptide complex: Bcl-1 is a novel BH3-only protein. *J Biol Chem*. 282:13123-13132.
567. Ojha N, Roy S, Radtke J, et al. 2008. Characterization of the structural and functional changes in the myocardium following focal ischemia-reperfusion injury. *Am J Physiol Heart Circ Physiol*. 294:H2435-2443.
568. Olivetti G, Giordano G, Corradi D, et al. 1995. Gender differences and aging: effects on the human heart. *J Am Coll Cardiol*. 26:1068-1079.
569. Olivetti G, Quaini F, Sala R, et al. 1996. Acute myocardial infarction in humans is associated with activation of programmed myocyte cell death in the surviving portion of the heart. *J Mol Cell Cardiol*. 28:2005-2016.
570. Pagano PJ, Clark JK, Cifuentes-Pagano ME, et al. 1997. Localization of a constitutively active, phagocyte-like NADPH oxidase in rabbit aortic adventitia: enhancement by angiotensin II. *Proc Natl Acad Sci U S A*. 94:14483-14488.
571. Palmer BR, Pilbrow AP, Frampton CM, et al. 2008. Plasma aldosterone levels during hospitalization are predictive of survival post-myocardial infarction. *Eur Heart J*. 29:2489-2496.

572. Palmer BS, Hadziahmetovic M, Veci T, et al. 2004. Global ischemic duration and reperfusion function in the isolated perfused rat heart. *Resuscitation*. 62:97-106.
573. Palojoki E, Saraste A, Eriksson A, et al. 2001. Cardiomyocyte apoptosis and ventricular remodeling after myocardial infarction in rats. *Am J Physiol Heart Circ Physiol*. 280:H2726-2731.
574. Pan JA, Fan Y, Gandhirajan RK, et al. 2013. Hyperactivation of the mammalian degenerin MDEG promotes caspase-8 activation and apoptosis. *J Biol Chem*. 288:2952-2963.
575. Pankiv S, Clausen TH, Lamark T, et al. 2007. p62/SQSTM1 binds directly to Atg8/LC3 to facilitate degradation of ubiquitinated protein aggregates by autophagy. *J Biol Chem*. 282:24131-24145.
576. Papakonstantinou NA, Stamou MI, Baikoussis NG, et al. 2013. Sex differentiation with regard to coronary artery disease. *J Cardiol*.
577. Paradies G, Petrosillo G, Pistolese M, et al. 2004. Decrease in mitochondrial complex I activity in ischemic/reperfused rat heart: involvement of reactive oxygen species and cardiolipin. *Circ Res*. 94:53-59.
578. Park Y, Kanekal S, and Kehrer JP. 1991. Oxidative changes in hypoxic rat heart tissue. *Am J Physiol*. 260:H1395-1405.
579. Pascual-Le Tallec L, and Lombes M. 2005. The mineralocorticoid receptor: a journey exploring its diversity and specificity of action. *Mol Endocrinol*. 19:2211-2221.
580. Passarelli C, Tozzi G, Pastore A, et al. 2010. GSSG-mediated Complex I defect in isolated cardiac mitochondria. *Int J Mol Med*. 26:95-99.
581. Patni H, Mathew JT, Luan L, et al. 2007. Aldosterone promotes proximal tubular cell apoptosis: role of oxidative stress. *Am J Physiol Renal Physiol*. 293:F1065-1071.
582. Patten RD, Pourati I, Aronovitz MJ, et al. 2004. 17beta-estradiol reduces cardiomyocyte apoptosis in vivo and in vitro via activation of phospho-inositide-3 kinase/Akt signaling. *Circ Res*. 95:692-699.
583. Pattingre S, Tassa A, Qu X, et al. 2005. Bcl-2 antiapoptotic proteins inhibit Beclin 1-dependent autophagy. *Cell*. 122:927-939.
584. Pawlak M, Lefebvre P, and Staels B. 2012. General molecular biology and architecture of nuclear receptors. *Curr Top Med Chem*. 12:486-504.
585. Pearce P, and Funder JW. 1987. High affinity aldosterone binding sites (type I receptors) in rat heart. *Clin Exp Pharmacol Physiol*. 14:859-866.
586. Pedram A, Razandi M, and Levin ER. 2006a. Nature of functional estrogen receptors at the plasma membrane. *Mol Endocrinol*. 20:1996-2009.
587. Pedram A, Razandi M, Wallace DC, et al. 2006b. Functional estrogen receptors in the mitochondria of breast cancer cells. *Mol Biol Cell*. 17:2125-2137.

588. Pelzer T, Schumann M, Neumann M, et al. 2000. 17beta-estradiol prevents programmed cell death in cardiac myocytes. *Biochem Biophys Res Commun.* 268:192-200.
589. Penumathsa SV, Thirunavukkarasu M, Koneru S, et al. 2007. Statin and resveratrol in combination induces cardioprotection against myocardial infarction in hypercholesterolemic rat. *J Mol Cell Cardiol.* 42:508-516.
590. Perez-Lopez FR, Larrad-Mur L, Kallen A, et al. 2010. Gender differences in cardiovascular disease: hormonal and biochemical influences. *Reprod Sci.* 17:511-531.
591. Perez-Reyes E, Kim HS, Lacerda AE, et al. 1989. Induction of calcium currents by the expression of the alpha 1-subunit of the dihydropyridine receptor from skeletal muscle. *Nature.* 340:233-236.
592. Perrelli MG, Pagliaro P, and Penna C. 2011. Ischemia/reperfusion injury and cardioprotective mechanisms: Role of mitochondria and reactive oxygen species. *World J Cardiol.* 3:186-200.
593. Perrier R, Richard S, Sainte-Marie Y, et al. 2005. A direct relationship between plasma aldosterone and cardiac L-type Ca²⁺ current in mice. *J Physiol.* 569:153-162.
594. Peshavariya HM, Dusting GJ, and Selemidis S. 2007. Analysis of dihydroethidium fluorescence for the detection of intracellular and extracellular superoxide produced by NADPH oxidase. *Free Radic Res.* 41:699-712.
595. Pessoa BS, Peixoto EB, Papadimitriou A, et al. 2012. Spironolactone improves nephropathy by enhancing glucose-6-phosphate dehydrogenase activity and reducing oxidative stress in diabetic hypertensive rat. *J Renin Angiotensin Aldosterone Syst.* 13:56-66.
596. Peters SC, and Piper HM. 2007. Reoxygenation-induced Ca²⁺ rise is mediated via Ca²⁺ influx and Ca²⁺ release from the endoplasmic reticulum in cardiac endothelial cells. *Cardiovasc Res.* 73:164-171.
597. Petrosillo G, Ruggiero FM, Di Venosa N, et al. 2003. Decreased complex III activity in mitochondria isolated from rat heart subjected to ischemia and reperfusion: role of reactive oxygen species and cardiolipin. *Faseb J.* 17:714-716.
598. Phillips GB, Castelli WP, Abbott RD, et al. 1983. Association of hyperestrogenemia and coronary heart disease in men in the Framingham cohort. *Am J Med.* 74:863-869.
599. Pippal JB, and Fuller PJ. 2008. Structure-function relationships in the mineralocorticoid receptor. *J Mol Endocrinol.* 41:405-413.
600. Pitt B, Kober L, Ponikowski P, et al. 2013. Safety and tolerability of the novel non-steroidal mineralocorticoid receptor antagonist BAY 94-8862 in patients with chronic heart failure and mild or moderate chronic kidney disease: a randomized, double-blind trial. *Eur Heart J.*
601. Pitt B, Remme W, Zannad F, et al. 2003. Eplerenone, a selective aldosterone blocker, in patients with left ventricular dysfunction after myocardial infarction. *N Engl J Med.* 348:1309-1321.

602. Pitt B, Williams G, Remme W, et al. 2001. The EPHEBUS trial: eplerenone in patients with heart failure due to systolic dysfunction complicating acute myocardial infarction. Eplerenone Post-AMI Heart Failure Efficacy and Survival Study. *Cardiovasc Drugs Ther.* 15:79-87.
603. Pitt B, Zannad F, Remme WJ, et al. 1999. The effect of spironolactone on morbidity and mortality in patients with severe heart failure. Randomized Aldactone Evaluation Study Investigators. *N Engl J Med.* 341:709-717.
604. Plumier JC, Robertson HA, and Currie RW. 1996. Differential accumulation of mRNA for immediate early genes and heat shock genes in heart after ischaemic injury. *J Mol Cell Cardiol.* 28:1251-1260.
605. Pollak N, Dolle C, and Ziegler M. 2007. The power to reduce: pyridine nucleotides--small molecules with a multitude of functions. *Biochem J.* 402:205-218.
606. Portera-Cailliau C, Sung CH, Nathans J, et al. 1994. Apoptotic photoreceptor cell death in mouse models of retinitis pigmentosa. *Proc Natl Acad Sci U S A.* 91:974-978.
607. Potts MB, Vaughn AE, McDonough H, et al. 2005. Reduced Apaf-1 levels in cardiomyocytes engage strict regulation of apoptosis by endogenous XIAP. *J Cell Biol.* 171:925-930.
608. Preston GA, Lyon TT, Yin Y, et al. 1996. Induction of apoptosis by c-Fos protein. *Mol Cell Biol.* 16:211-218.
609. Prossnitz ER, Arterburn JB, and Sklar LA. 2007. GPR30: A G protein-coupled receptor for estrogen. *Mol Cell Endocrinol.* 265-266:138-142.
610. Prossnitz ER, Arterburn JB, Smith HO, et al. 2008. Estrogen signaling through the transmembrane G protein-coupled receptor GPR30. *Annu Rev Physiol.* 70:165-190.
611. Przyklenk K, Ovize M, Bauer B, et al. 1995. Gender does not influence acute myocardial infarction in adult dogs. *Am Heart J.* 129:1108-1113.
612. Purim-Shem-Tov YA, Melgoza N, Haw J, et al. 2012. Achieving high quality in ST-segment elevation myocardial infarction care: one urban academic medical center experience. *Crit Pathw Cardiol.* 11:32-39.
613. Pyo JO, Nah J, Kim HJ, et al. 2008. Protection of cardiomyocytes from ischemic/hypoxic cell death via Drbp1 and pMe2GlyDH in cardio-specific ARC transgenic mice. *J Biol Chem.* 283:30707-30714.
614. Qi XL, Nguyen TL, Andries L, et al. 1998. Vascular endothelial dysfunction contributes to myocardial depression in ischemia-reperfusion in the rat. *Can J Physiol Pharmacol.* 76:35-45.
615. Qian J, Ren X, Wang X, et al. 2009. Blockade of Hsp20 phosphorylation exacerbates cardiac ischemia/reperfusion injury by suppressed autophagy and increased cell death. *Circ Res.* 105:1223-1231.

616. Qin F, Simeone M, and Patel R. 2007. Inhibition of NADPH oxidase reduces myocardial oxidative stress and apoptosis and improves cardiac function in heart failure after myocardial infarction. *Free Radic Biol Med.* 43:271-281.
617. Qin W, Rudolph AE, Bond BR, et al. 2003. Transgenic model of aldosterone-driven cardiac hypertrophy and heart failure. *Circ Res.* 93:69-76.
618. Qin Y, Vanden Hoek TL, Wojcik K, et al. 2004. Caspase-dependent cytochrome c release and cell death in chick cardiomyocytes after simulated ischemia-reperfusion. *Am J Physiol Heart Circ Physiol.* 286:H2280-2286.
619. Qu S, Zhu H, Wei X, et al. 2010. Oxidative stress-mediated up-regulation of myocardial ischemic preconditioning up-regulated protein 1 gene expression in H9c2 cardiomyocytes is regulated by cyclic AMP-response element binding protein. *Free Radic Biol Med.* 49:580-586.
620. Quigley CA, De Bellis A, Marschke KB, et al. 1995. Androgen receptor defects: historical, clinical, and molecular perspectives. *Endocr Rev.* 16:271-321.
621. Quinn SJ, and Williams GH. 1988. Regulation of aldosterone secretion. *Annu Rev Physiol.* 50:409-426.
622. Raedschelders K, Ansley DM, and Chen DD. 2012. The cellular and molecular origin of reactive oxygen species generation during myocardial ischemia and reperfusion. *Pharmacol Ther.* 133:230-255.
623. Rajagopalan S, Duquaine D, King S, et al. 2002. Mineralocorticoid receptor antagonism in experimental atherosclerosis. *Circulation.* 105:2212-2216.
624. Ram RV, and Trivedi AV. 2012. Behavioral risk factors of coronary artery disease: A paired matched case control study. *J Cardiovasc Dis Res.* 3:212-217.
625. Rao L, Perez D, and White E. 1996. Lamin proteolysis facilitates nuclear events during apoptosis. *J Cell Biol.* 135:1441-1455.
626. Redel A, Jazbutyte V, Smul TM, et al. 2008. Impact of ischemia and reperfusion times on myocardial infarct size in mice in vivo. *Exp Biol Med (Maywood).* 233:84-93.
627. Redout EM, Wagner MJ, Zuidwijk MJ, et al. 2007. Right-ventricular failure is associated with increased mitochondrial complex II activity and production of reactive oxygen species. *Cardiovasc Res.* 75:770-781.
628. Reimer KA, Ideker RE, and Jennings RB. 1981. Effect of coronary occlusion site on ischaemic bed size and collateral blood flow in dogs. *Cardiovasc Res.* 15:668-674.
629. Reimer KA, Jennings RB, and Tatum AH. 1983. Pathobiology of acute myocardial ischemia: metabolic, functional and ultrastructural studies. *Am J Cardiol.* 52:72A-81A.
630. Ren D, Tu HC, Kim H, et al. 2010. BID, BIM, and PUMA are essential for activation of the BAX- and BAK-dependent cell death program. *Science.* 330:1390-1393.
631. Ren R, Oakley RH, Cruz-Topete D, et al. 2012. Dual role for glucocorticoids in cardiomyocyte hypertrophy and apoptosis. *Endocrinology.* 153:5346-5360.

632. Revankar CM, Cimino DF, Sklar LA, et al. 2005. A transmembrane intracellular estrogen receptor mediates rapid cell signaling. *Science*. 307:1625-1630.
633. Revankar CM, Mitchell HD, Field AS, et al. 2007. Synthetic estrogen derivatives demonstrate the functionality of intracellular GPR30. *ACS Chem Biol*. 2:536-544.
634. Revollo JR, Grimm AA, and Imai S. 2007. The regulation of nicotinamide adenine dinucleotide biosynthesis by Nampt/PBEF/visfatin in mammals. *Curr Opin Gastroenterol*. 23:164-170.
635. Ricchiuti V, Lapointe N, Pojoga L, et al. 2011. Dietary sodium intake regulates angiotensin II type 1, mineralocorticoid receptor, and associated signaling proteins in heart. *J Endocrinol*. 211:47-54.
636. Rickard AJ, Morgan J, Bienvenu LA, et al. 2012. Cardiomyocyte mineralocorticoid receptors are essential for deoxycorticosterone/salt-mediated inflammation and cardiac fibrosis. *Hypertension*. 60:1443-1450.
637. Rickard AJ, Morgan J, Tesch G, et al. 2009. Deletion of mineralocorticoid receptors from macrophages protects against deoxycorticosterone/salt-induced cardiac fibrosis and increased blood pressure. *Hypertension*. 54:537-543.
638. Riedl SJ, Renatus M, Schwarzenbacher R, et al. 2001. Structural basis for the inhibition of caspase-3 by XIAP. *Cell*. 104:791-800.
639. Riehle C, Wende AR, Zaha VG, et al. 2011. PGC-1beta deficiency accelerates the transition to heart failure in pressure overload hypertrophy. *Circ Res*. 109:783-793.
640. Rigsby CS, Burch AE, Ogbi S, et al. 2007. Intact female stroke-prone hypertensive rats lack responsiveness to mineralocorticoid receptor antagonists. *Am J Physiol Regul Integr Comp Physiol*. 293:R1754-1763.
641. Robin E, Guzy RD, Loor G, et al. 2007. Oxidant stress during simulated ischemia primes cardiomyocytes for cell death during reperfusion. *J Biol Chem*. 282:19133-19143.
642. Rockhold RW. 1993. Cardiovascular toxicity of anabolic steroids. *Annu Rev Pharmacol Toxicol*. 33:497-520.
643. Roger VL, Go AS, Lloyd-Jones DM, et al. 2012. Heart disease and stroke statistics--2012 update: a report from the American Heart Association. *Circulation*. 125:e2-e220.
644. Rogerson FM, and Fuller PJ. 2003. Interdomain interactions in the mineralocorticoid receptor. *Mol Cell Endocrinol*. 200:45-55.
645. Rong F, Peng Z, Ye MX, et al. 2009. Myocardial apoptosis and infarction after ischemia/reperfusion are attenuated by kappa-opioid receptor agonist. *Arch Med Res*. 40:227-234.
646. Rosano GM, Cornoldi A, and Fini M. 2005. Effects of androgens on the cardiovascular system. *J Endocrinol Invest*. 28:32-38.
647. Rosano GM, Leonardo F, Pagnotta P, et al. 1999. Acute anti-ischemic effect of testosterone in men with coronary artery disease. *Circulation*. 99:1666-1670.

648. Rosenbaum DM, Degtarev A, David J, et al. 2010. Necroptosis, a novel form of caspase-independent cell death, contributes to neuronal damage in a retinal ischemia-reperfusion injury model. *J Neurosci Res*. 88:1569-1576.
649. Rosner W, Hankinson SE, Sluss PM, et al. 2013. Challenges to the measurement of estradiol: an endocrine society position statement. *J Clin Endocrinol Metab*. 98:1376-1387.
650. Rossier MF, Lenglet S, Vetterli L, et al. 2008. Corticosteroids and redox potential modulate spontaneous contractions in isolated rat ventricular cardiomyocytes. *Hypertension*. 52:721-728.
651. Rossol-Haseroth K, Zhou Q, Braun S, et al. 2004. Mineralocorticoid receptor antagonists do not block rapid ERK activation by aldosterone. *Biochem Biophys Res Commun*. 318:281-288.
652. Rothermel BA, and Hill JA. 2008. The heart of autophagy: deconstructing cardiac proteotoxicity. *Autophagy*. 4:932-935.
653. Rousseau MF, Gurne O, Duprez D, et al. 2002. Beneficial neurohormonal profile of spironolactone in severe congestive heart failure: results from the RALES neurohormonal substudy. *J Am Coll Cardiol*. 40:1596-1601.
654. Rubio-Gayosso I, Ramirez-Sanchez I, Ita-Islas I, et al. 2013. Testosterone metabolites mediate its effects on myocardial damage induced by ischemia/reperfusion in male Wistar rats. *Steroids*. 78:362-369.
655. Rude MK, Duhaney TA, Kuster GM, et al. 2005. Aldosterone stimulates matrix metalloproteinases and reactive oxygen species in adult rat ventricular cardiomyocytes. *Hypertension*. 46:555-561.
656. Ruixing Y, Al-Ghazali R, Wenwu L, et al. 2006. Pretreatment with probucol attenuates cardiomyocyte apoptosis in a rabbit model of ischemia/reperfusion. *Scand J Clin Lab Invest*. 66:549-558.
657. Ruiz-Meana M, Abellan A, Miro-Casas E, et al. 2007. Opening of mitochondrial permeability transition pore induces hypercontracture in Ca²⁺ overloaded cardiac myocytes. *Basic Res Cardiol*. 102:542-552.
658. Ruiz-Meana M, Inserte J, Fernandez-Sanz C, et al. 2011. The role of mitochondrial permeability transition in reperfusion-induced cardiomyocyte death depends on the duration of ischemia. *Basic Res Cardiol*. 106:1259-1268.
659. Sa MP, Ferraz PE, Escobar RR, et al. 2013. Five-year outcomes following PCI with DES versus CABG for unprotected LM coronary lesions: meta-analysis and meta-regression of 2914 patients. *Rev Bras Cir Cardiovasc*. 28:83-92.
660. Saartok T, Dahlberg E, and Gustafsson JA. 1984. Relative binding affinity of anabolic-androgenic steroids: comparison of the binding to the androgen receptors in skeletal muscle and in prostate, as well as to sex hormone-binding globulin. *Endocrinology*. 114:2100-2106.
661. Sader MA, Griffiths KA, McCredie RJ, et al. 2001. Androgenic anabolic steroids and arterial structure and function in male bodybuilders. *J Am Coll Cardiol*. 37:224-230.

662. Sader MA, McGrath KC, Hill MD, et al. 2005. Androgen receptor gene expression in leucocytes is hormonally regulated: implications for gender differences in disease pathogenesis. *Clin Endocrinol (Oxf)*. 62:56-63.
663. Sahara S, Aoto M, Eguchi Y, et al. 1999. Acinus is a caspase-3-activated protein required for apoptotic chromatin condensation. *Nature*. 401:168-173.
664. Sakahira H, Enari M, and Nagata S. 1998. Cleavage of CAD inhibitor in CAD activation and DNA degradation during apoptosis. *Nature*. 391:96-99.
665. Sakahira H, Enari M, Ohsawa Y, et al. 1999. Apoptotic nuclear morphological change without DNA fragmentation. *Curr Biol*. 9:543-546.
666. Sala-Mercado JA, Wider J, Undyala VV, et al. 2010. Profound cardioprotection with chloramphenicol succinate in the swine model of myocardial ischemia-reperfusion injury. *Circulation*. 122:S179-184.
667. Salmon M, Gomez D, Greene E, et al. 2012. Cooperative binding of KLF4, pELK-1, and HDAC2 to a G/C repressor element in the SM22alpha promoter mediates transcriptional silencing during SMC phenotypic switching in vivo. *Circ Res*. 111:685-696.
668. Saotome M, Katoh H, Yaguchi Y, et al. 2009. Transient opening of mitochondrial permeability transition pore by reactive oxygen species protects myocardium from ischemia-reperfusion injury. *Am J Physiol Heart Circ Physiol*. 296:H1125-1132.
669. Saraste A, and Pulkki K. 2000. Morphologic and biochemical hallmarks of apoptosis. *Cardiovasc Res*. 45:528-537.
670. Saraste A, Pulkki K, Kallajoki M, et al. 1997. Apoptosis in human acute myocardial infarction. *Circulation*. 95:320-323.
671. Sartorio CL, Fraccarollo D, Galuppo P, et al. 2007. Mineralocorticoid receptor blockade improves vasomotor dysfunction and vascular oxidative stress early after myocardial infarction. *Hypertension*. 50:919-925.
672. Sasano H, Murakami H, Shizawa S, et al. 1999. Aromatase and sex steroid receptors in human vena cava. *Endocr J*. 46:233-242.
673. Sato A, and Funder JW. 1996. High glucose stimulates aldosterone-induced hypertrophy via type I mineralocorticoid receptors in neonatal rat cardiomyocytes. *Endocrinology*. 137:4145-4153.
674. Saunders PT, Maguire SM, Gaughan J, et al. 1997. Expression of oestrogen receptor beta (ER beta) in multiple rat tissues visualised by immunohistochemistry. *J Endocrinol*. 154:R13-16.
675. Savolainen H, Frosen J, Petrov L, et al. 2001. Expression of estrogen receptor sub-types alpha and beta in acute and chronic cardiac allograft vasculopathy. *J Heart Lung Transplant*. 20:1252-1264.
676. Sbarouni E, Iliodromitis EK, Bofilis E, et al. 1998. Short-term estrogen reduces myocardial infarct size in oophorectomized female rabbits in a dose-dependent manner. *Cardiovasc Drugs Ther*. 12:457-462.

677. Scarabelli T, Stephanou A, Rayment N, et al. 2001. Apoptosis of endothelial cells precedes myocyte cell apoptosis in ischemia/reperfusion injury. *Circulation*. 104:253-256.
678. Scarabelli TM, Knight RA, Rayment NB, et al. 1999. Quantitative assessment of cardiac myocyte apoptosis in tissue sections using the fluorescence-based tunel technique enhanced with counterstains. *J Immunol Methods*. 228:23-28.
679. Scarabelli TM, Stephanou A, Pasini E, et al. 2002. Different signaling pathways induce apoptosis in endothelial cells and cardiac myocytes during ischemia/reperfusion injury. *Circ Res*. 90:745-748.
680. Scarabelli TM, Stephanou A, Pasini E, et al. 2004. Minocycline inhibits caspase activation and reactivation, increases the ratio of XIAP to smac/DIABLO, and reduces the mitochondrial leakage of cytochrome C and smac/DIABLO. *J Am Coll Cardiol*. 43:865-874.
681. Schafer FQ, and Buettner GR. 2001. Redox environment of the cell as viewed through the redox state of the glutathione disulfide/glutathione couple. *Free Radic Biol Med*. 30:1191-1212.
682. Schafer N, Lohmann C, Winnik S, et al. 2013. Endothelial mineralocorticoid receptor activation mediates endothelial dysfunction in diet-induced obesity. *Eur Heart J*.
683. Schenkel PC, Tavares AM, Fernandes RO, et al. 2010. Redox-sensitive prosurvival and proapoptotic protein expression in the myocardial remodeling post-infarction in rats. *Mol Cell Biochem*. 341:1-8.
684. Schierbeck LL, Rejnmark L, Tofteng CL, et al. 2012. Effect of hormone replacement therapy on cardiovascular events in recently postmenopausal women: randomised trial. *Bmj*. 345:e6409.
685. Schmidt BM, Horisberger K, Feuring M, et al. 2005. Aldosterone blunts human baroreflex sensitivity by a nongenomic mechanism. *Exp Clin Endocrinol Diabetes*. 113:252-256.
686. Schmidt BM, Montealegre A, Janson CP, et al. 1999. Short term cardiovascular effects of aldosterone in healthy male volunteers. *J Clin Endocrinol Metab*. 84:3528-3533.
687. Schmidt BM, Oehmer S, Delles C, et al. 2003. Rapid nongenomic effects of aldosterone on human forearm vasculature. *Hypertension*. 42:156-160.
688. Schmidt K, Tissier R, Ghaleh B, et al. 2010. Cardioprotective effects of mineralocorticoid receptor antagonists at reperfusion. *Eur Heart J*. 31:1655-1662.
689. Schoeniger LO, Curtis W, Esnaola NF, et al. 1994. Myocardial heat shock gene expression in pigs is dependent on superoxide anion generated at reperfusion. *Shock*. 1:31-35.
690. Schuit SC, de Jong FH, Stolk L, et al. 2005. Estrogen receptor alpha gene polymorphisms are associated with estradiol levels in postmenopausal women. *Eur J Endocrinol*. 153:327-334.

691. Schwarz ER, Somoano Y, Hale SL, et al. 2000. What is the required reperfusion period for assessment of myocardial infarct size using triphenyltetrazolium chloride staining in the rat? *J Thromb Thrombolysis*. 10:181-187.
692. Searle J, Kerr JF, and Bishop CJ. 1982. Necrosis and apoptosis: distinct modes of cell death with fundamentally different significance. *Pathol Annu*. 17 Pt 2:229-259.
693. Seiferth A, Ruhs S, Mildenerger S, et al. 2012. The phosphatase calcineurin PP2BA β mediates part of mineralocorticoid receptor transcriptional activity. *Faseb J*. 26:2327-2337.
694. Seli E, Guzeloglu-Kayisli O, Cakmak H, et al. 2006. Estradiol increases apoptosis in human coronary artery endothelial cells by up-regulating Fas and Fas ligand expression. *J Clin Endocrinol Metab*. 91:4995-5001.
695. Selye H, Bajusz E, Grasso S, et al. 1960. Simple techniques for the surgical occlusion of coronary vessels in the rat. *Angiology*. 11:398-407.
696. Sgobbo P, Pacelli C, Grattagliano I, et al. 2007. Carvedilol inhibits mitochondrial complex I and induces resistance to H₂O₂ -mediated oxidative insult in H9C2 myocardial cells. *Biochim Biophys Acta*. 1767:222-232.
697. Shan L, Li J, Wei M, et al. 2010. Disruption of Rac1 signaling reduces ischemia-reperfusion injury in the diabetic heart by inhibiting calpain. *Free Radic Biol Med*. 49:1804-1814.
698. Shapiro AL, Vinuela E, and Maizel JV, Jr. 1967. Molecular weight estimation of polypeptide chains by electrophoresis in SDS-polyacrylamide gels. *Biochem Biophys Res Commun*. 28:815-820.
699. Shapiro J, Christiana J, and Frishman WH. 1999. Testosterone and other anabolic steroids as cardiovascular drugs. *Am J Ther*. 6:167-174.
700. Shaw LJ, Bairey Merz CN, Pepine CJ, et al. 2006. Insights from the NHLBI-Sponsored Women's Ischemia Syndrome Evaluation (WISE) Study: Part I: gender differences in traditional and novel risk factors, symptom evaluation, and gender-optimized diagnostic strategies. *J Am Coll Cardiol*. 47:S4-S20.
701. Sheppard KE, and Autelitano DJ. 2002. 11 β -hydroxysteroid dehydrogenase 1 transforms 11-dehydrocorticosterone into transcriptionally active glucocorticoid in neonatal rat heart. *Endocrinology*. 143:198-204.
702. Shibata S, Mu S, Kawarazaki H, et al. 2011. Rac1 GTPase in rodent kidneys is essential for salt-sensitive hypertension via a mineralocorticoid receptor-dependent pathway. *J Clin Invest*. 121:3233-3243.
703. Shibata S, Nagase M, Yoshida S, et al. 2008. Modification of mineralocorticoid receptor function by Rac1 GTPase: implication in proteinuric kidney disease. *Nat Med*. 14:1370-1376.
704. Shilkrut M, Yaniv G, Asleh R, et al. 2003. Tyrosine kinases inhibitors block Fas-mediated deleterious effects in normoxic and hypoxic ventricular myocytes. *J Mol Cell Cardiol*. 35:1229-1240.

705. Shimizu S, and Tsujimoto Y. 2000. Proapoptotic BH3-only Bcl-2 family members induce cytochrome c release, but not mitochondrial membrane potential loss, and do not directly modulate voltage-dependent anion channel activity. *Proc Natl Acad Sci U S A.* 97:577-582.
706. Shintani-Ishida K, Inui M, and Yoshida K. 2012. Ischemia-reperfusion induces myocardial infarction through mitochondrial Ca(2)(+) overload. *J Mol Cell Cardiol.* 53:233-239.
707. Shiomi T, Tsutsui H, Hayashidani S, et al. 2002. Pioglitazone, a peroxisome proliferator-activated receptor-gamma agonist, attenuates left ventricular remodeling and failure after experimental myocardial infarction. *Circulation.* 106:3126-3132.
708. Shirani J, Berezowski K, and Roberts WC. 1994. Out-of-hospital sudden death from left ventricular free wall rupture during acute myocardial infarction as the first and only manifestation of atherosclerotic coronary artery disease. *Am J Cardiol.* 73:88-92.
709. Sies H, and Cadenas E. 1985. Oxidative stress: damage to intact cells and organs. *Philos Trans R Soc Lond B Biol Sci.* 311:617-631.
710. Sievers RE, Schmiedl U, Wolfe CL, et al. 1989. A model of acute regional myocardial ischemia and reperfusion in the rat. *Magn Reson Med.* 10:172-181.
711. Silander K, Alanne M, Kristiansson K, et al. 2008. Gender differences in genetic risk profiles for cardiovascular disease. *PLoS One.* 3:e3615.
712. Simoncini T, Hafezi-Moghadam A, Brazil DP, et al. 2000. Interaction of oestrogen receptor with the regulatory subunit of phosphatidylinositol-3-OH kinase. *Nature.* 407:538-541.
713. Singh A, Lee KJ, Lee CY, et al. 1989. Relation between myocardial glutathione content and extent of ischemia-reperfusion injury. *Circulation.* 80:1795-1804.
714. Smith CC, and Yellon DM. 2011. Necroptosis, necrostatins and tissue injury. *J Cell Mol Med.* 15:1797-1806.
715. Soderberg O, Gullberg M, Jarvius M, et al. 2006. Direct observation of individual endogenous protein complexes in situ by proximity ligation. *Nature methods.* 3:995-1000.
716. Soderberg O, Leuchowius KJ, Gullberg M, et al. 2008. Characterizing proteins and their interactions in cells and tissues using the in situ proximity ligation assay. *Methods.* 45:227-232.
717. Srinivasula SM, Hegde R, Saleh A, et al. 2001. A conserved XIAP-interaction motif in caspase-9 and Smac/DIABLO regulates caspase activity and apoptosis. *Nature.* 410:112-116.
718. St-Pierre J, Lin J, Krauss S, et al. 2003. Bioenergetic analysis of peroxisome proliferator-activated receptor gamma coactivators 1alpha and 1beta (PGC-1alpha and PGC-1beta) in muscle cells. *J Biol Chem.* 278:26597-26603.
719. Stanczyk FZ, Lee JS, and Santen RJ. 2007. Standardization of steroid hormone assays: why, how, and when? *Cancer Epidemiol Biomarkers Prev.* 16:1713-1719.

720. Stanton RC, Seifter JL, Boxer DC, et al. 1991. Rapid release of bound glucose-6-phosphate dehydrogenase by growth factors. Correlation with increased enzymatic activity. *J Biol Chem.* 266:12442-12448.
721. Steenbergen C, Murphy E, Levy L, et al. 1987. Elevation in cytosolic free calcium concentration early in myocardial ischemia in perfused rat heart. *Circ Res.* 60:700-707.
722. Stennicke HR, Jurgensmeier JM, Shin H, et al. 1998. Pro-caspase-3 is a major physiologic target of caspase-8. *J Biol Chem.* 273:27084-27090.
723. Stokes KI, Benguzzi HA, and Cameron JA. 2000. Physiological responses associated with sustained delivery of T, DHT, and AED in male rats. *Biomed Sci Instrum.* 36:209-214.
724. Stoner JD, Angelos MG, and Clanton TL. 2004. Myocardial contractile function during postischemic low-flow reperfusion: critical thresholds of NADH and O₂ delivery. *Am J Physiol Heart Circ Physiol.* 286:H375-380.
725. Stowe DF, and Camara AK. 2009. Mitochondrial reactive oxygen species production in excitable cells: modulators of mitochondrial and cell function. *Antioxid Redox Signal.* 11:1373-1414.
726. Straface E, Gambardella L, Brandani M, et al. 2012. Sex differences at cellular level: "cells have a sex". *Handb Exp Pharmacol:*49-65.
727. Straface E, Vona R, Gambardella L, et al. 2009. Cell sex determines anoikis resistance in vascular smooth muscle cells. *FEBS Lett.* 583:3448-3454.
728. Strober W. 2001. Trypan blue exclusion test of cell viability. *Curr Protoc Immunol.* Appendix 3:Appendix 3B.
729. Struthers AD. 1996. Aldosterone escape during angiotensin-converting enzyme inhibitor therapy in chronic heart failure. *J Card Fail.* 2:47-54.
730. Stuck BJ, Lenski M, Bohm M, et al. 2008. Metabolic switch and hypertrophy of cardiomyocytes following treatment with angiotensin II are prevented by AMP-activated protein kinase. *J Biol Chem.* 283:32562-32569.
731. Subjeck JR, and Shyy TT. 1986. Stress protein systems of mammalian cells. *Am J Physiol.* 250:C1-17.
732. Sukoyan GV, Andriadze NA, Guchua EI, et al. 2005. Effect of NAD on recovery of adenine nucleotide pool, phosphorylation potential, and stimulation of apoptosis during late period of reperfusion damage to myocardium. *Bull Exp Biol Med.* 139:46-49.
733. Sullivan ML, Martinez CM, Gennis P, et al. 1998. The cardiac toxicity of anabolic steroids. *Prog Cardiovasc Dis.* 41:1-15.
734. Sun CK, Chang LT, Sheu JJ, et al. 2007. Losartan preserves integrity of cardiac gap junctions and PGC-1 alpha gene expression and prevents cellular apoptosis in remote area of left ventricular myocardium following acute myocardial infarction. *Int Heart J.* 48:533-546.
735. Sun Y, Zhang J, Lu L, et al. 2002. Aldosterone-induced inflammation in the rat heart : role of oxidative stress. *Am J Pathol.* 161:1773-1781.

736. Surder D, Schwitter J, Moccetti T, et al. 2010. Cell-based therapy for myocardial repair in patients with acute myocardial infarction: rationale and study design of the SWISS multicenter Intracoronary Stem cells Study in Acute Myocardial Infarction (SWISS-AMI). *Am Heart J.* 160:58-64.
737. Suzuki J, Iwai M, Mogi M, et al. 2006. Eplerenone with valsartan effectively reduces atherosclerotic lesion by attenuation of oxidative stress and inflammation. *Arterioscler Thromb Vasc Biol.* 26:917-921.
738. Swerdloff RS, and Wang C. 1998. Dihydrotestosterone: a rationale for its use as a non-aromatizable androgen replacement therapeutic agent. *Baillieres Clin Endocrinol Metab.* 12:501-506.
739. Takagi H, Matsui Y, Hirofani S, et al. 2007. AMPK mediates autophagy during myocardial ischemia in vivo. *Autophagy.* 3:405-407.
740. Takahashi M. 2011. Role of the inflammasome in myocardial infarction. *Trends Cardiovasc Med.* 21:37-41.
741. Takeda M, Tatsumi T, Matsunaga S, et al. 2007. Spironolactone modulates expressions of cardiac mineralocorticoid receptor and 11beta-hydroxysteroid dehydrogenase 2 and prevents ventricular remodeling in post-infarct rat hearts. *Hypertens Res.* 30:427-437.
742. Tallec LP, Kirsh O, Lecomte MC, et al. 2003. Protein inhibitor of activated signal transducer and activator of transcription 1 interacts with the N-terminal domain of mineralocorticoid receptor and represses its transcriptional activity: implication of small ubiquitin-related modifier 1 modification. *Mol Endocrinol.* 17:2529-2542.
743. Talukder MA, Elnakish MT, Yang F, et al. 2013. Cardiomyocyte-specific overexpression of an active form of Rac predisposes the heart to increased myocardial stunning and ischemia-reperfusion injury. *Am J Physiol Heart Circ Physiol.* 304:H294-302.
744. Tan CY, Ban H, Kim YH, et al. 2009. The heat shock protein 27 (Hsp27) operates predominantly by blocking the mitochondrial-independent/extrinsic pathway of cellular apoptosis. *Mol Cells.* 27:533-538.
745. Tan DX, Manchester LC, Reiter RJ, et al. 1998. Ischemia/reperfusion-induced arrhythmias in the isolated rat heart: prevention by melatonin. *J Pineal Res.* 25:184-191.
746. Tan WQ, Wang JX, Lin ZQ, et al. 2008. Novel cardiac apoptotic pathway: the dephosphorylation of apoptosis repressor with caspase recruitment domain by calcineurin. *Circulation.* 118:2268-2276.
747. Tanaka N, Yonekura H, Yamagishi S, et al. 2000. The receptor for advanced glycation end products is induced by the glycation products themselves and tumor necrosis factor-alpha through nuclear factor-kappa B, and by 17beta-estradiol through Sp-1 in human vascular endothelial cells. *J Biol Chem.* 275:25781-25790.
748. Tavernarakis N. 2007. Cardiomyocyte necrosis: alternative mechanisms, effective interventions. *Biochim Biophys Acta.* 1773:480-482.

749. Tawa P, Hell K, Giroux A, et al. 2004. Catalytic activity of caspase-3 is required for its degradation: stabilization of the active complex by synthetic inhibitors. *Cell Death Differ.* 11:439-447.
750. Taylor AH, and Al-Azzawi F. 2000. Immunolocalisation of oestrogen receptor beta in human tissues. *J Mol Endocrinol.* 24:145-155.
751. Thirunavukkarasu M, Penumathsa SV, Juhasz B, et al. 2006. Niacin-bound chromium enhances myocardial protection from ischemia-reperfusion injury. *Am J Physiol Heart Circ Physiol.* 291:H820-826.
752. Thomas JA, Poland B, and Honzatko R. 1995. Protein sulfhydryls and their role in the antioxidant function of protein S-thiolation. *Arch Biochem Biophys.* 319:1-9.
753. Tivesten A, Bollano E, Nystrom HC, et al. 2006. Cardiac concentric remodelling induced by non-aromatizable (dihydro-)testosterone is antagonized by oestradiol in ovariectomized rats. *J Endocrinol.* 189:485-491.
754. Toth A, Jeffers JR, Nickson P, et al. 2006. Targeted deletion of Puma attenuates cardiomyocyte death and improves cardiac function during ischemia-reperfusion. *Am J Physiol Heart Circ Physiol.* 291:H52-60.
755. Touyz RM, Chen X, Tabet F, et al. 2002. Expression of a functionally active gp91phox-containing neutrophil-type NAD(P)H oxidase in smooth muscle cells from human resistance arteries: regulation by angiotensin II. *Circ Res.* 90:1205-1213.
756. Tsai KH, Wang WJ, Lin CW, et al. 2012. NADPH oxidase-derived superoxide anion-induced apoptosis is mediated via the JNK-dependent activation of NF-kappaB in cardiomyocytes exposed to high glucose. *J Cell Physiol.* 227:1347-1357.
757. Tsybouleva N, Zhang L, Chen S, et al. 2004. Aldosterone, through novel signaling proteins, is a fundamental molecular bridge between the genetic defect and the cardiac phenotype of hypertrophic cardiomyopathy. *Circulation.* 109:1284-1291.
758. Tunstall-Pedoe H. 1998. Myth and paradox of coronary risk and the menopause. *Lancet.* 351:1425-1427.
759. Turan RG, Bozdogan TI, Ortak J, et al. 2011. Improved functional activity of bone marrow derived circulating progenitor cells after intra coronary freshly isolated bone marrow cells transplantation in patients with ischemic heart disease. *Stem Cell Rev.* 7:646-656.
760. Usal A, Acarturk E, Yuregir GT, et al. 1996. Decreased glutathione levels in acute myocardial infarction. *Jpn Heart J.* 37:177-182.
761. Vaccarino V, Abramson JL, Veledar E, et al. 2002. Sex differences in hospital mortality after coronary artery bypass surgery: evidence for a higher mortality in younger women. *Circulation.* 105:1176-1181.
762. Vaccarino V, Badimon L, Corti R, et al. 2011. Ischaemic heart disease in women: are there sex differences in pathophysiology and risk factors? Position paper from the working group on coronary pathophysiology and microcirculation of the European Society of Cardiology. *Cardiovasc Res.* 90:9-17.

763. Valentim L, Laurence KM, Townsend PA, et al. 2006. Urocortin inhibits Beclin1-mediated autophagic cell death in cardiac myocytes exposed to ischaemia/reperfusion injury. *J Mol Cell Cardiol.* 40:846-852.
764. van Eickels M, Patten RD, Aronovitz MJ, et al. 2003. 17-beta-estradiol increases cardiac remodeling and mortality in mice with myocardial infarction. *J Am Coll Cardiol.* 41:2084-2092.
765. Vanden Hoek TL, Li C, Shao Z, et al. 1997a. Significant levels of oxidants are generated by isolated cardiomyocytes during ischemia prior to reperfusion. *J Mol Cell Cardiol.* 29:2571-2583.
766. Vanden Hoek TL, Shao Z, Li C, et al. 1997b. Mitochondrial electron transport can become a significant source of oxidative injury in cardiomyocytes. *J Mol Cell Cardiol.* 29:2441-2450.
767. Vandenaabeele P, Declercq W, Van Herreweghe F, et al. 2010. The role of the kinases RIP1 and RIP3 in TNF-induced necrosis. *Sci Signal.* 3:re4.
768. Vanlangenakker N, Vanden Berghe T, Krysko DV, et al. 2008. Molecular mechanisms and pathophysiology of necrotic cell death. *Curr Mol Med.* 8:207-220.
769. Verbunt RJ, van Dockum WG, Bastiaanse EM, et al. 1995. Glutathione disulfide as an index of oxidative stress during postischemic reperfusion in isolated rat hearts. *Mol Cell Biochem.* 144:85-93.
770. Vickers MR, MacLennan AH, Lawton B, et al. 2007. Main morbidities recorded in the women's international study of long duration oestrogen after menopause (WISDOM): a randomised controlled trial of hormone replacement therapy in postmenopausal women. *Bmj.* 335:239.
771. Vidavalur R, Swarnakar S, Thirunavukkarasu M, et al. 2008. Ex vivo and in vivo approaches to study mechanisms of cardioprotection targeting ischemia/reperfusion (i/r) injury: useful techniques for cardiovascular drug discovery. *Curr Drug Discov Technol.* 5:269-278.
772. Viengchareun S, Le Menuet D, Martinerie L, et al. 2007. The mineralocorticoid receptor: insights into its molecular and (patho)physiological biology. *Nucl Recept Signal.* 5:e012.
773. von Harsdorf R, Li PF, and Dietz R. 1999. Signaling pathways in reactive oxygen species-induced cardiomyocyte apoptosis. *Circulation.* 99:2934-2941.
774. von Lueder TG, Sangaralingham SJ, Wang BH, et al. 2013. Renin-angiotensin blockade combined with natriuretic peptide system augmentation: novel therapeutic concepts to combat heart failure. *Circ Heart Fail.* 6:594-605.
775. Walther RF, Atlas E, Carrigan A, et al. 2005. A serine/threonine-rich motif is one of three nuclear localization signals that determine unidirectional transport of the mineralocorticoid receptor to the nucleus. *J Biol Chem.* 280:17549-17561.
776. Wang M, Crisostomo P, Wairiuko GM, et al. 2006. Estrogen receptor-alpha mediates acute myocardial protection in females. *Am J Physiol Heart Circ Physiol.* 290:H2204-2209.

777. Wang M, Tsai BM, Kher A, et al. 2005. Role of endogenous testosterone in myocardial proinflammatory and proapoptotic signaling after acute ischemia-reperfusion. *Am J Physiol Heart Circ Physiol*. 288:H221-226.
778. Wang M, Wang Y, Abarbanell A, et al. 2009. Both endogenous and exogenous testosterone decrease myocardial STAT3 activation and SOCS3 expression after acute ischemia and reperfusion. *Surgery*. 146:138-144.
779. Wang QD, Swardh A, and Sjoquist PO. 2001. Relationship between ischaemic time and ischaemia/reperfusion injury in isolated Langendorff-perfused mouse hearts. *Acta Physiol Scand*. 171:123-128.
780. Watkins SJ, Borthwick GM, and Arthur HM. 2011. The H9C2 cell line and primary neonatal cardiomyocyte cells show similar hypertrophic responses in vitro. *In Vitro Cell Dev Biol Anim*. 47:125-131.
781. Webb CM, McNeill JG, Hayward CS, et al. 1999. Effects of testosterone on coronary vasomotor regulation in men with coronary heart disease. *Circulation*. 100:1690-1696.
782. Webster KA. 2006. Puma joins the battery of BH3-only proteins that promote death and infarction during myocardial ischemia. *Am J Physiol Heart Circ Physiol*. 291:H20-22.
783. Webster KA, Discher DJ, and Bishopric NH. 1994. Regulation of fos and jun immediate-early genes by redox or metabolic stress in cardiac myocytes. *Circ Res*. 74:679-686.
784. Wehling M, Bauer MM, Ulsenheimer A, et al. 1996. Nongenomic effects of aldosterone on intracellular pH in vascular smooth muscle cells. *Biochem Biophys Res Commun*. 223:181-186.
785. Wehling M, Neylon CB, Fullerton M, et al. 1995. Nongenomic effects of aldosterone on intracellular Ca²⁺ in vascular smooth muscle cells. *Circ Res*. 76:973-979.
786. Wehling M, Spes CH, Win N, et al. 1998. Rapid cardiovascular action of aldosterone in man. *J Clin Endocrinol Metab*. 83:3517-3522.
787. Wehr E, Pilz S, Boehm BO, et al. 2011. Low free testosterone is associated with heart failure mortality in older men referred for coronary angiography. *Eur J Heart Fail*. 13:482-488.
788. Wei C, Li H, Han L, et al. 2013. Activation of autophagy in ischemic postconditioning contributes to cardioprotective effects against ischemia/reperfusion injury in rat hearts. *J Cardiovasc Pharmacol*. 61:416-422.
789. Wei GZ, Zhou JJ, Wang B, et al. 2007. Diastolic Ca²⁺ overload caused by Na⁺/Ca²⁺ exchanger during the first minutes of reperfusion results in continued myocardial stunning. *Eur J Pharmacol*. 572:1-11.
790. Wei Y, Whaley-Connell AT, Habibi J, et al. 2009. Mineralocorticoid receptor antagonism attenuates vascular apoptosis and injury via rescuing protein kinase B activation. *Hypertension*. 53:158-165.

791. Weil BR, Manukyan MC, Herrmann JL, et al. 2010. Signaling via GPR30 protects the myocardium from ischemia/reperfusion injury. *Surgery*. 148:436-443.
792. Weinberger C, Hollenberg SM, Ong ES, et al. 1985. Identification of human glucocorticoid receptor complementary DNA clones by epitope selection. *Science*. 228:740-742.
793. Weir RA, Tsoralis IK, Steedman T, et al. 2011. Aldosterone and cortisol predict medium-term left ventricular remodelling following myocardial infarction. *Eur J Heart Fail*. 13:1305-1313.
794. Weiss JN, Korge P, Honda HM, et al. 2003. Role of the mitochondrial permeability transition in myocardial disease. *Circ Res*. 93:292-301.
795. Welder AA, Robertson JW, Fugate RD, et al. 1995. Anabolic-androgenic steroid-induced toxicity in primary neonatal rat myocardial cell cultures. *Toxicol Appl Pharmacol*. 133:328-342.
796. Wenger NK. 2002. Clinical characteristics of coronary heart disease in women: emphasis on gender differences. *Cardiovasc Res*. 53:558-567.
797. Werns SW, Fantone JC, Ventura A, et al. 1992. Myocardial glutathione depletion impairs recovery of isolated blood-perfused hearts after global ischaemia. *J Mol Cell Cardiol*. 24:1215-1220.
798. WHO. 2011. World Health Organization. The top 10 causes of death. Fact Sheet no. 310. www.who.int/mediacentre/factsheets/fs310_2008.pdf Date last accessed: 30 October 2012.
799. Wild S, Pierpoint T, McKeigue P, et al. 2000. Cardiovascular disease in women with polycystic ovary syndrome at long-term follow-up: a retrospective cohort study. *Clin Endocrinol (Oxf)*. 52:595-600.
800. Wildling L, Hinterdorfer P, Kusche-Vihrog K, et al. 2009. Aldosterone receptor sites on plasma membrane of human vascular endothelium detected by a mechanical nanosensor. *Pflugers Arch*. 458:223-230.
801. Williams GH, Burgess E, Kolloch RE, et al. 2004. Efficacy of eplerenone versus enalapril as monotherapy in systemic hypertension. *Am J Cardiol*. 93:990-996.
802. Williams TA, Verhovez A, Milan A, et al. 2006. Protective effect of spironolactone on endothelial cell apoptosis. *Endocrinology*. 147:2496-2505.
803. Williamson DH, and Fennell DJ. 1975. The use of fluorescent DNA-binding agent for detecting and separating yeast mitochondrial DNA. *Methods Cell Biol*. 12:335-351.
804. Wilson JD, Griffin JE, and Russell DW. 1993. Steroid 5 alpha-reductase 2 deficiency. *Endocr Rev*. 14:577-593.
805. Wingard DL, Suarez L, and Barrett-Connor E. 1983. The sex differential in mortality from all causes and ischemic heart disease. *Am J Epidemiol*. 117:165-172.
806. Wong VW, Mardini M, Cheung NW, et al. 2011. High-dose insulin in experimental myocardial infarction in rabbits: protection against effects of hyperglycaemia. *J Diabetes Complications*. 25:122-128.

807. Wu G, Fang YZ, Yang S, et al. 2004. Glutathione metabolism and its implications for health. *J Nutr.* 134:489-492.
808. Wyllie AH, Kerr JF, and Currie AR. 1980. Cell death: the significance of apoptosis. *Int Rev Cytol.* 68:251-306.
809. Xhyheri B, and Bugiardini R. 2010. Diagnosis and treatment of heart disease: are women different from men? *Prog Cardiovasc Dis.* 53:227-236.
810. Xiao J, Zhu X, He B, et al. 2011. MiR-204 regulates cardiomyocyte autophagy induced by ischemia-reperfusion through LC3-II. *J Biomed Sci.* 18:35.
811. Xiao L, Pimentel DR, Wang J, et al. 2002. Role of reactive oxygen species and NAD(P)H oxidase in alpha(1)-adrenoceptor signaling in adult rat cardiac myocytes. *Am J Physiol Cell Physiol.* 282:C926-934.
812. Xu Y, Arenas IA, Armstrong SJ, et al. 2003. Estrogen modulation of left ventricular remodeling in the aged heart. *Cardiovasc Res.* 57:388-394.
813. Xu YC, Jing XL, Ke Y, et al. 2008. [Expression of brain natriuretic peptide and c-fos gene in rat after acute myocardial ischemia and its medicolegal significance]. *Fa Yi Xue Za Zhi.* 24:1-4.
814. Yan L, Sadoshima J, Vatner DE, et al. 2006. Autophagy: a novel protective mechanism in chronic ischemia. *Cell Cycle.* 5:1175-1177.
815. Yan L, Vatner DE, Kim SJ, et al. 2005. Autophagy in chronically ischemic myocardium. *Proc Natl Acad Sci U S A.* 102:13807-13812.
816. Yanagibashi K, Haniu M, Shively JE, et al. 1986. The synthesis of aldosterone by the adrenal cortex. Two zones (fasciculata and glomerulosa) possess one enzyme for 11 beta-, 18-hydroxylation, and aldehyde synthesis. *J Biol Chem.* 261:3556-3562.
817. Yang J, and Fuller PJ. 2012. Interactions of the mineralocorticoid receptor--within and without. *Mol Cell Endocrinol.* 350:196-205.
818. Yang SH, Liu R, Perez EJ, et al. 2004. Mitochondrial localization of estrogen receptor beta. *Proc Natl Acad Sci U S A.* 101:4130-4135.
819. Yang W, Guastella J, Huang JC, et al. 2003. MX1013, a dipeptide caspase inhibitor with potent in vivo antiapoptotic activity. *Br J Pharmacol.* 140:402-412.
820. Yang Z, Cheng B, Song J, et al. 2007. Estrogen accelerates G1 to S phase transition and induces a G2/M phase-predominant apoptosis in synthetic vascular smooth muscle cells. *Int J Cardiol.* 118:381-388.
821. Yao X, Tan G, He C, et al. 2012. Hydrogen sulfide protects cardiomyocytes from myocardial ischemia-reperfusion injury by enhancing phosphorylation of apoptosis repressor with caspase recruitment domain. *Tohoku J Exp Med.* 226:275-285.
822. Yaoita H, Ogawa K, Maehara K, et al. 1998. Attenuation of ischemia/reperfusion injury in rats by a caspase inhibitor. *Circulation.* 97:276-281.

823. Yarbrough WM, Mukherjee R, Stroud RE, et al. 2010. Caspase inhibition modulates left ventricular remodeling following myocardial infarction through cellular and extracellular mechanisms. *J Cardiovasc Pharmacol.* 55:408-416.
824. Yasojima K, Kilgore KS, Washington RA, et al. 1998. Complement gene expression by rabbit heart: upregulation by ischemia and reperfusion. *Circ Res.* 82:1224-1230.
825. Yellon DM, and Hausenloy DJ. 2007. Myocardial reperfusion injury. *N Engl J Med.* 357:1121-1135.
826. Yi X, Yin XM, and Dong Z. 2003. Inhibition of Bid-induced apoptosis by Bcl-2. tBid insertion, Bax translocation, and Bax/Bak oligomerization suppressed. *J Biol Chem.* 278:16992-16999.
827. Yokota K, Shibata H, Kobayashi S, et al. 2004. Proteasome-mediated mineralocorticoid receptor degradation attenuates transcriptional response to aldosterone. *Endocr Res.* 30:611-616.
828. Yoshida M, Ma J, Tomita T, et al. 2005. Mineralocorticoid receptor is overexpressed in cardiomyocytes of patients with congestive heart failure. *Congest Heart Fail.* 11:12-16.
829. Young M, Fullerton M, Dilley R, et al. 1994. Mineralocorticoids, hypertension, and cardiac fibrosis. *J Clin Invest.* 93:2578-2583.
830. Young MJ, and Funder JW. 1996. The renin-angiotensin-aldosterone system in experimental mineralocorticoid-salt-induced cardiac fibrosis. *Am J Physiol.* 271:E883-888.
831. Ytrehus K, Liu Y, Tsuchida A, et al. 1994. Rat and rabbit heart infarction: effects of anesthesia, perfusate, risk zone, and method of infarct sizing. *Am J Physiol.* 267:H2383-2390.
832. Ytrehus K, Myklebust R, and Mjos OD. 1986. Influence of oxygen radicals generated by xanthine oxidase in the isolated perfused rat heart. *Cardiovasc Res.* 20:597-603.
833. Yusuf S, Reddy S, Ounpuu S, et al. 2001. Global burden of cardiovascular diseases: part I: general considerations, the epidemiologic transition, risk factors, and impact of urbanization. *Circulation.* 104:2746-2753.
834. Zalckvar E, Berissi H, Eisenstein M, et al. 2009. Phosphorylation of Beclin 1 by DAP-kinase promotes autophagy by weakening its interactions with Bcl-2 and Bcl-XL. *Autophagy.* 5:720-722.
835. Zaman MA, Oparil S, and Calhoun DA. 2002. Drugs targeting the renin-angiotensin-aldosterone system. *Nature reviews. Drug discovery.* 1:621-636.
836. Zannad F, McMurray JJ, Krum H, et al. 2011. Eplerenone in patients with systolic heart failure and mild symptoms. *N Engl J Med.* 364:11-21.
837. Zaugg M, Jamali NZ, Lucchinetti E, et al. 2001. Anabolic-androgenic steroids induce apoptotic cell death in adult rat ventricular myocytes. *J Cell Physiol.* 187:90-95.

838. Zennaro MC, Keightley MC, Kotelevtsev Y, et al. 1995. Human mineralocorticoid receptor genomic structure and identification of expressed isoforms. *J Biol Chem.* 270:21016-21020.
839. Zhan E, Keimig T, Xu J, et al. 2008. Dose-dependent cardiac effect of oestrogen replacement in mice post-myocardial infarction. *Exp Physiol.* 93:982-993.
840. Zhang J, Qi XY, Wan YF, et al. 2011. Establishment of a reperfusion model in rabbits with acute myocardial infarction. *Cell Biochem Biophys.* 60:249-258.
841. Zhang S, Zhang M, Goldstein S, et al. 2013. The effect of c-fos on acute myocardial infarction and the significance of metoprolol intervention in a rat model. *Cell Biochem Biophys.* 65:249-255.
842. Zhang SX, Bentel JM, Ricciardelli C, et al. 1998. Immunolocalization of apolipoprotein D, androgen receptor and prostate specific antigen in early stage prostate cancers. *J Urol.* 159:548-554.
843. Zhang X, Zheng X, Sun H, et al. 2006. Prevention of renal ischemic injury by silencing the expression of renal caspase 3 and caspase 8. *Transplantation.* 82:1728-1732.
844. Zhang YQ, and Herman B. 2006. ARC protects rat cardiomyocytes against oxidative stress through inhibition of caspase-2 mediated mitochondrial pathway. *J Cell Biochem.* 99:575-588.
845. Zhang YX, Fan H, Shi Y, et al. 2010. Prevention of lung ischemia-reperfusion injury by short hairpin RNA-mediated caspase-3 gene silencing. *J Thorac Cardiovasc Surg.* 139:758-764.
846. Zhao K, Zhao GM, Wu D, et al. 2004. Cell-permeable peptide antioxidants targeted to inner mitochondrial membrane inhibit mitochondrial swelling, oxidative cell death, and reperfusion injury. *J Biol Chem.* 279:34682-34690.
847. Zhao ZQ, Nakamura M, Wang NP, et al. 2000. Reperfusion induces myocardial apoptotic cell death. *Cardiovasc Res.* 45:651-660.
848. Zheng HY, Li Y, Dai W, et al. 2012. Imbalance of testosterone/estradiol promotes male CHD development. *Biomed Mater Eng.* 22:179-185.
849. Zheng X, Zhang X, Sun H, et al. 2006. Protection of renal ischemia injury using combination gene silencing of complement 3 and caspase 3 genes. *Transplantation.* 82:1781-1786.
850. Zheng Z, Yang M, Zhang F, et al. 2011. Gender-related difference of sevoflurane postconditioning in isolated rat hearts: focus on phosphatidylinositol-3-kinase/Akt signaling. *J Surg Res.* 170:e3-9.
851. Zhou ZX, Lane MV, Kempainen JA, et al. 1995. Specificity of ligand-dependent androgen receptor stabilization: receptor domain interactions influence ligand dissociation and receptor stability. *Mol Endocrinol.* 9:208-218.
852. Zhu CJ, Wang QQ, Zhou JL, et al. 2012. The mineralocorticoid receptor-p38MAPK-NFkappaB or ERK-Sp1 signal pathways mediate aldosterone-stimulated inflammatory and profibrotic responses in rat vascular smooth muscle cells. *Acta Pharmacol Sin.* 33:873-878.

853. Zornoff LA, Paiva SA, Minicucci MF, et al. 2009. Experimental myocardium infarction in rats: analysis of the model. *Arq Bras Cardiol.* 93:434-440, 426-432.
854. Zou H, Li Y, Liu X, et al. 1999. An APAF-1.cytochrome c multimeric complex is a functional apoptosome that activates procaspase-9. *J Biol Chem.* 274:11549-11556.
855. Zucker DR, Griffith JL, Beshansky JR, et al. 1997. Presentations of acute myocardial infarction in men and women. *J Gen Intern Med.* 12:79-87.
856. Zweier JL, Flaherty JT, and Weisfeldt ML. 1987. Direct measurement of free radical generation following reperfusion of ischemic myocardium. *Proc Natl Acad Sci U S A.* 84:1404-1407.
857. Zweier JL, Kuppusamy P, Williams R, et al. 1989. Measurement and characterization of postischemic free radical generation in the isolated perfused heart. *J Biol Chem.* 264:18890-18895.
858. Zweier JL, and Talukder MA. 2006. The role of oxidants and free radicals in reperfusion injury. *Cardiovasc Res.* 70:181-190.